

**The Synthesis, Structural Characterization and Biological
Evaluation of Potential Chemotherapeutic Agents**

by

Frankie P. Anderson B.Sc. (Hons)

A thesis presented for the degree of Doctor of Philosophy

at

Dublin City University



*Ollscoil Chathair Bhaile Átha Cliath
School of Chemical Sciences*

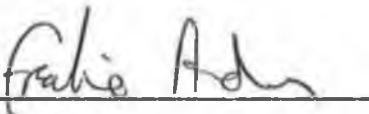
June 2005

To Mammy and Daddy

DECLARATION

I hereby certify that this material, which I now submit for assessment on the programme of study leading to the award of Ph.D is entirely my own work and has not been taken from the work of others save and to the extent that such work has been cited and acknowledged within the text of my work.

Signed:



Frankie P. Anderson

ID No. 97035157

Date:

18th August 2005

Acknowledgements

First and foremost I would like to thank my supervisors, Dr. Peter T. M. Kenny and Dr. John F. Gallagher, for giving me the opportunity to conduct research under their supervision, and for being so supportive and encouraging at both an academic and personal level.

I would also like to express my gratitude to:

The National Institute for Cellular Biotechnology (NICB) and Dublin City University for the funding of this project.

Dr. Alan J. Lough at the Department of Chemistry, University of Toronto, 80 St. George Street, Toronto, Ontario, Canada M5S 3H6 for obtaining X-ray crystallographic data.

Dr. Robert O'Connor and Paula Kinsella in the National Institute for Cellular Biotechnology, for carrying out cytotoxicity and synergistic toxicity studies.

Dr. John P. Dalton in the Institute for the Biotechnology of Infectious Diseases, University of Technology, Sydney, PO Box 123, Broadway, NSW 2007, Australia for generously donating *Fasciola hepatica* cathepsin L protease.

Dr. Ciarán Ó Fágáin, Dr. Brendan O'Connor, Dr. Deborah M. Ruth and Pamela O'Brien in the School of Biotechnology, Dublin City University for their assistance with the protease inhibition studies.

Dr. Steven R. Alley in the National Institute for Cellular Biotechnology for carrying out electrospray ionisation mass spectrometry on the synthesised compounds.

All of the technical staff in the School of Chemical Sciences, especially, Mick, Damien, Maurice, Ambrose, Veronica, Ann, John and Vinny.

All of the fourth year undergraduate students who worked on this project especially Eoin Murray, Louise O'Brien and Stephen Cloonan.

A special thanks to my colleagues, David Savage, Noel Brennan, Paula Kelly, Brian Moran and Alok Goel, members of the Kenny and Gallagher research groups.

All my fellow postgraduate researchers both past and present for their friendship and support particularly, Neil, Ray, Rob, Ger, Jai Feng, Mairead, Yang, Nameer, Rachel, Andrea, Ian, Fadi, Claire, Fiona, Noel, Tony, Karl, Johnny, Marco, Stefania and Jennifer.

Special thanks to my family, my parents John and Mary and my sister Jill for all their support and encouragement. A more wonderful family does not exist.

Finally, last but certainly not least, a huge thank you to Karen for being so supportive and putting up with me all this time. She has been an inspiration and there will be no one more delighted that I have finally completed my studies.

Abstract

The design and synthesis of potent chemotherapeutics offers one of the most successful routes for the treatment of disease. A series of amino acid, dipeptidyl and stilbenyl derivatives have been synthesised and evaluated as potential therapeutic agents. These compounds were fully characterised by a range of spectroscopic techniques including; IR, ^1H , ^{13}C , ^{19}F , ^{31}P , DEPT 135 and HMQC NMR in addition to ESIMS. X-ray crystal structures were also obtained in certain cases.

Multidrug resistance (MDR) is used to define resistance whereby cells become resistant to different drugs with no obvious structural resemblance and with different cellular targets. The preparation of *N*-fluorobenzoyl amino acid derivatives has resulted in the synthesis of multidrug resistance modulators. *N*-pentafluorobenzoyl-L-alanine methyl ester **81** was the most potent derivative. This compound although relatively non-toxic was shown to increase the potency of the anticancer drug epirubicin by 65%.

Fasciolosis is not only an important human disease but also affects cattle and sheep worldwide causing economic losses of approx 2 billion dollars. Potent inhibitors of *Fasciola hepatica* cathepsin L endoproteases have been developed. These dipeptidyl derivatives were synthesised by using the standard 1,3-dicyclohexylcarbodiimide (DCC) or 1-ethyl-3-(3-dimethylaminopropyl)carbodiimide (EDC), 1-hydroxybenzotriazole (HOBt) protocol. *N*-4-fluorobenzoyl-L-leucine-glycine nitrile **151** was shown to be the most active compound with an IC_{50} value of 2.78 μM recorded.

α -Chymotrypsin has served as a prototypical enzyme for the serine proteases and has been very useful as a model target enzyme for the development of compounds of pharmacological interest. A series of dipeptidyl phosphonate esters were prepared by standard EDC/HOBt protocol. *N*-4-fluorobenzenesulphonyl-glycine-phenylalanine^p-(OPh)₂ **165** was the most potent derivative with an IC_{50} value of 16.15 μM against α -chymotrypsin.

Resveratrol found in grapes is a naturally occurring phytoalexin formed in response to fungal infections. It has been shown to exhibit various biological properties including antifungal, anticancer, estrogenic and heart protecting activities. The synthesis of fluorinated analogues of this bioactive compound were carried out using a decarbonylative Heck reaction with preliminary biological results indicating that (*E*)-1-(4-acetoxystyryl)-3,5-difluorobenzene **192** was a potent growth inhibitor of breast, lung and central nervous system cancer lines. At a concentration of 100 μM the growth of central nervous system cancer was limited by 99%.

Table of Contents

Title Page	i
Dedication	ii
Declaration	iii
Acknowledgements	iv
Abstract	v
Chapter 1. Literature Review	
1.1 Proteases and their inhibition	
1.1.1 Introduction	1
1.1.2 Protease mechanism	2
1.1.3 Protease inhibitors	5
1.1.4 Categories of protease inhibitor	7
1.1.5 Non-specific protease inhibitors	8
1.1.6 Serine protease inhibitors	10
1.1.7 Cysteine protease inhibitors	14
1.1.8 Aspartic protease inhibitors	19
1.1.9 Metalloprotease inhibitors	24
1.1.10 Fluorine containing protease inhibitors	28
1.1.11 Conclusion	32
1.2 Cancer and cancer resistance	
1.2.1 Introduction	33
1.2.2 Modulators of P-glycoprotein associated cancer resistance	34
1.2.3 Synthetic inhibitors of MRP-1 associated cancer resistance	38
1.2.4 Glutathione <i>S</i> -transferase associated cancer resistance	38
1.2.5 Cancer resistance related to the topoisomerases	40
1.2.6 Conclusion	42
1.3 References	43
Chapter 2. Synthesis, characterisation and biological activity of novel modified amino acid derivatives	
2.1 Introduction	50
2.2 Synthesis of <i>N</i> -fluorobenzoyl amino acid esters	52
2.2.1 Synthesis of <i>N</i> -fluorobenzoyl-L-alanine methyl esters	54
2.2.2 ¹ H NMR studies of the <i>N</i> -fluorobenzoyl-L-alanine methyl esters	55

2.2.3	Synthesis of <i>N</i> -fluorobenzoyl-L-phenylalanine methyl esters	57
2.2.4	Electrospray ionisation mass spectrometry studies of the <i>N</i> -fluorobenzoyl-L-phenylalanine methyl esters	58
2.2.5	¹³ C NMR studies of the <i>N</i> -fluorobenzoyl-L-phenylalanine derivatives	59
2.2.6	Synthesis of <i>N</i> -fluorobenzoyl-glycine ethyl esters	60
2.2.7	Infrared study of the <i>N</i> -fluorobenzoyl-glycine derivatives	61
2.2.8	¹⁹ F NMR study of the <i>N</i> -fluorobenzoyl-glycine derivatives	63
2.2.9	Synthesis of <i>N</i> -fluorobenzoyl-L-leucine methyl esters	63
2.2.10	HMQC study of <i>N</i> -3-fluorobenzoyl-L-leucine methyl ester	64
2.3	Structural study of the <i>N</i> -fluorobenzoyl amino acid esters	67
2.4	<i>N</i> -fluorobenzoyl amino acid derivatives as potential multidrug resistance inhibitors	
2.4.1	Introduction	76
2.4.2	Cytotoxicity of the <i>N</i> -fluorobenzoyl amino acid derivatives	77
2.4.3	Combination toxicity of <i>N</i> -fluorobenzoyl amino acid derivatives and epirubicin	79
2.5	Conclusion	81
2.6	Experimental	82
2.7	References	107

Chapter 3. Fluorobenzoyl dipeptidyl derivatives as inhibitors of the *Fasciola hepatica* cathepsin L endoproteases

3.1	Introduction	110
3.2	Synthesis of dipeptidyl derivatives	111
3.2.1	Synthesis and characterisation of <i>N</i> -fluorobenzoyl dipeptidyl benzyl esters	113
3.2.2	¹ H NMR Study of the <i>N</i> -fluorobenzoyl dipeptidyl benzyl esters	114
3.2.3	Synthesis and characterisation of <i>N</i> -pentafluorobenzoyl dipeptidyl methyl esters	116
3.2.4	¹³ C NMR study of the <i>N</i> -pentafluorobenzoyl-L-alanine dipeptidyl methyl esters	119
3.2.5	Synthesis and characterisation of <i>N</i> -fluorobenzoyl dipeptidyl nitrile derivatives	120

3.2.6	HMQC study of 4-fluorobenzoyl-L-leucine-glycine nitrile	122
3.3	Protease inhibitory activity of <i>N</i> -fluorobenzoyl dipeptidyl derivatives against the <i>Fasciola hepatica</i> cysteine cathepsin L endoproteases	
3.3.1	Introduction	124
3.3.2	Fluorescent assay to determine the inhibitory potency of dipeptidyl derivatives	124
3.3.3	Protease inhibition of the <i>N</i> -fluorobenzoyl dipeptidyl benzyl ester derivatives	125
3.3.4	Protease inhibition of the <i>N</i> -pentafluorobenzoyl dipeptidyl methyl ester derivatives	127
3.3.5	Protease inhibition of the <i>N</i> -fluorobenzoyl dipeptidyl nitrile derivatives	128
3.3.6	True inhibitory activity of the most potent protease inhibitors	129
3.4	Conclusion	130
3.5	Experimental	132
3.6	References	152

Chapter 4. Dipeptidyl phosphonate diphenyl esters as inhibitors of the serine protease bovine pancrease α -chymotrypsin

4.1	Introduction	154
4.2	Synthesis and structural characterisation of diphenyl- α -amino phosphonates	157
4.3	Dipeptidyl phosphonate diphenyl esters	
4.3.1	Synthesis and structural characterisation of <i>N</i> -4-fluorobenzenesulphonyl dipeptidyl phosphonate diphenyl esters	159
4.3.2	¹ H NMR study of <i>N</i> -4-fluorobenzenesulphonyl dipeptidyl phosphonate esters	161
4.3.3	Synthesis and structural characterisation of <i>N</i> -cinnamoyl dipeptidyl phosphonate diphenyl esters	162
4.3.4	¹³ C NMR study of <i>N</i> -cinnamoyl dipeptidyl phosphonate esters	164
4.3.5	Synthesis and structural characterisation of <i>N</i> -trifluoroacetyl dipeptidyl phosphonate diphenyl esters	166
4.3.6	HMQC Study of <i>N</i> -trifluoroacetyl dipeptidyl phosphonate esters	167
4.4	Structural study of the dipeptidyl phosphonate esters	169

4.5	Protease inhibitory activity of dipeptidyl phosphonate esters	
4.5.1	Introduction	179
4.5.2	Assay to determine the inhibitory potency of dipeptidyl phosphonate esters on bovine pancreas α -chymotrypsin serine protease	179
4.5.3	Protease inhibition of the <i>N</i> -4-fluorobenzenesulphonyl dipeptidyl phosphonate ester derivatives	180
4.5.4	Protease inhibition of the <i>N</i> -cinnamoyl dipeptidyl phosphonate ester derivatives	181
4.5.5	Protease inhibition of the <i>N</i> -trifluoroacetyl dipeptidyl phosphonate ester derivatives	183
4.6	Conclusion	184
4.7	Experimental	186
4.8	References	202
Chapter 5. Fluorinated analogues of resveratrol as potential anticancer agents		
5.1	Introduction	205
5.2	Biosynthetic pathway of resveratrol	206
5.3	Syntheses of resveratrol	207
5.4	Synthesis and structural characterisation of fluorinated analogues of resveratrol	211
5.4.1	¹ H NMR study of the fluorinated resveratrol analogues	216
5.4.2	¹³ C NMR study of the fluorinated resveratrol analogues	217
5.5	Biological activity of the fluorinated resveratrol analogues	
5.5.1	Introduction	219
5.5.2	Anticancer potential of fluorinated resveratrol analogues	220
5.6	Synthesis and characterisation of 3,5-difluorophenyl resveratrol analogues	221
5.6.1	HMQC study of (<i>E</i>)-4-(3,5-difluorostyryl)phenylmethanesulphonate	224
5.7	Conclusion	226
5.8	Experimental	227
5.9	References	235
Appendix I- List of abbreviations		238

Chapter 1

Literature Review

1.1 Proteases and their inhibition

1.1.1 Introduction

A proteinase or protease as it is commonly known, catalyses the cleavage of peptide bonds. Proteolytic cleavage of peptide bonds is one of the most common and important enzymatic modifications of proteins. Proteases only catalyse the hydrolysis of a peptide bond but their diversity of function make them one of the most fascinating group of enzymes. Their control over protein synthesis enables them to regulate physiological processes such as fertilization, growth and differentiation. The inhibition of such proteases has led to the treatment of conditions such as cancer and HIV.¹

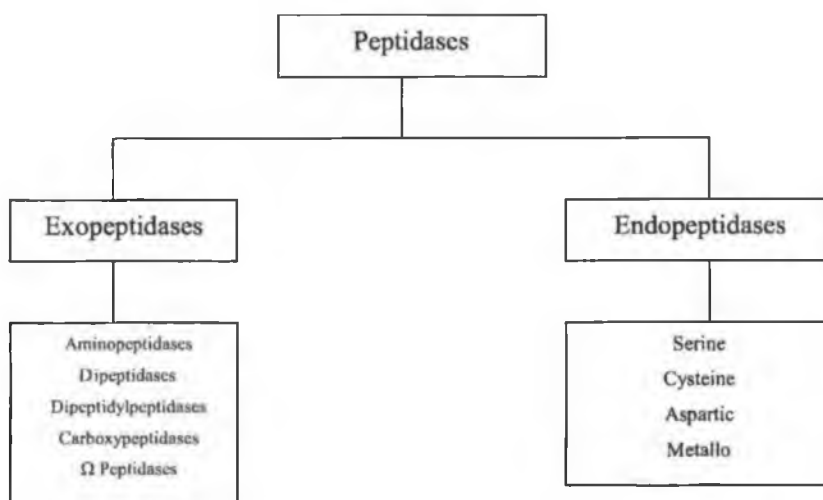


Figure 1.1 Classes of peptidases.

Investigations into kinetics, inhibition and single crystal X-ray structures of proteases have led to the identification of their active sites. Proteases can be divided into certain groups, with members of each group having similar structures and analogous mechanisms of action. Proteolytic enzymes are members of the peptidase family indicating that they hydrolyse peptide bonds. Enzymes that require the presence of an unsubstituted *N*- or *C*- terminus in the substrate are termed exopeptidases and those that do not are known as endopeptidases. The secondary and tertiary structure of protein substrates usually prevents attack by the exopeptidases. The presence of a free *N*- or *C*- terminus is usually not favoured by endopeptidases. Exopeptidases remove a

single amino acid, dipeptide or tripeptide from the *N*- or *C*- terminus, actions that determine its classification.

Four mechanistic classes of endopeptidases are recognised by the International Union of Biochemistry, namely serine, cysteine, aspartic and metalloproteases.² Each class of protease is characterised by a distinct set of functional amino acid residues arranged in a particular order to

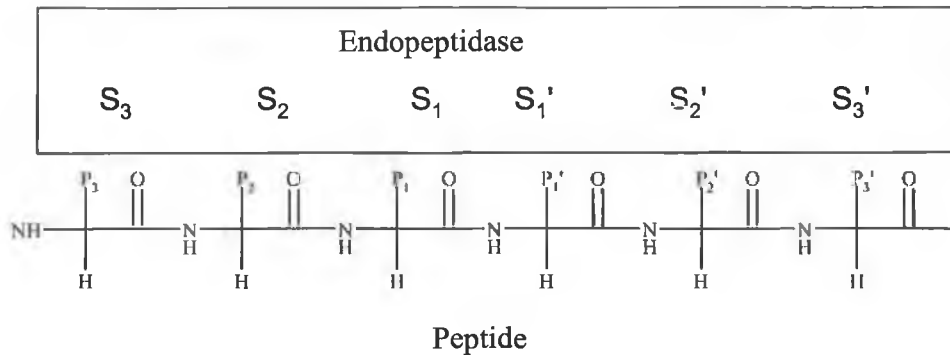


Figure 1.2 Substrate-Enzyme binding sites

form the active site. The nomenclature to describe the interaction of a substrate with a protease has been described.³ The amino acids of the polypeptide chain bind with the subsites in the enzyme active site. The subsite is referred to as *S* and the substrate amino acids *P*. The amino acids adjacent to the scissile site on the *N*-terminus are labeled P₁, P₂, P₃ etc and on the *C*-terminus P₁', P₂', P₃' etc with the P₁/P₁' being closest to the cleavage site. The complementary sites on the enzyme are labeled S₁, S₂, S₁', S₂' etc. The specificity of different proteases is due to differing amino acid residue substitution in the primary substrate binding site P₁/P₁' and minor differences in the secondary binding sites (P₂-P₈/P₂'-P₈'). A prime example is the serine protease α -chymotrypsin. It prefers an aromatic side chain on the substrate at P₁'.⁴ This is because the bulky aromatic group can fit snugly into a slit-like hydrophobic pocket near the active site.

1.1.2 Protease Mechanism.

The general mechanism for the four classes of proteolytic enzyme, differ, only in a minor manner with the overall process, *i.e.* hydrolysis of the peptide bond, similar in all cases. Serine proteases have been the most studied group of enzymes in the protease field with trypsin, α -chymotrypsin, trypsin, elastase and thrombin implicated in a variety of conditions. Their mode of action involves the substrate binding in the active site to form a Michaelis complex.

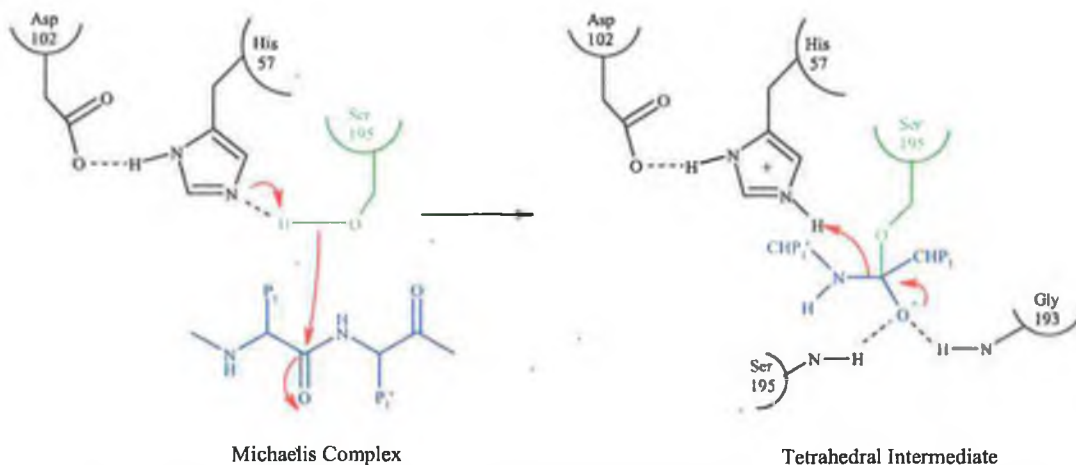


Figure 1.3 Tetrahedral intermediate formed by attack of a serine hydroxyl at amide bond.

The trigonal carbonyl group of the scissile amide bond is exposed to nucleophilic attack by the active site serine hydroxyl. The imidazole side chain of His⁵⁷ activates this hydroxyl group. The resulting tetrahedral intermediate is stabilized by hydrogen bonding to the N-H backbone of Ser¹⁹⁵ and Gly¹⁹³, hence forming the oxyanion hole.

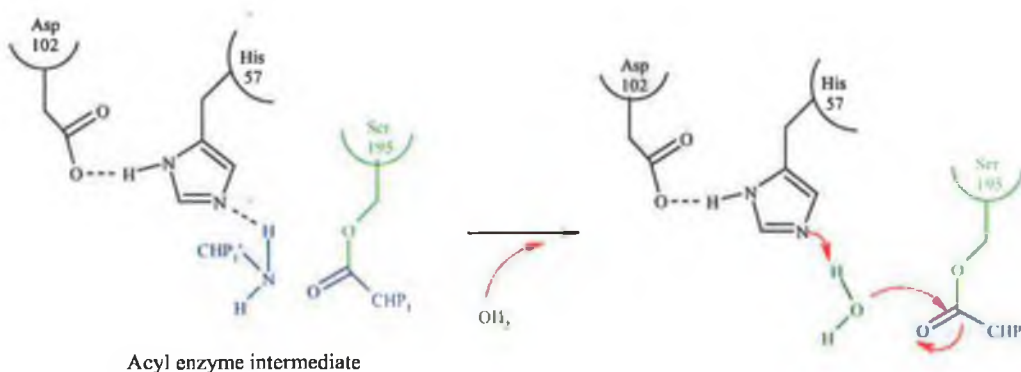


Figure 1.4 Deacylation of acyl enzyme intermediate facilitated by attack of a water molecule.

Proton transfer from the His⁵⁷ residue to the amine of the tetrahedral intermediate eliminates the C-terminal fragment as a leaving group. The covalent acyl-enzyme complex is attacked by a water molecule activated by the imidazole side chain of histidine⁵⁷, with formation of a new tetrahedral intermediate. This intermediate subsequently breaks down via acid catalysis to form the carboxy fragment of the cleaved substrate and regeneration of the Ser¹⁹⁵ residue of the active site.

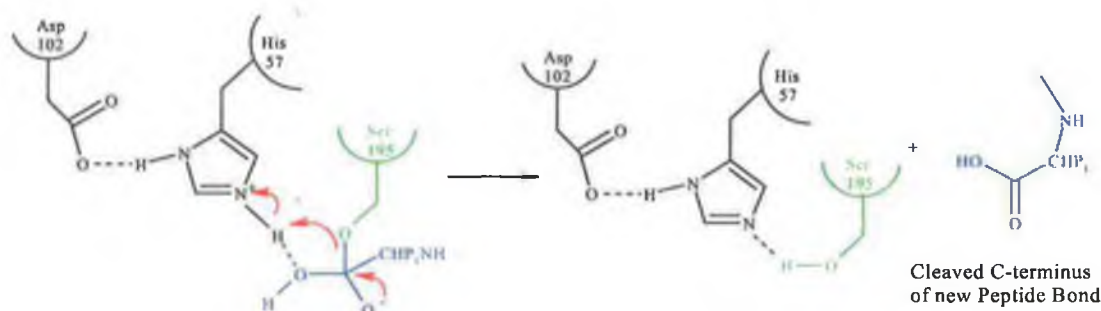


Figure 1.5 Peptide cleavage and regeneration of the serine¹⁹⁵ residue.

Cysteine proteases are believed to act in an analogous manner to the serine proteases. In their case it is the sulphur atom of a cysteine residue that is believed to act as the nucleophile. Resembling the mechanism of serine proteases, a histidine side chain is thought to be involved in hydrogen bonding to the oxygen anion formed from the attack of the nucleophile on the carbonyl. However it is still debatable whether the catalytic pair of Cys²⁵ and His¹⁵⁹ involved is sufficient for full catalytic activity.⁵

Aspartic proteases are understood to catalyse the cleavage of peptide bonds without the use of nucleophilic attack but by a functional group of the enzyme. Therefore, there is no tetrahedral intermediate formed between the enzyme and the substrate. Catalysis involves the involvement of two aspartic acid side chains. Nucleophilic attack is not involved, as the carboxyl group is not renowned as an effective nucleophile. The low pH optimum of this group of enzymes further strengthens the belief that the carboxyl groups are involved in the catalysis.

Metalloproteases like aspartic proteases do not form covalent intermediates. As an alternative of using hydrogen bonding via an 'oxyanion' hole to exert a catalytic effect on the carbonyl group, the metalloproteases are believed to use co-ordination to a metal ion to exert this effect. The metal involved is usually zinc. It provides a strong electrophilic interaction to assist the attack of a water molecule that is co-ordinated to the fourth tetrahedral site. The water molecule can be displaced during co-ordination of the substrate carbonyl to the metal atom but it is believed to remain at the active site. The water molecule is also hydrogen bonded to a glutamic acid. The carboxyl group acts as a base to remove a proton and assist the attack of the same water molecule on the peptide carbonyl. A proton must be transferred to the leaving nitrogen atom and perhaps this could be derived from glutamic acid.

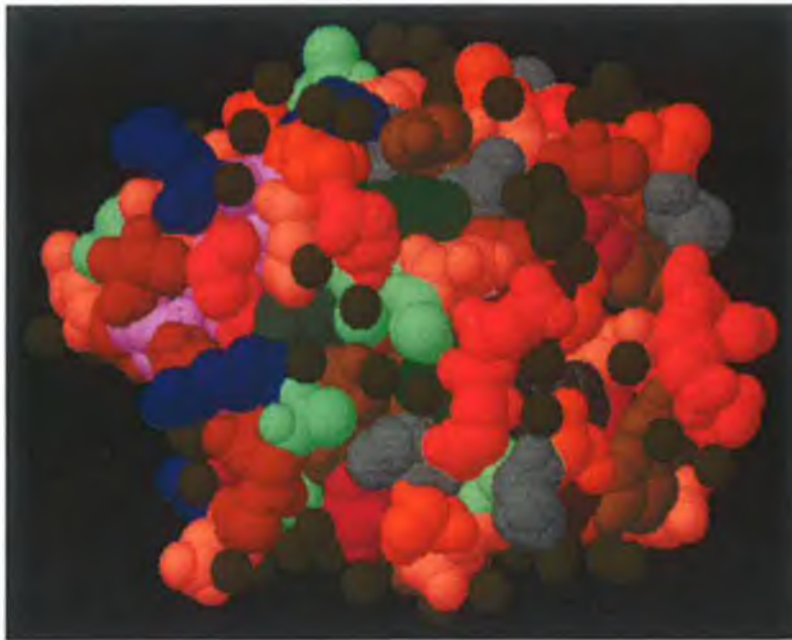
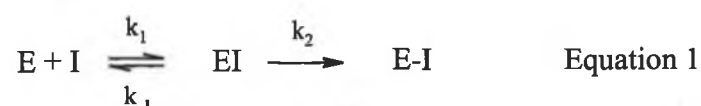


Figure 1.6 Zinc protease, a metalloprotease from the microorganism *Streptomyces caespitosus*. It is the smallest protease found to date. It consists of 132 amino acid residues.⁶

1.1.3 Protease Inhibitors.

Protease inhibitors are compounds that decrease the rate of hydrolysis of a given substrate with the kinetics of such a reaction fundamental to the degree of inhibition achieved. The kinetics of the reaction between a protease and its potential inhibitor determine the inhibitors effectiveness. The suppression of protease activity is regulated by the kinetic constants of the reaction between the protease and the inhibitor. The calculation of such parameters allows determination of both the quantity and the duration required to achieve efficient inhibition. Most protease inhibitors are defined as 'active site directed', *i.e.* they combine with the catalytic and substrate binding sites of the proteinase to form a tight and stable complex.² These inhibitors, natural or synthetic mimic a substrate.

Many protease inhibitors form irreversible covalent complexes with proteases. Irreversible or tight binding inhibitors (reversible inhibitors that bind to the enzyme with high affinity) decrease the number of active sites available for substrate. Protease inhibition can be described as a bimolecular reaction between protease (E) and inhibitor (I) that results in the formation of a stable complex (E-I) via an intermediate analogous to substrate binding (EI).² The



rates of the reactions are described by the rate constants k_1 , k_{-1} and k_2 (Equation 1). This equation describes an irreversible reaction. Irreversible inhibitors form covalent bonds with the enzyme and often these bonds remain when the enzyme is denatured. The parameters that govern the reaction of a protease with an irreversible inhibitor are the three rate constants. The most important quantity in this type of inhibition is the apparent rate of inhibition (or association) called k_{ass} (Equation 2). For inhibitors following the above mechanism, k_{ass} is defined as

$$k_{\text{ass}} = k_1 \cdot k_2 / k_{-1} \quad \text{Equation 2}$$

Under appropriate conditions all three rate constants can be measured, however for practical purposes k_{ass} is sufficient to describe the reaction rate of irreversible inhibitors.

Reversible inhibitors are bound to the enzyme through a combination of van der Waals, electrostatic, hydrogen bonding and hydrophobic forces. An equilibrium between the complexed form of an enzyme and free enzyme characterizes reversible inhibitors.



The equilibrium constant for the reaction, K_i is given by

$$K_i = [E][I]/[EI] = k_{-1}/k_1 \quad \text{Equation 4}$$

The practical use of these kinetic constants is the estimation of efficiency of the inhibitor. K_i and k_{ass} are constant for a particular enzyme-inhibitor reaction. It is from these values that parameters such as IC_{50} or $t_{1/2}$ can be calculated. The IC_{50} is the inhibitor concentration required to half the enzyme activity. It depends on substrate concentration (S) and k_m and is given by

$$IC_{50} = K_i (1 + S/k_m) \quad \text{Equation 5}$$

where k_m is the Michaelis constant. IC_{50} values represent one of the most common methods of comparing protease inhibitors.

For protease inhibitors to be effective as biological tools it is vital that not only are they very potent but also highly selective in binding to a particular protease. A key mechanistic feature of many protease inhibitors is the presence of a transition state isostere that simulates the

transition state of amide bond hydrolysis. The incorporation of such amide bond surrogates has proven to be a very successful strategy for rapidly converting protease substrates into inhibitors.⁷ Inhibitor composition has also been an important feature of protease inhibitor design to date. As drugs, protease inhibitors need on one hand to be designed to adopt an extended conformation and make hydrogen bonds to, and interact through hydrophobic effects with specific proteases, they also need to avoid degradation en route to the desired protease interactions with numerous other proteases in the digestive tract, in plasma and inside cells. This problem is compounded by the fact that natural peptide substrates for proteases are very susceptible to such degradation. Protease inhibitors also suffer from other major delivery problems such as low membrane permeability, high first pass metabolism and very low bioavailability. The most successful drugs based on protease inhibition to date have tended to be small organic molecules with few or no peptide bonds, significant lipophilicity and high selectivity for both the specific protease and the clinical objective being targeted.

1.1.4 Categories of protease inhibitor

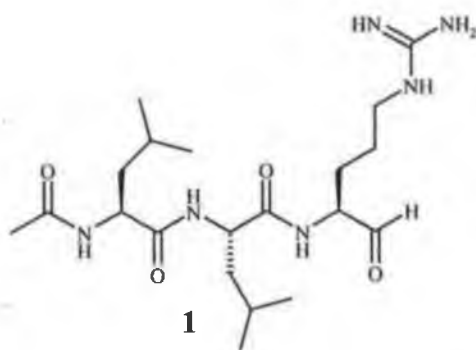
Protease inhibitors can be split into two general classes, the natural product derived inhibitors and the low molecular weight synthetic inhibitors. Over one hundred natural peptide based protease inhibitors have been isolated from plant, animal and bacterial sources. They behave as tight binding reversible or pseudo-irreversible inhibitors of proteases preventing substrate access to the active site through steric hindrance. As such they are usually large protein chains but are extremely variable in size from fifty residues (Bovine Pancreatic Trypsin Inhibitor) to over four hundred residues (α -1-proteinase inhibitor).²

The low molecular weight inhibitors can be either synthetic or of bacterial and fungal origin and irreversibly modify an amino acid residue of the protease active site. The huge diversity of protease inhibitors means that they are often grouped according to their reaction mechanism, origin or structural similarity. However, the most efficient method of separating different classes of inhibitors is by their specificity. As such they can be ordered according to which family of proteases they inhibit although some inhibitors are potent against multiple enzymes. Presently, the majority of research in the area of protease inhibition is concentrated on the design and synthesis of low molecular weight synthetic inhibitors with high specificity for individual proteolytic enzymes.

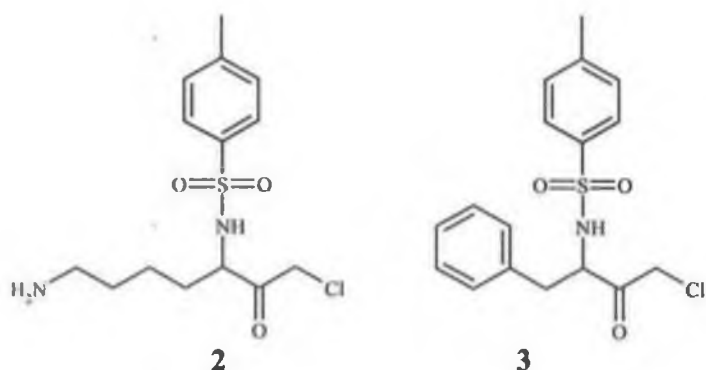
1.1.5 Non-specific protease inhibitors

α -Macroglobulins are a large group of natural protein protease inhibitors and for the most part extremely class specific. However, the human-plasma protein α_2 -macroglobulin fails to discriminate between the proteinase classes. It is a glycoprotein composed of four identical subunits. The inhibitory ability arises from a conformational change during the reaction that traps the enzyme allowing only small substrate molecules to enter and to be cleaved by the entrapped protease.⁸ This binding is irreversible and is mechanistically different to other inhibitors that tend to concentrate on active site deactivation. The α -macroglobulins are the only natural inhibitors that fail to discriminate among protease classes.

Peptide aldehydes are di-, tri- or tetrapeptides containing an aldehyde moiety in place of the usual carboxylate group. They are reversible inhibitors that are often referred to as 'transition state analogues' because they act by mimicking the tetrahedral intermediate formed during peptide bond hydrolysis. The most notable example is leupeptin **1**. Leupeptin inhibits serine (trypsin), plasmin (kallikrein) and cysteine proteases (papain).² The structure of leupeptin is acetyl-leucyl-leucyl-arginal. A number of peptidyl aldehyde derivatives have been synthesized in attempts to improve specificity.⁹ Two major drawbacks limit their usefulness as selective or specific inhibitors. Firstly, the lack of selectivity allows for the inhibition of proteases other than those under investigation. Secondly, in aqueous solution most aldehydes exist primarily as inactive hydrates. Accordingly the rate limiting step for inhibition can be the formation of the aldehyde rather than the encounter with a suitable target enzyme.



Peptidyl chloromethyl ketones are irreversible inhibitors that represented one of the first approaches in the study of active site directed protease modification.¹⁰ The two best known members are tosyl-L-lysine chloromethyl ketone (TLCK) **2** and tosylamido-L-phenylethylchloromethyl ketone (TPCK) **3**.



The mechanism of inactivation of serine proteases shows that inhibition results from the protease binding the inhibitor in a substrate like manner followed by alkylation of the active site histidine by the chloromethyl moiety. It has been shown that halomethyl ketone inhibitors form an irreversible tetrahedral covalent adduct with the active site histidine residue of serine proteases.¹¹

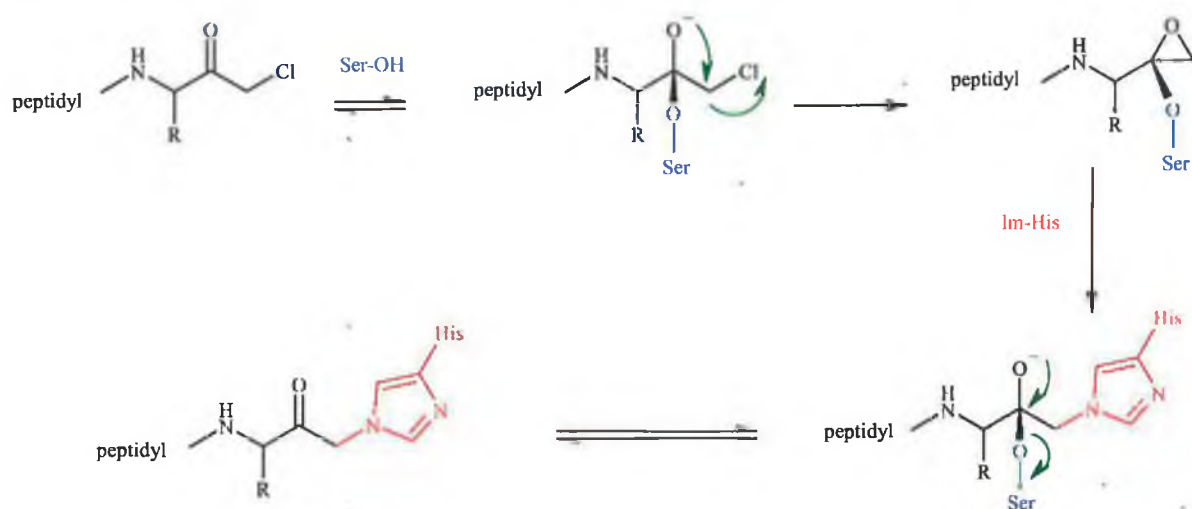


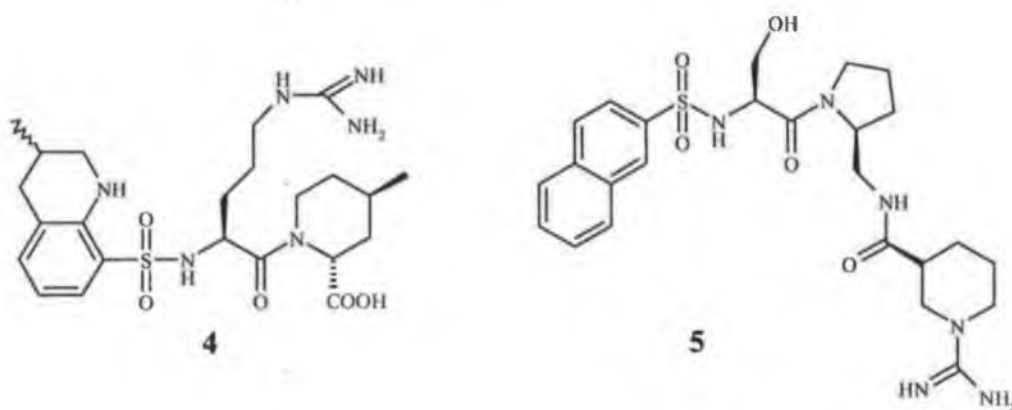
Figure 1.7 Proposed mechanism of inhibition of serine proteases by peptidyl chloromethyl ketones.

Unfortunately chloromethyl ketones also have the ability to inactivate cysteine proteases, by a similar mechanism to serine proteases. Considerable specificity for individual serine and cysteine proteases can be obtained by altering the peptide sequence of the inhibitor. It should be noted that many researchers claim specific inhibitors without actually demonstrating that the inhibitor does not react with the other potential target proteases. The use of chloromethyl ketones in cell culture and animal studies is limited by toxicity resulting from alkylation of cellular components.

1.1.6 Serine protease inhibitors

Serine proteases are classified by their substrate specificity with particular emphasis placed on the nature of the residue present at P1. The most common examples are trypsin like (positively charged residues Lys/Arg preferred at P1), elastase like (small hydrophobic residues Ala/Val at P1) and chymotrypsin like (large hydrophobic residues Phe/Tyr/Leu/Trp at P1). X-ray crystal structural data for the interactions of serine proteases and inhibitors is available for trypsin, α -chymotrypsin, γ -chymotrypsin, thrombin and human cathepsin G.⁶ The main goal of inhibitor design is to synthesise potent inhibitors that maximise selectivity for closely related proteases. Therefore the inhibitor should have the ability to inhibit only one protease in a mixture and such inhibitors should have an inhibition rate constant for the protease of one thousand fold less than for any other protease in the mixture.

Thrombin is a trypsin like serine protease that plays a central role in haemostasis and blood coagulation.¹² Thrombin hydrolyses the blood factors V, VII, XII and fibrinogen that generate fibrin.¹³ The polymerisation of fibrin produces the core of a blood clot. Thrombin essentially protects us from bleeding to death but an excess of this protease can lead to undesired thrombosis often causing death from stroke. The substrate pocket SI of thrombin is optimised to recognise an arginine side chain. Argatroban **4** is a potent arginine derivative that inhibits platelet aggregation by clot-associated thrombin.¹⁴ It is a 64:36 mixture of 21-(*R*) and 21-(*S*) diastereomers with the latter being twice as potent as the former in an *in vitro* assay but also less soluble in aqueous buffer. It has been approved for treating peripheral arterial occlusive disease



in Japan. Bristol-Myers Squibb have more recently developed a potent inhibitor of thrombin (BMS 189090) **5**.¹⁵ This was shown to have an IC₅₀ value of 16 nM when assayed against the chromogenic substrate S-2238. The crystal structure of thrombin complexed with **5** is shown in

Figure 1.8. It can be seen that the inhibitor binds in an antiparallel fashion to thrombin. BMS 189090 has also been shown to be an effective inhibitor in protecting mice from thrombin-induced lethality and in inhibiting arterial and venous thrombosis in rats. The administration of a 0.5 mg/kg dose resulted in almost complete inhibition of venous thrombosis.

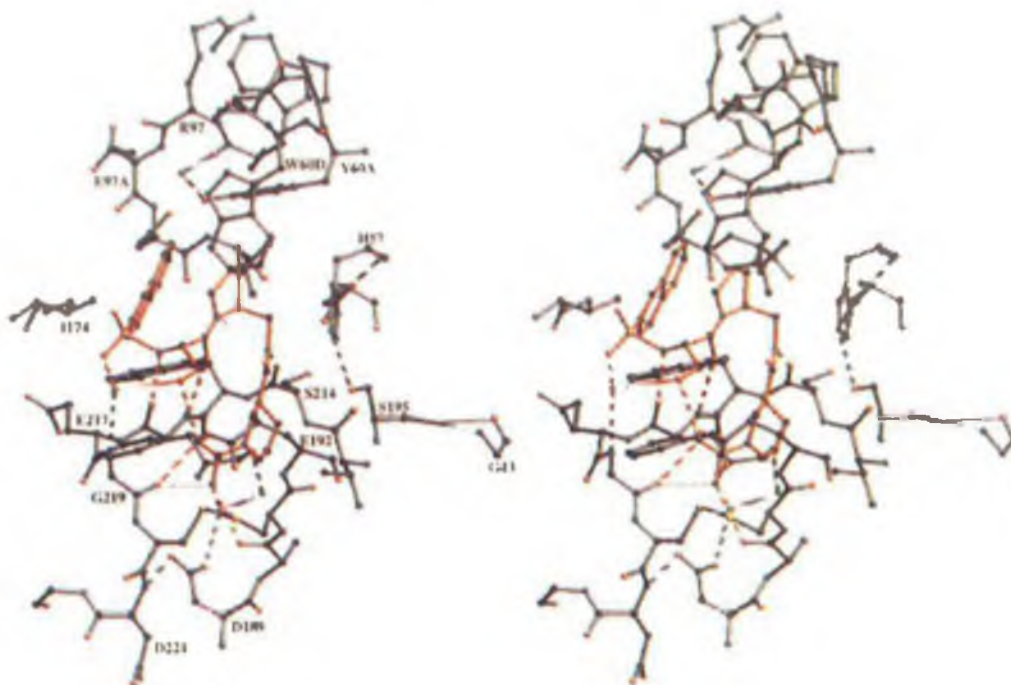
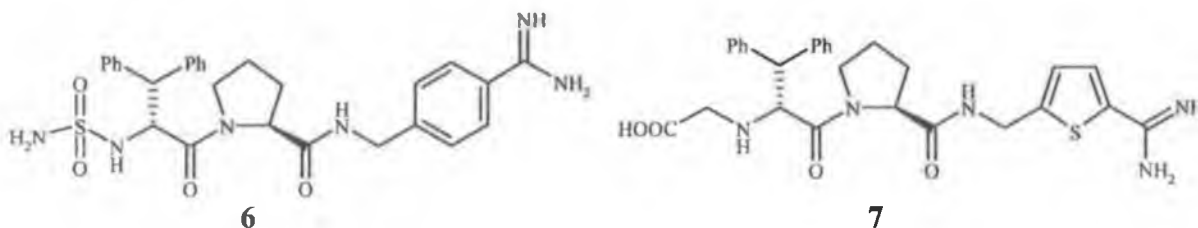


Figure 1.8 Three dimensional structure of thrombin complexed with compound **5** showing the bound confirmation of the inhibitor, the active site residues and solvent molecules in the active site.¹⁶

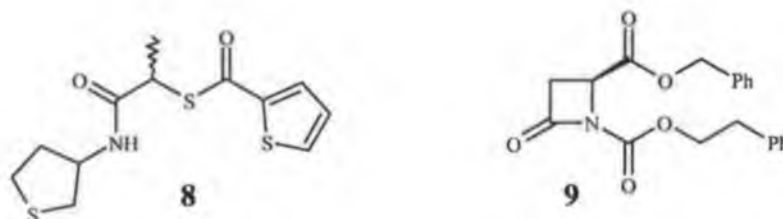
A potent orally active inhibitor of thrombin has been recently developed by Lee *et al.*¹⁷ This highly potent diphenylalanine derivative **7** ($K_i = 0.015$ nM) is based on an optimised highly efficient thrombin inhibitor **6**. Although this gave potent inhibition with a K_i value of 3 pM *in vitro*, clinical trials revealed a short duration of action and poor bioavailability. Optimisation of this derivative resulted in potent inhibition being achieved by the incorporation of a thiophenamidine in the P1 position. Although the inhibitory potency of **7** was slightly less than **6** the bioavailability of **7** was significantly superior with a maximum concentration of 3.8 $\mu\text{g/ml}$ recorded after oral dosage. **7** was also shown to be highly selective when assayed against other

serine proteases such as factor Xa, trypsin, and plasmin. Compound 7 has been recently selected for preclinical and clinical development.



Elastase is a serine protease implicated in cystic fibrosis and chronic bronchitis.¹⁸ Endogenous inhibitors such as the secretory leukocyte protease inhibitors tightly regulate elastase activity but an imbalance between proteases and antiproteases can lead to the degradation of healthy tissue and disease development. The inhibition of elastase has led to the development of numerous therapeutic agents. The cyclic thiol MR 889 **8** is in clinical evaluation for the treatment of chronic obstructive pulmonary disease (COPD).¹⁹ It is a reversible, slow binding inhibitor with specific activity towards neutrophil elastase ($K_i = 1.38 \mu\text{M}$) and may be given to COPD patients safely for a period of four weeks without any major side effects.

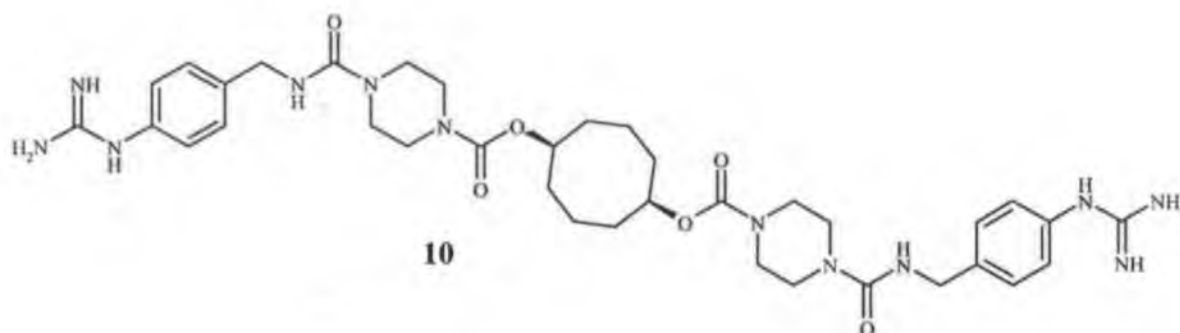
Gerard and co-workers have synthesised the β -lactam **9**. This has been shown to promote suicide inhibition of porcine pancreatic elastase. It is a potent reversible inhibitor ($K_i = 10 \mu\text{M}$) and only one in a series of β -lactams that have been developed as potential protease inhibitors.²⁰ Baylac *et al* have recently reported that the natural fragrant extracts of aromatic plants have the ability to successfully inhibit human leukocyte elastase.²¹ The most potent



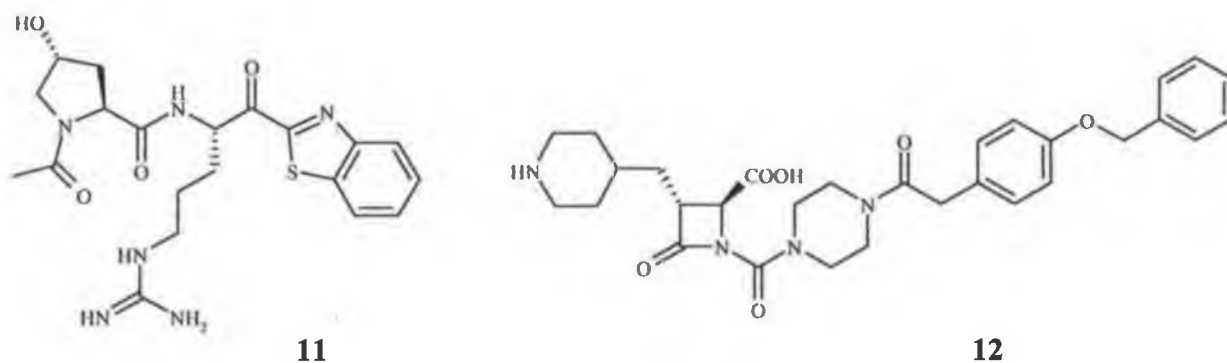
fragrant was shown to be the spice known as turmeric that was once used in the treatment of jaundice.²² This novel method of inhibition offers an alternative therapeutic route to the treatment of various diseases.

Tryptase is a trypsin like serine protease that has been implicated as a mediator in various inflammatory and allergic conditions such as conjunctivitis and asthma.²³ It is estimated that over

100 million people will suffer from asthma by the end of this decade. To lessen the severity of asthma, therapeutics attacking the underlying inflammatory processes are being investigated.²⁴ Tryptase is produced by mast cells and accounts for 20-25% of the total lung and skin mast cell protein. The S1 pocket of tryptase is large enough to accommodate a range of simple P1 nitrogen bases. The crystal structure of the enzyme has indicated preference for simple aromatic and aliphatic nitrogen bases at P1.²⁵ A piperazine based derivative **10** is a very selective and potent inhibitor of tryptase.²⁶ Compound **10** has a K_i value of 70 pM against tryptase and selectivity over trypsin and thrombin close to 10^5 fold. These dibasic inhibitors are C_2 symmetric with one end of the molecule fitting the S1 pocket with the other end of the molecule potentially docking into another S1 pocket of an adjacent tryptase monomer.



More recently Johnson and Johnson have developed potent selective inhibitors of human mast cell tryptase. The benzothiazole ketone derivative **11** has been reported to have a K_i value of 10 nM against tryptase and 8.1 nM against trypsin.²⁷ Although this compound potently inhibits trypsin it is highly selective against other serine proteases such as kallikrein, plasmin and thrombin. The benzothiazole derivatives were shown to be up to eight times more potent than their thiazole analogues. The success of aerosol administration of **11** into the sheep model of



asthma has led to the advancement of this compound into clinical trials. Bristol Myers Squibb have developed the piperidine derivative **12** as a potent and selective inhibitor of tryptase.²⁸ It has an IC₅₀ value of 1 nM against tryptase and 440 nM against trypsin. Although the presence of aromatic rings adjacent to the amide bond failed to improve the activity of **12** it managed to increase selectivity substantially.

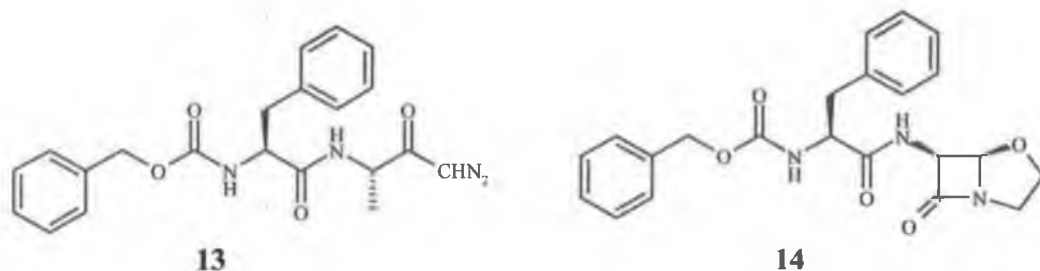
Serine protease inhibitors frequently have 3-5 amino acid residues and thus interact with only a small region of the enzyme. This leads to the increased problem of selectivity. For the development of therapeutically useful serine protease inhibitors, it has generally been accepted that reversible inhibitors are preferred over irreversible ones. Irreversible inhibitors would be expected to covalently bind with nucleophiles en route to the intended target most likely resulting in toxic side effects. Reversible transition state analogues usually possess an electrophilic isostere located at the C-terminus of P1 residues. Examples include aldehydes, boronic acids and activated ketones. The presence of a reactive electrophilic site in many reversible inhibitors will undoubtedly lead to pharmacological problems when administered to humans. For example, peptidyl aldehydes are easily oxidised to carboxylic acids and are prone to racemisation in the presence of acid or base if a chiral centre is present in the molecule.

1.1.7 Cysteine protease inhibitors.

Cysteine proteases exist in three structurally distinct classes that are either papain like (*eg* cathepsins), ICE (interleukin-1 converting enzyme) like (caspases) or picorna-viral (similar to serine proteases with cysteine replacing serine). Cathepsins have historically been the most studied cysteine proteases. Cysteine proteases hydrolyse amide bonds in much the same manner as serine proteases except for the fact that the thiol moiety of a cysteine residue is involved in catalysis compared to the hydroxy nucleophile of a serine residue in serine proteases. The biggest problem encountered in the design of cysteine protease inhibitors is the similarity in their substrate affinities and proteolytic mechanisms with serine proteases.

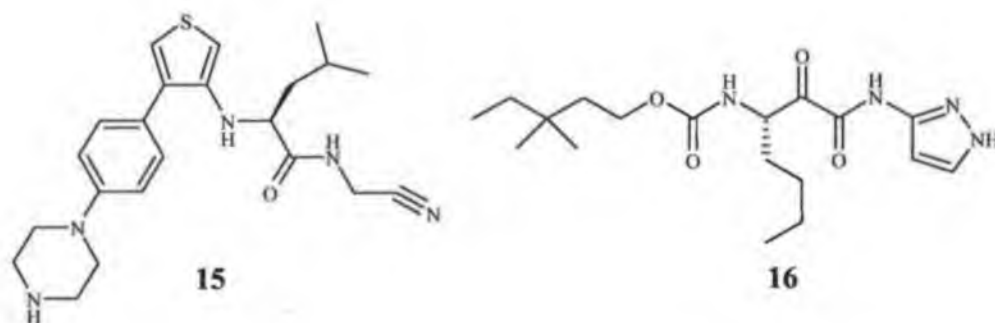
The term “cathepsin” was introduced by Willstätter and Bamann in 1929 to describe a protease that is active at acidic pH but can be differentiated from pepsin.⁵ Cathepsin A, B and C have been suggested as the intracellular counterparts of pepsin, trypsin and α -chymotrypsin.²⁹ Cathepsin inhibitors are promising therapeutics for the treatment of diseases characterized by excessive bone loss such as osteoporosis and inflammatory and traumatic processes such as

rheumatoid arthritis and cancer metastasis.³⁰ Among the earliest reported inhibitors were peptidyl diazomethyl ketones and aldehydes.



Diazomethyl ketones inactivate cathepsin B by alkylation of the active site cysteine residue. The most effective example is **13**. It has been reported to inactivate cathepsin B and C effectively.³¹ More recently, Zhou *et al* have synthesised a series of 6-substituted amino-4-oxa-1-azabicyclo[3,2,0]heptan-7-one derivatives **14** as cathepsin B protease inhibitors.³² Compound **14** was found to have an IC_{50} value of 1.76 μ M against cathepsin B protease. Molecular modelling studies carried out suggested that the 1-N atom in **14** can be involved in hydrogen bonding to the protonated histidine in the active site of cysteine proteases therefore acting as an effective inhibitor. Unfortunately **14** was also found to be extremely potent against cathepsin L, K and S with nanomolar inhibition often occurring.

Cathepsin K is a cysteine protease abundant in osteoclasts and is involved in the degradation of various bone proteins.³³ The peptidyl nitrile **15** is a potent inhibitor of cathepsin K and significantly reduces bone loss.³⁴ The leucine glycine nitrile scaffold of this inhibitor has previously been a successful design feature of potent cysteine protease inhibitors. Compound **15**



has an IC_{50} value of 0.2 nM against human cathepsin K and is shown to substantially reduce bone resorption at a concentration of 10 nM. GlaxoSmithKline have recently developed a series of highly potent ketoamide based inhibitors of cathepsin K.³⁵ Compound **16** was the most potent derivative with an IC_{50} value of 1.6 nM. Unfortunately this compound is not very selective with

cathepsin S also undergoing inhibition with an IC_{50} value of 2.56 nM. The key step in the synthesis of this derivative is the preparation of the α -ketoamide from the oxidation of a phosphorus ylide using ozone followed by loss of the nitrile moiety using the Wasserman procedure.³⁶

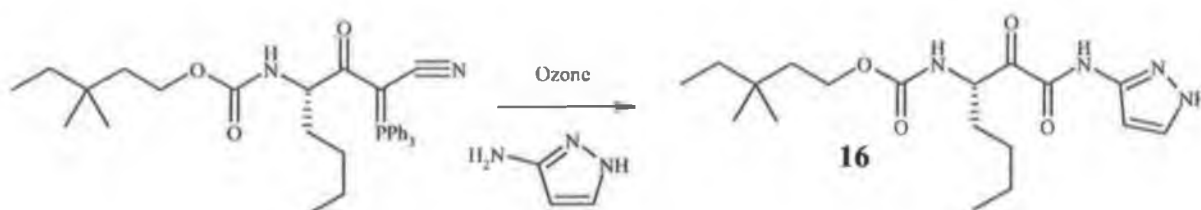
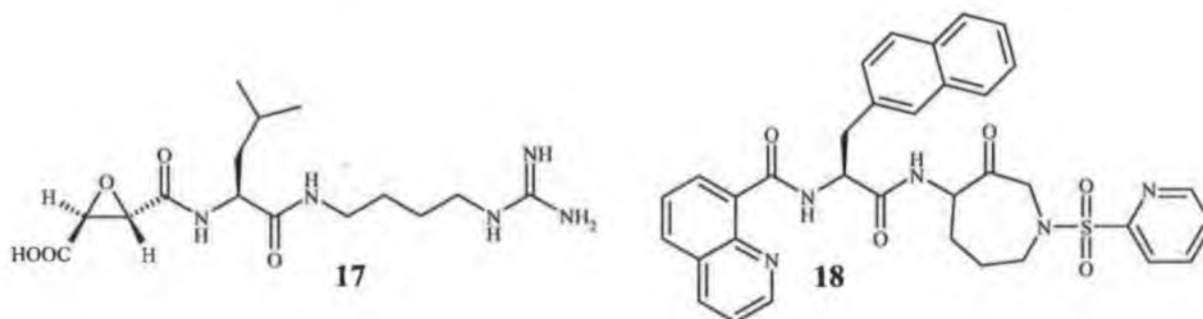


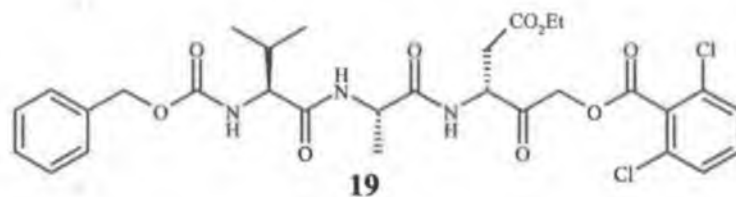
Figure 1.9 Key synthetic step in the synthesis of the GlaxoSmithKline cathepsin K inhibitor **16**

Cathepsin L has been implicated in tumor metastasis with the presence of metastatic human melanoma cells associated with the secretion of a cathepsin L protease.³⁷ E-64 **17** is a naturally occurring cysteine protease inhibitor with high potency against cathepsin B, F, K and L proteases.³⁸ Treatment with the epoxide E-64 inhibits cathepsin L protease in the nanomolar range and offers a potential treatment for metastasis. Lately, the azepanone scaffold has been used in the preparation of cathepsin L inhibitors. The potent inhibitor **18** is shown to be impressively selective over cathepsin K for cathepsin L with 50,000-fold selectivity.³⁹ It has a K_i value of 9.9 μ M against human cathepsin K compared to a K_i value of 503 nM for human cathepsin K.

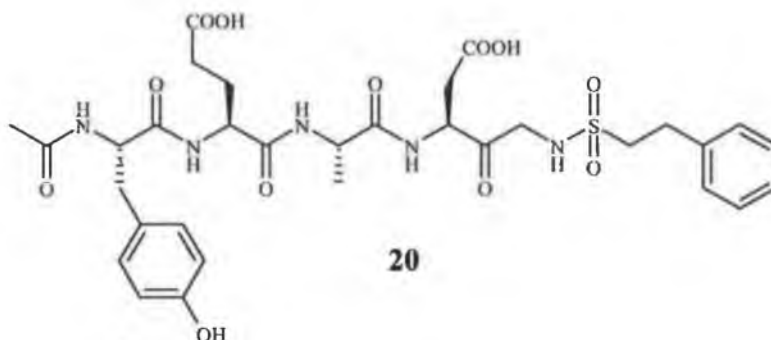


Caspase is a new term given to cysteine endoproteases with absolute specificity for aspartic acid at P1 in their substrates. They also have specificity for the four amino acids to the amino terminal side of the cleavage site. Caspases have become promising therapeutic candidates for the treatment of inflammatory and degenerative diseases such as rheumatoid arthritis, Alzheimer's disease and Parkinson's disease.⁴⁰ The first demonstration of an effective inhibitor in a chronic disease was the prodrug VE-13045 **19**.⁴¹ The aspartyl side chain ester in the

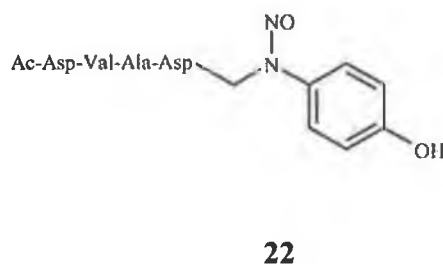
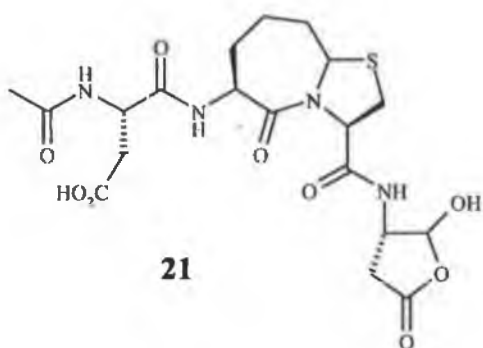
compound is rapidly hydrolysed *in vivo*, yielding a bioactive molecule based on the Cbz-Val-Ala-Asp template. The tripeptidyl derivative **19** was shown to reduce inflammation and progression of arthritis when administered to mice with established disease. Pfizer have recently



developed a potent caspase-1 inhibitor based on an alanyl-aspartyl sulphonamide scaffold.⁴² This derivative **20** has an IC_{50} value of 3.4 nM against caspase-1 and the presence of an aspartic acid residue at the P1 position along with the sulphonamide moiety is crucial for potent inhibition.

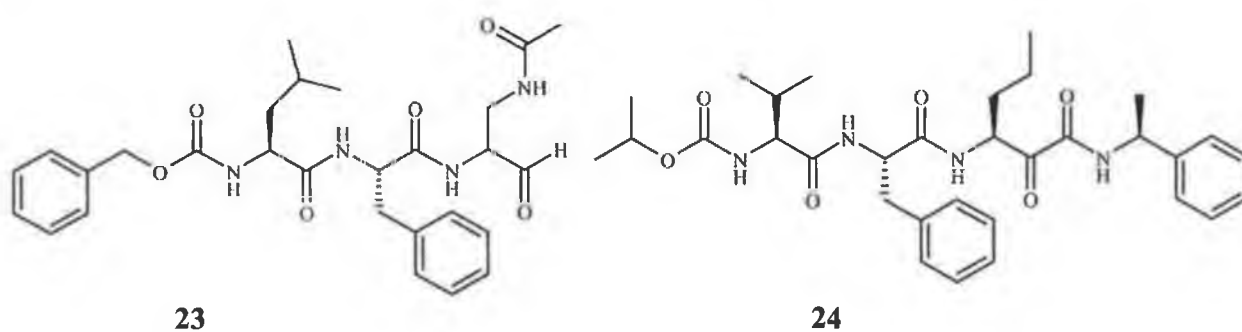


Caspase-3 is believed to be a key component in apoptosis and is involved in neurodegenerative diseases such as Alzheimer's, Parkinson's and Huntington's disease.⁴³ It has been well publicised that an aspartyl residue in the P4 position is crucial for caspase-3 inhibition. The potent caspase-3 inhibitor **21** has an IC_{50} value of 18 nM against caspase-3.⁴⁴ This conformationally constrained bicyclic caspase inhibitor is a potent caspase-3 inhibitor due to the aspartic acid residue present at P4. It has selectivity in the region of 577 fold relative to caspase-1. Researchers at Wayne State University, Detroit have recently reported structure-based design of irreversible, non-peptidyl inhibitors of caspase 3. The *N*-nitroso aniline **22** was designed as a



novel irreversible inhibitor.⁴⁵ Inhibition takes place by *S*-nitrosylation of the active site cysteine thiol moiety. The nitroso aniline moiety had very weak inhibitory activity by itself. Incorporation of a peptide analogue to a substrate of caspase-3 furnished a more potent inhibitor. Although the inhibition of caspase-3 was not remarkable these nitric oxide (NO) donating compounds provide a novel scaffold for the design of inhibitors to specifically deliver NO to the enzyme.

The rhinovirus 3C protease is a member of the picornaviral cysteine proteases. Human rhinoviruses (HRV) are the viruses that are responsible for the common cold. Since they occur in over one hundred different variants, the development of a vaccine seems unlikely, whereas the inhibition of their component cysteine proteases 2A and 3C that are essential for replication represents a possible strategy against the common cold. Rhinovirus 3C protease is a 20 kDa picornaviral protease that selectively catalyses the hydrolysis of glutamine-glycine peptide bonds. Glutamine based inhibitors have limitations due to the fact that they exist predominantly in the cyclic hemiaminal form. The design and synthesis of isosteres of the glutamine side chain are a possible method of potent inhibition. Compound **23** has been reported to inhibit the replication of several different HRV serotypes.⁴⁶ **23** has a K_i value of 6 nM against HRV 3C protease. This compound was able to reduce the levels of infectious virus even when administered late in the HRV life cycle. More recently Eli Lilly have described the synthesis and inhibitory potency of a series of tripeptidyl α -ketoamide derivatives.⁴⁷ Compound **24** was the most potent derivative with an IC_{50} value of 170 nM against HRV-14. This noncytotoxic compound also exhibits potent antiviral activity with an EC_{50} of 0.85 μ M against HRV-14.

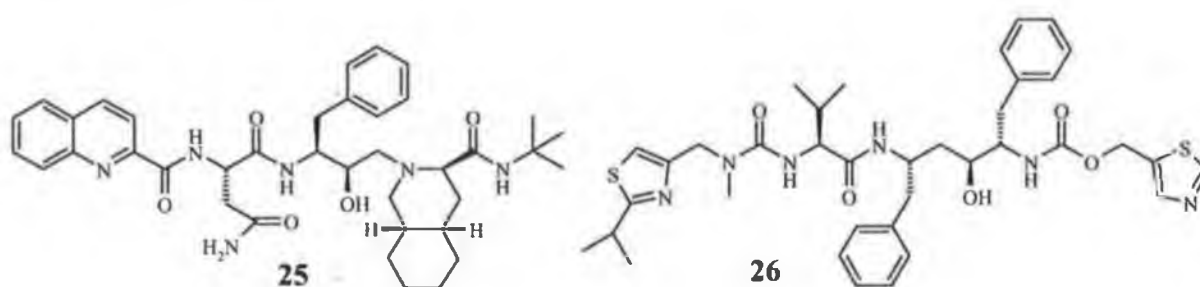


To date there are few electrophilic isosteres appropriate for developing selective, reversible inhibitors of cysteine proteases. This may explain why very few cysteine protease inhibitors have advanced to clinical trials. *C*-terminal aldehydes and ketones, which react with the active site cysteine to form reversible thioacetal transition state analogues, are the most used isosteres for developing reversible cysteine protease inhibitors. The main problem with aldehyde

isosteres is the fact that they are not very selective inhibitors. In contrast to this there have been many functional groups capable of irreversibly alkylating the active site cysteine incorporated into peptides including epoxides, nitriles and diazomethyl ketones. These functional groups are activated electrophiles that are generally quite selective for cysteine versus serine proteases. To date the majority of these compounds are still too reactive to various nucleophiles in the body. These concerns have severely limited the development of such irreversible inhibitors as therapeutic agents. It remains to be seen whether electrophilic analogues will provide irreversible cysteine inhibitors with the pharmacokinetic and pharmacological profiles required of therapeutic agents in the future.

1.1.8 Aspartic acid protease inhibitors.

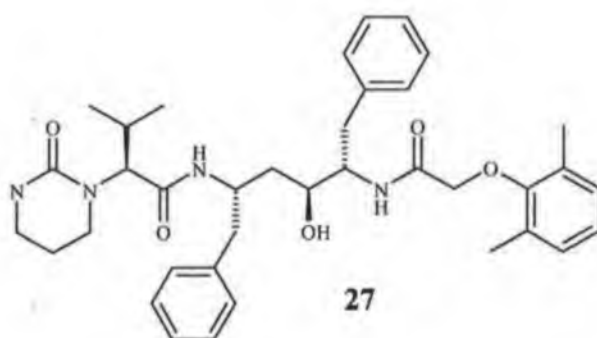
Aspartic proteases generally bind 6-10 amino acid residues of their polypeptide substrates and are typically processed with the aid of two catalytic aspartic acid residues in the active site. There is usually considerable scope for building efficient inhibitors for a particular aspartic protease by taking advantage of the numerous interactions on both sides of its scissile amide bond. Various aspartic proteases also contain one or more flaps that close down on top of the inhibitor further adding to inhibitor-protease interactions and increasing the basis for selectivity. The general acid-base mechanism that is considered most likely for peptide hydrolysis catalysed by aspartic proteases involves the scissile amide bond undergoing nucleophilic attack by a water molecule which is itself activated by a deprotonated aspartic acid residue.



The number of people living with HIV/AIDS is estimated at 38 million and approximately 3 million AIDS deaths were recorded in 2003.⁴⁸ The virally encoded protease of the human immunodeficiency virus (HIV-1 protease) has proved to be an attractive drug target due to its essential role in the replicative cycle of HIV and its inactivation has led to the formation of immature and non-infectious viral serotypes.⁴⁹ Several low molecular weight inhibitors of HIV-1 protease are now administered clinically including saquinavir **25** and

ritonavir **26**.⁵⁰ These are among the first successful examples of receptor-structure based designer drugs and were developed using structures of compounds bound in the active site of HIV-1 protease and with the knowledge of inhibitors of other aspartic acid proteases *e.g.* renin. All HIV-1 protease inhibitors developed so far target the active site substrate binding groove of the homodimeric enzyme, a long cylindrical cavity that binds 6-7 amino acids *via* ionic, van der Waals or hydrogen bonding interactions.⁵¹ Two catalytic aspartic acid residues present at the centre of this cavity promote amide bond hydrolysis.

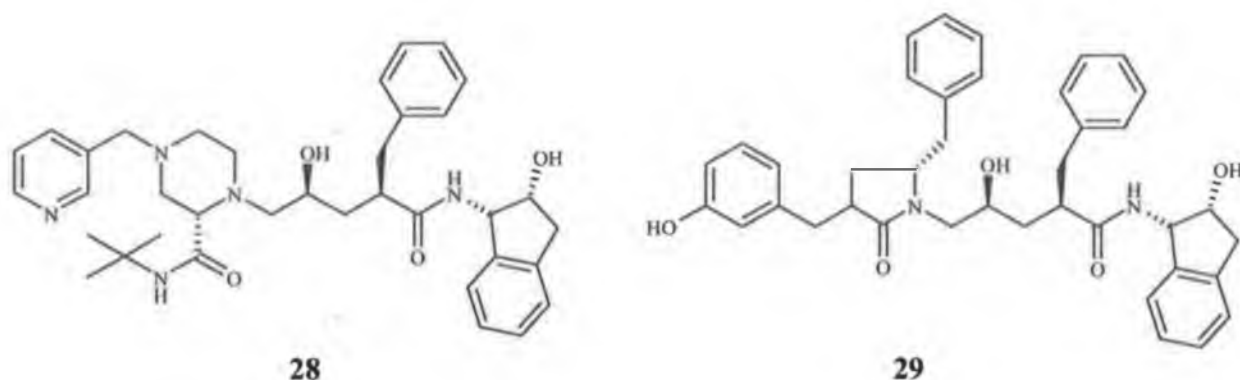
Saquinavir became the first HIV protease inhibitor to be approved for human use in 1996 despite low oral bioavailability due to poor adsorption and extensive first pass degradation by cytochrome P450.⁵⁰ It is generally administered in combination with nucleoside analogues for the treatment of advanced HIV infection and is active in cell culture against both HIV-1 and



HIV-2 viruses. The most common side effects experienced with **25** are gastrointestinal including diarrhoea and nausea. Ritonavir was approved in February 1996 for use in combination with nucleosides or as monotherapy for the treatment of HIV infection. **26** is metabolised primarily through cytochrome P4503A and is considered both as a potent inhibitor and an inducer of the cytochrome P450 metabolic pathway.⁵⁰ The most frequently reported adverse effects in 1,140 patients who received ritonavir included nausea and vomiting. The addition of ritonavir to a saquinavir course of therapy boosts levels of saquinavir by 20 fold based on ritonavir's potent inhibition of P4503A. Doses of both drugs can be reduced thereby potentially decreasing the side effects of both inhibitors.

Viral resistance to monotherapy with any of these drugs is a significant problem. Serial passages of HIV-1 *in vitro* in the presence of increasing concentrations of a protease inhibitor cause rapid emergence of drug resistant viral strains of HIV-1. Resistance is due to amino acid substitutions in the protease. However, cross resistance is not always observed for inhibitor

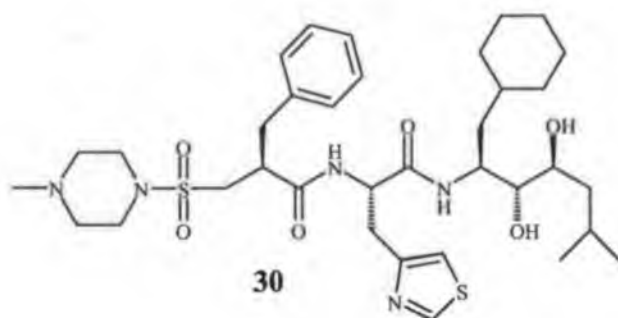
cocktails so HIV patients who experience clinical failure with one protease inhibitor may still benefit from another protease inhibitor.



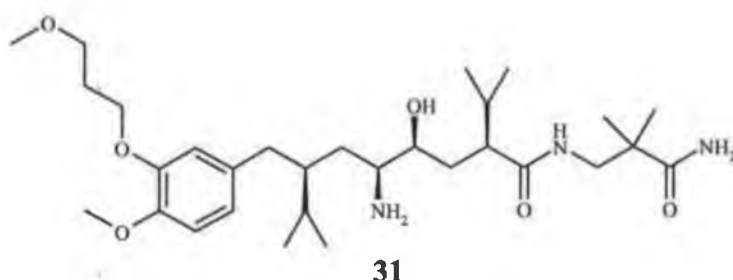
The HIV inhibitor Lopanavir **27** is the antiviral component of Kaletra™ (approved by the FDA in September 2000) that has been approved as a HIV protease inhibitor for the treatment of HIV infection.⁵² **27** possesses high potency against wild type and mutant HIV proteases with K_i values ranging from 1.3-28 pM.⁵³ Lopanavir also exhibits potent antiviral activity with an EC_{50} value of 100 nM recorded. The core unit of **27** is identical to that of ritonavir. The two benzyl groups at P1 and P1' are believed to be essential for efficient inhibition. GlaxoSmithKline have recently developed a series of pyrrolidone based derivatives as potent inhibitors of HIV-1 protease.⁵⁴ The inhibitors incorporate the P1'-P2' scaffold of the approved HIV drug Indinavir **28**. The phenolic derivative **29** was reported to have a K_i value of 0.05 nM against the HIV-1 protease compared to 0.07 nM for Indinavir. It also has increased water solubility due to the presence of the hydroxy group at the *meta* position. The majority of HIV protease inhibitors to date are based on the replacement of the scissile bond with non-hydrolysable isosteres. The peptidic nature of these derivatives limits their oral bioavailability and a short plasma half-life is often observed. Despite the success of the available inhibitors, viral resistance and cost of synthesis remains the main problems facing the inhibition of this fatal disease.

The aspartic acid protease renin is involved in the rate limiting first step of the renin-angiotensin system. Due to their specificity, renin inhibitors are antihypertensive agents similar in action to ACE (Angiotensin Converting Enzyme) inhibitors but free of some side effects associated with ACE administration. Zankiren **30** was the first peptidic renin inhibitor with 53% oral absorption.⁵⁵ It is also a potent inhibitor of human plasma renin at pH 7.4. A 10 mg/Kg intraduodenal dose in sodium depleted monkey's reduced mean arterial blood pressure by 37%

for 2 hours. Zankiren **30** has also been shown to reduce the incidence of dry cough associated with ACE treatment. Renin inhibitors have mainly been developed by modifying substrate fragments from the angiotensinogen cleavage site but their clinical progress has been hampered by their peptidic character that confers low stability and poor oral availability in humans. Another hurdle has been the high cost of production compared with antihypertensives such as ACE inhibitors. Renin inhibitors generally need to interact with 5 subsites (S4-S1') of the enzyme to bind tightly and selectively compared with only 3 for ACE inhibitors. Consequently, renin inhibitors tend to have a higher molecular weight, have more stereocentres and are thus more expensive to manufacture. Several renin inhibitors with low molecular weight, less peptidic character and improved oral bioavailability have emerged.

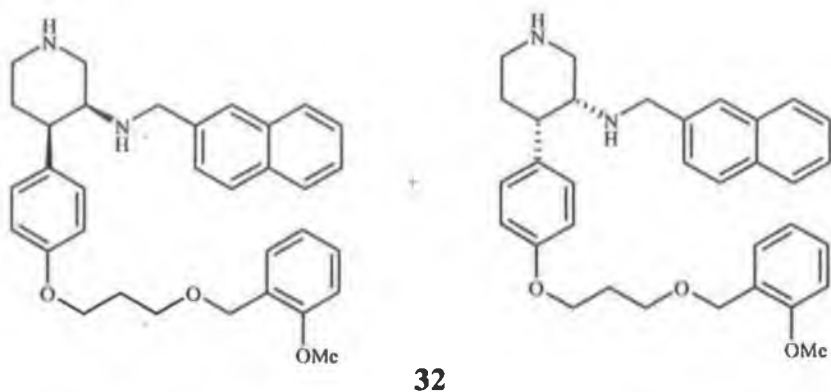


Aliskiren **31**, an orally active renin inhibitor has been shown to inhibit the production of angiotensin I and II.⁵⁶ It decreases blood pressure in hypertensive patients at daily doses of 75 and 150 mg. Exploratory studies testing the efficiency and safety of this renin inhibitor in patients with renal disease and congestive heart failure are currently underway. Pfizer have recently reported the synthesis of a series of non-peptidic *cis*-disubstituted amino-aryl-piperidine based renin inhibitors.⁵⁷ The racemic mixture **32** has IC₅₀ value of 61 nM against human renin.

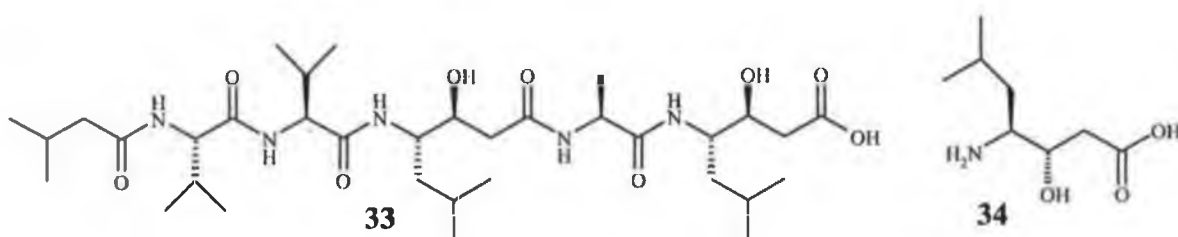


This compound is characterised by the *cis* orientation of the two stereocenters on the amino-aryl-piperidine template. It was also shown to have *in vivo* antihypertensive activity after oral dosage to mice (30 mg/kg) gave peak antihypertensive activity one and a half hours post dose.

Unfortunately this compound suffers from submicromolar interactions with cytochrome P 450 isoenzymes. This limits its potential for further development although these compounds can be used as a starting point for second generation renin inhibitors.



Pepstatin **33** is a naturally occurring inhibitor isolated by Umezawa *et al*, and provides a good example of the information that can be gained from the detailed study of a naturally occurring inhibitor by a variety of physical methods.⁵⁸ Pepstatin (Iva-Val-Val-Sta-Ala-Sta) which contains the novel amino acid statine **34** [(3*S*,4*S*)-4-amino-3-hydroxy-6-methyl heptanoic acid] inhibits most aspartic proteases except for renin. Existing data indicates that the (3*S*)-hydroxyl group is needed for maximal inhibition. Thus pepstatin analogues lacking a pro-(*S*) C-3



hydroxyl group are much weaker inhibitors of aspartic proteases than inhibitors containing the pro-(*S*) C-3 hydroxyl group found in natural statine.⁵⁹ The structure of statine provides an isosteric replacement for a dipeptidic unit. The structures of statine and the tetrahedral intermediate for amide hydrolysis illustrates that statine can be isosteric with the tetrahedral intermediate only from C3 through C7. Statine is either 2 atoms too long to be isosteric with a normal α -amino acid or one atom short to be isosteric with a dipeptide.

The majority of aspartic protease inhibitors developed to date bind to their target enzyme through non-covalent interactions. These compounds are therefore reversible inhibitors of proteases and inhibition relies on the enzyme having very much higher affinity for the inhibitor

than its natural substrate. High affinity for any particular aspartic acid protease has been achieved by trying to maximise the number of non-covalent interactions that the inhibitor makes with the enzyme. One approach that has proved successful is the introduction of a transition state isostere that can mimic the tetrahedral transition state of amide bond hydrolysis. It has been suggested that stable structures which can resemble the transition state for an enzyme reaction, will be bound more tightly than the substrate for the enzyme catalysed reaction. Studies carried out with pepstatin showed that increased affinity due to an isostere can be as great as 10^4 fold and is not only due to mimicry of the transition state of amide hydrolysis but also due to the displacement of the catalytic water molecule hydrogen bonded to the catalytic aspartic acid residues.

1.1.9 Metalloprotease inhibitors.

Metalloproteases like the aspartic acid proteases do not form covalent intermediates but instead utilize coordination to a metal center to achieve their catalytic effect of hydrolyzing peptide bonds.² All known metalloproteases to date use a zinc atom to effect amide bond hydrolysis but theoretically the use of metals such as nickel and copper could be feasible. The currently accepted catalytic mechanism involves a Zn^{2+} ion tetrahedrally coordinated to three donor groups from the enzyme and a water molecule. This water molecule is also hydrogen bonded to the carboxylic side chain of a glutamic acid and is therefore activated for nucleophilic attack as shown in Figure 1.10a. The coordination of the carbonyl moiety of the scissile amide bond to zinc is followed by nucleophilic attack by the water molecule with a proton transfer to the carboxylate giving a tetrahedral zinc intermediate (Figure 1.10b). The transfer of a proton from glutamic acid to the amide nitrogen is followed by collapse of the tetrahedral intermediate with the generation of a salt bridge between glutamic acid and the free amine of the cleaved substrate as shown in Figure 1.10c. The design of inhibitors has focused on attempts to bind the catalytic zinc atom. Synthetic inhibitors generally contain a moiety such as a thiol, carboxylic acid or hydroxamic acid moiety as the warhead, capable of coordinating to a zinc atom attached to a series of other groups that are designed to fit the specificity pockets of a particular protease.⁶⁰ This hypothesis of inhibition has turned out to be very successful with numerous potent and selective inhibitors of metalloproteases being approved for clinical administration.

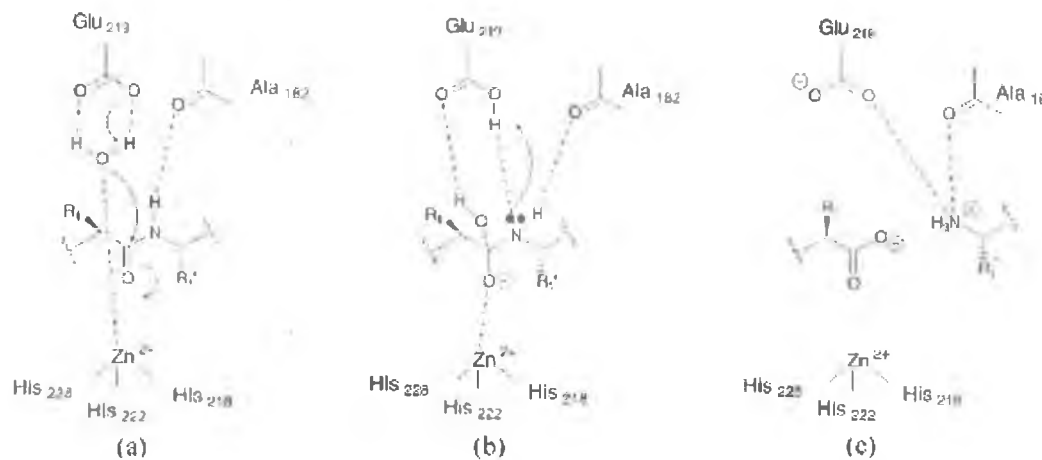
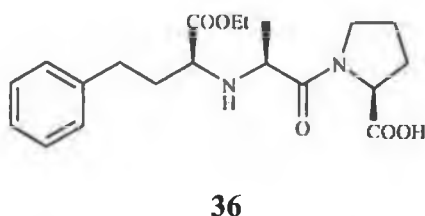
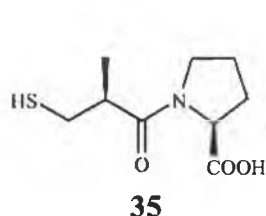


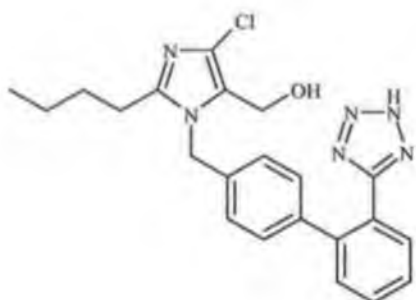
Figure 1.10 Proposed catalytic mechanism for the matrix metalloproteases.

Angiotensin converting enzyme (ACE) is a zinc metalloprotease that is expressed in many tissues including the heart, the lungs and several regions of the brain. ACE has received considerable attention due to its pivotal role in blood regulation by catalyzing the proteolysis of angiotensin I to the vasopressor angiotensin II.⁶¹ The inhibition of ACE decreases levels of angiotensin II in the body leading to a decrease in blood pressure.⁶² Angiotensin converting enzyme is one of the most studied drug design targets and inhibitor development has been extensively documented. Many ACE inhibitors have been approved for therapeutic use including

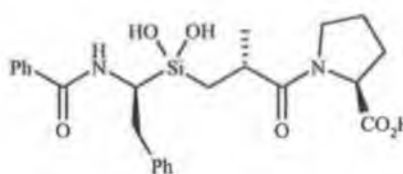


captopril **35** and enalapril **36**.⁶³ These inhibitors are not only useful for the treatment of hypertension but also for congestal heart failure and renal protection. These compounds are small, low molecular weight derivatives that generally only occupy the S1, S1' and S2' subsites of ACE. They all employ a chelating group that binds to the active site zinc resulting in high inhibitory potency and selectivity. ACE is a nonspecific enzyme that cleaves not only angiotensin converting enzyme I but also bradykinin and other peptide hormones. The inhibition of ACE leads to side effects such as cough and skin rash. These side effects are believed to be associated with a buildup of bradykinin caused by its inhibition by ACE.⁶⁴ In recent times, low molecular weight, lipophilic inhibitors of ACE have been developed that are devoid of side

effects. A prime example is that of losartan **37**.⁶⁵ Losartan is a nonpeptidyl angiotensin II receptor antagonist and differs from ACE inhibitors by producing direct antagonism of the angiotensin II receptor. It is beneficially devoid of side effects such as cough associated with other ACE inhibitors. This derivative may have the potential to compete effectively with ACE inhibitors as drugs of choice for the treatment of hypertension in the market place.

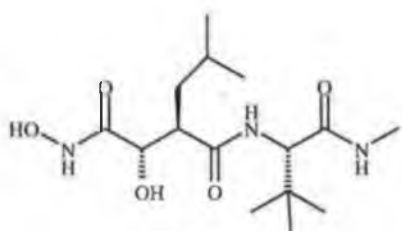


37

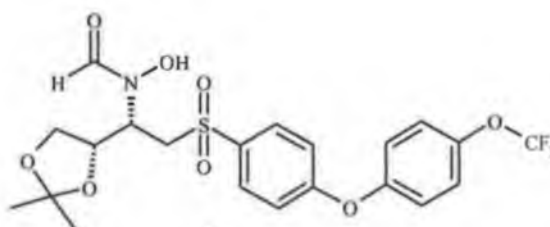


38

Kim *et al* have recently described the synthesis of silanediol peptidomimetics as ACE inhibitors.⁶⁶ These non-hydrolysable mimics act as transition state analogues replacing the scissile amide carbonyl of the protease substrate. The most potent derivative **38** was shown to have an IC_{50} value of 72 nM against angiotensin converting enzyme from rabbit lung. This was almost fifty times more potent than the carboxy analogue.



39



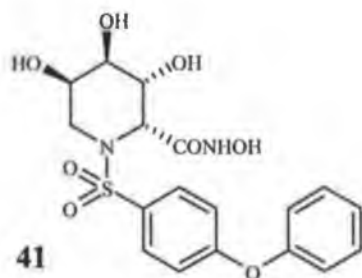
40

Matrix metalloproteases (MMP) are a family of proteases that were first described in 1962 when Gross and Lapiere identified an enzyme from a tadpole tail with proteolytic action capable of attacking collagen.⁶⁷ MMP's were initially characterized by their ability to degrade components of the extracellular matrix. These enzymes require a zinc ion at their active site and are inhibited by zinc and calcium chelating agents. Although matrix metalloproteases are inhibited naturally by locally produced tissue inhibitors of metalloproteases (TIMP), an imbalance caused by overexpression and activation of matrix metalloproteases results in tissue degradation. It is thought that matrix metalloproteases are important in the growth and spread of

malignant tumors and development of chronic diseases such as multiple sclerosis and arthritis.⁶⁸ For these reasons matrix metalloproteases are considered to be attractive targets for inhibitor development and the treatment of these disorders.

Various matrix metalloprotease inhibitors are undergoing evaluation in clinical trials for the treatment of cancer, arthritis and multiple sclerosis. Marimastat **39** is the most notably advanced and is a broad spectrum metalloprotease inhibitor having a low nanomolar activity against MMP-1 with an IC_{50} value of 10 nM recorded.⁶⁹ This peptidomimetic is the end result of years of substrate based inhibitor design based on the Gly-Ile and Gly-Leu collagenase (MMP-1) cleavage sites. The most important feature of these inhibitors is the zinc binding component, a terminal hydroxamate proving to be the most effective ligand for enhancing the potency. One of the main side effects of **39** is the onset of joint toxicity occurring predominantly in the upper limbs.

As a means of avoiding these side effects, Wada *et al* have recently synthesised a series of highly selective MMP inhibitors as antitumor agents.⁷⁰ Compound **40** has been shown to be the most potent of these inhibitors with an IC_{50} value of 0.50 nM recorded against MMP-9. It possesses greater selectivity than marimastat and has pharmacokinetics consistent with once a day dosage. Compound **40** exhibits significant inhibition of tumour growth in animal cancer models and to date is shown to have considerably less side effects than **39**. It is currently undergoing phase I clinical trials in cancer patients. More recently Moriyama *et al* have reported the synthesis of azasugar based MMP inhibitors as antipsoriatic agents.⁷¹ Psoriasis is a complex inflammatory skin disease that affects 2% of the population. Compound **41** gave a K_i value of 5.3 nM against MMP-1. It was shown to suppress psoriasis *in vivo* on a mouse (12-*O*-tetradecanoylphorbol-13-acetate) TPA induced epidermal hyperplasia model at doses between 1 and 100 μ g.



MMP inhibition offers a promising opportunity to develop novel and innovative therapies for many chronic diseases that currently lack effective treatment. Despite the strong strategic position of this class of compounds, only a few MMP inhibitors have entered clinical trials. In general the greatest potency has been obtained by designing inhibitors to interact with at least the S1, S1' and S2' subsites of the enzyme. Oral bioavailability has been the greatest stumbling block for these substrate based inhibitors. Second generation compounds with improved bioavailability and selectivity should accelerate the development of this class of inhibitors.

1.1.10 Fluorine containing protease inhibitors.

The incorporation of a fluorine atom into a drug molecule has been fundamental in the improvement of biological activity. The importance of fluorine substitution in pharmaceutical development is evident in the large number of fluorinated derivatives approved by the FDA for use as anticancer, antiviral, antidepressant and anesthetic agents. There are generally two consequences of introducing fluorine into a drug molecule. Firstly there are the physicochemical properties. Fluorine has the ability to simultaneously modulate electronic, lipophilic and steric parameters that can critically influence the pharmacological properties of a drug molecule. The introduction of a fluorine atom will generally increase lipophilicity, decrease basicity and alter the hydrogen bonding interactions of a molecule. Secondly, there is the influence of fluorine substitution on the biological stability of a drug molecule, *e.g.*, through altering susceptibility to metabolism (Figure 1.11).⁷² Fluorine has been used as a means to developing safer and more reactive pharmaceuticals due to the strength of the carbon-fluorine bond that is very difficult to metabolize so harmful and unproductive side reactions are unlikely to occur.

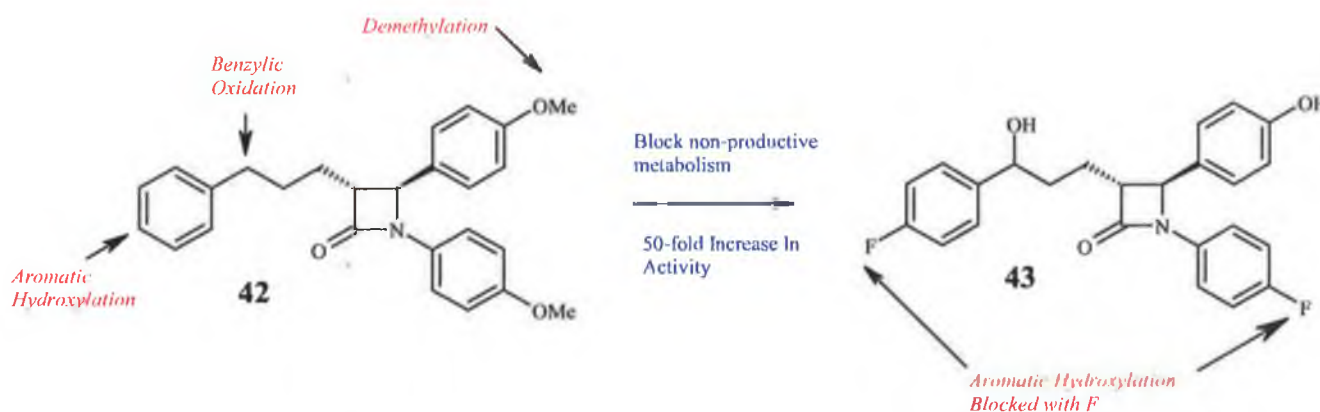
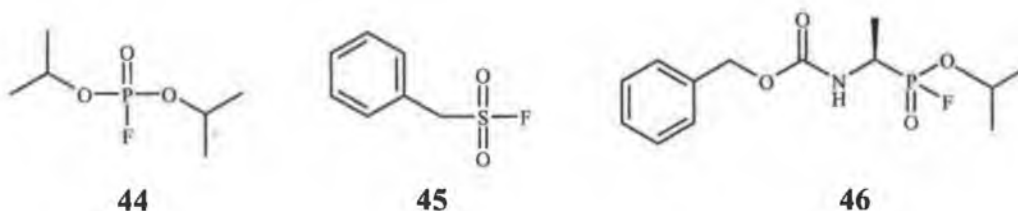


Figure 1.11 Prevention of metabolic deactivation

The lipid lowering agent **43** has been developed as a means of treating hyperlipidemia. Its half life of 22 hours is in part due to the presence of the fluorine atoms that block unfavourable metabolic processes. It is approved by the FDA for combination therapy with statin derivatives for the treatment of hypercholesterolemia.

The Van der Waals radius of the fluorine atom is 1.47 Å. This value is positioned between the values of hydrogen (1.20 Å) and oxygen (1.52 Å) allowing it to mimic a hydroxyl group and to participate in hydrogen bonding interactions. The concept of replacing the hydroxyl moiety of a bioactive molecule with a fluorine atom has been a prevalent method for the enhancement of biological activity. Medicinal chemists have recognised for some time that fluorine and hydroxyl groups are chemical isosteres.⁷³ The introduction of a fluorine atom into a bioactive molecule also provides a marker for ¹⁹F NMR studies where drug-protein interactions can be assessed *in vitro* and *in vivo* due to the absence of fluorine in living tissue.

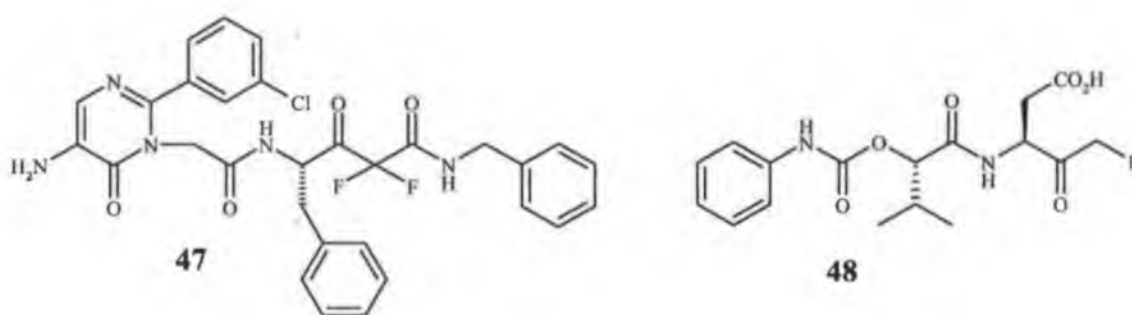
Phosphonyl and sulphonyl fluorides were the first reported fluorine containing protease inhibitors and were developed more than eighty years ago. The inhibitors diisopropylfluorophosphate (DFP) **44** and phenylmethylsulphonyl fluoride (PMSF) **45** are two of the most effective examples of protease inhibitors and are generally associated with serine inhibition.⁷⁴ These inhibitors phosphorylate or sulphonylate the active site serine hydroxy group due to the electrophilicity of the phosphorus or sulphur atom induced by the adjacent fluorine atom. Unfortunately these inhibitors are extremely toxic and suffer poor selectivity with both serine and cysteine proteases. Bartlett *et al* have synthesized increasingly selective phosphonyl fluorides. Compound **46** incorporates peptidyl character as a means of improving the selectivity of a potent phosphonyl fluoride. It is a potent inhibitor of elastase with 6-fold selectivity for elastase over α -chymotrypsin.⁷⁵



The incorporation of fluoromethyl ketone moieties into protease inhibitors has led to the development of potent transition state inhibitors for a variety of proteases including porcine pancreatic elastase and cathepsin B.⁷⁶ The introduction of a fluorine atom into a methyl ketone

creates a highly reactive carbon center that readily undergoes nucleophilic attack. Peptidyl derivatives containing fluoroketones have the ability to be potent inhibitors of proteases due to the vastly increased electrophilic nature of this carbon center. Both di- and trifluoromethyl ketones exist in water almost entirely in the hydrated form and thus it seems likely that fluoro ketones would form a hemiketal at the active site of a serine protease or as it hydrates, bind tightly to both metallo and aspartyl proteases.⁷⁷ In contrast to chloromethyl ketones, the C-F bond in fluoromethyl ketones is much stronger than the C-Cl bond in the chloro analogues. This suggests that fluoromethyl ketones should be much poorer alkylating agents than chloromethyl ketones. This property should reduce the side effects associated with the use of chloromethyl ketones.

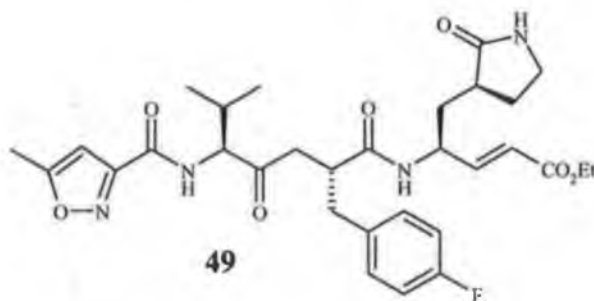
Akahoshi *et al* have developed a series of protease inhibitors incorporating a difluoromethylene ketone.⁷⁸ These derivatives were potent human chymase inhibitors with high enzymatic selectivity and satisfactory metabolic stability. It has previously been reported that the inclusion of a difluoromethyl ketone moiety increased affinity and selectivity for human chymase compared to other chymotrypsin like serine proteases.⁷⁹ The most potent derivative **47** has a K_i value of 2.62 nM against the serine protease human heart chymase and is 1600-fold more selective for this serotype of chymase than rat peritoneal chymase. *In vivo* analysis carried out showed that **47** had satisfactory pharmacokinetics with oral bioavailability of 32% in dogs and 17% in rats. Due to its biological and pharmacokinetic profile this compound is currently being evaluated for its therapeutic potential against chymase induced diseases such as asthma.



More recently Cai *et al* have described a series of dipeptidyl aspartyl fluoromethyl ketone derivatives as broad spectrum inhibitors of the caspases.⁸⁰ Compound **48** was the most potent derivative with an IC₅₀ value of 17 nM against human caspase-3 protease. This compound was also shown to provide 50% cell protection against apoptosis induced by tumour necrosis factor- α

(TNF- α) at a concentration of 0.2 μ M. Unfortunately it was also shown to inhibit caspases 1, 3, 6, 7, 8 and 9 with IC₅₀ values between 11 and 50 nM. However, this compound was selective against non-caspase proteolytic enzymes with 10⁵ selectivity over cathepsin B, calpain-1 and Factor Xa recorded. Compound **48** was also found to be active in a mouse liver apoptosis model. The intravenous administration of **48** at a dosage of 10 mg/kg showed that there was 83% increase in the number of mice surviving after 3 days.

Perhaps the most successful example of a fluorinated protease inhibitor is the tripeptidyl Michael acceptor containing human rhinovirus (HRV) inhibitor RupintrivirTM **49**. RupintrivirTM is a potent irreversible inhibitor of HRV 3C protease with an EC₅₀ value of 5 nM recorded. This compound was a selective inhibitor of HRV 3C protease with no inhibition of serine or cathepsin proteases occurring at a concentration of 10 nM and was shown to be stable in human plasma, dog plasma and α -chymotrypsin with half lives of greater than 60 minutes recorded. This drug is currently in phase three clinical trials for intranasal delivery and was one of the first drugs utilised as a potential inhibitor of the SARS outbreak in 2003.⁸¹



The incorporation of a fluorine atom has been shown to improve bioactivity and has led to development of some of the most successful pharmaceuticals to date. Despite this there are still very few examples of fluorinated protease inhibitors approved for clinical use. The most potent series of derivatives have been based on a fluoromethyl ketone scaffold. Examples of such derivatives have shown potent inhibition of serine and cysteine proteases. They are considerably more stable than their chlorine analogues although their alkylating ability often induces toxic side effects. The introduction of a trifluoromethyl moiety may be a more successful route for the inhibition of nucleophilic proteases given that the steric size of the trifluoromethyl moiety is similar to a chlorine atom and also it has the ability to induce an electrophilic center. The development of potent selective inhibitors such as **49** furnishes optimism for the development of further fluorinated protease inhibitors.

1.1.11 Conclusion

The design and synthesis of protease inhibitors offers the potential for potent and selective chemotherapeutic agents. Historically, the design of protease inhibitors has incorporated highly reactive electrophilic warheads that alkylate, acylate, phosphonylate or sulphonylate the active site residues of serine and cysteine proteases. These first generation inhibitors although very potent were shown to suffer from severe side effects due to their reactivity and poor selectivity due to their lack of peptide character. The design of aspartic acid protease inhibitors has concentrated on the incorporation of transition state isosteres that mimic the tetrahedral transition state of amide bond hydrolysis. This is due to the fact that aspartic acid protease inhibitors bind to their target enzyme through non-covalent interactions. This method of design has been particularly successful with inhibitors of the HIV-1 protease. The replacement of the peptide backbone of peptide inhibitors with peptidomimetics has been successful in improving the bioavailability and stability of aspartic acid protease inhibitors in biological systems. Finally, metalloproteases have been most effectively inhibited by the incorporation of moieties such as thiols and hydroxymates capable of binding to the Zn^{2+} ion. Although potent and selective inhibitors have been developed the majority of these derivatives have suffered from very poor bioavailability. More recently inhibition design has begun to utilise molecular modelling in tandem with the crystal structures of enzyme-inhibitor complexes. These complexes offer a clear picture of how the conformation of the inhibitor is related to the active site of the enzyme and guides the design of future inhibitors. This mechanism of design has been particularly fruitful when used in combination with library screening.

The inhibition of proteases offers great potential for the treatment of various diseases. Unfortunately there are very few inhibitors that have reached the market as drugs. The main problems that are encountered by inhibitors are their lack of selectivity, poor bioavailability and toxicity. The active sites of serine and cysteine proteases are very similar and often a potent inhibitor of a serine protease will also effectively inhibit similar cysteine proteases. The peptide nature of inhibitors limits their bioavailability and toxicity due to reactive warheads incorporated into design is observed. Alternatively, protease inhibition has been extremely successful in the treatment of hypertension, HIV and parasitic diseases. HIV protease inhibitors such as saquinavir and lopinavir have not only revolutionised the treatment of this horrendous disease but have also increased the expectation that potent inhibitors of other proteases will be developed as drugs.

1.2 Cancer and cancer resistance

1.2.1 Introduction

Cancer is a set of diseases characterized by unregulated cell growth leading to invasion of surrounding tissues and metastasis. It is an ancient condition and was known to the early Egyptians. Cancer is a major cause of premature death in the western world second only to heart disease.⁸² It is caused by a variety of factors including smoking, pollution, diet and lifestyle. The best form of treatment is prevention with initiatives such as smoking control and dietary awareness becoming more prevalent. The next best approach is early detection. The smaller the number and less malignant the nature of the cancer cells the greater the probability of finding a cure. Screening programmes are now in place for the early detection of cervical, breast, prostate and colon cancers.

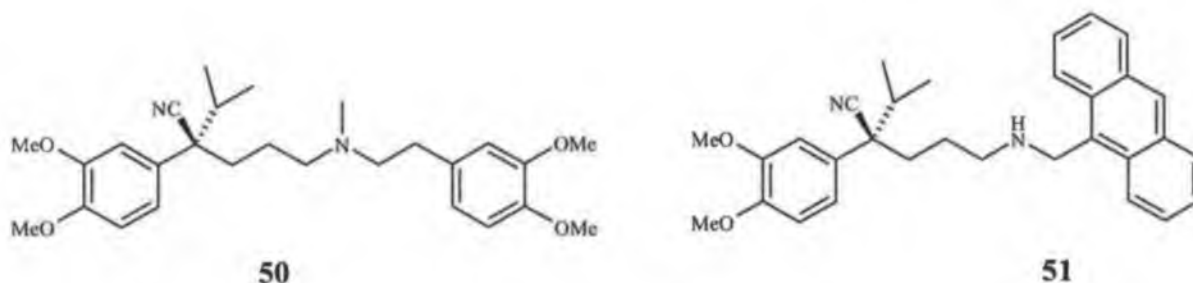
Chemotherapy is the most effective treatment for metastatic tumors. It is the treatment of choice for patients who have cancers that do not respond to surgery or radiation. The appearance of tumor cells resistant to a range of cytotoxic drugs is a serious problem in cancer chemotherapy. Clinical drug resistance is a major barrier to overcome before chemotherapy can become curative for patients presenting with metastatic cancer. There are two main types of cancer resistance. Intrinsic drug resistance is present at the time of diagnosis, in tumors that fail to respond to first line chemotherapy while acquired drug resistance occurs in tumors that are initially often highly responsive to initial treatment but on tumor recurrence appear to be strongly resistant to the original treatment.⁸³ They become resistant to both previously used drugs and new agents with different structures and modes of action. A number of specific resistance mechanisms that occur at a molecular level have been described *in vivo* and *in vitro*. The three main proposed mechanisms include the reduction of the intracellular accumulation of anticancer drugs by increased drug efflux (MDR), alterations in drug targets (topoisomerase II) or activation of detoxifying systems (glutathione-S-transferases). The absence of a structural relationship between the various types of cancer resistance modulators increases the difficulty in eradicating resistance to chemotherapeutics. Compounds as diverse as non-steroidal anti-inflammatory's, calcium channel blockers and protease inhibitors have all been used successfully to treat cancer resistance.

The broad spectrum resistance to structurally and mechanistically diverse anticancer agents is known as multidrug resistance (MDR). It results from the over expression of adenosine

triphosphate (ATP) binding cassette (ABC) transporters.⁸⁴ The ABC transporters are a large family of transmembrane proteins that use the energy of ATP hydrolysis to transport their substrates across biological membranes. They function as a mechanism of eliminating harmful substances from the body. The two most studied ABC transporters are P-glycoprotein (Pgp) and multidrug resistance associated protein (MRP-1). Pgp and MRP-1 are drug efflux pumps typically coexpressed with other ABC transporters such as breast cancer resistance protein (BCRP) and lung cancer resistance protein (LRP).⁸⁴ Although Pgp and MRP-1 belong to the same family of transporters there are some distinct differences between them. Pgp is expressed by secretory cells such as capillary endothelial cells in the brain and testis and at sites within the pancreas, kidney and liver whereas MRP-1 has been observed in virtually every type of tissue.⁸⁵ An additional difference relates to their expression in human tumors. The levels of Pgp are often increased in tumor cells from patients undergoing chemotherapy. In contrast, although MRP-1 is expressed in a high percentage of tumors, its over expression is not consistently found in tumors. For example MRP-1 levels in lung tumors were found to be lower than those in normal lung tissue.⁸⁵ Therefore it seems that over expression of Pgp activity is clinically more significant than the elevation of MRP-1 levels.

1.2.2 Modulators of P-glycoprotein associated cancer resistance

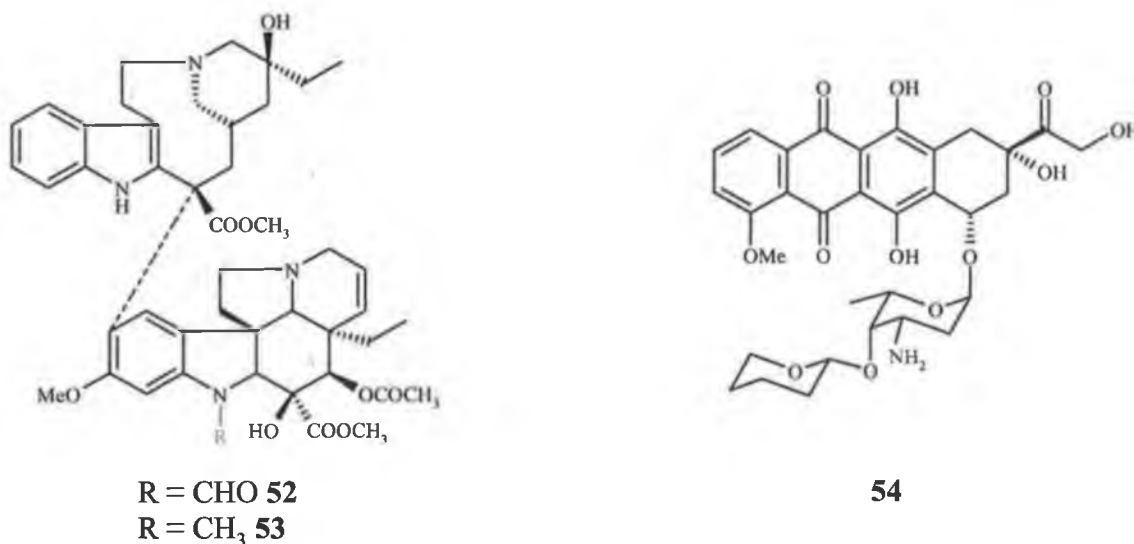
P-glycoprotein was the first protein implicated in multidrug resistance and confers resistance by pumping drugs out of the cell. Inhibition of Pgp has been employed to improve the effectiveness of chemotherapy. The inactivation of Pgp should have no side effects as studies on mice have concluded that the protein is not essential for their survival.⁸⁶ Chemosensitizers is the term now used to describe drugs that act by blocking Pgp. Verapamil **50** was the first compound



reported to overcome vincristine **52** resistance in P388 leukemia *in vivo* and *in vitro*.⁸⁷ Structural studies showed that **50** directly interacts with Pgp and inhibits the binding of Pgp transported agents to the pump, thus blocking drug efflux. This calcium channel antagonist is a potent

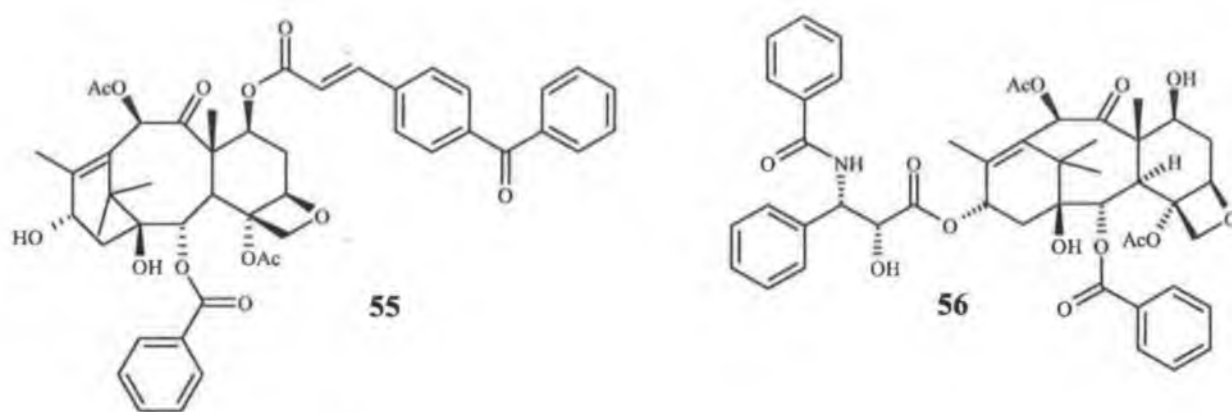
inhibitor of Pgp *in vitro* but the plasma concentrations of **50** required to efficiently block Pgp transport are rarely achieved clinically despite the administration of sufficient verapamil **50** to induce cardiotoxicity.⁸⁸

Teodori *et al* have synthesized a series of verapamil analogues with additional aromatic rings adjacent to the amino moiety.⁸⁸ Previous research has shown that besides the overall lipophilicity of the molecule, weak polar interactions such as those produced by the overlapping of π orbitals of aromatic rings can play an important role in stabilizing the binding of MDR reversing agents to Pgp.⁸⁹ The transmembrane segments of Pgp are believed to be rich in aromatic amino acid residues. The phenanthrene derivative **51** was shown to be a nanomolar MDR reverter with a dosage of 50 nM increasing the nuclear concentration of pirarubicin **54** in resistant erythroleukemia K 562 cells by 50%. This compound was more than 30-fold more potent than verapamil in reversing MDR. Its inactivity as a vasodilator limits its potential cardiotoxicity. **51** also presents a pharmacological profile that makes it a promising drug candidate to treat MDR.



A series of novel taxane based multidrug resistant reversal agents have been described.⁹⁰ The synthesis of these compounds is based on the fact that natural taxanes from the Japanese yew tree, *Taxus cuspidate* increase the cellular accumulation of vincristine in MDR tumor cells as much as verapamil.⁹¹ The incorporation of a hydrophobic conjugated ring has been shown to be a common theme in previous structure-activity relationship studies of structurally different classes of MDR reversal agents. The noncytotoxic compound **55** with a hydrophobic benzoyl-

cinnamoyl moiety reached 99.8% recovery of the original antitumor activity of paclitaxel **56** against the resistant breast tumor cell line MCF7-R when administered at a 1 μ M level. The Pgp transporter is known for its ability to non-selectively eliminate hydrophobic agents from cells but this study suggests that the presence of a hydrophobic moiety bonded to a taxane based derivative furnishes effective reversal agents. The taxol derivative **55** was confirmed as a modulator against P-glycoprotein overexpression in drug resistant cell lines, it was also shown to inhibit efflux pumps mediated by the ABC transporters MRP-1 and BCRP and offers a lead compound for the revitalization of well studied anticancer agents.



The naturally occurring steroid hormone progesterone **57** has been described as a potent modulator of Pgp.⁹² Clarke *et al* have recently designed and synthesized a series of Pgp inhibitors based on the progesterone skeleton.⁹³ Their hypothesis involved substitution at the C-7 position with an aromatic moiety would exhibit reduced Pgp affinity, increased anti-Pgp activity and reduced affinity for progesterone receptors. This is one of the first examples of the rational design of Pgp inhibitors. To date the majority of Pgp inhibitors have not been designed as MDR reverters thus side effects related to the normal function of these agents may be induced at concentrations required to affect Pgp function. These inhibitors have been evaluated for their Pgp modulating activity with breast cancer models that have Pgp expression as the only mechanism present to produce MDR.

The methylbenzyl amine derivative **60** was shown to be the most potent Pgp inhibitor. This compound was synthesized by firstly preparing 6-dehydroprogesterone **58** from the reaction of **57** with the oxidizing agent 2,3-dichloro-5,6-dicyano-1,4-benzoquinone (DDQ) and *p*-toluenesulphonic acid. This was then reacted with 4-aminothiophenol and sodium hydroxide to

furnish a substituted aminothiophenol derivative **59**. Reaction of this compound with α -methylbenzylisocyanate in the presence of dichloromethane yielded **60**. This noncytotoxic compound has an IC_{50} value greater than $20 \mu\text{M}$ against breast cancer cells independent of progesterone receptors. Because Pgp is an efflux pump the ability of **60** to influence the intracellular accumulation of the cytotoxic drug vinblastine **53** was measured. Vinblastine content in Pgp positive cells exposed to media containing **53** was approx. 6-fold lower than in Pgp negative cells. At a concentration of $0.7 \mu\text{M}$ **60** was shown to decrease the difference in accumulation of vinblastine in Pgp positive and Pgp negative cells by 50%. This was 28-fold more potent than **57** and more than four times more potent than verapamil. It was also shown not to bind to its predicted cellular target, progesterone receptors at concentrations that inhibit Pgp activity. This progesterone analogue significantly increased anti-Pgp activity when compared with progesterone and verapamil, lost its ability to activate progesterone receptors and is predicted to exhibit relatively low intrinsic toxicity *in vivo*.

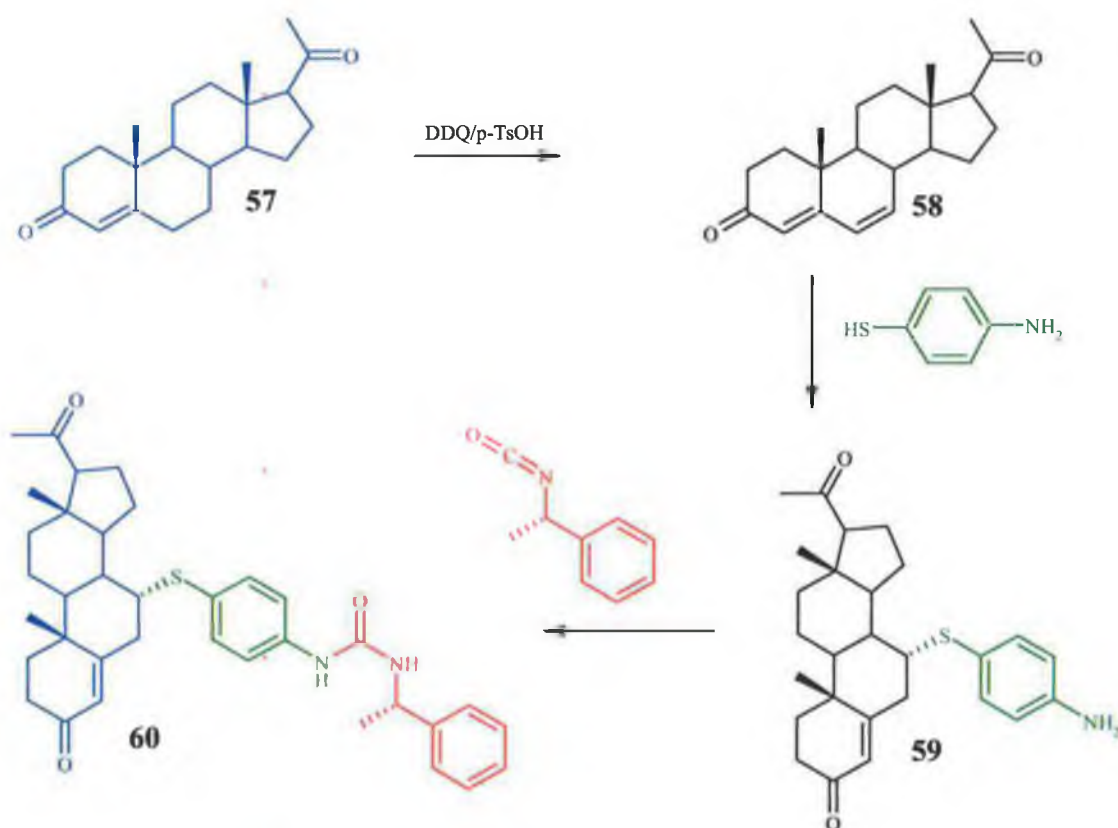
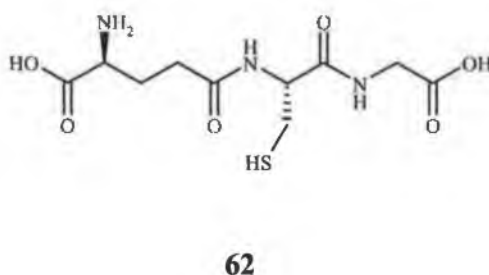
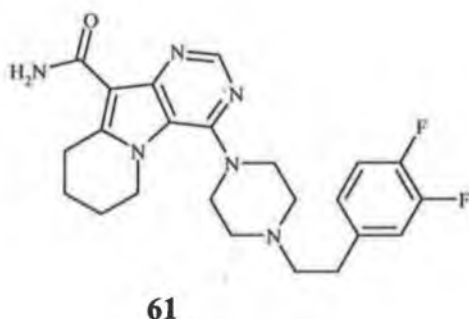


Figure 1.12 Synthesis of the progesterone based P-glycoprotein inhibitor **60**

1.2.3 Synthetic inhibitors of MRP-1 associated cancer resistance

The drug efflux pump MRP-1, a member of the ABC transporters, is a 190 Kda protein localized mainly in the plasma membrane.⁹⁴ Resistance associated with MRP-1 is different than Pgp mediated resistance although many anticancer drugs are affected by both mechanisms. The overexpression of MRP-1 in tumor cells confers resistance to anthracyclines and vinca alkaloids but in contrast to Pgp taxanes are poor substrates for MRP-1.⁹⁵ Although various inhibitors of Pgp have entered clinical trials the development of selective MRP-1 inhibitors is in its infancy. Scientists at Xenova Ltd. have recently described potent, selective inhibitors of MRP-1.⁹⁵ The pyrrolopyrimidine derivative **61** was shown to have an IC₅₀ value of 138 nM against the MRP-1 expressing cell line CORL23/R. This compound was more than 362-fold more selective for MRP-1 than Pgp. Cytochrome P450's (CYP) are a major class of oxidative enzymes involved in drug metabolism. Potential MRP-1 modulators will be administered with cytotoxic agents and it is essential that these modulators will not inhibit CYP. Compound **61** exhibited minor inhibition against CYP with an IC₅₀ value of 45.8 μM recorded. It was also shown to have bioavailability of 71.6% when administered orally at 50 mg/kg in mice. More importantly the plasma concentrations of this compound were 10-fold greater than their IC₅₀ value for several hours after dosing. Finally, the *in vivo* efficacy of **61** was assessed with mice bearing CORL23/R tumors. The antitumor activity of vincristine was improved by 35 %. In contrast, both vincristine and **57** alone had no effect on tumor growth in this MRP-1 resistant tumor model.

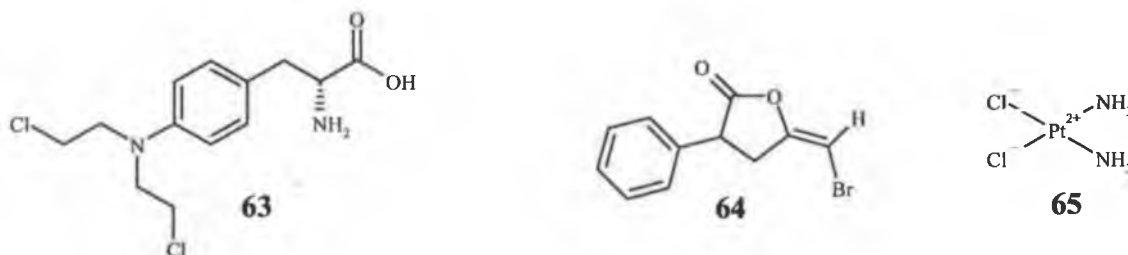


1.2.4 Glutathione S-transferase associated cancer resistance

The overexpression of glutathione S-transferase (GST) particularly the GST-π isozyme has been proposed to be one of the biochemical mechanisms responsible for drug resistance in cancer chemotherapy and offers a therapeutic target for the inhibition of GST mediated drug resistance.⁹⁶ The glutathione S-transferases are a family of enzymes that catalyze the addition of

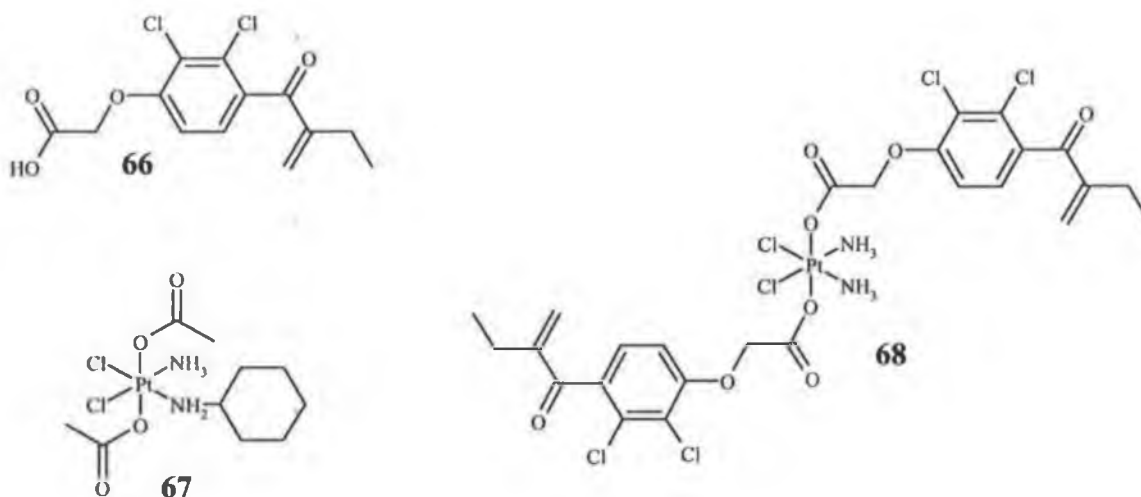
the tripeptide glutathione **62** to endogenous substrates that have electrophilic functional groups.⁹⁷ The glutathione **62** adducts produced have increased solubility in water and are subsequently enzymatically degraded to mercapturates and excreted. GST has been shown to deactivate a number of chemotherapeutic drugs including the alkylating agent melphalan **63**.⁹⁸ The over-expression of three GST isozymes (α , μ and π) have been found in cultured tumor cells resistant to cancer chemotherapy with the human GST- π isozyme being overexpressed in carcinoma of the colon, lung, kidney and pancreas.⁹⁹ GST- π inactivates chemotherapeutic substances by conjugating them to glutathione **62** and their inhibition offers a potential method for cancer resistance.

Zheng *et al* have reported the synthesis of a series of haloenol lactones as potent inhibitors of human GST- π isoenzyme.⁹⁹ The bromoenolfin **64** was the most potent inhibitor with GST activity reducing by 0.1504% min^{-1} over a twelve minute duration. The method of inhibition was proposed to involve the enzymatic hydrolysis of the haloenol lactone by the Cys⁴⁷ residue of the GST- π active site. This proposal was confirmed by electrospray ionisation mass spectrometry (ESIMS) of proteolytic fragments from haloenol lactone modified GST- π indicated that the haloenol lactone is covalently bonded to the protein at Cys⁴⁷.



Cisplatin **65** has been one of the most successful examples of a chemotherapeutic agent and is used in approx. 70% of all cancer treatments. Despite this success, drug resistance to cisplatin remains a serious problem. GST is known to catalyze the conjugation of glutathione with cisplatin *in vitro* that leads to elimination of toxic compounds.¹⁰⁰ Ethacrynic acid **66**, a diuretic in clinical use has been shown to be a potent inhibitor of GST enzymes. Satraplatin **67** is a Pt(IV) anticancer drug currently undergoing Phase 3 clinical trials for combination therapy in patients with prostate cancer. It functions as a prodrug releasing its cytotoxic Pt(II) payload after losing its axial aceto-ligands by reduction *in vivo*. It has been shown to be suitable for oral administration. Dyson *et al* have recently synthesized a Pt(IV) prodrug **68** incorporating two molecules of **66** as ligands.¹⁰⁰ This compound will be reduced *in vivo* in analogous manner to **67**

but releasing the ethacrynic acid moiety as well as a cytotoxic Pt(II) center thus reversing cisplatin associated drug resistance. Compound **68** was shown to be a more potent inhibitor of GST than cisplatin or ethacrynic acid when assayed directly against the GST- α -isoenzymes GSTP1-1 and GSTA1-1, and was capable of reducing the activity of both enzymes to less than 10%. Mass spectrometric analysis indicated that a GST induced cleavage of the platinum-ethacrynic acid carboxylate bond could be responsible for inhibition although the mechanism of carboxylate bond cleavage may not be the same as GST conjugation. Compound **68** was also shown to have broad spectrum anticancer activity and significantly more cytotoxic than cisplatin against the cisplatin resistant breast tumor cell line MCF-7. **68** was shown to have an IC_{50} value of 31.85 μ M compared to $> 80 \mu$ M for **65** 24 hours after exposure.



1.2.5 Cancer resistance related to the topoisomerases

Topoisomerases are a series of enzymes that catalyze topological changes in DNA and are essential for cell division and replication.¹⁰¹ There are three types of mammalian topoisomerases with type II existing in α and β isoforms.¹⁰² Topoisomerase II is a major target for chemotherapeutic agents used in the treatment of cancer. Topoisomerase II directed agents are able to stabilize the covalent DNA-topoisomerase II complex and are traditionally known as topoisomerase poisons.¹⁰³ Rather than inhibiting the overall catalytic activity of the enzyme, poisons act by stabilizing covalent DNA-topoisomerase II complexes that eventually results in the generation of lethal DNA double strand breaks in treated cells. These poisons convert essential enzymes into potent cellular toxins that facilitate apoptosis.

1.2.6 Conclusion

Clinical drug resistance is a multi-facet problem with often more than one drug resistance phenotype prevailing in the cell. The quantity and complexity of these drug resistant mechanisms renders their modulation challenging. To date there is still a distinct lack of understanding relating to many of these phenotypes and this has led to the majority of modulators being developed serendipitously. Although some potent inhibitors have been developed their extreme side effects often limits their employment. The design of specific drug resistance modulators has been limited. The use of traditional drug discovery tools such as SAR and QSAR have not produced many potent inhibitors of drug resistance due to the unrelated structures of many common inhibitors. Genome studies correlating drug response with DNA microarray datasets have identified many of the genes and proteins involved in drug resistance. The identification of specific biomarkers offers the potential for the selection of optimal treatment for individual patients and the most promising solution for the eradication of drug resistance.

1.13 References

- 1 a) Johnson, L.L., Dyer, R., Hupe D.J., *Curr. Opin. Chem. Biol.* **1998**, 466. b) Chino, M.,
2 Wakao, M., Ellman, J.A., *Tetrahedron* **2002**, 58, 6305.
- 3 Baynon, R.J., Bond, J., “*Proteolytic Enzymes*”, Oxford University Press, **1992**, 2nd
4 edition.
- 5 Schechter, I., Berger, A., *Biochem. Biophys. Res. Comm.* **1967**, 27, 157.
- 6 Harel, M., Su, C.T., Frolow, F., Silman, I., Sussman, J.L., *Biochemistry* **1991**, 30,
7 5217.
- 8 Otto, H.H., Schirmeister, T., *Chem. Rev.* **1997**, 97, 133.
- 9 PDB: www.rcsb.org/pdb
- 10 Rich, D.H., *J. Med. Chem.* **1985**, 28, 263.
- 11 Barrett, A.J., Starkey, P.M., *Biochem. J.* **1973**, 133, 709.
- 12 Fukiage, C., Azuma, M., Nakamura, Y., Tamada, Y., Nakamura, M., Shearer, T.,
13 *Biochem. Biophys. Acta* **1997**, 1361, 304.
- 14 Shaw, E., Mares-Guia, M., Cohen, W., *Biochemistry* **1965**, 4, 2219.
- 15 Rauber, P., Angliker, H., Walker, B., Shaw, E., *Biochem. J.* **1986**, 239, 633.
- 16 De Simone, G., Menchise, V., Omaggio, S., Pedone, C., Scozzafava, A., Supuran, C.T.,
17 *Biochemistry* **2003**, 42, 9013.
- 18 Danilewicz, J.C., Abel, S.M., Brown, A.D., Fish, P.V., Hawkeswood, E., Holland, S.J.,
James, K., McElroy, A.B., Overington, J., Powling, M.J., Rance, D.J., *J. Med. Chem.*
2002, 45, 2432.
- 19 Rawson, T.E., Van Gorp, K.A., Yang, J., Kogan, T.P., *J. Pharm. Sci.* **1993**, 82, 672.
- 20 Das, J., Kimball, D., Reid, J.A., Wang, T.C., Lau, W.F., Roberts, D.G.M., Seiler, S.M.,
21 Schumacher, W.A., Ogletree, M.L., *Bioorg. Med. Chem. Lett.* **2002**, 12, 41.
- 22 Malley, M.F., Taberner, L., Chang, C.Y., Ohringer, S., Roberts, D.G.M., Das, J., Sack,
23 J.S., *Protein Sci.* **1996**, 5, 221.
- 24 Lee, K., Park, C.W., Jung, W.H., Park, H.D., Lee, S.H., Chung, K.H., Park, S.K.,
25 Kwon, O.H., Kang, M., Park, D.H., Lee, S.K., Kim, E.E., Yoon, S.K., Kim, A., *J.*
26 *Med. Chem.* **2003**, 46, 3612.
- 27 Hlasta, D.J., Subramanyam, C., Bell, M.R., Carabateas, P.M., Court, J.J., Desai, R.C.,

-
- Drozd, M.L., Eickhoff, W.M., Ferguson, E.W., Gordon, R.J., Johnson, J.A., Kumar, V., Maycock, A.L., Mueller, K.R., Pagani, E.D., Robinson, D.T., Saindane, M.T., Silver, P.J., Subramanian, S., *J. Med. Chem.* **1995**, *38*, 739.
- 19 Luisetti, M., Sturani, C., Sella, D., Madonini, E., Galvavotti, V., Bruno, G., Peona, V., Kucich, U., Dagnino, G., Rosenbloom, J., Starcher, B., Grassi, C., *Eur. Respir. J.* **1996**, *9*, 1482.
- 20 Gerard, S., Dive, G., Clamot, B., Touillaux, R., Marchand-Brynaert, J., *Tetrahedron* **2002**, *58*, 2423.
- 21 Baylac, S., Racine, P., *Int. J. Aromatherapy* **2004**, *14*, 179.
- 22 <http://www.botanical.com/botanical/mgmh/t/turmer30.html>
- 23 Schaschke, N., Dominik, A., Matschiner, G., Sommerhoff, C.P., *Bioorg. Med. Chem. Lett.* **2002**, *12*, 985.
- 24 Sutton, J.C., Bolton, S.A., Hartl, K.S., Huang, M.H., Jacobs, G., Meng, W., Ogletree, M.L., Pi, Z., Schumacher, W.A., Seiler, S.M., Slusarchyk, W.A., Treuner, U., Zahler, R., Zhao, G., Bisacchi, G.S., *Bioorg. Med. Chem. Lett.* **2002**, *12*, 3229.
- 25 Stubbs, M., Morenweiser, R., Sturzebecher, J., Bauer, M., Bode, W., Huber, R., Piechottka, G.P., Matschiner, G., Somerhoff, C.P., Fritz, H., Auerswald, E.A., *J. Biol. Chem.* **1997**, *272*, 19931.
- 26 Rice, K.D., Gangloff, A.R., Kuo, E.Y., Dener, J.M., Wang, W.R., Lum, R., Newcomb, W.S., Havel, C., Putnam, D., Cregar, L., Wong, M., Warne, R.L., *Bioorg Med. Chem. Lett.* **2000**, *10*, 2357.
- 27 Costanzo, M.J., Yabut, S.C., Almond, H.R., Andrade-Gordon, P., Corcoran, T.W., de Garavilla, L., Kauffman, J.A., Abraham, W.M., Recacha, R., Chattopadhyay, D., Maryanoff, B.E., *J. Med. Chem.* **2003**, *46*, 3865.
- 28 Sutton, J.C., Bolton, S.A., Davis, M.E., Hartl, K.S., Jacobsen, B., Mathur, A., Ogletree, M.L., Slusarchyk, W.A., Zahler, R., Seiler, S.M., Bisacchi, G.S., *Bioorg. Med. Chem. Lett.* **2004**, *14*, 2233.
- 29 Tallen, H., Jones, M., Fruton, J., *J. Biol. Chem.* **1952**, *194*, 793.
- 30 Mendonca, R.V., Venkatraman, S., Palmer, J.T., *Bioorg Med. Chem. Lett.* **2002**, *12*,

2887.

- 31 Fried, B., Graczyk, T.K., "Advances in Trematode Biology", CRC Press, LLC, New
York, 1997.
- 32 Zhou, N.E., Guo, D., Kaleta, J., Purisima, E., Menard, R., Micetich, R.G., Singh, R.,
Bioorg. Med. Chem. Lett. **2002**, *12*, 3413.
- 33 Altmann, E., Green, J., Tintelnot-Blomley, M., *Bioorg. Med. Chem. Lett.* **2003**, *13*, 1997.
- 34 Robichaud, J., Bayly, C., Oballa, R., Prasit, P., Mellon, C., Falguyret, J.P., Percival,
M.D., Wesolowski, G., Rodan, S.B., *Bioorg. Med. Chem. Lett.* **2004**, *14*, 4291.
- 35 Tavares, F.X., Deaton, D.N., Miller, A.B., Miller, L.R., Wright, L.L., Zhou, H.Q., *J.*
Med. Chem. **2004**, *47*, 5049.
- 36 Wasserman, H.H., Ho, W.B., *J. Org. Chem.* **1994**, *59*, 4364.
- 37 Rousselet, N., Mills, L., Jean, D., Tellez, C., Bar-Eli, M., Frade, R., *Cancer Res.* **2004**,
64, 146.
- 38 Barrett, A.J., Kembhavi, A.A., Brown, M.A., Kirschke, H., Knight, C.G., Tamai, M.,
Hanada, K., *Biochem. J.* **1982**, *201*, 189.
- 39 James, I.E., Marquis, R.W., Blake, S.M., Hwang, S.M., Gress, C.J., Ru, Y.,
Zembryki, D., Yamashita, D.S., McQueney, M.S., Tomaszek, T.A., Oh, H.J.,
Gowen, M., Veber, D.F., Lark, M.W., *J. Biol. Chem.* **2001**, *276*, 11507.
- 40 Linton, S.D., Karanewsky, D.S., Ternansky, R.J., Wu, J.C., Pham, B., Kodandapani, L.,
Smidt, R., Diaz, J.L., Fritz, L.C., Tomaselli, K.J., *Bioorg. Med. Chem. Lett.* **2002**, *12*,
2969.
- 41 Revesz, L., Briswalter, C., Heng, R., Leutwiler, A., Mueller, R., Wuethrich, H.J., *Tet.*
Lett. **1994**, *35*, 9693.
- 42 Harter, W.G., Albrect, H., Brady, K., Caprathe, B., Dunbar, J., Gilmore, J., Hays, S.,
Kostlan, C.R., Lunney, B., Walker, N., *Bioorg. Med. Chem. Lett.* **2004**, *14*, 809.
- 43 Cohen, G.M., *Biochem. J.* **1997**, *326*, 1.
- 44 Karanewsky, D.S., Bai, X., Linton, S., Krebs, J.F., Wu, J., Pham, B., Tomaselli, K.J.,
Bioorg. Med. Chem. Lett. **1998**, *8*, 2757.
- 45 Guo, Z., Xian, M., Zhang, W., McGill, A., Wang, P.G., *Bioorg. Med. Chem.* **2001**, *9*, 99.

- 46 Webber, S.E., Okano, K., Little, T.L., Reich, S.H., Xin, Y., Fuhrman, S.A., Matthews, D.A., Love, R.A., Hendrickson, T.F., Patick, A.K., Meador III, J.W., Ferre, R.A., Brown, E.L., Ford, C.E., Binford, S.L., Worland, S.T., *J. Med. Chem* **1998**, *41*, 2786.
- 47 Chen, S.H., Lamar, J., Victor, F., Snyder, N., Johnson, R., Heinz, B.A., Wakulchik, M., Wang, Q.M., *Bioorg. Med. Chem. Lett.* **2003**, *13*, 3531.
- 48 Ax, A., Schaal, W., Vrang, L., Samuelsson, B., Hallberg, A., Karlén, A., *Bioorg. Med. Chem.* **2005**, *13*, 755.
- 49 Bouzide, A., Sauv e, G., Yelle, J., *Bioorg. Med. Chem. Lett.* **2005**, *15*, 1509.
- 50 Pakyz, A., Israel, D., *J. Am. Pharm. Assoc.* **1997**, *5*, 543.
- 51 Hwang, Y.S., Chmielewski, J., *J. Med. Chem.* **2005**, *48*, 2239.
- 52 Sham, H.L., Zhao, C., Li, L., Betebenner, D.A., Saldivar, A., Vasavanonda, S., Kempf, D.J., Plattner, J.L., Norbeck, D.W., *Bioorg. Med. Chem. Lett.* **2002**, *12*, 3101.
- 53 <http://www.albmolecular.com/features/tekreps/vol08/no14/>
- 54 Kazmierski, W.M., Andrews, W., Furfine, E., Spaltenstein, A., Wright, L., *Bioorg. Med. Chem. Lett.* **2004**, *14*, 5689.
- 55 Kleinert, H.D., Stein, H.H., Boyd, S., Fung, A.K., Baker, W.R., Verburg, K.M., Polakowski, J.S., Kovar, P., Barlow, J., Cohen, J., *Hypertension* **1992**, *20*, 768.
- 56 Stanton, A., Barton, J., Jensen, C., Bobillier, B., Mann, J., O'Brien, E., *Am. J. Hypertension* **2002**, *4*, 56A.
- 57 Cody, W.L., Holsworth, D.D., Powell, N.A., Jalaie, M., Zhang, E., Wang, W., Samas, B., Bryant, J., Ostroski, R., Ryan, M.J., Edmunds, J.J., *Bioorg. Med. Chem. Lett.* **2005**, *13*, 59.
- 58 Rich, D.H., *J. Med. Chem.*, **1985**, *3*, 263.
- 59 Rich, D.H., Sun, E.T.O., Ulm, E., *J. Med. Chem.* **1980**, *23*, 27.
- 60 Hanessian, S., Moitessier, N., Gauchet, C., Viau, M., *J. Med. Chem.* **2001**, *44*, 3066.
- 61 Natesh, R., Schwager, S.L.U., Evans, H.R., Sturrock, E.D., Acharya, K.R., *Biochemistry* **2004**, *43*, 8718.
- 62 Kim, W., Lee, S., Kang, S.K., Yu, H.C., Cho, B.H., Park, S.K., *Transplantation Proceedings* **2002**, *34*, 3223.

- 63 Burris, J.F., *J. Clin. Pharm.* **1995**, *35*, 337.
- 64 Almansa, C., Gómez, L.A., Cavalcanti, F.L., de Arriba, A.F., García-Rafanell, J., Forn, J., *J. Med. Chem.* **1997**, *40*, 547.
- 65 Croquet, V., Moal, F., Veal, N., Wang, J., Oberti, F., Roux, J., Vuillemin, E., Gallois, Y., Douay, O., Chappard, D., Cales, P., *J. Hepatology* **2002**, *37*, 773.
- 66 Kim, J., Sieburth, S. McN. *Bioorg. Med. Chem. Lett.* **2004**, *14*, 2853.
- 67 Foda, H.D., Zucker, S., *Drug Discovery Today* **2001**, *9*, 478.
- 68 Whittaker, M., Floyd, C.D., Brown, P., Gearing, A.J.H., *Chem. Rev.* **1999**, *99*, 2735.
- 69 Beckett, R.P., Davidson, A.H., Drummond, A.H., Whittaker, M., *Drug Discovery Today* **1996**, *1*, 16.
- 70 Wada, C.K., Holms, J.H., Curtin, M.L., Dai, Y., Florjancic, A.S., Garland, R.B., Guo, Y., Heyman, R.H., Stacey, J.R., Steinman, D.H., Albert, D.H., Bouska, J.J., Elmore, I.N., Goodfellow, C.L., Marcotte, P.A., Tapang, P., Morgan, D.W., Michaelides, M.R., Davidsen, S.K., *J. Med. Chem.* **2002**, *45*, 219.
- 71 Moriyama, H., Tsukida, T., Inoue, Y., Yokota, K., Yoshino, K., Kondo, H., Miura, N., Nishimura, S.I., *J. Med. Chem.* **2004**, *47*, 1930.
- 72 Park, B.K., Kitteringham, N.R., O'Neill, P.M., *Annu. Rev. Pharmacol. Toxicol.* **2001**, *41*, 443.
- 73 Welch, J.T., Eswarakrishnan, S., "*Fluorine in Bioorganic Chemistry*", Wiley and Sons, New York **1991**.
- 74 Ni, L.M., Powers, J.C., *Bioorg. Med. Chem. Lett.* **1998**, *6*, 1776.
- 75 Bartlett, P.A., Lamden, L.A., *Bioorg. Chem.* **1986**, *14*, 356.
- 76 a) Imperali, B., Abeles, R.H., *Biochemistry* **1986**, *25*, 3760. b) Shaw, E., Angliker, H., Rauber, P., Walker, B., Wikstrom, P., *Biomed. Biochim. Acta.* **1986**, *45*, 1397.
- 77 Gelb, M.H., Svaren, J.P., Abeles, R.H., *Biochemistry* **1985**, *24*, 1813.
- 78 Akahoshi, F., Ashimori, A., Sakashita, H., Yoshimura, T., Eda, M., Imada, T., Nakajima, M., Mitsutomi, N., Kuwahara, S., Ohtsuka, T., Fukaya, C., Miyazaki, M., Nakamura, N., *J. Med. Chem.* **2001**, *44*, 1297.
- 79 Eda, M., Ashimori, A., Akahoshi, F., Yoshimura, T., Inoue, Y., Fukaya, C., Nakajima, M., Fukuyama, H., Imada, T., Nakamura, N., *Bioorg. Med. Chem. Lett.* **1998**, *8*, 919.

- 80 Wang, Y., Guan, L., Jia, S., Tseng, B., Drewe, J., Cai, S.X., *Bioorg. Med. Chem. Lett.*
2005, 15, 1379.
- 81 http://www.casg.uab.edu/Presentations/2004/2004_annual_meeting_presentation.htm
- 82 King, R.J.B., “*Cancer Biology*”, Pearson Education 2000, 2nd edition.
- 83 Baird, R.D., Kaye, S.B., *Eur. J. Cancer* 2003, 39, 2450.
- 84 Filipits, M., *Drug Discovery Today: Disease Mechanisms* 2004, 1, 229.
- 85 Lawrence, D.S., Copper, J.E., Smith, C.D., *J. Med. Chem.* 2001, 44, 594.
- 86 Loo, T.W., Bartlett, M.C., Clarke, D.M., *Mol. Pharmaceut.* 2004, 1, 426.
- 87 Tsuruo, T., Iida, H., Tsukagoshi, S., Sakurai, Y., *Cancer Res.* 1981, 41, 1967.
- 88 Teodori, E., Dei, S., Quidu, P., Budriesi, R., Chiarini, A., Garnier-Suillerot, A., Gualtieri,
F., Manetti, D., Romanelli, M.N., Scapecchi, S., *J. Med. Chem.* 1999, 42, 1687.
- 89 Klopman, G., Shi, L.M., Ramu, A., *Mol. Pharmacol.* 1997, 52, 323.
- 90 Ojima, I., Borella, C.P., Wu, X., Bounaud, P.Y., Oderda, C.F., Sturm, M., Miller, M.L.,
Chakravarty, S., Chen, J., Huang, Q., Pera, P., Brooks, T.A., Baer, M.R., Bernacki, R.J.,
J. Med. Chem. 2005, 48, 2218.
- 91 Kobayashi, J., Ogiwara, A., Hosoyama, H., Shigemori, H., Yoshida, N., Sasaki, T., Li,
Y., Iwasaki, S., Naito, M., Tsuruo, T., *Tetrahedron* 1994, 50, 7401.
- 92 Yang, C.P.H., DePinho, S.G., Greenberger, L.M., Arceci, R.J., Horwitz, S.B., *J. Biol.*
Chem. 1989, 264, 782.
- 93 Leonessa, F., Kim, J.H., Ghiorghis, A., Kulawiec, R.J., Hammer, C., Talebian, A.,
Clarke, R., *J. Med. Chem.* 2002, 45, 390.
- 94 Bredel, M., Zentner, J., *Lancet Oncology* 2002, 3, 397.
- 95 Wang, S., Folkes, A., Chuckowree, I., Cockcroft, X., Sohal, S., Miller, W., Milton, J.,
Wren, S.P., Vicker, N., Depledge, P., Scott, J., Smith, L., Jones, H., Mistry, P., Faint, R.,
Thompson, D., Cocks, S., *J. Med. Chem.* 2004, 47, 1329.
- 96 Su, F., Hu, X., Jia, W., Gong, C., Song, E., Hamar, P., *J. Surg. Res.* 2003, 113, 102.
- 97 http://www.cstl.nist.gov/biotech/carb/gilliland_group/molecules/gst.html
- 98 Kupczyk-Subotkowska L., Siahaan, T.J., Basile, A.S., Friedman, H.S., Higgins, P.E.,
Song, D., Gallo, J.M., *J. Med. Chem.* 1997, 40, 1726.
- 99 Wu, Z., Minhas, G.S., Wen, D., Jiang, H., Chen, K., Zimniak, P., Zheng, J., *J. Med.*

Chem. **2004**, *47*, 3282.

¹⁰⁰ Ang, W.H., Khalaila, I., Allardyce, C.S., Juillerat-Jeanneret, L., Dyson, P.J., *J. Am. Chem. Soc.* **2005**, *127*, 1382.

¹⁰¹ Robert, J., Larsen, A.K., *Biochimie* **1998**, *80*, 247.

¹⁰² Renodon-Cornière, A., Jensen, L.H., Nitiss, J.L., Jensen, P.B., Sehested, M., *Biochemistry* **2003**; *42*, 9749.

¹⁰³ Larsen, A.K., Escargueil, A.E., Skladanowski, A., *Pharmacol. Therapeut.* **2003**, *99*, 167.

¹⁰⁴ Duca, M., Guianvarc'h, D., Meresse, P., Bertounesque, E., Dauzonne, D., Kraus-Berthier, L., Thiot, S., Léonce, S., Pierré, A., Pfeiffer, B., Renard, P., Arimondo, P.B., Monneret, C., *J. Med. Chem.* **2005**, *48*, 593.

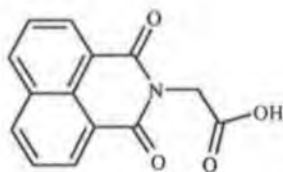
¹⁰⁵ Kingma, P.S., Burden, D.A., Osheroff, N., *Biochemistry* **1999**, *38*, 3457.

Chapter 2

Synthesis, characterization and biological activity of novel modified amino acid derivatives

2.1 Introduction

N-benzoyl peptides have been shown to have a wide range of biological activity varying from the treatment of diabetes and rheumatoid arthritis to the improved drug delivery of certain potential pharmaceuticals.¹ The benzoylation of a *N*-terminal amino acid increases the lipophilicity of the amino acid and substitution on such a group is often crucial for its biological activity. Alrestatin **71**, a benzoylglycine derivative is an effective aldose reductase inhibitor. It has been used to delay the development of long-term diabetes complications such as cataract and neuropathy.² The planar structure in addition to a carboxylic or another acidic proton is believed to be essential for the inhibitory effect.



71

A series of *N*-fluorobenzoyl glycine methyl esters have been previously described.³ These derivatives have been used to probe the structure of substrate-enzyme complexes using resonance Raman spectroscopy. From this study it was shown that enzyme-substrate contacts between papain and the *N*-fluorobenzoyl glycine methyl esters involve fluorine atoms at both the *meta* and *ortho* positions in the phenyl ring. The introduction of a fluorine atom onto the phenyl ring has been shown to enhance biological activity.⁴ There are generally two consequences of introducing fluorine into a drug molecule. Firstly there are the physicochemical properties, *i.e.* increased lipophilicity, increased acidity, decreased basicity and a change in hydrogen bonding properties. Lipophilicity is an important consideration in the design of biologically active compounds since it often controls absorption, transport or receptor binding.⁵ Secondly, there is the influence of fluorine substitution on the biological stability of a drug molecule. Fluorine substitution at different positions around the aromatic ring has led to improvements in selectivity and affinity along with a reduction in oxidative metabolism.⁶ Although heavier halogens and

The introduction of fluorine into the bioactive molecules as markers also provide a valuable tool for ^{19}F NMR studies by taking advantage of the fact that fluorine is virtually absent in living tissue. *N*-fluorobenzoylamino acid esters also can be very useful chiral building blocks for organic synthesis (Figure 2.1). A number of one step reactions can readily turn the amino acid esters into very interesting bioactive molecules such as thiazoles, hydrazides and lactones. For example the reaction of *N*-4-fluorobenzoyl-L-Ala-OMe with phosphorus oxychloride can furnish the corresponding oxazole derivative. The benzoyl derivatives of such compounds have been prepared but to date very little work has taken place on their fluoro analogues. Besides the utility of fluorobenzoyl amino acid esters as versatile synthetic intermediates they may have intrinsic importance as a pharmacophore of various therapeutic agents since the benzoyl amino acid skeleton is found in numerous pharmacologically active molecules possessing antihepatitis, anticonvulsant and anti-HIV activities.⁷ Herein the synthesis and structural characterization of a series of fluorobenzoyl amino acid esters is presented.

2.2 Synthesis of *N*-fluorobenzoyl amino acid esters

There are potentially three alternative procedures for the synthesis of *N*-fluorobenzoyl amino acid esters (Figure 2.2). The first route involves fluorination of *N*-aminobenzoyl amino acid esters using diazotisation and sodium tetrafluoroborate that furnish fluorobenzoyl amino acid esters although such reactions have shown poor yields.⁵ The introduction of a fluorine atom onto the phenyl ring can be achieved by a number of ways. Historically fluorination was carried out by selectively chlorinating the aromatic ring using FeCl_3 and Cl_2 gas followed by halogen exchange using metal fluorides, HF or antimony halide/HF as fluorinating agents. Halex (halogen exchange) methodology involves the displacement of a heavier halogen from a ring carbon by a fluorine atom in the form of a fluoride ion. The reaction does not proceed at an acceptable rate unless the leaving group is activated. Activation can be achieved by introducing electron withdrawing groups at the *ortho* or *para* positions to the halogen being exchanged.⁸ Alternative methodologies include the use of organometallic, radical and electrophilic reagents but all of these suffer from environmental and safety issues.

Elemental fluorine F_2 has also been used successfully to halogenate phenyl rings. However its use has been quite limited due to the uncontrollable nature of the reaction that leads to decomposition products. Furthermore it has been shown that *para*-disubstituted benzene with

two ortho/para directing groups can be fluorinated with high selectivity.⁹ Elemental fluorine is therefore of use as a fluorinating agent for aromatic molecules when the directing effects of the groups on the ring are complimentary. Deaminative fluorination is by far the most effective method of introducing fluorine into an aromatic ring. The first step of this procedure is diazotisation with nitrous acid and sodium tetrafluoroborate to produce arenediazonium tetrafluoroborates (ArN_2BF_4) followed by fluorinative decomposition to furnish fluoroarene derivatives. The *Balz-Schiemann* reaction as it is known is the most convenient and practical method for the regiospecific introduction of fluorine onto aromatic rings.¹⁰ However many difficulties arise with isolation of some ArN_2BF_4 and yields are often low. The use of HF for the diazotization of aminoarenes greatly simplified the transformation of ArNH_2 to ArF .¹¹ This procedure offers the advantage of a one pot deaminative fluorination of ArNH_2 due to the fact that the diazonium salts do not have to be isolated. More recently Olah and his group have recorded yields of up to 90% by the diazotisation of ArNH_2 using a pyridinium polyhydrogen fluoride ($\text{Py}\cdot 9\text{HF}$) solution.¹² The only disadvantage to this procedure is the extreme corrosive nature of the reagent used.

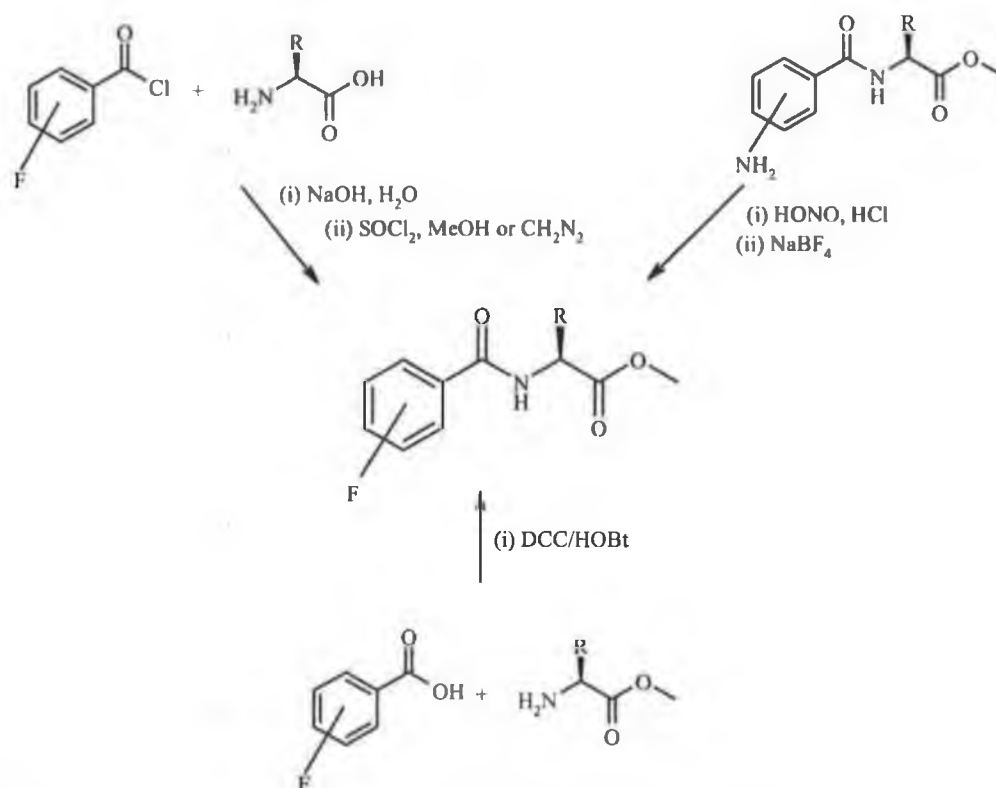
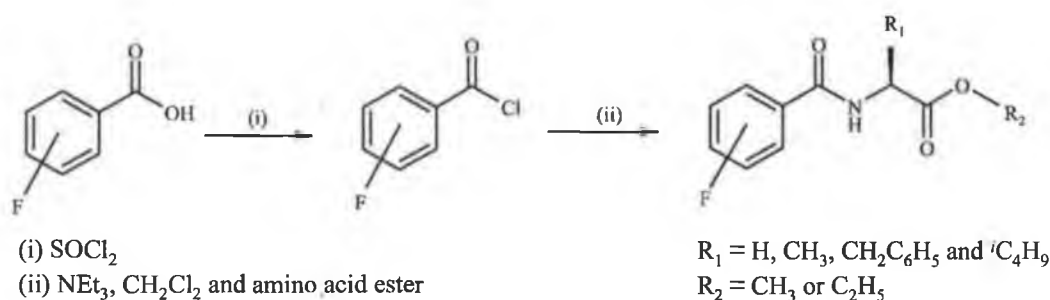


Figure 2.2 Alternative syntheses of *N*-fluorobenzoyl amino acid esters.

Alternatively peptide coupling using 1,3-dicyclohexylcarbodiimide (DCC) and 1-hydroxybenzotriazole (HOBt) is another useful method. The main disadvantage to this process is the formation of the *N*-acylurea byproduct that reduces the total yield to less than 50% in certain cases. The third procedure for the synthesis of fluorobenzoyl amino acid esters involves the preparation of the acid derivatives followed by esterification of the free acid group by diazomethane or thionyl chloride/methanol yielding the esters in good yields. The synthesis of the acid derivatives usually results in the formation of the fluorobenzoic acid by-product. Isolation of the *N*-fluorobenzoyl amino acids can often be difficult. The logic behind the selection of our synthetic route was increased yields and ease of purification by recrystallisation.

A series of novel *N*-fluorobenzoyl amino acid esters have been synthesized using the amino acids L-alanine, L-phenylalanine, glycine and L-leucine as starting materials. A series of mono-, di- and pentafluoro compounds have been synthesized. The first step of the synthesis involves the preparation of the appropriate fluorobenzoyl chloride. This is formed from the reaction of the benzoic acid derivative and the chlorinating agent thionyl chloride. Excess thionyl chloride is distilled off to give the acid chloride in almost quantitative yield. The acid chloride thus formed is then reacted with an equimolar amount of an amino acid ester and an excess of triethylamine in dichloromethane to form the *N*-fluorobenzoyl amino acid derivatives. The reaction is shown in Scheme 2.1. This reaction is analogous to the *Schotten-Baumann* reaction.¹⁰



Scheme 2.1 Synthesis of *N*-fluorobenzoyl amino acid esters.

2.2.1 Synthesis of *N*-fluorobenzoyl-L-alanine methyl esters

A series of ten *N*-fluorobenzoyl-L-alanine methyl esters were prepared. The compounds are presented in Table 2.1. Compound **72** has been previously reported as a root growth promoting agent.¹³ Compound **74** furnishes the highest yield with a value of 78%. The superior yields of the monofluoro derivatives are probably due to a solubility effect. The monofluoro

derivatives **72-74** were found to be soluble in most organic solvents. The lowest yield of 41 % was recorded for *N*-pentafluorobenzoyl-L-alanine methyl ester **81**. This compound was found to have poor solubility in both polar and non-polar organic solvents. The effect of five fluorine atoms on the benzoyl ring may result in steric hindrance but if this was the case a similar discrepancy in yield would be expected between the 2-fluoro and 4-fluoro analogues. The addition of sodium hydroxide to the amino acid for the synthesis of the *N*-pentafluorobenzoyl amino acid derivative **82** furnished an increased value of 73%.

Table 2.1 *N*-fluorobenzoyl-L-alanine derivatives.

Compound	R ₁	R ₂	% Yield
<i>N</i> -2-fluorobenzoyl-L-Ala-OMe 72	2-F-C ₆ H ₄ CO-	-CH ₃	74
<i>N</i> -3-fluorobenzoyl-L-Ala-OMe 73	3-F-C ₆ H ₄ CO-	-CH ₃	69
<i>N</i> -4-fluorobenzoyl-L-Ala-OMe 74	4-F-C ₆ H ₄ CO-	-CH ₃	78
<i>N</i> -2,3-difluorobenzoyl-L-Ala-OMe 75	2,3-(F) ₂ -C ₆ H ₃ CO-	-CH ₃	47
<i>N</i> -2,4-difluorobenzoyl-L-Ala-OMe 76	2,4-(F) ₂ -C ₆ H ₃ CO-	-CH ₃	53
<i>N</i> -2,5-difluorobenzoyl-L-Ala-OMe 77	2,5-(F) ₂ -C ₆ H ₃ CO-	-CH ₃	43
<i>N</i> -2,6-difluorobenzoyl-L-Ala-OMe 78	2,6-(F) ₂ -C ₆ H ₃ CO-	-CH ₃	62
<i>N</i> -3,4-difluorobenzoyl-L-Ala-OMe 79	3,4-(F) ₂ -C ₆ H ₃ CO-	-CH ₃	58
<i>N</i> -3,5-difluorobenzoyl-L-Ala-OMe 80	3,5-(F) ₂ -C ₆ H ₃ CO-	-CH ₃	53
<i>N</i> -pentafluorobenzoyl-L-Ala-OMe 81	2,3,4,5,6-(F) ₅ -C ₆ CO-	-CH ₃	41
<i>N</i> -pentafluorobenzoyl-L-Ala-OH 82	2,3,4,5,6-(F) ₅ -C ₆ CO-	-H	73

2.2.2 ¹H NMR studies of the *N*-fluorobenzoyl-L-alanine derivatives

One of the most interesting results recorded is the effect of ¹³C-¹⁹F and ¹H-¹⁹F coupling on the NMR spectra. Presently it is impossible to decouple the ¹³C-¹⁹F and ¹³C-¹H interactions simultaneously on the available NMR instrument. The effects of this coupling have been shown to extend to a four-bond distance. Theoretical calculations of the chemical shifts expected with fluoro substitution on the phenyl ring were very accurate and invaluable in assigning each carbon and hydrogen.¹⁴ The ¹H NMR spectrum of *N*-2,4-difluorobenzoyl-L-alanine methyl ester **76** is shown in Figure 2.3. The solvent used was deuterated dimethyl sulphoxide (DMSO-d₆). The amide peak present at δ ~8.73 is a doublet with a coupling constant of 6.8 Hz due to coupling

with the α hydrogen. This chemical shift is attributed to a hydrogen bond interaction between the amide proton and the polar S=O bond in the sulphoxide group of DMSO- d_6 . The characteristic splitting pattern for a 2,4-difluoro substituted benzene ring is seen as a multiplet centered at $\delta \sim 7.7$, a multiplet centered at $\delta \sim 7.35$ and a multiplet centered at $\delta \sim 7.18$ each of which integrate for one proton each. The reason these all appear as multiplets is due to the effect of ^1H - ^{19}F coupling on the phenyl ring. The α -hydrogen integrating for one proton shows up as a multiplet centered at $\delta \sim 4.48$. This can be explained by its proximity to both the amide proton and the methyl side chain of alanine. The alanine methyl group is coupled to the α -hydrogen and appears as a doublet at $\delta \sim 1.38$ with a coupling constant of 7 Hz. The characteristic methyl ester signal appears as a singlet at $\delta \sim 3.67$. The ^1H NMR spectrum of *N*-2,4-difluorobenzoyl-L-alanine methyl ester **76** is shown in Figure 2.3.

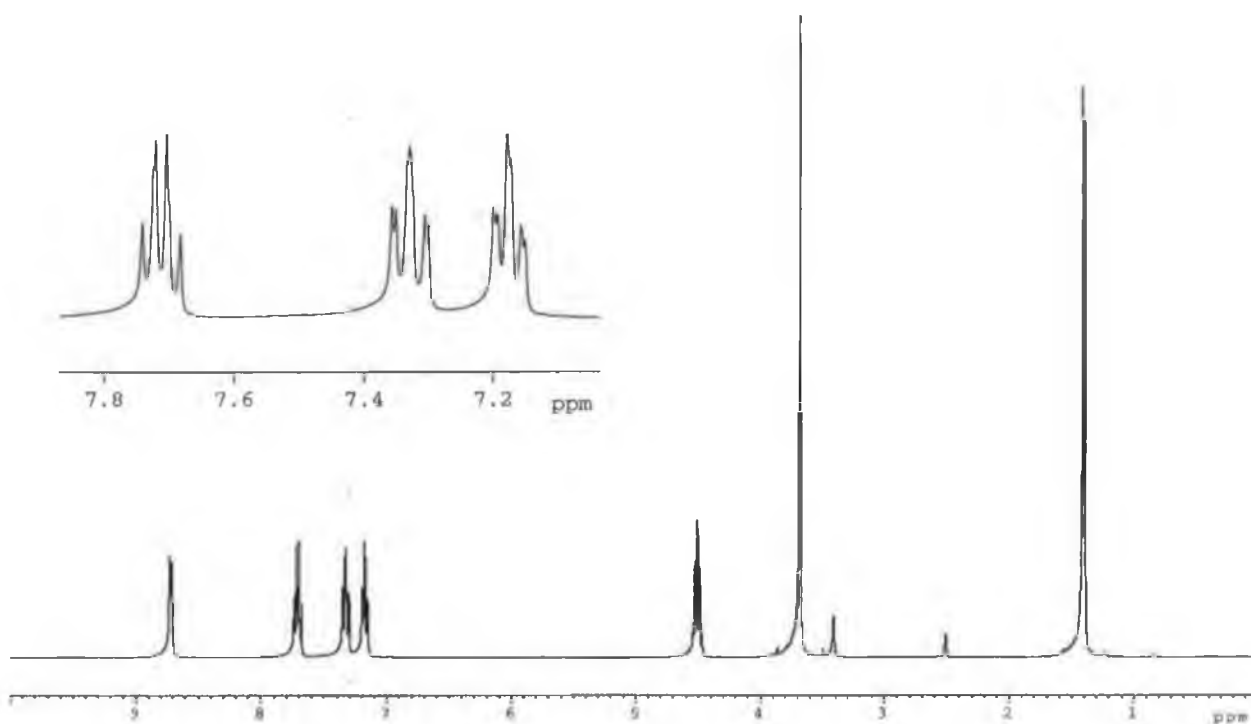


Figure 2.3 ^1H NMR spectrum of 2,4-difluorobenzoyl-L-alanine methyl ester **76**.

A measure of the electron withdrawing nature of the fluorobenzoyl moiety is recorded by the chemical shift of the amide protons. The most electron withdrawing substituent pentafluorobenzoyl, shifts the amide proton chemical shift down to δ 9.42. A similar effect is seen with the 2,6-difluoro analogue with the amide proton appearing at δ 9.19. Therefore this indicates a fluorine atom present in the 2- and 6- positions have the greatest influence over the

chemical shift of the amide proton. Selected chemical shift values for the *N*-fluorobenzoyl-L-alanine derivatives are present in Table 2.2.

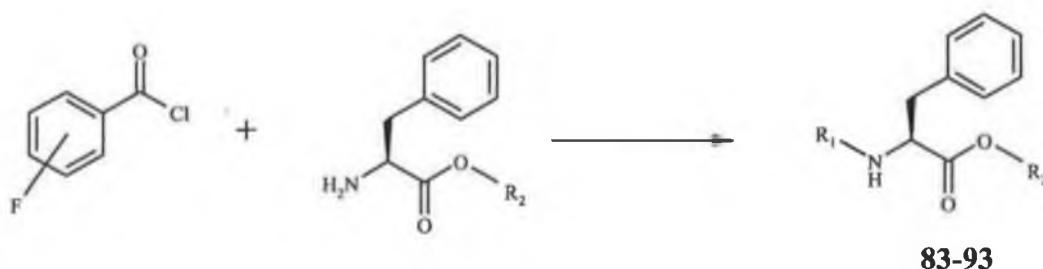
Table 2.2 Selected ^1H NMR data (δ) for the *N*-fluorobenzoyl-L-alanine derivatives.

Compound No.	NH	α -H	-OCH ₃	-CH ₃
72	8.75	4.45-4.52	3.67	1.39
74	8.84	4.47-4.54	3.65	1.41
76	8.73	4.46-4.50	3.67	1.38
78	9.19	4.47-4.51	3.67	1.35
81	9.42	4.47-4.55	3.68	1.37

2.2.3 Synthesis of *N*-fluorobenzoyl-L-phenylalanine methyl esters

Phenylalanine (Phe) is an essential amino acid used as a precursor for neurotransmitter biosynthesis.¹⁵ Phenylalanine has been shown to promote the division of existing melanoma cells.¹⁶ The artificial sweetener Aspartame is comprised of 50% L-phenylalanine. It is often crucially important in biologically active peptides to elicit bioactivity where the side chain phenyl group often plays an essential role in the ligand-receptor interaction.¹⁷ The molecular mechanism of this hydrophobic interaction is believed to involve interaction of phenylalanine with the alkyl side chains of amino acids whereby the Phe-phenyl π system is believed to function as a hydrogen acceptor.

The phenylalanine derivatives prepared are shown in Table 2.3. *N*-pentafluorobenzoyl-L-phenylalanine methyl ester **92** was prepared in the lowest yield of 39% due to its poor solubility in organic solvents. A similar observation was made in the case of the alanine derivatives. The introduction of sodium hydroxide gives compound **93** in the highest yield of 78 %. The melting points of the L-phenylalanine derivatives substantially higher than the L-alanine derivatives with highest being the 158-159 °C of the acid **93**.



Scheme 2.2 Synthesis of *N*-fluorobenzoyl-L-phenylalanine derivatives

Table 2.3 *N*-fluorobenzoyl-L-phenylalanine derivatives.

Compound	R ₁	R ₂	% Yield
<i>N</i> -2-fluorobenzoyl-L-Phe-OMe 83	2-F-C ₆ H ₄ CO-	-CH ₃	56
<i>N</i> -3-fluorobenzoyl-L-Phe-OMe 84	3-F-C ₆ H ₄ CO-	-CH ₃	45
<i>N</i> -4-fluorobenzoyl-L-Phe-OMe 85	4-F-C ₆ H ₄ CO-	-CH ₃	49
<i>N</i> -2,3-difluorobenzoyl-L-Phe-OMe 86	2,3-(F) ₂ -C ₆ H ₃ CO-	-CH ₃	56
<i>N</i> -2,4-difluorobenzoyl-L-Phe-OMe 87	2,4-(F) ₂ -C ₆ H ₃ CO-	-CH ₃	62
<i>N</i> -2,5-difluorobenzoyl-L-Phe-OMe 88	2,5-(F) ₂ -C ₆ H ₃ CO-	-CH ₃	48
<i>N</i> -2,6-difluorobenzoyl-L-Phe-OMe 89	2,6-(F) ₂ -C ₆ H ₃ CO-	-CH ₃	42
<i>N</i> -3,4-difluorobenzoyl-L-Phe-OMe 90	3,4-(F) ₂ -C ₆ H ₃ CO-	-CH ₃	44
<i>N</i> -3,5-difluorobenzoyl-L-Phe-OMe 91	3,5-(F) ₂ -C ₆ H ₃ CO-	-CH ₃	51
<i>N</i> -pentafluorobenzoyl-L-Phe-OMe 92	2,3,4,5,6-(F) ₅ -C ₆ CO-	-CH ₃	39
<i>N</i> -pentafluorobenzoyl-L-Phe-OH 93	2,3,4,5,6-(F) ₅ -C ₆ CO-	-H	78

2.2.4 Electrospray Ionization Mass Spectrometry (ESIMS) studies of the *N*-fluorobenzoyl-L-phenylalanine derivatives

Electrospray is the term that refers to the small flow of liquid from a capillary needle when a potential difference is applied between the end of the capillary and a cylindrical electrode.¹⁸ Under these conditions the samples leaving the capillary do not leave as liquids but as fine mists. These mists consist of droplets that are highly charged and may be either positive or negative depending on the sign of the voltage applied to the capillary. Upon evaporation of the solvent droplets, a molecular ion of the sample is obtained in a desolvated state. These ions are then transported into the ion analyzer by an electric field. The evaporation process yields either [M+H]⁺ or [M-H]⁻ adducts with their generation promoting desolvation, as repulsive Coloumbic forces become stronger than the cohesive forces of the droplet. Electrospray ionization (ESI) is a particularly effective technique for the production of molecular ions from polar molecules. ESI mass spectrometry was carried out on compounds **83-86** on a Bruker Esquire 3000 series LC/MS.

The positive ion mode mass spectrum of **84** shows an intense peak at *m/z* 324 when a cone voltage of 20 was applied. The appearance of this peak confirms the molecular mass of the compound and reveals the presence of a [M+Na]⁺ adduct. Relatively intense peaks also appear at *m/z* 340 and 625 respectively. The presence of the peak at *m/z* 340 can be attributed to the [M+K]⁺

adduct while the peak at m/z 625 is due to a $[2M+Na]^+$ species. A weak peak is also present at m/z 120 responsible for the phenylalanine side chain derivative as shown in Figure 2.4. When the cone voltage is increased to 40 volts there is the appearance of one intense peak, the $[M+Na]^+$ adduct. There is also the presence of weak peaks at m/z 242 and m/z 123 that represent phenylalanine methyl ester and the fluorobenzoyl moiety that are present after fragmentation. The mass spectrum of **83** displays a similar pattern except a distinct weak peak appears at m/z 302 representing the $[M+H]^+$ species.

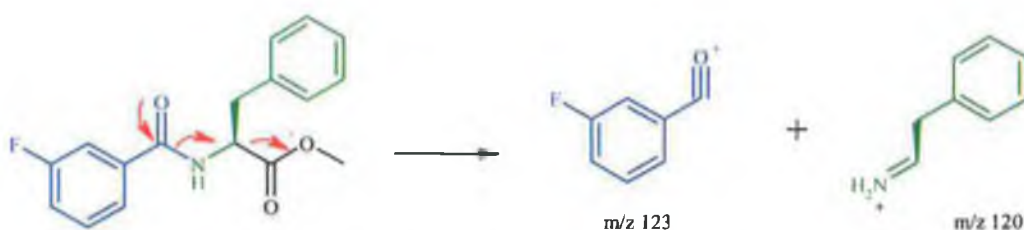


Figure 2.4 Fragmentation of *N*-3-fluorobenzoyl-L-phenylalanine **84**.

2.2.5 ^{13}C NMR Studies of the *N*-fluorobenzoyl-L-phenylalanine derivatives **83-93**

A ^{13}C NMR and DEPT 135 study was carried out on all compounds synthesised. The ^{13}C NMR of *N*-3,5-difluorobenzoyl-L-phenylalanine methyl ester **91** is shown in Figure 2.5. In the ^{13}C NMR spectrum, the amide carbonyl peak appears at $\delta \sim 164$ as a triplet due to the effect of ^{13}C - ^{19}F coupling and the ester carbonyl peak appears at $\delta \sim 172$. Each of the carbon atoms on the fluorinated aromatic ring appear as doublets and triplets due to the affect of ^{13}C - ^{19}F on the ring.

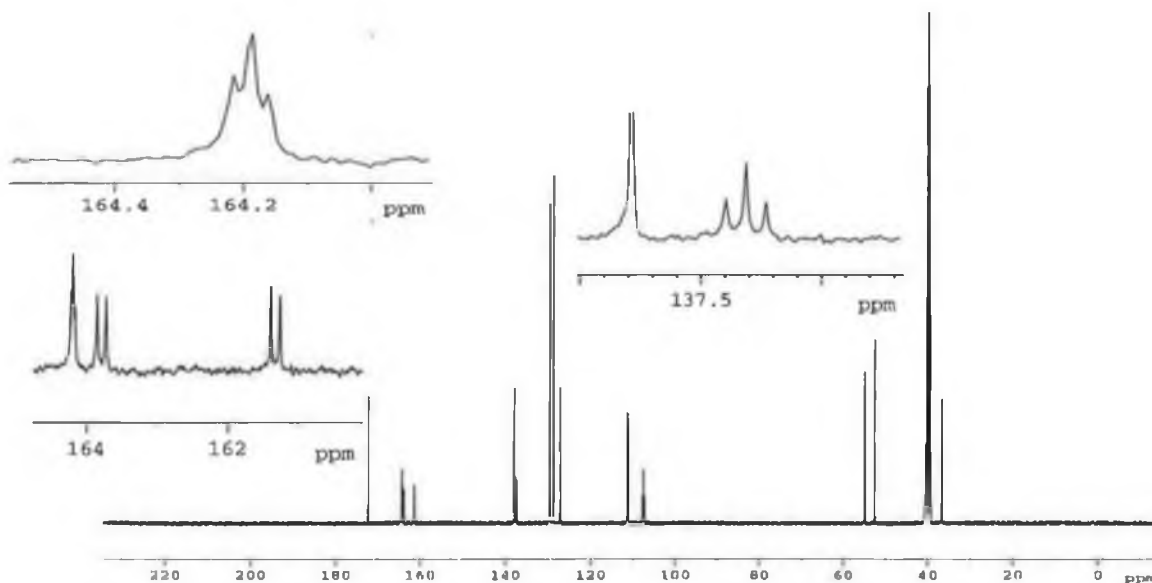


Figure 2.5 ^{13}C NMR spectrum of *N*-3,5-difluorobenzoyl-L-phenylalanine methyl ester **91**.

The carbon atoms to which fluorine is bonded appear at $\delta \sim 163$ and $\delta \sim 161$. The four other carbons on the ring appear at $\delta \sim 111$, ~ 110 , ~ 107 with the quaternary carbon appearing at $\delta \sim 137.3$. The phenylalanine phenyl ring shows peaks at $\delta \sim 137$, ~ 129 , ~ 128 and ~ 126 . The methyl ester peak appears downfield at $\delta \sim 52$ due to the deshielding effect of the attached oxygen atom. The signal for the α -carbon appears at $\delta \sim 54$. The methylene carbon of L-phenylalanine group is present at $\delta \sim 36$. This is confirmed by the ^{13}C DEPT 135 spectra.

The fluorobenzoyl moiety has a distinct effect on the chemical shift of the amide carbonyl. The compounds **92** and **93** with the most electron withdrawing substituent, the pentafluorobenzoyl moiety have a chemical shift of $\delta \sim 157$. This is in contrast to the monofluorobenzoyl derivatives **83** and **85** that have a chemical shift further downfield at $\delta 164.2$ and $\delta 165.7$ respectively.

Table 2.4 Selected ^{13}C NMR data (δ) for the *N*-fluorobenzoyl-L-phenylalanine derivatives.

Compound No.	C=O _{Ester}	C=O _{Amide}	C-F	α -C
83	172.1	164.2	159.6	54.5
85	172.5	165.8	164.3	54.7
87	172.0	163.3	163.9, 160.2	54.5
89	171.7	160.2	160.4, 158.0	54.4
92	171.4	157.1	144.6, 141.5, 142.1, 138.4, 136.0	54.5

Although each of the compounds differ substantially in relation to the chemical shifts of their aromatic carbon atoms, each compound has six distinct peaks representing the aromatic carbons even if certain atoms would appear to be in the same chemical environment. This effect is due to ^{19}F - ^{13}C coupling in the ^{13}C NMR spectra.

2.2.6 Synthesis of *N*-fluorobenzoyl-glycine ethyl esters

A series of *N*-fluorobenzoyl-glycine derivatives are presented in Table 2.5. In contrast to the alanine and phenylalanine derivatives the highest yield 72% was obtained for the pentafluoro analogue **103**. This is due to the increased solubility of the glycine derivatives in organic solvents and also perhaps the fact that the lack of a substantial side chain in glycine limits the amount of steric hindrance possible. This is reinforced by the fact that *N*-pentafluorobenzoyl-glycine nitrile **104** has a yield of 68% that is greater than the L-alanine or L-phenylalanine pentafluorobenzoyl analogues.

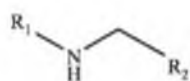


Table 2.5 *N*-fluorobenzoyl-glycine derivatives.

Compound	R ₁	R ₂	m.p. °C	% Yield
<i>N</i> -2-fluorobenzoyl-Gly-OEt 94	2-F-C ₆ H ₄ CO-	-COOEt	oil	58
<i>N</i> -3-fluorobenzoyl-Gly-OEt 95	3-F-C ₆ H ₄ CO-	-COOEt	60-62	52
<i>N</i> -4-fluorobenzoyl-Gly-OEt 96	4-F-C ₆ H ₄ CO-	-COOEt	101-103	63
<i>N</i> -2,3-difluorobenzoyl-Gly-OEt 97	2,3-(F) ₂ -C ₆ H ₃ CO-	-COOEt	54-56	69
<i>N</i> -2,4-difluorobenzoyl-Gly-OEt 98	2,4-(F) ₂ -C ₆ H ₃ CO-	-COOEt	77-79	61
<i>N</i> -2,5-difluorobenzoyl-Gly-OEt 99	2,5-(F) ₂ -C ₆ H ₃ CO-	-COOEt	51-52	55
<i>N</i> -2,6-difluorobenzoyl-Gly-OEt 100	2,6-(F) ₂ -C ₆ H ₃ CO-	-COOEt	67-68	66
<i>N</i> -3,4-difluorobenzoyl-Gly-OEt 101	3,4-(F) ₂ -C ₆ H ₃ CO-	-COOEt	91-92	61
<i>N</i> -3,5-difluorobenzoyl-Gly-OEt 102	3,5-(F) ₂ -C ₆ H ₃ CO-	-COOEt	80-81	52
<i>N</i> -pentafluorobenzoyl-Gly-OEt 103	2,3,4,5,6-(F) ₅ -C ₆ CO-	-COOEt	79-80	72
<i>N</i> -pentafluorobenzoyl-Gly-CN 104	2,3,4,5,6-(F) ₅ -C ₆ CO-	-CN	126-127	68

2.2.7 Infrared study of the *N*-fluorobenzoyl-glycine derivatives

Infrared (IR) spectroscopy is a spectroscopic technique by which many functional groups can be identified. Compounds absorb IR radiation and various molecular vibrations are induced. The IR spectra of these compounds typically show two bands between 3460 and 3400 cm⁻¹ (Amide I and II) as shown in Figure 2.6. These bands are representative of secondary amide N-H groups, however, upon hydrogen bonding or if the sample is in the solid state these N-H groups

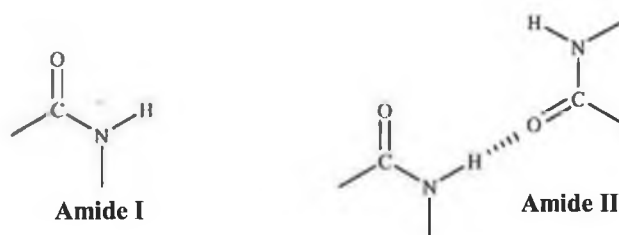


Figure 2.6 Configuration of amides giving rise to two bands in the IR spectrum.

will appear at a lower wavelength. The appearance of two bands can be attributed to two types of amide absorptions.¹⁹ Hydrogen bonding lowers and broadens N-H stretching frequencies albeit to a lesser degree than is the case with O-H groups as the intensity of the N-H absorption is

usually less than that of O-H absorptions. The amide carbonyl (Amide I) is observed stretching between 1695 and 1680 cm^{-1} . At 1550 cm^{-1} the N-H (Amide II) bending occurs. The aromatic system of these compounds produce bands between 1500 and 1600 cm^{-1} . Further bands due to aromaticity are present in the fingerprint region but these are of little diagnostic value.

The Infrared spectrum of *N*-3,4-difluorobenzoyl-glycine ethyl ester **101** is shown in Figure 2.7. The IR spectrum was obtained as a potassium bromide disk. The bands due to amide and ester carbonyls appear at 1646 and 1739 cm^{-1} respectively. Peaks at 1542 cm^{-1} can be attributed to N-H bending and C-N stretching of the C-N-H group. At 3306 cm^{-1} a peak due to N-H stretching is observed. Selected IR values for the *N*-fluorobenzoyl-glycine derivatives are presented in Table 2.6.

Table 2.6 Selected IR values (cm^{-1}) for the *N*-fluorobenzoyl-glycine derivatives.

Compound No.	N-H	C=O _{Ester}	C=O _{Amide}	Aryl C-H
94	3309	1737	1645	701
96	3277	1748	1648	670
98	3411	1749	1656	772
100	3278	1734	1654	800
103	3271	1737	1658	786

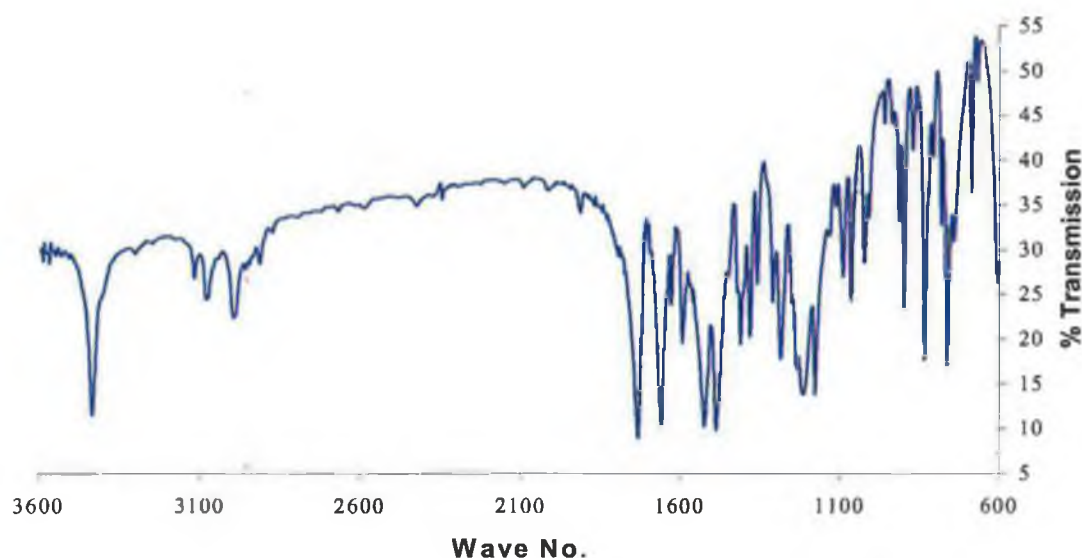


Figure 2.7 Infrared spectrum of *N*-3,4-difluorobenzoyl-glycine ethyl ester **101**.

2.2.8 ^{19}F NMR study of *N*-fluorobenzoyl-glycine derivatives

The ^{19}F NMR spectrum of compound *N*-2,5-difluorobenzoyl-glycine ethyl ester **99** is shown in Figure 2.8. There are two multiplets present, one centred at $\delta \sim -118.5$ and the other centred at $\delta \sim -119.6$. These peaks appear as multiplets due to ^1H - ^{19}F and ^{19}F - ^{19}F coupling between the fluorine atoms and the aromatic protons. These chemical shifts become $\delta \sim -42.8$ and $\delta \sim -43.8$ when trifluoroacetic acid is used as an external standard. These two multiplets integrate for one fluorine atom each. The pentafluoro derivatives **103** and **104** show a distinctive pattern in the ^{19}F NMR. The fluorine atom in the *para* position appears as a triplet at $\delta \sim -77.7$ due to coupling with two fluorine atoms and integrates for one fluorine. The fluorine atoms in the *ortho* positions appear as a double doublet at $\delta \sim -66.6$. The fluorine atoms couple with the *meta* fluorine atoms to give a coupling constant of ~ 23 Hz and with each other giving an decreased coupling constant of ~ 6 Hz. The integration of this peak gives a value of two. The fluorine atoms in the *meta* positions appear as a multiplet centred at $\delta \sim -86.3$. The fluorine atoms in these positions couple with each other, the *ortho* fluorine atoms and the *para* fluorine atom. Finally the pattern for a 3,5-difluorosubstituted phenyl ring appears as a triplet with a coupling constant ~ 8 Hz. The fluorine atoms couple with protons in the *ortho* and *para* positions. The results from the ^{19}F NMR study shows that fluorine atom has the ability to couple with both the hydrogen and fluorine nuclei in NMR.

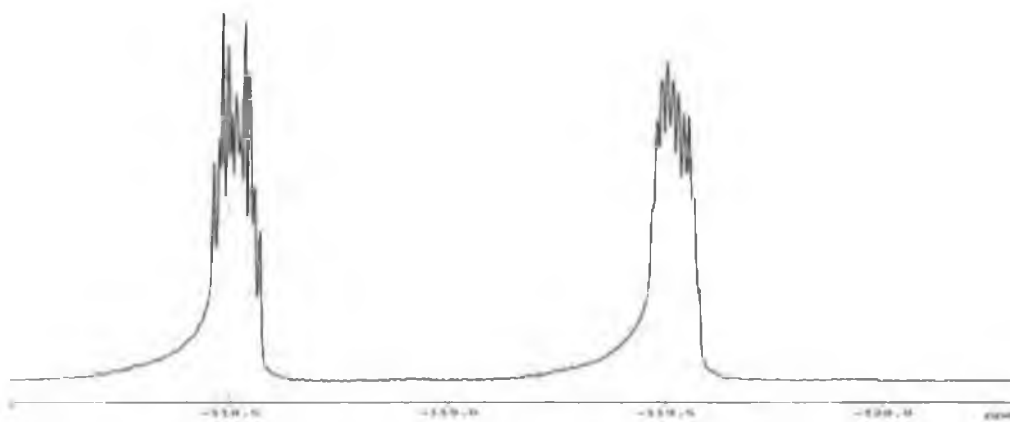


Figure 2.8 ^{19}F NMR spectrum of *N*-2,5-difluorobenzoyl-glycine ethyl ester **99**.

2.2.9 Synthesis of *N*-fluorobenzoyl-leucine methyl esters

The final class of fluorobenzoyl amino acid derivatives prepared were the L-leucine analogues. *N*-fluorobenzoyl-L-leucine methyl esters **105-114** were prepared in the highest yields.

However these derivatives turned out to be the least crystalline with a number of compounds oils. This may be due to the bulky hydrophobic nature of the ^tbutyl side chain. The highest yield recorded was for compound **106** with a value of 79 %. The *N*-pentafluorobenzoyl derivative compound **114** was obtained in a yield of 45 %. This yield is superior to the yields recorded for the alanine and phenylalanine analogues but it is still lower than the yields of the mono- and difluorobenzoyl-*L*-leucine methyl esters. This decreased yield is related to the reduced solubility of a pentafluorobenzoyl derivative in organic solvent.

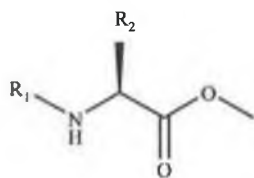


Table 2.7 *N*-fluorobenzoyl-*L*-leucine derivatives.

Compound	R ₁	R ₂	% Yield
<i>N</i> -2-fluorobenzoyl-Leu-OMe 105	2-F-C ₆ H ₄ CO-	-CH ₂ CH(CH ₃) ₂	62
<i>N</i> -3-fluorobenzoyl- <i>L</i> -Leu-OMe 106	3-F-C ₆ H ₄ CO-	-CH ₂ CH(CH ₃) ₂	79
<i>N</i> -4-fluorobenzoyl- <i>L</i> -Leu-OMe 107	4-F-C ₆ H ₄ CO-	-CH ₂ CH(CH ₃) ₂	76
<i>N</i> -2,3-difluorobenzoyl- <i>L</i> -Leu-OMe 108	2,3-(F) ₂ -C ₆ H ₃ CO-	-CH ₂ CH(CH ₃) ₂	65
<i>N</i> -2,4-difluorobenzoyl- <i>L</i> -Leu-OMe 109	2,4-(F) ₂ -C ₆ H ₃ CO-	-CH ₂ CH(CH ₃) ₂	71
<i>N</i> -2,5-difluorobenzoyl- <i>L</i> -Leu-OMe 110	2,5-(F) ₂ -C ₆ H ₃ CO-	-CH ₂ CH(CH ₃) ₂	59
<i>N</i> -2,6-difluorobenzoyl- <i>L</i> -Leu-OMe 111	2,6-(F) ₂ -C ₆ H ₃ CO-	-CH ₂ CH(CH ₃) ₂	63
<i>N</i> -3,4-difluorobenzoyl- <i>L</i> -Leu-OMe 112	3,4-(F) ₂ -C ₆ H ₃ CO-	-CH ₂ CH(CH ₃) ₂	51
<i>N</i> -3,5-difluorobenzoyl- <i>L</i> -Leu-OMe 113	3,5-(F) ₂ -C ₆ H ₃ CO-	-CH ₂ CH(CH ₃) ₂	73
<i>N</i> -pentafluorobenzoyl- <i>L</i> -Leu-OMe 114	2,3,4,5,6-(F) ₅ -C ₆ CO-	-CH ₂ CH(CH ₃) ₂	45

2.2.10 HMQC study of *N*-3-fluorobenzoyl-*L*-leucine methyl ester **106**

The ¹H NMR spectra of the *N*-fluorobenzoyl-*L*-leucine derivatives show the two methyl groups of the ^tbutyl side chain as two individual doublets even though they appear to reside in the same chemical environment. A similar result is observed in the ¹³C NMR where the two methyl groups appear at δ ~21 and δ ~23. The hydrogen atoms of the methine and methylene groups of the ^tbutyl side chain generally overlap with a multiplet appearing centred at δ ~1.7.

HMQC (Heteronuclear multiple quantum correlation) is a 2D NMR spectroscopic technique which correlates the carbon and proton spectra and hence total structural elucidation can be achieved. HMQC is a C-H correlation method that is frequently used to resolve the overlapping proton signals in complex structures.¹⁹ This is of great assistance when assigning both carbon and proton peaks and elucidating a structure. As quaternary carbons and carbonyls do not bear hydrogen, no representative peak appears in the HMQC spectrum. These spectra yield such useful information so as to remove many ambiguities regarding the structure of the compound that is being characterised. Table 2.8 and Figure 2.9 shows the C-H correlation spectrum for *N*-3-fluorobenzoyl-L-leucine methyl ester **106**.

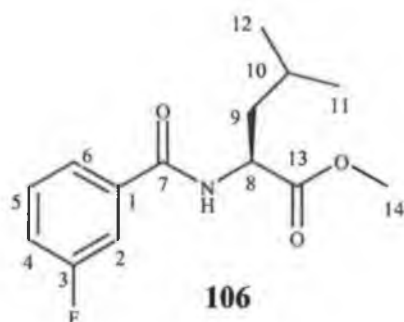


Table 2.8 C-H correlation of *N*-3-fluorobenzoyl-L-leucine methyl ester **106**.

Site	¹ H	¹³ C	HMQC
1		136.3	
2	7.68-7.72		114.5
3		162.3	
4	7.36-7.41		118.7
5	7.50-7.56		130.8
6	7.68-7.72		124.0
7		165.1	
8	4.49-4.55		51.3
9	1.49-1.83		39.5
10	1.49-1.83		24.7
11	0.91		23.1
12	0.87		21.3
13		173.3	
14	3.67		52.2

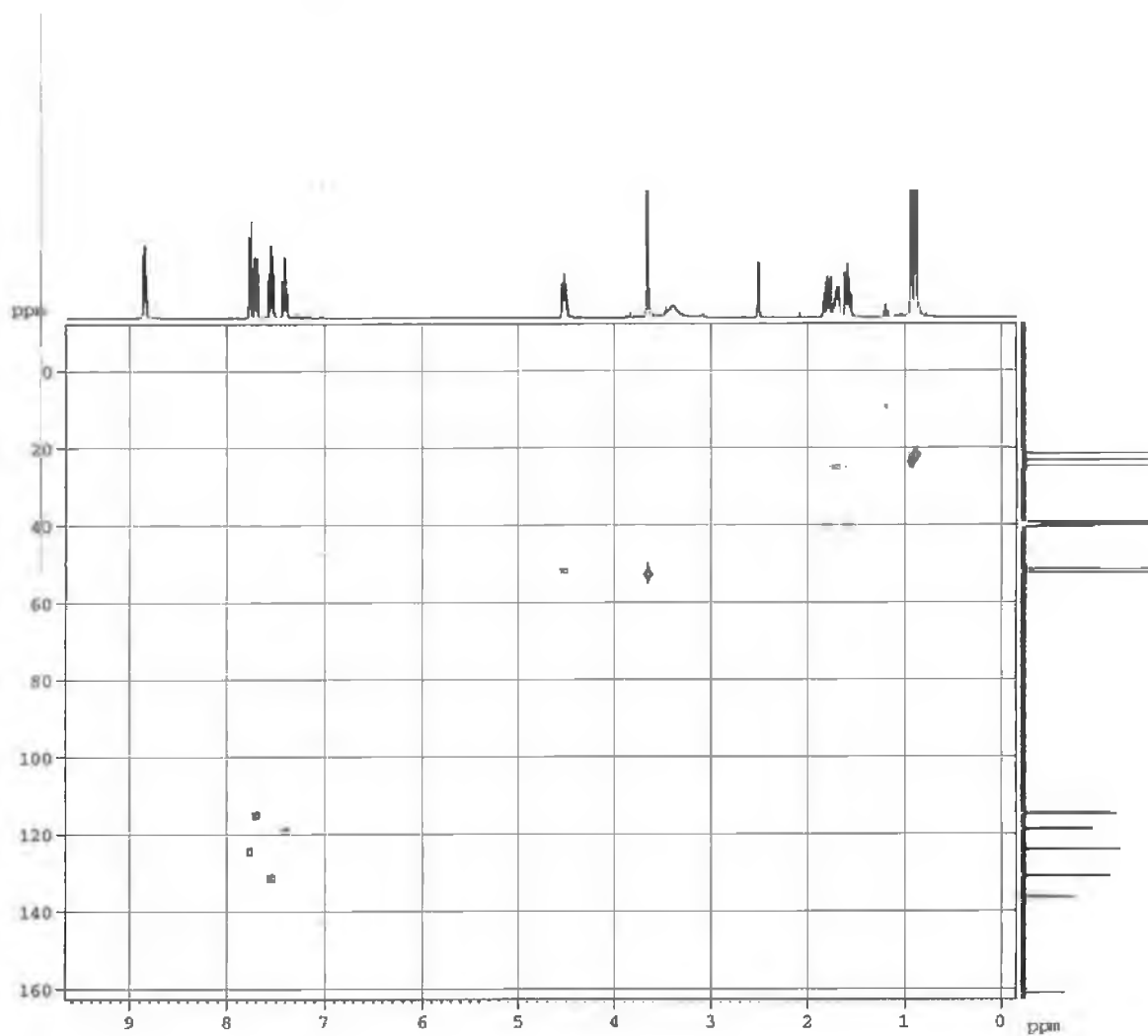


Figure 2.9 HMQC Spectrum of *N*-3-fluorobenzoyl-L-leucine methyl ester **106**.

2.3 Structural study of the *N*-fluorobenzoyl amino acid esters

Crystals suitable for single crystal x-ray crystallographic determinations of **76**, **81**, **101** and **114** were grown from hexane, yielding colourless block shaped crystals. All pertinent crystallographic information is summarized in Tables 2.9 and 2.11 and selected bond distances and angles of non-hydrogen atoms are given in Tables 2.10 and 2.12. Figures 2.10 - 2.18 show perspective views of each crystal structure with the atomic numbering scheme.

Compound **76** crystallizes in the monoclinic space group $P2_1$ (No. 4) with two independent molecules per asymmetric unit. The range of the phenyl C-C bond distances is 1.361(5) to 1.396(4) Å (mean 1.380(4) Å). The carbonyl C=O distance for molecule A is 1.289(9) Å but molecule B has a carbonyl bond distance of 1.228(10) Å. The F-C-C bond angles range from 117.2(3)° to 119.6(4)°. The amide C(O)-N distances C(1A)-N(1A) 1.318(3) Å and C(1B)-N(1B) 1.447(3) Å exhibit a lot of single bond character. The principle interactions in **76** involve the amide N-H and carbonyl groups of neighbouring residues interacting as N-H...O=C and forming a one-dimensional chain (Figure 2.13).

Refinement has shown that there are two types of disorder associated with **76**. The amide carbonyl oxygen atom is disordered over two sites O1A/O1B which differ in their orientation with respect to the amide moiety and with site occupancy factors subsequently fixed at 50% each. Secondly, the 2,4-difluorophenyl ring is disordered over two orientations with site occupancies of 0.938(6) and 0.062(6) for the major and minor sites respectively. This was detected by analysis of the difference maps.

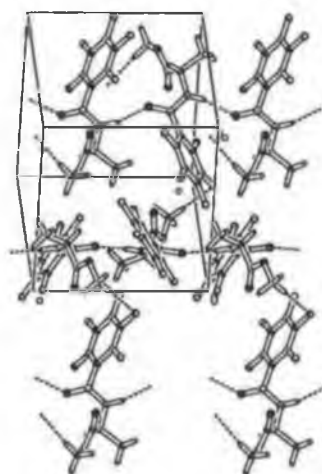


Figure 2.10 PLATON drawing of the X-ray crystal structure of *N*-pentafluorobenzoyl-L-alanine methyl ester **76** depicting the intermolecular interactions.

Compound **81** crystallizes in the orthorhombic space group $P2_12_12_1$ (No.19) with four independent molecules per asymmetric unit. The range of the phenyl C-C bond distances is 1.373(4) to 1.396(3) Å (mean 1.382(4) Å). The carbonyl C=O distance for **81** is 1.221(3) Å. The F-C-C bond angles range from 117.9(2)° to 121.1(3)°. The torsion angle between the phenyl ring and the amide functionality is -53.6(3)°. This is in contrast to the values of **76** which are 54.2(6)° for molecule A and 21.8(6)° for molecule B. The value of 21.8(6)° for molecule B makes the three atom plane O=C-N almost co-planar with respect to the phenyl ring system. The principle interactions in **81** involve the amide N-H and carbonyl groups linked as one-dimensional chains (Figure 2.10).

Table 2.9 Crystal data and structure refinement for *N*-2,4-difluorobenzoyl-L-alanine methyl ester **76** and *N*-pentafluorobenzoyl-L-alanine methyl ester **81**.

	76	81
Empirical formula	C ₁₁ H ₁₁ N ₁ O ₃ F ₂	C ₁₁ H ₈ N ₁ O ₃ F ₅
M _r	243.21	297.18
Crystal color	Colourless, block	Colourless, block
Crystal System	Monoclinic	Orthorhombic
Space group	P2 ₁ (#4)	P2 ₁ 2 ₁ 2 ₁ (#19)
a/Å	5.0014(8)	9.649(4)
b/Å	18.571(2)	10.613(4)
c/Å	6.2184(9)	11.879(5)
β/°	92.496(11)	-
V/Å ³	577.02	1216.47(9)
Z	2	4
Temperature/K	294	150
D _{calc} /gcm ⁻³	1.4	1.623
F ₍₀₀₀₎	252	600
μ/mm ⁻¹	0.123	0.166
Crystal dimensions/mm	0.47 x 0.38 x 0.25	0.42 x 0.22 x 0.12
Index ranges	<i>h</i> , -6-6; <i>k</i> , -22-22; <i>l</i> , -7-7	<i>h</i> , -11-12; <i>k</i> , -13-13; <i>l</i> , -15-15
Max. and min. transmission	0.945 to 0.97	0.933 to 0.980
Refinement method	Full matrix on F ²	Full matrix on F ²
Reflections collected/unique	2612/1177	4975/1574
Data/parameters	1094/174	1377/188
Goodness of fit	1.04	1.07
Final <i>R</i> indices (I>2σ(I))	0.033(R ₁), 0.083(R _w)	0.041(R ₁), 0.101(R _w)
Density range in final diff. map/eÅ ³	-0.12, +0.13	-0.25, +0.26

Table 2.10 Selected bond distances (Å) and angles (°) for **76** and **81** with estimated standard deviations.

	76	81
(a) Bond distances		
C(12)-F(2)	1.353(3), 1.31(3)	1.339(3)
C(14)-F(4)	1.341(4)	1.335(3)
O(1)-C(1)	1.289(9), 1.228(10)	1.221(3)
N(1)-C(1)	1.318(3)	1.336(3)
C(1)-C(11)	1.497(4)	1.510(3)
(b) Bond angles		
O(1)-C(1)-C(11)	114.7(5), 123.4(5)	121.1(2)
F(2)-C(12)-C(11)	119.0(3)	120.4(2)
C(11)-C(1)-N(1)	118.01(19)	114.8(2)
O(1)-C(1)-N(1)	117.3(5), 124.2(5)	124.1(2)

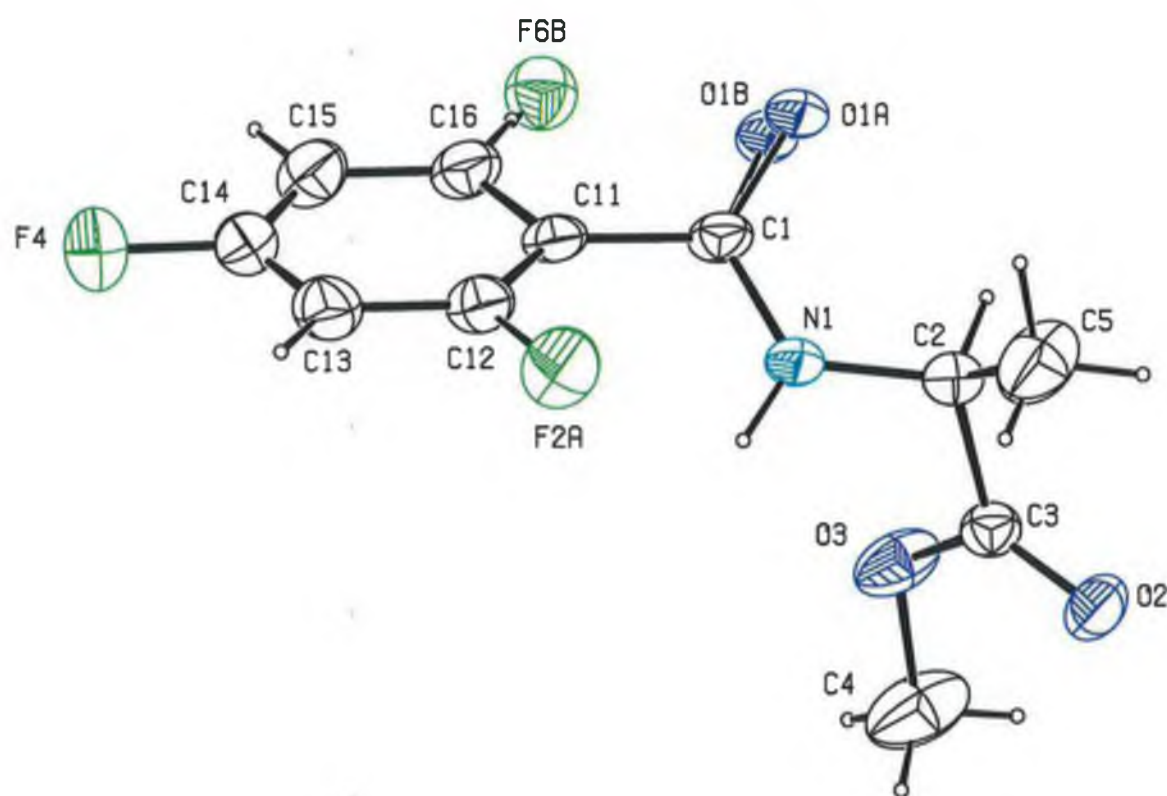


Figure 2.11 ORTEP view of the X-ray crystal structure of *N*-2,4-difluorobenzoyl-L-alanine methyl ester **76**.

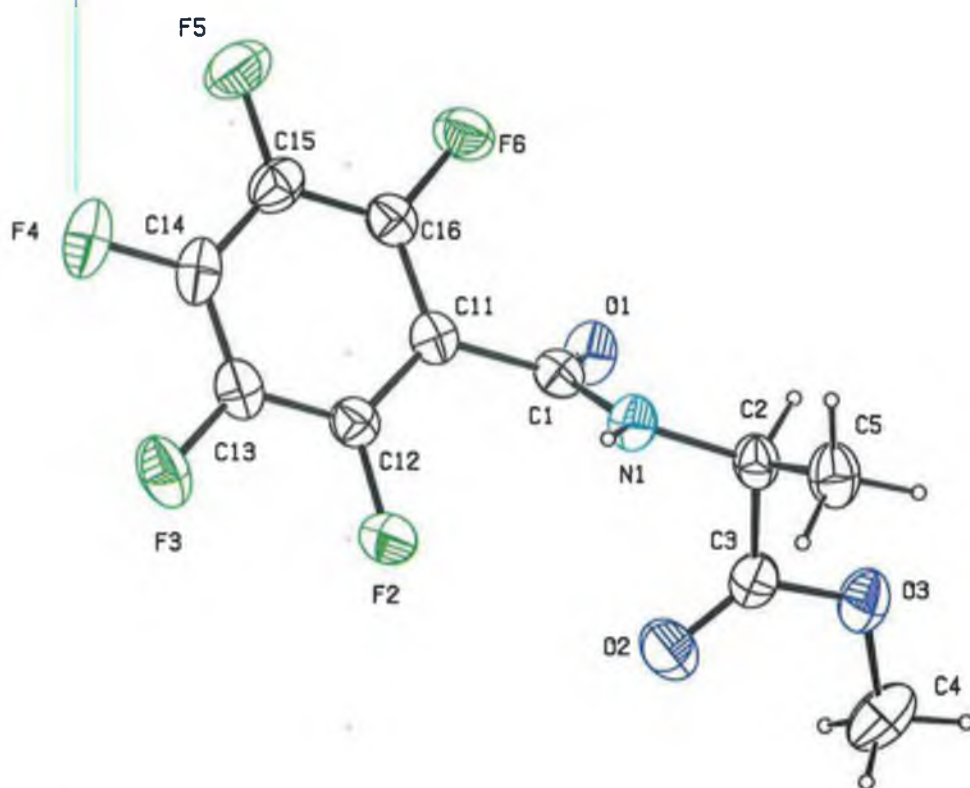


Figure 2.12 ORTEP view of the X-ray crystal structure of *N*-pentafluorobenzoyl-L-alanine methyl ester **81**.

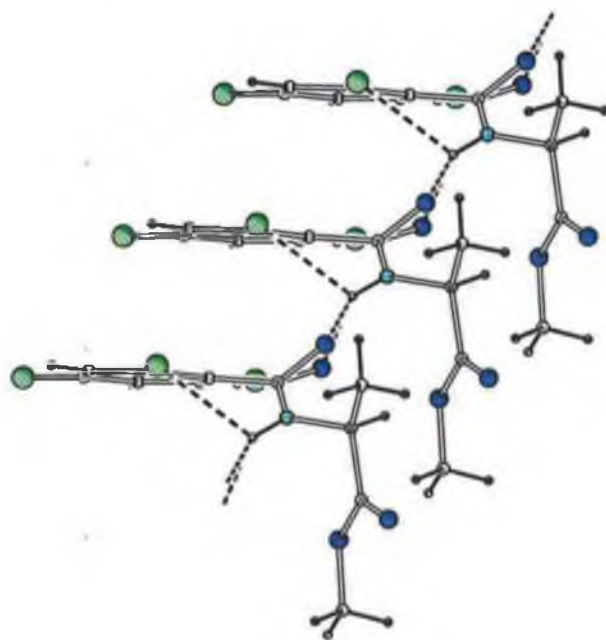


Figure 2.13 PLATON drawing of the X-ray crystal structure of *N*-2,4-difluorobenzoyl-L-alanine methyl ester **76** depicting the intermolecular interactions.

Compound **101** crystallizes in the monoclinic space group $P2_1/c$ with four independent molecules per asymmetric unit. The range of the phenyl C-C bond distances is 1.349(6) to 1.388(4) Å (mean 1.367(4) Å). The phenyl C=O distance for this molecule is 1.244(4) Å but the ester moiety has a carbonyl bond distance of 1.175(5) Å. The F-C-C bond angles range from 117.9(6)° to 121.3(5)°. The amide C(O)-N distance C(1)-N(1) 1.328(4) Å exhibits a lot of single bond character. The principle interactions in **101** involve the amide N-H and carbonyl groups of neighbouring residues interacting as N-H...O=C and forming a one-dimensional chain. There is also a weak intermolecular hydrogen bond formed between the carbonyl of C(1) and C(12) of the aromatic ring (Figure 2.14).

Table 2.11 Crystal data and structure refinement for *N*-3,4-difluorobenzoyl-glycine ethyl ester **101** and *N*-pentafluorobenzoyl-L-leucine methyl ester **114**.

	101	114
Empirical formula	C ₁₁ H ₁₁ N ₁ O ₃ F ₂	C ₁₄ H ₁₄ N ₁ O ₃ F ₅
M _r	243.21	339.26
Crystal color	Colourless, needle	Colourless, block
Crystal System	Monoclinic	Monoclinic
Space group	P2 ₁ /c	P2 ₁
a/Å	4.901(7)	11.878(2)
b/Å	24.729(4)	8.765(18)
c/Å	9.910(2)	15.568(3)
β/°	93.465(13)	106.91(3)
V/Å ³	1198.6(3)	1550.7(5)
Z	4	4
Temperature/K	294	150
D _{calc} /gcm ⁻³	1.348	1.453
F ₍₀₀₀₎	504	696
μ/mm ⁻¹	0.118	0.140
Crystal dimensions/mm	0.40 x 0.40 x 0.10	0.20 x 0.16 x 0.10
Index ranges	<i>h</i> , -6-1; <i>k</i> , -1-29; <i>l</i> , -11-11	<i>h</i> , -15-15; <i>k</i> , -11-9; <i>l</i> , -20-20
Max. and min. transmission	0.954 to 0.988	0.972 to 0.986
Refinement method	Full matrix on F ²	Full matrix on F ²
Reflections collected/unique	3048/2121	13297/3791
Data/parameters	919/175	2549/422
Goodness of fit	1.009	0.994
Final <i>R</i> indices (<i>I</i> >2σ(<i>I</i>))	0.065(<i>R</i> ₁), 0.148(<i>R</i> _w)	0.042(<i>R</i> ₁), 0.091(<i>R</i> _w)
Density range in final diff. map/eÅ ³	-0.15, +0.15	-0.18, +0.20

Refinement has shown that there is disorder associated with **101**. The ester carbonyl oxygen atom is disordered over two sites O1A/O1B which differ in their orientation with respect to the ester moiety and with site occupancy factors subsequently fixed at 50% each.

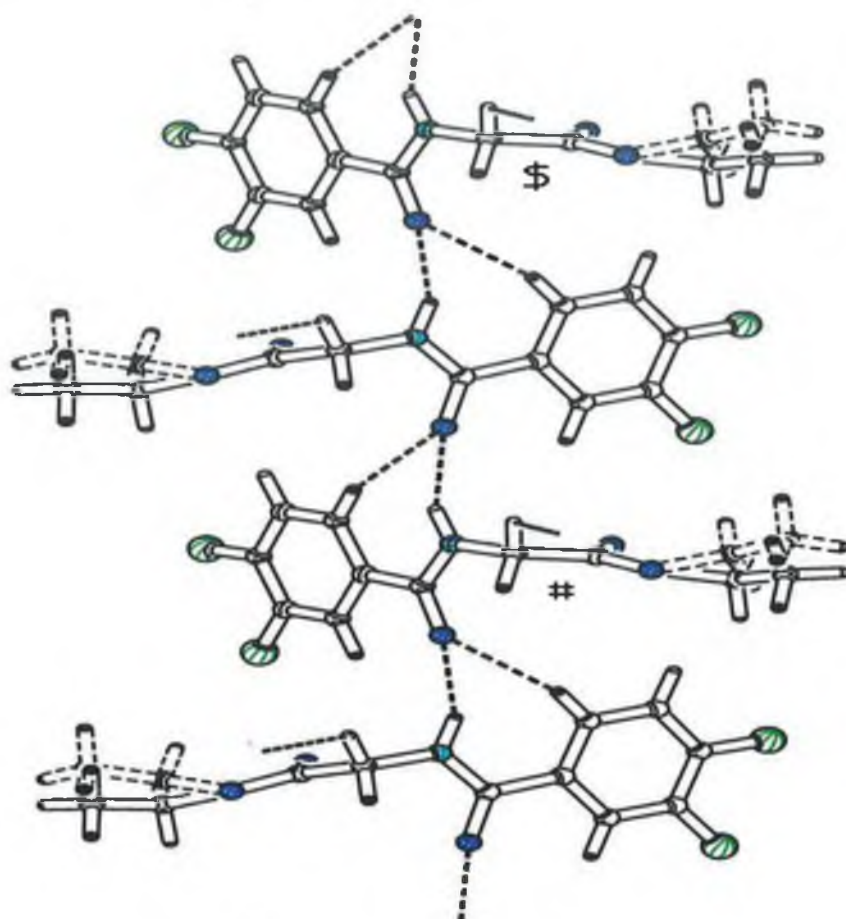


Figure 2.14 PLATON drawing of the X-ray crystal structure of *N*-3,4-difluorobenzoyl-glycine ethyl ester **101** depicting the intermolecular interactions.

Compound **114** crystallizes in the monoclinic space group $P2_1$ with four independent molecules per asymmetric unit. The range of the phenyl C-C bond distances is 1.361(5) to 1.391(4) Å (mean 1.377(5) Å). The carbonyl C=O distance for **114** is 1.237(4) Å. The F-C-C bond angles range from 117.7(3)° to 121.0(3)°. The torsion angle between the phenyl ring and the amide functionality is 54.7(5)°. This value compares favorably with the value of -53.6(3)° for compound **81**. The principle interactions in **114** involve the amide N-H and carbonyl groups linked as one-dimensional chains (Figure 2.17).

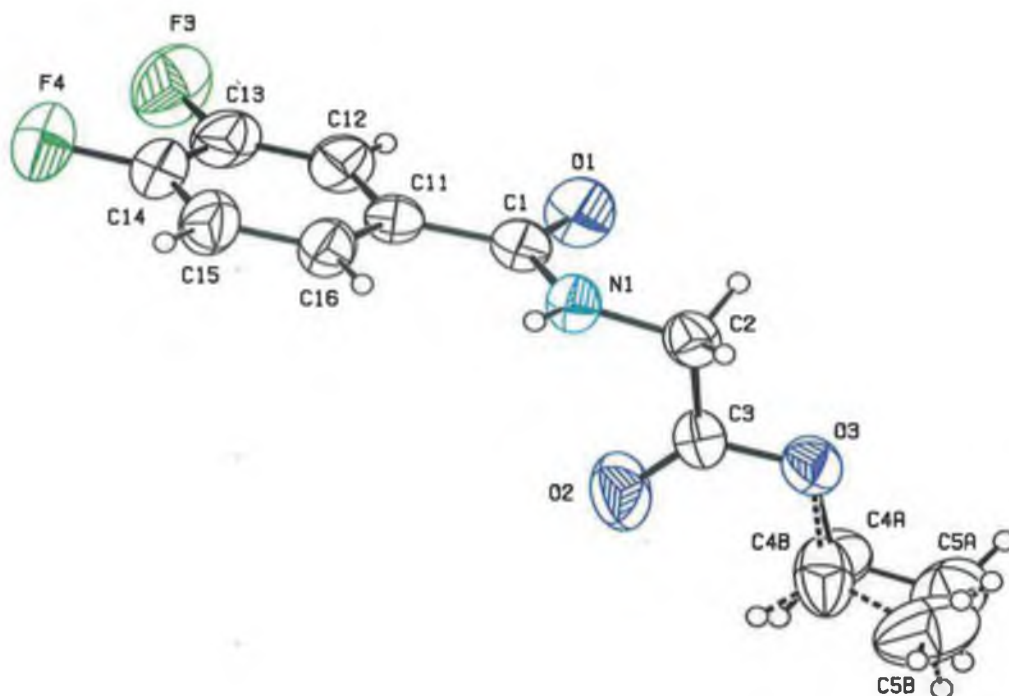


Figure 2.15 ORTEP view of the X-ray crystal structure of *N*-3,4-difluorobenzoyl-glycine ethyl ester **3h**.

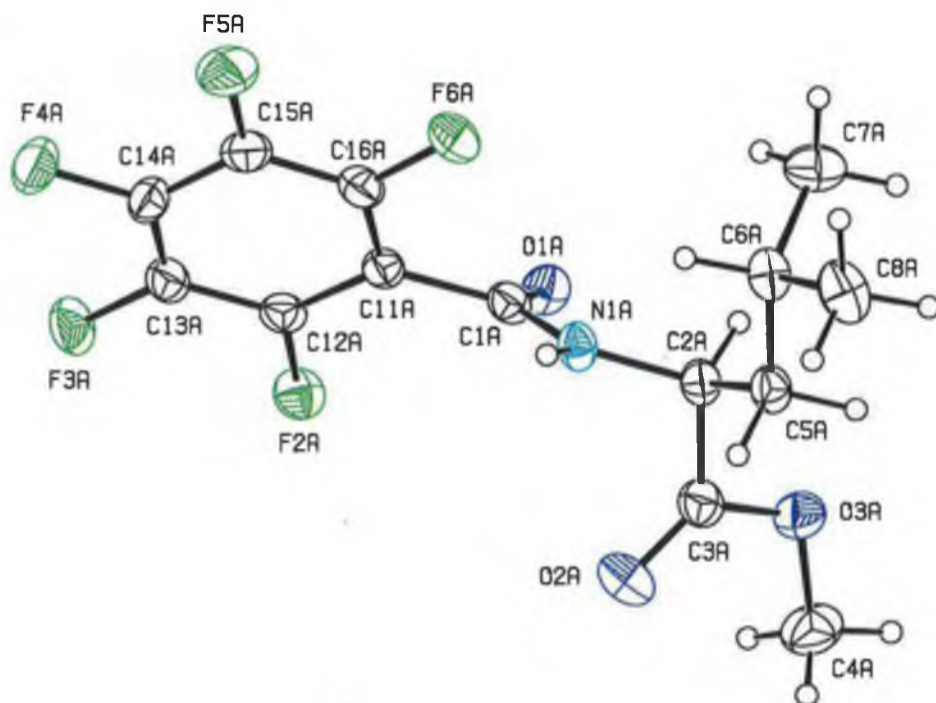


Figure 2.16 ORTEP view of the X-ray crystal structure of *N*-pentafluorobenzoyl-L-leucine methyl ester **114**

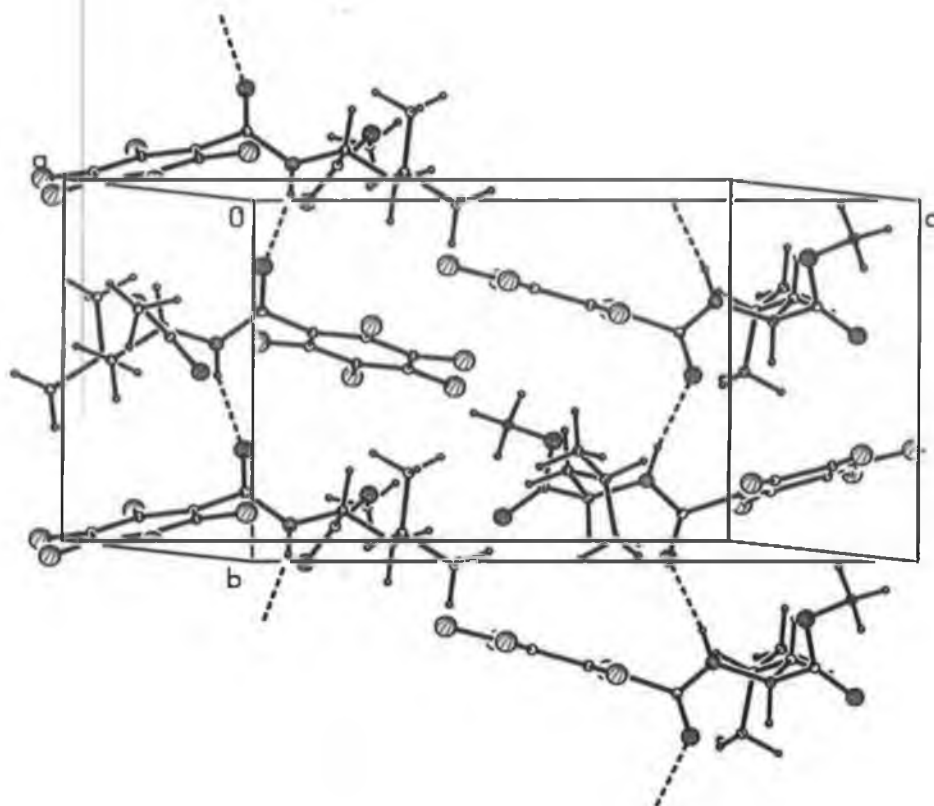


Figure 2.17 PLATON drawing of the X-ray crystal structure of *N*-pentafluorobenzoyl-L-leucine methyl ester **114** depicting the intermolecular interactions.

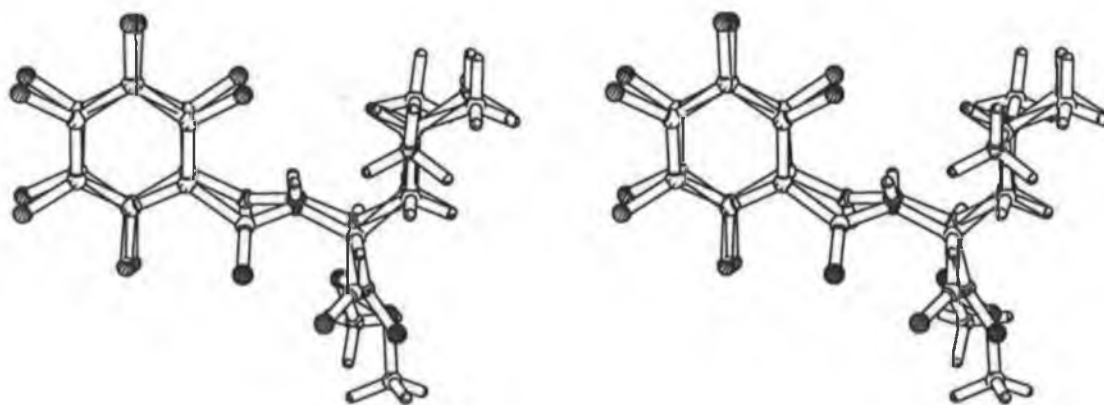


Figure 2.18 PLATON drawing of the X-ray crystal structure of *N*-pentafluorobenzoyl-L-leucine methyl ester **114** depicting the best fit between the two molecules in **114**.

Table 2.12 Selected bond distances (Å) and angles (°) for **101** and **114** with estimated standard deviations.

	101	114
(a) Bond distances		
C(13)-F(3)	1.361(5)	1.3474(4)
C(14)-F(4)	1.353(4)	1.3477(4)
O(1)-C(1)	1.244(4)	1.236(4)
N(1)-C(1)	1.328(4)	1.329(4)
C(1)-C(11)	1.481(5)	1.492(5)
(b) Bond angles		
O(1)-C(1)-C(11)	120.87(4)	121.19(3)
F(3)-C(13)-C(12)	121.3(5)	120.14(3)
F(4)-C(14)-C(13)	119.2(5)	120.75(3)
C(11)-C(1)-N(1)	119.81(3)	115.4(3)
O(1)-C(1)-N(1)	119.32(4)	123.4(3)

At present there is only one example of a *N*-fluorobenzoyl amino acid derivative deposited with the Cambridge Crystallographic Data Center. This derivative *N*-4-fluorobenzoyl-L-valine **116** reported by Coates *et al* has many similarities with compounds **76**, **81**, **101** and **114**.²⁰ The length of the carbon-fluorine bond is 1.359 Å that compares favorably with 1.341 Å (**76**), 1.335 Å (**81**), 1.353 Å (**101**) and 1.347 Å (**114**). The bond distances of compounds **81** and **114** are slightly smaller due to the fact that these compounds are pentafluorobenzoyl derivatives and the selected bond lengths are the length of the carbon-fluorine bond in the *para* position. According to the Cambridge Crystallographic Database April 2004 version the average length of an aromatic carbon-fluorine is 1.348 Å. The length of the amide bond in these derivatives is very similar. Compound **116** has an amide bond length of 1.319 Å compared to of 1.318 Å compound **76**. Compound **101** has an amide bond angle (O1)-(C1)-(N1) of 119.32°. The *N*-4-fluorobenzoyl-L-valine derivative **116** has a similar amide bond angle of 122.37°. Finally the torsion angle between the phenyl ring and the amide shows compounds **76** and **116** to be comparable. Compound **76** has a torsion angle of 21.8° whereas compound **116** has a torsion angle of 26.3° between the phenyl plane and the amide bond.

A gene named MRP-1 (Multidrug Resistance-associated Protein) with a molecular weight of \approx 190 Kda from H69AR cell line has been isolated.²³ MRP-1 is a 1531 amino acid membrane phosphoprotein encoded by a 6.5 kilobase mRNA and is a member of the ATP binding cassette (ABC) family of transmembrane transporters. MRP-1 has also been shown to play a crucial role in protecting tissues from toxin induced damage.²⁶

2.4.2 Cytotoxicity of the *N*-fluorobenzoyl amino acid derivatives

The toxicity of compounds **72-115** was examined. Firstly an IC_{50} of selected compounds was carried out. The IC_{50} is used to determine the concentration of a drug at which 50% cell survival is seen and it is a good indication of the toxicity of a drug. This involved the use of DLKP cells, a lung cancer derived cell line. Each drug was used at a variety of concentrations ranging from 5 μ M to 200 μ M. This involved the incubation of the cells with the drugs for approximately one week, after which the plates were then read using an alkaline phosphatase assay. The results of which were then graphed plotting concentration of the drug in micromoles, against the percentage of cell survival.

Table 2.13 IC_{50} values of the fluorobenzoyl amino acids against DLKP cells

Compound	IC_{50} μ M
74	> 200
76	> 200
81	16
82	> 200
85	> 200
92	17
93	> 200
104	15
114	24
115	17

Compounds **74**, **76**, **82**, **85** and **93** were shown to be relatively non-toxic. A very high percentage of cell survival was seen with all drug concentrations. Due to their non-toxic nature an IC_{50} could not be determined. The remaining compounds tested showed mild toxicity. Compound **81** was

found to be a relatively toxic compound with only 8 % cell survival seen at 200 μ M. An IC₅₀ of this compound was seen at about 16 μ M. *N*-pentafluorobenzoyl-glycine nitrile **104** was shown to be the most potent compound with an IC₅₀ value of 15 μ M.

Cytotoxicity studies on the L-alanine derivatives showed that the pentafluorobenzoyl derivatives **81** and **82**, were more cytotoxic than their difluoro **76** or monofluoro **74** analogues. This could be due to increased lipophilicity and increased acidity of the pentafluoro derivatives. To assess what effect cellular hydrolysis might have on the toxicity of the L-Ala derivatives, the pentafluorobenzoyl acid **82** was analysed. This compound should not undergo hydrolysis due to its lack of an ester moiety and its toxicity was ultimately reduced by more than 12 fold. This shows that perhaps a cellular hydrolytic process or the increased lipophilicity of the ester derivatives is responsible for the cytotoxic nature of the pentafluoro ester compounds. Analysis of the L-phenylalanine derivatives gave similar results with the pentafluorobenzoyl derivative **92** being far more cytotoxic than its monofluoro **85** or acid analogue **93**. The L-leucine analogues also gave analogous results. The pentafluorobenzoyl derivative **114** was once again a cytotoxic agent but when the side chain was increased in size from an 'propyl to an indole group toxicity was increased by 30%. The increased activity of compound **115** must be due to the hydrophobic side chain of tryptophan. Compound **104** was also cytotoxic and this further indicated that a form of hydrolysis was perhaps responsible for the cytotoxic nature of these compounds as the nitrile group has been shown to be a target of hydrolysis.²⁷

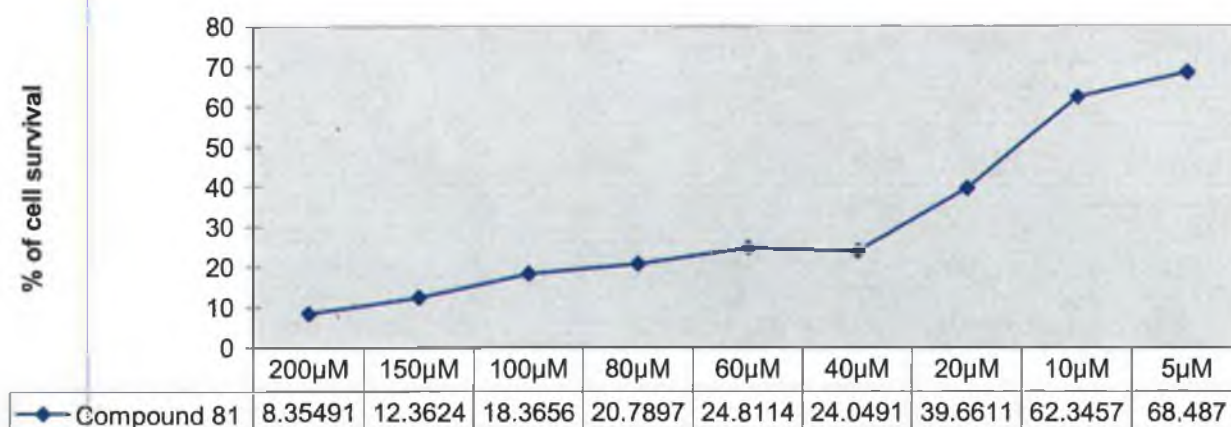
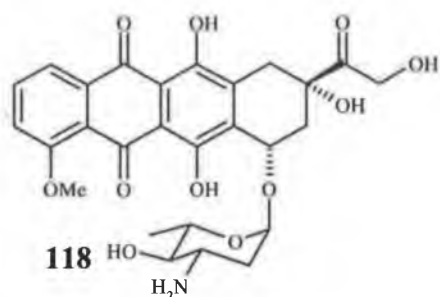


Figure 2.19 Line graph representing the % cell survival of DLKP cells when treated with varying concentrations of *N*-pentafluorobenzoyl-L-alanine methyl ester **81**.

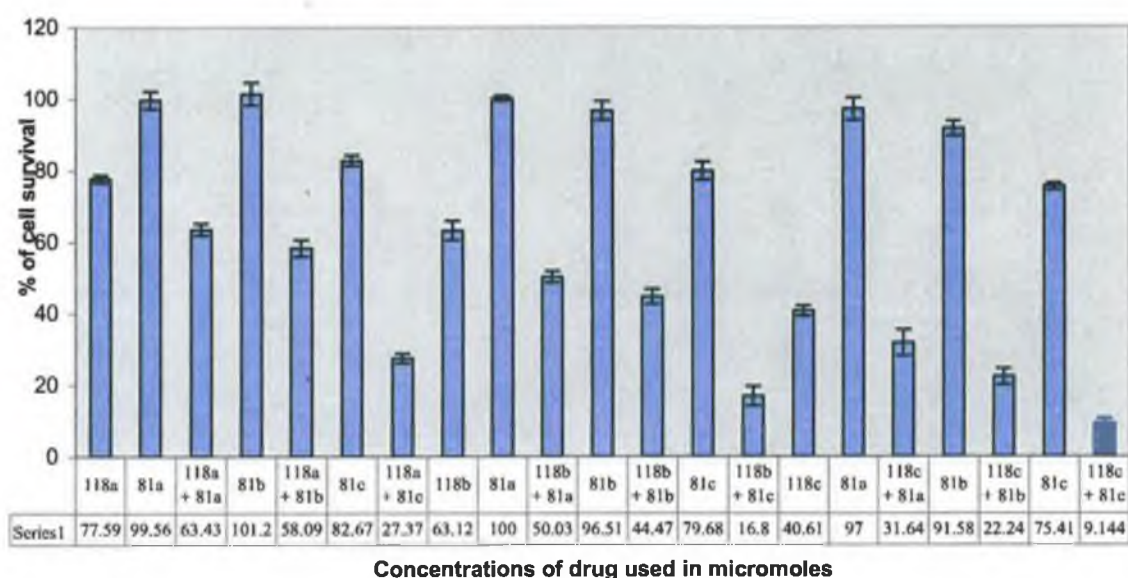
2.4.3 Combination toxicity of *N*-fluorobenzoyl amino acid derivatives and epirubicin

Epirubicin **118** is a potent anthracycline antibiotic. It was first approved for clinical use in France in 1982.²⁸ It is the 4' epimer of doxorubicin with the hydroxy group in an equatorial position. It exerts its effects on cancer cells in three ways. Firstly it inhibits the activity of the enzyme topoisomerase II that is crucial to DNA replication and transcription. It also intercalates between base pairs of DNA and inhibits DNA dependent RNA synthesis. Finally it is known to generate free radicals that cause membrane damage and DNA strand breaks.²⁹ It has broad spectrum anti cancer activity against Hodgkins disease, leukemia, prostate, lung and ovarian



carcinomas.³⁰ Epirubicin or Ellence[®] as it is commercially known is generally used in combination with other chemotherapy drugs to treat breast cancer that has spread to the lymph nodes under the arm following breast cancer surgery.³¹ Its metabolites are relatively non-cytotoxic although adverse effects such as nausea and congestive heart failure have been reported.³² It is generally administered as an intravenous infusion. Epirubicin has increased lipophilicity in comparison to doxorubicin and hence has increased cell penetration. Resistance to epirubicin is caused by two different processes, namely increased inactivation of free radicals caused by an increase in the levels of glutathione dependent enzymes and also increased drug efflux caused by MRP-1 and P-gp.³³

Compounds **81**, **92**, **104**, **114** and **115** were found to be the only compounds exhibiting toxicity and these were combined with epirubicin, to further test their toxicity, and to examine their synergistic toxicity with epirubicin. To do so, a combination toxicity assay involving the fluorobenzoyl amino acid derivatives, compound **118**, and DLKP cells, was carried out. Relatively non-toxic concentrations of these fluorobenzoyl amino acids were combined with various concentrations of epirubicin. Combination toxicity assays involving the non-toxic amino acid derivatives **82** and **93** were also carried out but only after the potency of the toxic analogues was assessed.



Compound **118**; **a** = 0.011 μ M, **b** = 0.013 μ M, **c** = 0.019 μ M.

Compound **81**; **a** = 2 μ M, **b** = 4.5 μ M, **c** = 16 μ M.

Figure 2.20 Combination assay of *N*-pentafluorobenzoyl-L-alanine methyl ester **81** and epirubicin **118** with DLKP.

This combination assay confirmed the toxicity of compound **81**. Compound **81** showed synergistic toxicity with epirubicin. This gives a preliminary indication that this agent may be a substrate and/or inhibitor of the MRP-1 cancer resistance mechanism that is found in DLKP cells. Table 2.14 displays the concentration of each agent used, the cell survival when administered alone and also the cell survival achieved when both agents are administered in combination.

Table 2.14 Synergistic toxicity of the fluorobenzoyl amino acid derivatives

Epirubicin (E) μ M	% Cell Survival	Compound (C)	% Cell Survival	E+C % Cell Survival
19	40.61	81 - 2 μ M	97.02	31.64
6	54.61	82 - 2 μ M	98.64	51.29
4	94.07	92 - 1 μ M	100	88.13
6	55.20	93 - 2 μ M	100	51.17
7	66.37	104 - 2 μ M	95.38	57.06
8	78.22	114 - 1 μ M	94.08	71.22
8	78.22	115 - 1 μ M	95.87	68.46

In terms of cytotoxicity the three most potent compounds were **81**, **104** and **115**. They also showed the best synergistic results when combined with epirubicin. *N*-pentafluorobenzoyl-L-alanine methyl ester **81** improved the cytotoxicity of epirubicin by up to 8.4%. Similar results were recorded for the L-tryptophan **115** and glycine **104** analogues with increased toxicity of up to 10% with compound **115**. Compounds **92** and **114** although not as toxic as compounds **81**, **93** or **104** showed synergistic toxicity, with the toxicity of epirubicin increasing by up to 7%. These results indicate that the more cytotoxic the agent the greater the synergism. Two completely non-toxic derivatives **82** and **93**, were tested for any possible synergism when combined with epirubicin. These compounds showed minor synergistic toxicity when combined with epirubicin with the toxicity of epirubicin increasing between 3-4%. From these results it can be said that the fluorobenzoyl amino acid motif is a substrate and/or inhibitor of the MRP-1 cancer resistance mechanism that is found in DLKP cells.

2.5 Conclusion

The synthesis, structural characterization and biological activity of a series of *N*-fluorobenzoyl amino acid derivatives has been carried out. *N*-fluorobenzoyl amino acid derivatives have been shown to be inhibitors of the MRP-1 cancer resistance mechanism. Further research will be focused on the development of more cytotoxic benzoyl amino acid derivatives as it has been shown that increased cytotoxicity generally equals increased synergistic toxicity. This can be accomplished in three ways. Firstly alternative substitutions with hydroxy or nitro groups on the benzoyl ring that are relatively isosteric to the fluorine atom may increase the polar nature of the compound. Variation in the size and polarity of the amino acid side chain of the amino acid must also be carried out. Finally, the introduction of more electrophilic *C*-terminal substituents such as boronic acids or aldehydes may improve the toxicity of these compounds as the electrophilic nitrile moiety has shown to increase the cytotoxicity of the fluorobenzoyl amino acid esters. Electrophilic isosteres have been shown to be potent inhibitors of the MRP-1 cancer resistance mechanism.³⁴ These factors will be important in developing more cytotoxic agents. We have shown that the indole side chain of L-Try has been shown to be the most effective group to date.

2.6 Experimental

General Procedures.

All chemicals were purchased from Sigma/Aldrich and used as received. When necessary solvents were purified prior to use and stored under nitrogen. Dichloromethane was distilled from CaH₂ and triethylamine was distilled and stored over potassium hydroxide pellets. Commercial grade reagents were used without further purification. Riedel-de Haën silica gel was used for thin layer and column flash chromatography. Melting points were determined using a Griffin melting point apparatus and are uncorrected. Specific rotation $[\alpha]_D$ studies were recorded on a Perkin Elmer 241 polarimeter. Infrared spectra were recorded on a Nicolet 405 FT-IR spectrometer and elemental analysis was carried out by the Microanalytical Laboratory at University College Dublin. Electrospray mass spectra were recorded on a Q-ToF Ultima equipped with a Waters 2790 LC system and a Bruker Esquire 3000 series LC/MS. NMR spectra were obtained on a Bruker AC 400 NMR spectrometer operating at 400 MHz for ¹H NMR, 376 MHz for ¹⁹F NMR and 100 MHz for ¹³C NMR. The ¹H and ¹³C NMR chemical shifts (ppm) are relative to tetramethylsilane and the ¹⁹F NMR chemical shifts (ppm) are relative to trifluoroacetic acid. All coupling constants (*J*) are in Hertz.

General procedure for the synthesis of N-fluorobenzoyl-L-alanine methyl esters 72-81

N-2-fluorobenzoyl-L-alanine methyl ester 72

A solution of 2-fluorobenzoyl chloride (2.00 g, 12.6 mmol) in dichloromethane (20 mls) was added dropwise to a solution of L-alanine methyl ester (1.76 g, 12.6 mmol) and triethylamine (2.55 g) in dichloromethane (20 mls). The solution was stirred for 8 hrs then washed with 5% NaHCO₃, 5% HCl and water. The organic extract was then dried over MgSO₄ and the solvent was removed *in vacuo* to yield a crude oil. Recrystallisation from hexane gave the title product **72** as white crystalline needles (2.11 g, 74%).

m.p. 38-40 °C. $[\alpha]_D^{25} = -6.2^\circ$ (c, 1.32, EtOH).

Anal. calcd. for C₁₁H₁₂N₁O₃F₁: C, 58.66; H, 5.37; N, 6.21; F, 8.44.

Found C, 58.46; H, 5.35; N, 6.10; F, 8.75.

Mass Spectrum: $[M+Na]^+$ found 248.1.

C₁₁H₁₂N₁O₃F₁Na₁ requires 248.2.

IR (KBr): ν 3268, 3101, 1756, 1656, 1504, 1215, 994 cm⁻¹.

¹H-NMR (400 MHz, DMSO): δ 8.75 (1H, d, *J* = 6.8 Hz, -NH-), 7.59-7.64 (1H, m, -ArH 6), 7.52-7.58 (1H, m, -ArH 4), 7.26-7.31 (2H, m, -ArH 3 & 5), 4.45-4.52 (1H, m, α-H), 3.67 (3H, s, -OCH₃), 1.39 (3H, d, *J* = 7.2 Hz, -CH₃).

¹³C-NMR (100 MHz, DMSO): δ 173.2 (-COOCH₃), 164.1 (-ArCO-), 159.5 (d, -ArC 2), 132.9 (d, -ArC 4), 130.4 (d, -ArC 6), 124.7 (d, -ArC 5), 123.8 (d, -ArC 1), 116.4 (d, -ArC 3), 52.3 (-OCH₃), 48.5 (α-C), 17.0 (-CH₃).

¹⁹F-NMR (376 MHz, DMSO): δ -38.9 - -38.6 (m).

***N*-3-fluorobenzoyl-L-alanine methyl ester 73**

3-Fluorobenzoyl chloride (2.00 g, 12.6 mmol) was used. Recrystallisation from hexane yielded **73** as a white powder (1.97 g, 69%).

m.p. 41-43 °C. [α]_D²⁵ = -14.2° (c, 4.0, EtOH).

Anal. calcd. for C₁₁H₁₂N₁O₃F₁: C, 58.66; H, 5.37; N, 6.21; F, 8.44.

Found C, 58.35; H, 5.30; N, 6.10; F, 8.84.

Mass Spectrum: [M+Na]⁺ found 248.1.

C₁₁H₁₂N₁O₃F₁Na₁ requires 248.2.

IR (KBr): ν 3322, 3072, 1748, 1641, 1542, 1227, 756 cm⁻¹.

¹H-NMR (400 MHz, DMSO): δ 8.91 (1H, d, *J* = 6.8 Hz, -NH-), 7.68-7.77 (2H, m, -ArH 2 & 6), 7.51-7.57 (1H, m, -ArH 5), 7.38-7.43 (1H, m, -ArH 4), 4.45-4.52 (1H, m, α-H), 3.67 (3H, s, -OCH₃), 1.41 (3H, d, *J* = 7.2 Hz, -CH₃).

¹³C-NMR (100 MHz, DMSO): δ 173.4 (-COOCH₃), 165.2 (d, -ArCO-), 163.3 (d, -ArC 3), 136.3 (d, -ArC 1), 130.7 (d, -ArC 5), 123.9 (d, -ArC 6), 118.6 (d, -ArC 4), 114.5 (d, -ArC 2), 52.2 (-OCH₃), 48.7 (α-C), 16.9 (-CH₃).

¹⁹F-NMR (376 MHz, DMSO): δ -37.3 - -37.2 (m).

***N*-4-fluorobenzoyl-L-alanine methyl ester 74**

4-Fluorobenzoyl chloride (2.00 g, 12.6 mmol) was used. Recrystallisation from hexane furnished **74** as white crystalline needles (2.22 g, 78%).

m.p. 70-72 °C. [α]_D²⁵ = -10.2° (c, 3.4, EtOH).

Anal. calcd. for C₁₁H₁₂N₁O₃F₁: C, 58.66; H, 5.37; N, 6.21; F, 8.44.

Found C, 58.87; H, 5.40; N, 6.10; F, 8.82.

Mass Spectrum: [M+Na]⁺ found 248.1.

$C_{11}H_{12}N_1O_3F_1Na_1$ requires 248.2.

IR (KBr): ν 3290, 3083, 1755, 1642, 1548, 1215, 846 cm^{-1} .

1H -NMR (400 MHz, DMSO): δ 8.84 (1H, d, $J = 6.8$ Hz, -NH-), 7.97-8.00 (2H, m, -ArH 2 & 6), 7.27-7.31 (2H, m, -ArH 3 & 5), 4.47-4.54 (1H, m, α -H), 3.65 (3H, s, -OCH₃), 1.41 (3H, d, $J = 7.6$ Hz, -CH₃).

^{13}C -NMR (100 MHz, DMSO): δ 173.5 (-COOCH₃), 165.6 (-ArCO-), 164.3 (d, -ArC 4), 130.5 (-ArC 2), 130.45 (-ArC 1), 130.4 (-ArC 6), 115.5 (-ArC 3), 115.3 (-ArC 5), 52.1 (-OCH₃), 48.7 (α -C), 16.9 (-CH₃).

^{19}F -NMR (376 MHz, DMSO): δ -33.8 - -33.6 (m).

***N*-2,3-difluorobenzoyl-L-alanine methyl ester 75**

2,3-Difluorobenzoyl chloride (2.00 g, 11 mmol) and L-alanine methyl ester (1.54 g, 11 mmol) were used. Recrystallisation from hexane furnished **75** as a white powder (1.26 g, 47%).

m.p. 46-48 °C. $[\alpha]_D^{25} = -10.7^\circ$ (c, 7.2, EtOH).

Anal. calcd. for $C_{11}H_{11}N_1O_3F_2$: C, 54.32; H, 4.55; N, 5.75; F, 15.62.

Found C, 54.18; H, 4.47; N, 5.38; F, 15.39.

Mass Spectrum: $[M+Na]^+$ found 266.1.

$C_{11}H_{11}N_1O_3F_2Na_1$ requires 266.1.

IR (KBr): ν 3303, 3059, 1760, 1643, 1536, 1482, 762 cm^{-1} .

1H -NMR (400 MHz, DMSO): δ 8.92 (1H, d, $J = 6.8$ Hz, -NH-), 7.42-7.57 (1H, m, -ArH 6), 7.38-7.42 (1H, m, -ArH 5), 7.27-7.32 (1H, m, -ArH 4), 4.46-4.53 (1H, m, α -H), 3.68 (3H, s, -OCH₃), 1.39 (3H, d, $J = 7.6$ Hz, -CH₃).

^{13}C -NMR (100 MHz, DMSO): δ 172.9 (-COOCH₃), 163.0 (d, -ArCO-), 148.6 (dd, -ArC 3), 147.5 (dd, -ArC 2), 126.2 (d, -ArC 1), 125.3 (t, -ArC 4), 125.2 (d, -ArC 5), 119.6 (d, -ArC 6), 52.2 (-OCH₃), 48.5 (α -C), 16.9 (-CH₃).

^{19}F -NMR (376 MHz, DMSO): δ -63.1 - -63.0 (m), -65.1 - -65.0 (m).

***N*-2,4-difluorobenzoyl-L-alanine methyl ester 76**

2,4-Difluorobenzoyl chloride (2.00 g, 11 mmol) was used. Recrystallisation from hexane furnished **76** as colourless block shaped crystals (1.42 g, 53%) which were of sufficient quality for an X-ray diffraction study.

m.p. 59-61 °C. $[\alpha]_D^{25} = -6.5^\circ$ (c, 8.3, EtOH).

Anal. calcd. for C₁₁H₁₁N₁O₃F₂: C, 54.32; H, 4.55; N, 5.75; F, 15.62.

Found C, 54.42; H, 4.56; N, 5.62; F, 15.83.

Mass Spectrum: [M+Na]⁺ found 266.1.

C₁₁H₁₁N₁O₃F₂Na₁ requires 266.1.

IR (KBr): ν 3306, 3073, 1739, 1646, 1542, 1276, 966 cm⁻¹.

¹H-NMR (400 MHz, DMSO): δ 8.73 (1H, d, J = 6.8 Hz, -NH-), 7.66-7.72 (1H, m, -ArH 6), 7.32-7.38 (1H, m, -ArH 5), 7.15-7.20 (1H, m, -ArH 3), 4.46-4.50 (1H, m, α -H), 3.67 (3H, s, -OCH₃), 1.38 (3H, d, J = 7.2 Hz, -CH₃).

¹³C-NMR (100 MHz, DMSO): δ 173.0 (-COOCH₃), 164.1 (dd, -ArC 4), 163.2 (d, -ArCO-), 160.1 (dd, -ArC 2), 132.2 (dd, -ArC 6), 120.4 (dd, -ArC 1), 112.0 (dd, -ArC 3), 104.9 (t, -ArC 5), 52.2 (-OCH₃), 48.5 (α -C), 17.0 (-CH₃).

¹⁹F-NMR (376 MHz, DMSO) δ : -30.7 (qt, J = 8 Hz), -33.6 (q, J = 8 Hz).

***N*-2,5-difluorobenzoyl-L-alanine methyl ester 77**

2,5-Difluorobenzoyl chloride (2.00 g, 11 mmol) was used. Recrystallisation from hexane furnished **77** as brown crystalline needles (1.15 g, 43%).

m.p. 50-52 °C. [α]_D²⁵ = -5.8° (c, 2.0, EtOH).

Anal. calcd. for C₁₁H₁₁N₁O₃F₂: C, 54.32; H, 4.55; N, 5.75; F, 15.62.

Found C, 54.27; H, 4.55; N, 5.72; F, 15.94.

Mass Spectrum: [M+Na]⁺ found 266.1.

C₁₁H₁₁N₁O₃F₂Na₁ requires 266.1.

IR (KBr): ν 3304, 3073, 1760, 1647, 1542, 1184, 747 cm⁻¹.

¹H-NMR (400 MHz, DMSO): δ 8.83 (1H, d, J = 6.8 Hz, -NH-), 7.34-7.45 (3H, m, -ArH 3, 4 & 6), 4.44-4.51 (1H, m, α -H), 3.67 (3H, s, -OCH₃), 1.39 (3H, d, J = 7.2 Hz, -CH₃).

¹³C-NMR (100 MHz, DMSO): δ 174.1 (-COOCH₃), 163.1 (-ArCO-), 158.1 (dd, -ArC 5), 155.7 (dd, -ArC 2), 125.0 (dd, -ArC 1), 119.4 (dd, -ArC 4), 118.3 (dd, -ArC 3), 116.5 (dd, -ArC 6), 52.3 (-OCH₃), 48.5 (α -C), 17.0 (-CH₃).

¹⁹F-NMR (376 MHz, DMSO): δ -42.9 - -42.8 (m), -44.1 - -44.0 (m).

***N*-2,6-difluorobenzoyl-L-alanine methyl ester 78**

2,6-Difluorobenzoyl chloride (2.00 g, 11 mmol) was used. Recrystallisation from hexane furnished **78** as white crystalline needles (1.65 g, 62%).

m.p. 62-64 °C. $[\alpha]_D^{25} = -16.2^\circ$ (c, 6.5, EtOH).

Anal. calcd. for $C_{11}H_{11}N_1O_3F_2$: C, 54.32; H, 4.55; N, 5.75; F, 15.62.

Found C, 54.40; H, 4.62; N, 5.72; F, 15.42.

Mass Spectrum: $[M+Na]^+$ found 266.1.

$C_{11}H_{11}N_1O_3F_2Na_1$ requires 266.1.

IR (KBr): ν 3308, 3002, 1735, 1656, 1623, 1006, 793 cm^{-1} .

1H -NMR (400 MHz, DMSO): δ 9.19 (1H, d, $J = 6.8$ Hz, -NH-), 7.51-7.55 (1H, m, -ArH 4), 7.15-7.19 (2H, m, -ArH 3 & 5), 4.47-4.51 (1H, m, α -H), 3.67 (3H, s, -OCH₃), 1.35 (3H, d, $J = 7.2$ Hz, -CH₃).

^{13}C -NMR (100 MHz, DMSO): δ 172.7 (-COOCH₃), 160.4 (d, -ArC 2), 159.9 (-ArCO-), 157.9 (d, -ArC 6), 132.1 (t, -ArC 4), 115.2 (-ArC 1), 112.3 (d, -ArC 3), 112.1 (d, -ArC 5), 52.3 (-OCH₃), 48.4 (α -C), 17.1 (-CH₃).

^{19}F -NMR (376 MHz, DMSO): δ -38.0 (t, $J = 7.6$ Hz).

***N*-3,4-difluorobenzoyl-L-alanine methyl ester 79**

3,4-Difluorobenzoyl chloride (2.00 g, 11 mmol) was used. Recrystallisation from hexane furnished **79** as white crystalline needles (1.57 g, 58%).

m.p. 72-74 °C. $[\alpha]_D^{25} = -12.1^\circ$ (c, 5.0, EtOH).

Anal. calcd. for $C_{11}H_{11}N_1O_3F_2$: C, 54.32; H, 4.55; N, 5.75; F, 15.62.

Found C, 54.30; H, 4.57; N, 5.72; F, 15.81.

Mass Spectrum: $[M+Na]^+$ found 266.1.

$C_{11}H_{11}N_1O_3F_2Na_1$ requires 266.1.

IR (KBr): ν 3291, 3083, 1747, 1641, 1547, 1218, 777 cm^{-1} .

1H -NMR (400 MHz, DMSO): δ 8.92 (1H, d, $J = 6.8$ Hz, -NH-), 7.81-7.96 (1H, m, -ArH 6), 7.78-7.81 (1H, m, -ArH 2), 7.52-7.59 (1H, m, -ArH 5), 4.46-4.49 (1H, m, α -H), 3.66 (3H, s, -OCH₃), 1.41 (3H, d, $J = 7.2$ Hz, -CH₃).

^{13}C -NMR (100 MHz, DMSO): δ 173.3 (-COOCH₃), 164.3 (d, -ArCO), 152.0 (dd, -ArC 4), 149.4 (dd, -ArC 3), 131.2 (t, -ArC 1), 125.3 (dd, -ArC 2), 117.8 (d, -ArC 5), 117.1 (d, -ArC 6), 52.3 (-OCH₃), 48.5 (α -C), 17.0 (-CH₃).

^{19}F -NMR (376 MHz, DMSO): δ -58.9 - -58.7 (m), -62.6 - -62.5 (m).

***N*-3,5-difluorobenzoyl-L-alanine methyl ester 80**

3,5-Difluorobenzoyl chloride (2.00 g, 11 mmol) was used. Recrystallisation from hexane furnished **80** as white crystalline needles (1.42 g, 53%).

m.p. 64-66 °C. $[\alpha]_D^{25} = -13.6^\circ$ (c, 8.0, EtOH).

Anal. calcd. for $C_{11}H_{11}N_1O_3F_2$: C, 54.32; H, 4.55; N, 5.75; F, 15.62.

Found C, 53.93; H, 4.41; N, 5.78; F, 15.98.

Mass Spectrum: $[M+Na]^+$ found 266.1.

$C_{11}H_{11}N_1O_3F_2Na_1$ requires 266.1.

IR (KBr): ν 3330, 3097, 1746, 1647, 1535, 1126, 988 cm^{-1} .

1H -NMR (400 MHz, DMSO): δ 8.91 (1H, d, $J = 6.8$ Hz, -NH-), 7.50-7.54 (2H, m, -ArH 2 & 6), 7.33-7.38 (1H, m, -ArH 4), 4.39-4.46 (1H, m, α -H), 3.59 (3H, s, -OCH₃), 1.34 (3H, d, $J = 7.2$ Hz, -CH₃).

^{13}C -NMR (100 MHz, DMSO): δ 173.3 (-COOCH₃), 164.3 (t, -ArCO-), 163.7 (d, -ArC 3), 161.3 (d, -ArC 5), 137.3 (-ArC 1), 111.1 (d, -ArC 2), 110.9 (d, -ArC 6), 107.1 (t, -ArC 4), 52.3 (-OCH₃), 48.5 (α -C), 17.0 (-CH₃).

^{19}F -NMR (376 MHz, DMSO): δ -33.5 (t, $J = 9$ Hz).

***N*-pentafluorobenzoyl-L-alanine methyl ester 81**

Pentafluorobenzoyl chloride (1.52 g, 6.6 mmol) and L-alanine methyl ester (0.92 g, 6.6 mmol) were used. Recrystallisation from hexane furnished **81** as white crystalline needles (0.81 g, 41%) that were of sufficient quality for an X-ray diffraction study.

m.p. 83-85 °C. $[\alpha]_D^{25} = -5.6^\circ$ (c, 7.2, EtOH).

Mass Spectrum: $[M+H]^+$ found 298.0502.

$C_{11}H_9N_1O_3F_5$ requires 298.0503.

IR (KBr): ν 3296, 3102, 1759, 1658, 1565, 1357 cm^{-1} .

1H -NMR (400 MHz, DMSO): δ 9.42 (1H, d, $J = 6.8$ Hz, -NH-), 4.47-4.55 (1H, m, α -H), 3.68 (3H, s, -OCH₃), 1.37 (3H, d, $J = 7.2$ Hz, -CH₃).

^{13}C -NMR (100 MHz, DMSO): δ 172.4 (-COOCH₃), 156.9 (-ArCO-), 144.7-144.8 (m, -ArC 2), 140.3-142.8 (m, -ArC 4), 142.1-142.3 (m, -ArC 6), 138.4-138.6 (m, -ArC 3), 135.9-136.1 (m, -ArC 5), 112.4 (t, -ArC 1), 52.4 (-OCH₃), 48.6 (α -C), 17.0 (-CH₃).

^{19}F -NMR (376 MHz, DMSO): δ -66.5 (dd, 2F, $J^4 = 6.8$ Hz, $J^3 = 22$ Hz), -77.6 (t, 1F, $J = 16.8$ Hz), -86.2 - -86.3 (m, 2F).

***N*-pentafluorobenzoyl-L-alanine 82**

L-Alanine (0.45 g, 5.0 mmol) was added to a solution of water (5 mls) and sodium hydroxide (0.4 g, 10 mmol) at room temperature. The reaction mixture was then heated to 85 °C and pentafluorobenzoyl chloride (1.16 g, 5mmol) was added over a period of 20 mins. After the addition was complete the reaction was left stirring for an additional 30 mins. The solution was then cooled and acidified with conc. HCl. This was washed with water and recrystallisation from EtOH gave the title product as a white powder (1.03g, 73%).

m.p. 136-138 °C. $[\alpha]_{\text{D}}^{25} = -12.8^\circ$ (c, 7.2, EtOH).

Mass Spectrum: $[\text{M}+\text{Na}]^+$ found 305.9.

$\text{C}_{10}\text{H}_6\text{N}_1\text{O}_3\text{F}_5\text{Na}_1$ requires 306.14.

IR (KBr): ν 3497, 3297, 1661, 1555, 1489, 813 cm^{-1} .

^1H -NMR (400 MHz, DMSO): δ 12.89 (1H, s, -OH), 9.31 (1H, d, $J = 7.6$ Hz, -NH-), 4.37-4.45 (1H, m, α -H), 1.36 (3H, d, $J = 7.6$ Hz, -CH₃).

^{13}C -NMR (100 MHz, DMSO): δ 173.4 (-COOH), 156.7 (-ArCO-), 144.5-144.7 (m, -ArC 2), 140.2-142.7 (m, -ArC 4), 142.1-142.3 (m, -ArC 6), 138.3-138.6 (m, -ArC 3), 135.9-136.1 (m, -ArC 5), 112.5 (t, -ArC 1), 48.6 (α -C), 17.2 (-CH₃).

^{19}F -NMR (376 MHz, DMSO): δ -66.5 (dd, 2F, $J^4 = 6.4$ Hz, $J^3 = 22.9$ Hz), -77.9 (t, 1F, $J = 22.1$ Hz), -86.4 - -86.5 (m, 2F).

General procedure for the synthesis of N-fluorobenzoyl-L-phenylalanine methyl esters 83-92

***N*-2-fluorobenzoyl-L-phenylalanine methyl ester 83**

A solution of 2-fluorobenzoyl chloride (2.00 g, 12.6 mmol) in dichloromethane (20 mls) was added dropwise to a solution of L-phenylalanine methyl ester (2.72 g, 12.6 mmol) and triethylamine (2.55 g) in dichloromethane (20 mls). The solution was stirred for 8 hrs then washed with 5% NaHCO₃, 5% HCl and water. The organic extract was then dried over MgSO₄ and the solvent was removed *in vacuo* to yield a crude orange oil. Recrystallisation from ethyl acetate gave the title product as a yellow solid (2.22 g, 56%).

m.p. 47-48 °C. $[\alpha]_{\text{D}}^{25} = -3.8^\circ$ (c, 5.0, EtOH).

Anal. calcd. for $\text{C}_{17}\text{H}_{16}\text{N}_1\text{O}_3\text{F}_1$: C, 67.76; H, 5.35; N, 4.65; F, 6.31.

Found C, 67.38; H, 5.16; N, 4.58; F, 6.50.

Mass Spectrum: $[M+Na]^+$ found 324.2.

$C_{17}H_{16}N_1O_3F_1Na_1$ requires 324.2.

IR (KBr): ν 3276, 3032, 1736, 1647, 1542, 1216, 759 cm^{-1} .

1H -NMR (400 MHz, DMSO): δ 8.73 (1H, d, $J = 5.6$ Hz, -NH-), 7.50-7.60 (2H, m, -ArH 4 & 6), 7.23-7.35 (7H, m, -ArH 3 & 5, -PhH), 4.75-4.81 (1H, m, α -H), 3.69 (3H, s, -OCH₃), 3.23 (1H, dd, $J^3 = 5.2$ Hz, $J^2 = 14.0$ Hz, -CH₂-), 3.13 (1H, dd, $J^3 = 9.6$ Hz, $J^2 = 13.6$ Hz, -CH₂-).

^{13}C -NMR (100 MHz, DMSO): δ 172.1 (-COOCH₃), 164.2 (-ArCO-), 159.6 (d, -ArC 2), 137.6 (-PhC 1), 133.0 (d, -ArC 4), 130.4 (d, -ArC 6), 129.4 (-PhC 3 & 5), 128.5 (-PhC 2 & 6), 126.9 (-PhC 4), 124.7 (d, -ArC 5), 123.5 (d, -ArC 1), 116.4 (d, -ArC 3), 54.5 (α -C), 52.3 (-OCH₃), 36.7 (-CH₂-, -VE DEPT).

^{19}F -NMR (376 MHz, DMSO): δ -38.5 - -38.7(m).

***N*-3-fluorobenzoyl-L-phenylalanine methyl ester 84**

3-Fluorobenzoyl chloride (2.00 g, 12.6 mmol) was used. Recrystallisation from ethyl acetate furnished **84** as a pale brown solid (1.78 g, 45%).

m.p. 63-65 °C. $[\alpha]_D^{25} = -44.5^\circ$ (c, 7.5, EtOH).

Anal. calcd. for $C_{17}H_{16}N_1O_3F_1$: C, 67.76; H, 5.35; N, 4.65; F, 6.31.

Found C, 67.51; H, 5.16; N, 4.43; F, 6.08.

Mass Spectrum: $[M+Na]^+$ found 324.2.

$C_{17}H_{16}N_1O_3F_1Na_1$ requires 324.2.

IR (KBr): ν 3313, 3063, 1741, 1638, 1527, 621 cm^{-1} .

1H -NMR (400 MHz, DMSO): δ 9.03 (1H, d, $J = 7.6$ Hz, -NH-), 7.68-7.70 (1H, m, -ArH 6), 7.61-7.64 (1H, m, -ArH 2), 7.48-7.54 (1H, m, -ArH 5), 7.14-7.17 (6H, m, -ArH 4 & -PhH), 4.67-4.73 (1H, m, α -H), 3.67 (3H, s, -OCH₃), 3.20 (1H, dd, $J^3 = 5.2$ Hz, $J^2 = 13.6$ Hz, -CH₂-), 3.12 (1H, dd, $J^3 = 10.4$ Hz, $J^2 = 13.6$ Hz, -CH₂-).

^{13}C -NMR (100 MHz, DMSO): δ 172.3 (-COOCH₃), 165.4 (d, -ArCO-), 163.2 (d, -ArC 3), 137.9 (-PhC 1), 136.2 (d, -ArC 1), 130.8 (d, -ArC 5), 129.4 (-PhC 3 & 5) 128.5 (-PhC 2 & 6), 126.8 (-PhC 4), 123.9 (d, -ArC 6), 118.7 (d, -ArC 4), 114.5 (d, -ArC 2), 54.7 (α -C), 52.3 (-OCH₃), 36.5 (-CH₂-, -VE DEPT).

^{19}F -NMR (376 MHz, DMSO): δ -37.5 - -37.6 (m).

***N*-4-fluorobenzoyl-L-phenylalanine methyl ester 85**

4-Fluorobenzoyl chloride (2.00 g, 12.6 mmol) was used. Recrystallisation from ethyl acetate furnished **85** as a yellow solid (1.98 g, 49%).

m.p. 70-72 °C. $[\alpha]_D^{25} = -47^\circ$ (c, 2.5, EtOH).

Anal. calcd. for $C_{17}H_{16}N_1O_3F_1$: C, 67.76; H, 5.35; N, 4.65; F, 6.31.

Found C, 67.34; H, 5.21; N, 4.43; F, 6.32.

Mass Spectrum: $[M+Na]^+$ found 324.2.

$C_{17}H_{16}N_1O_3F_1Na_1$ requires 324.2.

IR (KBr): ν 3310, 3075, 1737, 1637, 1501, 770 cm^{-1} .

1H -NMR (400 MHz, DMSO): δ 8.96 (1H, d, $J = 8.0$ Hz, -NH-), 7.92-7.96 (2H, m, -ArH 2 & 6), 7.17-7.35 (7H, m, -ArH 3&5, -PhH), 4.72-4.78 (1H, m, α -H), 3.66 (3H, s, -OCH₃), 3.23 (1H, dd, $J^3 = 5.2$ Hz, $J^2 = 14.0$ Hz, -CH₂-), 3.15 (1H, dd, $J^3 = 10.0$ Hz, $J^2 = 13.6$ Hz, -CH₂-).

^{13}C -NMR (100 MHz, DMSO): δ 172.5 (-COOCH₃), 165.8 (d, -ArCO-), 164.3 (d, -ArC 4), 138.0 (-PhC 1), 130.4 (-ArC 1), 130.4 (-ArC 2), 130.4 (-ArC 6), 129.3 (-PhC 3 & 5), 128.5 (-PhC 2 & 6), 126.8 (-PhC 4), 115.6 (-ArC 3), 115.3 (-ArC 5), 54.7 (α -C), 52.2 (-OCH₃), 36.4 (-CH₂-, -VE DEPT).

^{19}F -NMR (376 MHz, DMSO): δ -33.6 - -33.7 (m).

***N*-2,3-difluorobenzoyl-L-phenylalanine methyl ester 86**

2,3-Difluorobenzoyl chloride (2.23 g, 12.6 mmol) was used. Recrystallisation from ethyl acetate/pet ether 40-60 °C furnished **86** as a white solid (2.25 g, 56%).

m.p. 76-78 °C. $[\alpha]_D^{25} = -18.5^\circ$ (c, 5.4, EtOH).

Anal. calcd. for $C_{17}H_{15}N_1O_3F_2$: C, 63.95; H, 4.74; N, 4.39; F, 11.90.

Found C, 63.85; H, 4.71; N, 4.35; F, 11.61.

Mass Spectrum: $[M+Na]^+$ found 342.2.

$C_{17}H_{15}N_1O_3F_2Na_1$ requires 342.2.

IR (KBr): ν 3309, 2955, 1737, 1645, 1537, 701 cm^{-1} .

1H -NMR (400 MHz, DMSO): δ 8.80 (1H, d, $J = 7.6$ Hz, -NH-), 7.35-7.38 (1H, m, -ArH 6), 7.17-7.20 (5H, m, -PhH), 7.11-7.14 (2H, m, -ArH 4 & 5), 4.63-4.66 (1H, m, α -H), 3.57 (3H, s, -OCH₃), 3.10 (1H, dd, $J^3 = 5.2$ Hz, $J^2 = 14.0$ Hz, -CH₂-), 2.98 (1H, dd, $J^3 = 10.0$ Hz, $J^2 = 13.6$ Hz, -CH₂-).

^{13}C -NMR (100 MHz, DMSO): δ 171.9 (-COOCH₃), 163.2 (d, -ArCO-), 151.3 (d, -ArC 3), 148.9 (d, -ArC 2), 146.4 (d, -ArC 1), 137.5 (-PhC 1), 129.4 (-PhC 2 & 6), 128.5 (-PhC 3 & 5), 126.8 (-PhC 4), 126.0 (d, -ArC 4), 125.1 (dd, -ArC 5), 119.6 (d, -ArC 6), 54.5 (α -C), 52.2 (-OCH₃), 36.7 (-CH₂-, -VE DEPT).

^{19}F -NMR (376 MHz, DMSO): δ -63.0 - -63.1 (m), -64.8 - -64.9 (m).

***N*-2,4-difluorobenzoyl-L-phenylalanine methyl ester 87**

2,4-Difluorobenzoyl chloride (2.23 g, 12.6 mmol) was used. Recrystallisation from ethyl acetate/pet ether 40-60 °C furnished **87** as a yellow solid (2.49 g, 62%).

m.p. 37-38 °C. $[\alpha]_{\text{D}}^{25} = -13.2^\circ$ (c, 4.3, EtOH).

Anal. calcd. for C₁₇H₁₅N₁O₃F₂: C, 63.95; H, 4.74; N, 4.39; F, 11.90.

Found C, 63.90; H, 4.68; N, 4.37; F, 11.52.

Mass Spectrum: $[\text{M}+\text{Na}]^+$ found 342.2.

C₁₇H₁₅N₁O₃F₂Na₁ requires 342.2.

IR (KBr): ν 3244, 2953, 1751, 1618, 1497, 703 cm⁻¹.

^1H -NMR (400 MHz, DMSO): δ 8.68 (1H, d, $J = 7.8$ Hz, -NH-), 7.60-7.66 (1H, m, -ArH 6), 7.22-7.31 (6H, m, -ArH 5 & -PhH), 7.11-7.16 (1H, m, -ArH 3), 4.72-4.78 (1H, m, α -H), 3.68 (3H, s, -OCH₃), 3.21 (1H, dd, $J^3 = 5.2$ Hz, $J^2 = 14$ Hz, -CH₂-), 3.10 (1H, dd, $J^3 = 9.6$ Hz, $J^2 = 14$ Hz, -CH₂-).

^{13}C -NMR (100 MHz, DMSO): δ 172.0 (-COOCH₃), 163.9 (dd, -ArC 4), 163.3 (d, -ArCO-), 160.2 (dd, -ArC 2), 137.5 (-PhC 1), 132.1 (dd, -ArC 6), 129.4 (-PhC 2 & 6), 128.5 (-PhC 3 & 5), 126.8 (-PhC 4), 120.1 (dd, -ArC 1), 111.9 (dd, -ArC 3), 104.8 (t, -ArC 5), 54.5 (α -C), 52.2 (-OCH₃), 36.7 (-CH₂-, -VE DEPT).

^{19}F -NMR (376 MHz, DMSO): δ -30.7 (qt, $J = 7.5$ Hz), -33.6 (q, $J = 9.4$ Hz).

***N*-2,5-difluorobenzoyl-L-phenylalanine methyl ester 88**

2,5-Difluorobenzoyl chloride (2.23 g, 12.6 mmol) was used. Recrystallisation from ethyl acetate/pet ether 40-60 °C furnished **88** as a white solid (1.92 g, 48%).

m.p. 42-44 °C. $[\alpha]_{\text{D}}^{25} = -6.3^\circ$ (c, 3.0, EtOH).

Anal. calcd. for C₁₇H₁₅N₁O₃F₂: C, 63.95; H, 4.74; N, 4.39; F, 11.90.

Found C, 63.89; H, 4.59; N, 4.37; F, 11.78.

IR (KBr): ν 3318, 2956, 1740, 1638, 1491, 699 cm⁻¹.

¹H-NMR (400 MHz, DMSO): δ 8.83 (1H, d, $J = 7.2$ Hz, -NH-), 7.22-7.41 (8H, m, -ArH 3, 4, 6 & PhH), 4.70-4.76 (1H, m, α-H), 3.68 (3H, s, -OCH₃), 3.20 (1H, dd, $J^3 = 5.2$ Hz, $J^2 = 14.0$ Hz, -CH₂-), 3.08 (1H, dd, $J^3 = 9.6$ Hz, $J^2 = 13.6$ Hz, -CH₂-).

¹³C-NMR (100 MHz, DMSO): δ 171.9 (-COOCH₃), 163.3 (-ArCO), 158.0 (dd, -ArC 5), 155.6 (dd, -ArC 2), 137.5 (-PhC 1), 129.4 (-PhC 2 & 6), 128.5 (-PhC 3 & 5), 126.9 (-PhC 4), 124.8 (dd, -ArC 1), 119.5 (dd, -ArC 4), 118.4 (dd, -ArC 3), 116.4 (dd, -ArC 6), 54.5 (α-C), 52.3 (-OCH₃), 36.6 (-CH₂-, -VE DEPT).

¹⁹F-NMR (376 MHz, DMSO): δ -43.0 - -43.1 (m), -44.0 - -44.1 (m).

***N*-2,6-difluorobenzoyl-L-phenylalanine methyl ester 89**

2,6-Difluorobenzoyl chloride (2.23 g, 12.6 mmol) was used. Recrystallisation from ethyl acetate/pet ether 40-60 °C furnished **89** as a white solid (1.68 g, 42%).

m.p. 78-80 °C. $[\alpha]_D^{25} = -24^\circ$ (c, 1.5, EtOH).

Anal. calcd. for C₁₇H₁₅N₁O₃F₂: C, 63.95; H, 4.74; N, 4.39; F, 11.90.

Found C, 63.87; H, 4.66; N, 4.36; F, 11.59.

IR (KBr): ν 3301, 2923, 1737, 1656, 1541, 704 cm⁻¹.

¹H-NMR (400 MHz, DMSO): δ 9.30 (1H, d, $J = 7.6$ Hz, -NH-), 7.48-7.52 (1H, m, -ArH 4), 7.29-7.34 (5H, m, -PhH), 7.13-7.16 (2H, m, -ArH 3 & 5), 4.70-4.73 (1H, m, α-H), 3.68 (3H, s, -OCH₃), 3.17 (1H, dd, $J^3 = 5.2$ Hz, $J^2 = 13.6$ Hz, -CH₂-), 3.02 (1H, dd, $J^3 = 10.0$ Hz, $J^2 = 14.0$ Hz, -CH₂-).

¹³C-NMR (100 MHz, DMSO): δ 171.7 (-COOCH₃), 160.4 (d, -ArC 2), 160.2 (-ArCO-), 158.0 (d, -ArC 6), 137.4 (-PhC 1), 132.0 (t, -ArC 4), 129.4 (-PhC 3 & 5), 128.5 (-PhC 2 & 6), 126.9 (-PhC 4), 115.1 (t, -ArC 1), 112.2 (d, -ArC 3), 112.0 (d, -ArC 5), 54.4 (α-C), 52.3 (-OCH₃), 36.7 (-CH₂-, -VE DEPT).

¹⁹F-NMR (376 MHz, DMSO): δ -38.1 (t, $J = 7.1$ Hz).

***N*-3,4-difluorobenzoyl-L-phenylalanine methyl ester 90**

3,4-Difluorobenzoyl chloride (1.12 g, 6.3 mmol) and L-phenylalanine methyl ester (1.36 g, 6.3 mmol) were used. Recrystallisation from ethyl acetate/pet ether 40-60 °C furnished **90** as a white solid (0.86 g, 44%).

m.p. 97-98 °C. $[\alpha]_D^{25} = -49.1^\circ$ (c, 4.5, EtOH).

Anal. calcd. for C₁₇H₁₅N₁O₃F₂: C, 63.95; H, 4.74; N, 4.39; F, 11.90.

Found C, 63.55; H, 4.61; N, 4.34; F, 11.56.

IR (KBr): ν 3292, 3066, 1741, 1648, 1560, 878 cm^{-1} .

$^1\text{H-NMR}$ (400 MHz, DMSO): δ 9.04 (1H, d, $J = 7.6$ Hz, -NH-), 7.86-7.91 (1H, m, -ArH 6), 7.76-7.78 (1H, m, -ArH 2), 7.16-7.47 (6H, m, -PhH & -ArH 5), 4.76-4.82 (1H, m, α -H), 3.82 (3H, s, -OCH₃), 3.17 (1H, dd, $J^3 = 5.2$ Hz, $J^2 = 14$ Hz, -CH₂-), 3.02 (1H, dd, $J^3 = 10.4$ Hz, $J^2 = 13.6$ Hz, -CH₂-).

$^{13}\text{C-NMR}$ (100 MHz, DMSO): δ 172.3 (-COOCH₃), 164.7 (-ArCO-), 152.0 (dd, -ArC 4), 149.4 (dd, -ArC 3), 137.8 (-PhC 1), 131.2 (t, -ArC 1), 129.3 (-PhC 3 & 5), 128.5 (-PhC 2 & 6), 126.7 (-PhC 4), 125.1 (dd, -ArC 2), 117.6 (d, -ArC 5), 117.1 (d, -ArC 6), 54.8 (α -C), 52.1 (-OCH₃), 36.6 (-CH₂-, -VE DEPT).

$^{19}\text{F-NMR}$ (376 MHz, DMSO): δ -58.8 - -58.9 (m), -62.5 - -62.6 (m).

***N*-3,5-difluorobenzoyl-L-phenylalanine methyl ester 91**

3,5-Difluorobenzoyl chloride (1.12 g, 6.3 mmol) was used. Recrystallisation from ethyl acetate/pet ether 40-60 °C furnished **91** as a white solid (1.01 g, 51%).

m.p. 78-79 °C. $[\alpha]_{\text{D}}^{25} = -54^\circ$ (c, 3.5, EtOH).

Anal. calcd. for C₁₇H₁₅N₁O₃F₂: C, 63.95; H, 4.74; N, 4.39; F, 11.90.

Found C, 63.83; H, 4.71; N, 4.32; F, 11.55.

IR (KBr): ν 3326, 2978, 1750, 1647, 1593, 700 cm^{-1} .

$^1\text{H-NMR}$ (400 MHz, DMSO): δ 9.09 (1H, d, $J = 8.0$ Hz, -NH-), 7.55-7.59 (2H, m, -ArH 2 & 6), 7.16-7.33 (6H, m, -PhH & -ArH 4), 4.77-4.83 (1H, m, α -H), 3.67 (3H, s, -OCH₃), 3.23 (1H, dd, $J^3 = 5.2$ Hz, $J^2 = 14$ Hz, -CH₂-), 3.15 (1H, dd, $J^3 = 10.4$ Hz, $J^2 = 13.8$ Hz, -CH₂-).

$^{13}\text{C-NMR}$ (100 MHz, DMSO): δ 172.2 (-COOCH₃), 164.3 (t, -ArCO-), 163.7 (d, -ArC 3), 161.3 (d, -ArC 5), 137.8 (-PhC 1), 137.3 (t, -ArC 1), 129.2 (-PhC 3 & 5), 128.4 (-PhC 2 & 6), 126.7 (-PhC 4), 111.1 (d, -ArC 2), 110.9 (d, -ArC 6), 107.0 (t, -ArC 4), 54.8 (α -C), 52.1 (-OCH₃), 36.6 (-CH₂-, -VE DEPT).

$^{19}\text{F-NMR}$ (376 MHz, DMSO): δ -33.5 (t, $J = 8.5$ Hz).

***N*-pentafluorobenzoyl-L-phenylalanine methyl ester 92**

Pentafluorobenzoyl chloride (2.95 g, 12.6 mmol) and L-phenylalanine methyl ester (2.72 g, 12.6 mmol) were used. Recrystallisation from ethyl acetate/pet ether 40-60 °C furnished **92** as a pale yellow solid (1.83 g, 39%).

m.p. 104-106 °C. $[\alpha]_D^{25} = -24.1^\circ$ (c, 2.75, EtOH).

Anal. calcd. for $C_{17}H_{12}N_1O_3F_5$: C, 54.70; H, 3.24; N, 3.75; F, 25.45.

Found C, 54.94; H, 3.26; N, 3.72; F, 25.09.

IR (KBr): ν 3318, 3034, 1736, 1660, 1518, 699 cm^{-1} .

1H -NMR (400 MHz, DMSO): δ 9.48 (1H, d, $J = 8.0$ Hz, -NH-), 7.22-7.33 (5H, m, -PhH), 4.71-4.77 (1H, m, α -H), 3.69 (3H, s, -OCH₃), 3.19 (1H, dd, $J^3 = 4.8$ Hz, $J^2 = 14.0$ Hz, -CH₂-), 2.99 (1H, dd, $J^3 = 9.6$ Hz, $J^2 = 13.6$ Hz, -CH₂-).

^{13}C -NMR (100 MHz, DMSO): δ 171.4 (-COOCH₃), 157.1 (-ArCO-), 144.6-144.7 (m, -ArC 2), 140.3-142.8 (m, -ArC 4), 142.0-142.2 (m, -ArC 6), 138.3-138.5 (m, -ArC 3), 137.0 (-PhC 1), 135.9-136.1 (m, -ArC 5), 129.4 (-PhC 3 & 5), 128.5 (-PhC 2 & 6), 126.9 (-PhC 4), 112.3 (t, -ArC 1), 54.5 (α -C), 52.4 (-OCH₃), 36.7 (-CH₂-, -VE DEPT).

^{19}F -NMR (376 MHz, DMSO): δ -66.3 (dd, 2F, $J^4 = 6.8$ Hz, $J^3 = 22.9$ Hz), -77.5 (t, 1F, $J = 21.8$ Hz), -86.1--86.2 (m, 2F).

***N*-pentafluorobenzoyl-L-phenylalanine 93**

L-Phenylalanine (0.83 g, 5.0 mmol) was added to a solution of water (5 mls) and sodium hydroxide (0.4 g, 10 mmol) at room temperature. The reaction mixture was then heated to 85 °C and pentafluorobenzoyl chloride (1.16 g, 5mmol) was added over a period of 20 mins. After the addition was complete the reaction was left stirring for an additional 30 mins. The solution was then cooled and acidified with conc. HCl. This was washed with water and recrystallisation from EtOH gave the title product as a white powder (1.40g, 78%).

m.p. 158-159 °C. $[\alpha]_D^{25} = -14.3^\circ$ (c, 2.75, EtOH).

Mass Spectrum: $[M+Na]^+$ found 382.0.

$C_{16}H_{10}N_1O_3F_5Na_1$ requires 382.24.

IR (KBr): ν 3292, 3092, 1720, 1669, 1521, 996 cm^{-1} .

1H -NMR (400 MHz, DMSO): δ 12.74 (1H, s, -OH), 9.36 (1H, d, $J = 8.0$ Hz, -NH-), 7.20-7.31 (5H, m, -PhH), 4.62-4.65 (1H, m, α -H), 2.92-3.22 (2H, m, -CH₂-).

^{13}C -NMR (100 MHz, DMSO): δ 172.3 (-COOH), 156.9 (-ArCO-), 144.7-144.8 (m, -ArC 2), 140.3-142.8 (m, -ArC 4), 142.1-142.3 (m, -ArC 6), 138.4-138.6 (m, -ArC 3), 137.5 (-PhC 1), 135.9-136.1 (m, -ArC 5), 129.4 (-PhC 3 & 5), 128.5 (-PhC 2 & 6), 126.8 (-PhC 4), 112.3 (t, -ArC 1), 54.6 (α -C), 36.8 (-CH₂-, -VE DEPT).

^{19}F -NMR (400 MHz, DMSO): δ -66.2 (dd, 2F, $J^4 = 6.8$ Hz, $J^3 = 23.3$ Hz), -77.9 (t, 1F, $J = 15.8$ Hz), -86.4 - -86.5 (m, 2F).

General procedure for the synthesis of *N*-fluorobenzoyl glycine ethyl esters 94-103

***N*-2-fluorobenzoyl-glycine ethyl ester 94**

A solution of 2-fluorobenzoyl chloride (2.00 g, 12.6 mmol) in dichloromethane (20 mls) was added dropwise to a solution of glycine ethyl ester (1.76 g, 12.6 mmol) and triethylamine (2.55 g, 25.2 mmol) in dichloromethane (20 mls). The solution was stirred for 8 hrs then washed with 5% NaHCO_3 , 5% HCl and water. The organic extract was then dried over MgSO_4 and the solvent was removed *in vacuo* to yield a crude yellow oil. Recrystallisation from ethyl acetate/pet ether 40-60 °C furnished **94** as a yellow oil (1.54 g, 58%).

Anal. calcd. for $\text{C}_{11}\text{H}_{12}\text{N}_1\text{O}_3\text{F}_1$: C, 58.66; H, 5.37; N, 6.21; F, 8.44.

Found C, 58.45; H, 5.25; N, 6.41; F, 8.64.

IR (Nujol): ν 3309, 2955, 1737, 1645, 1537, 701 cm^{-1} .

^1H -NMR (400 MHz, DMSO): δ 8.68 (1H, t, $J = 7.6$ Hz, -NH-), 7.68-7.72 (1H, m, -ArH 6), 7.54-7.56 (1H, m, -ArH 4), 7.26-7.31 (2H, m, -ArH 3 & 5), 4.12 (2H, q, $J = 7.2$ Hz, -OCH₂-), 4.02 (2H, d, $J = 6.0$ Hz, -CH₂-), 1.19 (3H, t, $J = 7.2$ Hz, -CH₃).

^{13}C -NMR (100 MHz, DMSO): δ 169.9 (-COOCH₂CH₃), 164.4 (-ArCO-), 159.7 (d, -ArC 2), 133.3 (d, -ArC 4), 130.6 (d, -ArC 6), 124.9 (d, -ArC 5), 122.9 (d, -ArC 1), 116.5 (d, -ArC 3), 60.9 (-OCH₂-, -VE DEPT), 41.6 (-CH₂-, -VE DEPT), 14.3 (-CH₃).

^{19}F -NMR (376 MHz, DMSO): δ -38.4 - -38.5(m).

***N*-3-fluorobenzoyl-glycine ethyl ester 95**

3-Fluorobenzoyl chloride (2.00 g, 12.6 mmol) was used. Recrystallisation from ethyl acetate/pet ether 40-60 °C furnished **95** as a white solid (1.38 g, 52%).

m.p. 60-62 °C.

Anal. calcd. for $\text{C}_{11}\text{H}_{12}\text{N}_1\text{O}_3\text{F}_1$: C, 58.66; H, 5.37; N, 6.21; F, 8.44.

Found C, 58.24; H, 5.25; N, 6.22; F, 8.44.

IR (KBr): ν 3315, 2986, 1755, 1641, 1542, 679 cm^{-1} .

^1H -NMR (400 MHz, DMSO): δ 9.03 (1H, t, $J = 7.6$ Hz, -NH-), 7.66-7.76 (2H, m, -ArH 2 & 6), 7.47-7.50 (1H, m, -ArH 5), 7.30-7.32 (1H, m, -ArH 4), 4.11 (2H, q, $J = 7.2$ Hz, -OCH₂-), 4.06 (2H, d, $J = 6.0$ Hz, -CH₂-), 1.18 (3H, t, $J = 7.2$ Hz, -CH₃).

^{13}C -NMR (100 MHz, DMSO): δ 170.0 (-COOCH₂CH₃), 166.0 (d, -ArCO-), 162.3 (d, -ArC 3), 136.2 (d, -ArC 1), 130.6 (d, -ArC 5), 123.5 (d, -ArC 6), 118.5 (d, -ArC 4), 114.4 (d, -ArC 2), 60.8 (-OCH₂-, -VE DEPT), 41.6 (-CH₂-, -VE DEPT), 14.1 (-CH₃).

^{19}F -NMR(376 MHz, DMSO): δ -37.4 - -37.5 (m).

***N*-4-fluorobenzoyl-glycine ethyl ester 96**

4-Fluorobenzoyl chloride (2.00 g, 12.6 mmol) was used. Recrystallisation from ethyl acetate/pet ether 40-60 °C furnished **96** as a pale yellow crystalline solid (1.67 g, 63%).

m.p. 101-103 °C. Lit.³⁵ m.p. 102-104 °C.

Anal. calcd. for C₁₁H₁₂N₁O₃F₁: C, 58.66; H, 5.37; N, 6.21; F, 8.44.

Found C, 58.66; H, 5.23; N, 5.92; F, 8.90.

IR (KBr): ν 3277, 2982, 1748, 1648, 1560, 670 cm⁻¹.

^1H -NMR (400 MHz, DMSO): δ 8.98 (1H, t, J = 6.0 Hz, -NH-), 7.92-8.02 (2H, m, -ArH 2 & 6), 7.25-7.30 (2H, m, -ArH 3 & 5), 4.09 (2H, q, J = 7.2 Hz, -OCH₂-), 4.01 (2H, d, J = 6.0 Hz, -CH₂-), 1.17 (3H, t, J = 7.2 Hz, -CH₃).

^{13}C -NMR (100 MHz, DMSO): δ 170.1 (-COOCH₂CH₃), 166.1 (-ArCO-), 164.4 (d, -ArC 4), 130.4 (d, -ArC 1), 130.2 (-ArC 2), 130.1 (-ArC 6), 115.7 (-ArC 3), 115.5 (-ArC 5), 60.8 (-OCH₂-, -VE DEPT), 41.6 (-CH₂-, -VE DEPT), 14.2 (-OCH₃).

^{19}F -NMR (376 MHz, DMSO): δ -33.5 - -33.6 (m).

***N*-2,3-difluorobenzoyl-glycine ethyl ester 97**

2,3-Difluorobenzoyl chloride (2.23 g, 12.6 mmol) was used. Recrystallisation from ethyl acetate/pet ether 40-60 °C furnished **97** as a white solid (1.99 g, 69%).

m.p. 54-56 °C.

Anal. calcd. for C₁₁H₁₁N₁O₃F₂: C, 54.32; H, 4.56; N, 5.76; F, 15.62.

Found C, 54.27; H, 4.46; N, 5.77; F, 15.93.

IR (KBr): ν 3283, 2988, 1764, 1660, 1542, 722 cm⁻¹.

^1H -NMR (400 MHz, DMSO): δ 8.87 (1H, t, J = 5.2 Hz, -NH-), 7.52-7.59 (1H, m, -ArH 6), 7.42-7.45 (1H, m, -ArH 5), 7.27-7.32 (1H, m, -ArH 4), 4.12 (2H, q, J = 7.0 Hz, -OCH₂-), 4.01 (2H, d, J = 5.6 Hz, -CH₂-), 1.20 (3H, t, J = 7.2 Hz, -CH₃).

^{13}C -NMR (100 MHz, DMSO): δ 169.7 (-COOCH₂CH₃), 163.5 (d, -ArCO-), 150.1 (dd, -ArC 3), 147.6 (dd, -ArC 2), 125.5 (d, -ArC 1), 125.4 (t, -ArC 4), 120.1 (-ArC 5), 119.9 (-ArC 6), 60.9 (-OCH₂-, -VE DEPT), 41.6 (-CH₂-, -VE DEPT), 14.3 (-CH₃).

^{19}F -NMR (376 MHz, DMSO): δ -62.9 - -63.0 (m), -65.0 - -65.1 (m).

***N*-2,4-difluorobenzoyl-glycine ethyl ester 98**

2,4-Difluorobenzoyl chloride (2.23 g, 12.6 mmol) was used. Recrystallisation from ethyl acetate/pet ether 40-60 °C furnished **98** as a white solid (1.76 g, 61%).

m.p. 77-79 °C. Lit.³⁵ m.p. 80-81 °C.

Anal. calcd. for C₁₁H₁₁N₁O₃F₂: C, 54.32; H, 4.56; N, 5.76; F, 15.62.

Found C, 54.06; H, 4.40; N, 5.80; F, 15.94.

IR (KBr): ν 3411, 2992, 1749, 1656, 1534, 772 cm⁻¹.

^1H -NMR (400 MHz, DMSO): δ 8.66 (1H, bs, -NH-), 7.75-7.81 (1H, m, -ArH 6), 7.29-7.34 (1H, m, -ArH 5), 7.15-7.19 (1H, m, -ArH 3), 4.12 (2H, q, J = 7.0 Hz, -OCH₂-), 4.02 (2H, d, J = 5.2 Hz, -CH₂-), 1.21 (3H, t, J = 7.2 Hz, -CH₃).

^{13}C -NMR (100 MHz, DMSO): δ 169.8 (-COOCH₂CH₃), 164.0 (dd, -ArC 4), 163.4 (-ArCO-), 160.3 (dd, -ArC 2), 132.5 (dd, -ArC 6), 119.7 (d, -ArC 1), 112.2 (d, -ArC 3), 104.9 (t, -ArC 5), 60.8 (-OCH₂-, -VE DEPT), 41.7 (-CH₂-, -VE DEPT), 14.2 (-CH₃).

^{19}F -NMR (376 MHz, DMSO): δ -30.5 (qt, J = 8.3 Hz), -33.5 (q, J = 9.8 Hz).

***N*-2,5-difluoro-benzoyl-glycine ethyl ester 99**

2,5-Difluorobenzoyl chloride (2.23 g, 12.6 mmol) was used. Recrystallisation from ethyl acetate/pet ether 40-60 °C furnished **99** as a white solid (1.58 g, 55%).

m.p. 51-52 °C.

Anal. calcd. for C₁₁H₁₁N₁O₃F₂: C, 54.32; H, 4.56; N, 5.76; F, 15.62.

Found C, 54.29; H, 4.53; N, 5.84; F, 15.23.

IR (KBr): ν 3436, 2995, 1732, 1659, 1523, 763 cm⁻¹.

^1H -NMR (400 MHz, DMSO): δ 8.78 (1H, t, J = 6.0 Hz, -NH-), 7.35-7.47 (3H, m, -ArH 3,4 & 6), 4.13 (2H, q, J = 7.2 Hz, -OCH₂-), 4.02 (2H, d, J = 6.0 Hz, -CH₂-), 1.21 (3H, t, J = 7.0 Hz, -CH₃).

^{13}C -NMR (100 MHz, DMSO): δ 169.7 (-COOCH₂CH₃), 163.1 (-ArCO-), 158.2 (dd, -ArC 5), 155.8 (dd, -ArC 2), 124.4 (dd, -ArC 1), 119.8 (dd, -ArC 4), 118.5 (dd, -ArC 3), 116.6 (dd, -ArC 6), 60.9 (-OCH₂-, -VE DEPT), 41.7 (-CH₂-, -VE DEPT), 14.3 (-CH₃).

¹⁹F-NMR (376 MHz, DMSO): δ -42.8 - -42.9 (m), -43.8 - -43.9 (m).

N*-2,6-difluorobenzoyl-glycine ethyl ester **100*

2,6-Difluorobenzoyl chloride (2.23 g, 12.6 mmol) was used. Recrystallisation from ethyl acetate/pet ether 40-60 °C furnished **100** as a yellow solid (1.90 g, 66%).

m.p. 67-68 °C.

Anal. calcd. for C₁₁H₁₁N₁O₃F₂: C, 54.32; H, 4.56; N, 5.76; F, 15.62.

Found C, 54.22; H, 4.43; N, 5.85; F, 15.39.

IR (KBr): ν 3278, 2985, 1734, 1654, 1543, 800 cm⁻¹.

¹H-NMR (400 MHz, DMSO): δ 9.17 (1H, t, *J* = 6.0 Hz -NH-), 7.50-7.54 (1H, m, -ArH 4), 7.13-7.17 (2H, m, -ArH 3 & 5), 4.16 (2H, q, *J* = 7.0 Hz, -OCH₂-), 4.06 (2H, d, *J* = 6.0 Hz, -CH₂-), 1.24 (3H, t, *J* = 7.2 Hz, -CH₃).

¹³C-NMR (100 MHz, DMSO): δ 169.4 (-COOCH₂CH₃), 160.7 (-ArCO-), 160.5 (d, -ArC 2), 158.0 (d, -ArC 6), 132.0 (t, -ArC 4), 115.1 (t, -ArC 1), 112.2 (d, -ArC 3), 112.0 (d, -ArC 5), 60.9 (-OCH₂-, -VE DEPT), 41.4 (-CH₂-, -VE DEPT), 14.1 (-CH₃).

¹⁹F-NMR (376 MHz, DMSO): δ -38.1 (t, *J* = 6.8 Hz).

N*-3,4-difluorobenzoyl-glycine ethyl ester **101*

3,4-Difluorobenzoyl chloride (1.12g, 6.3 mmol) and glycine ethyl ester (0.88 g, 6.3 mmol) were used. Recrystallisation from ethyl acetate/pet ether 40-60 °C furnished **101** as yellow crystals (0.89 g, 61%) which were of sufficient quality for an X-ray diffraction study.

m.p. 91-92 °C.

Anal. calcd. for C₁₁H₁₁N₁O₃F₂: C, 54.32; H, 4.56; N, 5.76; F, 15.62.

Found C, 54.04; H, 4.17; N, 5.49; F, 16.00.

IR (KBr): ν 3327, 2992, 1742, 1647, 1560, 760 cm⁻¹.

¹H-NMR (400 MHz, DMSO): δ 9.03 (1H, t, *J* = 5.6 Hz -NH-), 7.84-7.90 (1H, m, -ArH 6), 7.75-7.79 (1H, m, -ArH 2), 7.30-7.35 (1H, m, -ArH 5), 4.10 (2H, q, *J* = 7.2 Hz, -OCH₂-), 4.00 (2H, d, *J* = 5.6 Hz, -CH₂-), 1.19 (3H, t, *J* = 7.2Hz, -CH₃).

¹³C-NMR (100 MHz, DMSO): δ 170.0 (-COOCH₂CH₃), 164.8 (-ArCO-), 152.0 (dd, -ArC 4), 149.6 (dd, -ArC 3), 131.3 (t, -ArC 1), 125.0 (dd, -ArC 2), 118.1 (t, -ArC 5), 117.0 (d, -ArC 6), 60.8 (-OCH₂-, -VE DEPT), 41.6 (-CH₂-, -VE DEPT), 14.3 (-CH₃).

¹⁹F-NMR (376 MHz, DMSO): δ -58.8 - -58.9 (m), -62.4 - -62.5 (m).

***N*-3,5-difluorobenzoyl-glycine ethyl ester 102**

3,5-Difluorobenzoyl chloride (1.12 g, 6.3 mmol) was used. Recrystallisation from ethyl acetate/pet ether 40-60 °C furnished **102** as a yellow solid (0.75 g, 52%).

m.p. 80-81 °C.

Anal. calcd. for C₁₁H₁₁N₁O₃F₂: C, 54.32; H, 4.56; N, 5.76; F, 15.62.

Found C, 54.20; H, 4.43; N, 5.83; F, 15.27.

IR (KBr): ν 3403, 3075, 1723, 1667, 1536, 672 cm⁻¹.

¹H-NMR (400 MHz, DMSO): δ 9.08 (1H, t, J = 6.0 Hz -NH-), 7.55-7.58 (2H, m, -ArH 2 & 6), 7.23-7.28 (1H, m, -ArH 4), 4.12 (2H, q, J = 7.2 Hz, -OCH₂-), 4.04 (2H, d, J = 6.0 Hz, -CH₂-), 1.20 (3H, t, J = 7.2 Hz, -CH₃).

¹³C-NMR (100 MHz, DMSO): δ 169.7 (-COOCH₂CH₃), 164.5 (t, -ArCO-), 163.8 (d, -ArC 3), 161.4 (d, -ArC 5), 137.4 (t, -ArC 1), 110.9 (d, -ArC 2), 110.7 (d, -ArC 6), 106.8 (t, -ArC 4), 60.8 (-OCH₂-, -VE DEPT), 41.5 (-CH₂-, -VE DEPT), 14.0 (-CH₃).

¹⁹F-NMR (376 MHz, DMSO): δ -33.9 (t, J = 8.3 Hz).

***N*-pentafluorobenzoyl-glycine ethyl ester 103**

Pentafluorobenzoyl chloride (1.52 g, 6.6 mmol) and glycine ethyl ester (0.92 g, 6.6 mmol) were used. Recrystallisation from ethyl acetate/pet ether 40-60 °C furnished **103** as a yellow solid (1.28 g, 72%).

m.p. 79-80 °C.

Anal. calcd. for C₁₁H₈N₁O₃F₅: C, 44.46; H, 2.71; N, 4.71; F, 31.97.

Found C, 44.25; H, 2.58; N, 4.71; F, 32.01.

IR (KBr): ν 3271, 2989, 1737, 1658, 1519, 786 cm⁻¹.

¹H-NMR (400 MHz, DMSO): δ 9.39 (1H, t, J = 6.0 Hz -NH-), 4.15 (2H, q, J = 7.2 Hz, -OCH₂-), 4.08 (2H, d, J = 6.0 Hz, -CH₂-), 1.23 (3H, t, J = 7.2 Hz, -CH₃).

¹³C-NMR (100 MHz, DMSO): δ 169.2 (-COOCH₂CH₃), 157.6 (-ArCO-), 144.7-144.8 (m, -ArC 2), 140.4-142.9 (m, -ArC 4), 142.3-142.4 (m, -ArC 6), 138.4-138.6 (m, -ArC 3), 135.9-136.1 (m, -ArC 5), 112.3 (t, -ArC 1), 61.0 (-OCH₂-, -VE DEPT), 41.5 (-CH₂-, -VE DEPT), 14.2 (-CH₃).

¹⁹F-NMR (376 MHz, DMSO): δ -66.6 (dd, 2F, J^4 = 6.4 Hz, J^3 = 23.3 Hz), -77.7 (t, 1F, J = 15.8 Hz), -86.3 - -86.4(m, 2F).

***N*-pentafluorobenzoyl-glycine nitrile 104**

A solution of pentafluorobenzoyl chloride (2.90 g, 12.6 mmol) in dichloromethane (20 mls) was added dropwise to a solution of glycine nitrile hydrochloride (1.17 g, 12.6 mmol) and triethylamine (2.55 g, 25.2 mmol) in dichloromethane (20 mls). The solution was stirred for 8 hrs then washed with 5% NaHCO₃, 5% HCl and water. The organic extract was then dried over MgSO₄ and the solvent was removed *in vacuo* to yield a crude yellow oil. Recrystallisation from hexane/ethyl acetate furnished **104** as a yellow solid (2.15 g, 68%).

m.p. 126-127 °C.

Mass Spectrum: [M+Na]⁺ found 273.0.

C₆H₃N₂O₁F₅Na₁ requires 273.1.

IR (KBr): ν 3279, 2993, 2365, 1675, 1527, 988 cm⁻¹.

¹H-NMR (400 MHz, DMSO): δ 9.77 (1H, bs, -NH-), 4.41 (2H, bs, -CH₂-).

¹³C-NMR (100 MHz, DMSO): δ 157.8 (-ArCO-), 144.7-144.8 (m, -ArC 2), 140.7-143.2 (m, -ArC 4), 142.2-142.4 (m, -ArC 6), 138.5-138.7 (m, -ArC 3), 135.9-136.1 (m, -ArC 5), 117.1 (-CN), 111.3 (d, -ArC 1), 27.9 (-CH₂-, -VE DEPT).

¹⁹F-NMR (376 MHz, DMSO): δ -66.6 (dd, 2F, $J^4 = 6.4$ Hz, $J^3 = 23.5$ Hz), -77.7 (t, 1F, $J = 22.1$ Hz), -86.3 - -86.4(m, 2F).

General procedure for the synthesis of N-fluorobenzoyl-L-leucine methyl esters 105-114

***N*-2-fluorobenzoyl-L-leucine methyl ester 105**

A solution of 2-fluorobenzoyl chloride (2.00 g, 12.6 mmol) in dichloromethane (20 mls) was added dropwise to a solution of L-leucine methyl ester (2.28 g, 12.6 mmol) and triethylamine (2.55 g) in dichloromethane (20 mls). The solution was stirred for 8 hrs then washed with 5% NaHCO₃, 5% HCl and water. The organic extract was then dried over MgSO₄ and the solvent was removed *in vacuo* furnished **105** as a viscous brown oil (1.96 g, 62%).

$[\alpha]_D^{25} = -13^\circ$ (c, 1.5, EtOH).

Anal. calcd. for C₁₄H₁₈N₁O₃F₁: C, 62.91; H, 6.79; N, 5.24; F, 7.11.

Found C, 62.80; H, 6.83; N, 5.01; F, 7.33.

IR (Nujol): ν 3304, 2959, 1739, 1648, 1525, 731 cm⁻¹.

¹H-NMR (400 MHz, DMSO): δ 8.70 (1H, d, $J = 7.2$ Hz, -NH-), 7.55-7.62 (1H, m, -ArH 6), 7.51-7.54 (1H, m, -ArH 4), 7.25-7.31 (2H, m, -ArH 3 & 5), 4.50-4.56 (1H, m, α -H), 3.68 (3H, s, -

OCH₃), 1.57-1.79 (3H, m, -CH₂- & -CH-), 0.92 (3H, d, *J* = 6.8 Hz, -CH₃), 0.88 (3H, d, *J* = 6.4 Hz, -CH₃).

¹³C-NMR (100 MHz, DMSO): δ 173.0 (-COOCH₃), 164.5 (-ArCO-), 159.5 (d, -ArC 2), 132.8 (d, -ArC 4), 130.4 (d, -ArC 6), 124.6 (d, -ArC 5), 124.0 (d, -ArC 1), 116.4 (d, -ArC 3), 52.2 (-OCH₃), 51.2 (α-C), 39.7 (-CH₂-, -VE DEPT), 24.7 (-CH-), 23.0 (-CH₃), 21.3 (-CH₃).

¹⁹F-NMR (376 MHz, DMSO): δ -38.8 - -38.9 (m).

***N*-3-fluorobenzoyl-L-leucine methyl ester 106**

3-Fluorobenzoyl chloride (1.8 g, 11.3 mmol) and L-leucine methyl ester (2.05 g, 11.3 mmol) were used. Recrystallisation from ethyl acetate furnished **106** as a fine dark brown powder (2.41 g, 79%).

m.p. 92-94 °C. [α]_D²⁵ = -20° (c, 1.5, EtOH).

Anal. calcd. for C₁₄H₁₈N₁O₃F₁: C, 62.91; H, 6.79; N, 5.24; F, 7.11.

Found C, 62.70; H, 6.55; N, 5.31; F, 7.31.

IR (KBr): ν 3286, 3076, 1747, 1637, 1543, 757 cm⁻¹.

¹H-NMR (400 MHz, DMSO): δ 8.85 (1H, d, *J* = 7.6 Hz, -NH-), 7.68-7.72 (2H, m, -ArH 2 & 6), 7.50-7.56 (1H, m, -ArH 5), 7.36-7.41 (1H, m, -ArH 4), 4.49-4.55 (1H, m, α-H), 3.67 (3H, s, -OCH₃), 1.49-1.83 (3H, m, -CH₂- & -CH-), 0.91 (3H, d, *J* = 6.8 Hz, -CH₃), 0.87 (3H, d, *J* = 6.4 Hz, -CH₃).

¹³C-NMR (100 MHz, DMSO): δ 173.3 (-COOCH₃), 165.1 (d, -ArCO-), 162.3 (d, -ArC 3), 136.3 (d, -ArC 1), 130.8 (d, -ArC 5), 124.0 (d, -ArC 6), 118.7 (d, -ArC 4), 114.5 (d, -ArC 2), 52.2 (-OCH₃), 51.3 (α-C), 39.5 (-CH₂-, -VE DEPT), 24.7 (-CH-), 23.1 (-CH₃), 21.3 (-CH₃).

¹⁹F-NMR (376 MHz, DMSO): δ -37.5 - -37.6 (m).

***N*-4-fluorobenzoyl-L-leucine methyl ester 107**

4-Fluorobenzoyl chloride (1.8 g, 11.3 mmol) was used. Recrystallisation from ethyl acetate furnished **107** as a fine yellow powder (2.29 g, 76%).

m.p. 88-91 °C. [α]_D²⁵ = -17° (c, 1.5, EtOH).

Anal. calcd. for C₁₄H₁₈N₁O₃F₁: C, 62.91; H, 6.79; N, 5.24; F, 7.11.

Found C, 63.12; H, 6.54; N, 5.01; F, 6.99.

IR (KBr): ν 3279, 3077, 1747, 1637, 1506, 852 cm⁻¹.

$^1\text{H-NMR}$ (400 MHz, DMSO): δ 8.78 (1H, d, $J = 7.6$ Hz, -NH-), 7.95-8.00 (2H, m, -ArH 2 & 6), 7.27-7.33 (2H, m, -ArH 3 & 5), 4.48-4.54 (1H, m, α -H), 3.64 (3H, s, -OCH₃), 1.54-1.83 (3H, m, -CH₂- & -CH-), 0.91 (3H, d, $J = 6.4$ Hz, -CH₃), 0.88 (3H, d, $J = 6.4$ Hz, -CH₃).

$^{13}\text{C-NMR}$ (100 MHz, DMSO): δ 173.4 (-COOCH₃), 165.9 (-ArCO-), 164.3 (d, -ArC 4), 130.5 (-ArC 1), 130.4 (-ArC 2), 130.3 (d, -ArC 6), 115.6 (-ArC 3), 115.4 (-ArC 5), 52.2 (-OCH₃), 51.3 (α -C), 39.5 (-CH₂-, -VE DEPT), 24.7 (-CH-), 23.1 (-CH₃), 21.4 (-CH₃).

$^{19}\text{F-NMR}$ (376 MHz, DMSO): δ -33.7 - -33.8 (m).

***N*-2,3-difluorobenzoyl-L-leucine methyl ester 108**

2,3-Difluorobenzoyl chloride (1.99 g, 11.3 mmol) was used. Recrystallisation from ethyl acetate furnished **108** as a viscous orange oil (2.09 g, 65%).

$[\alpha]_{\text{D}}^{25} = -20^\circ$ (c, 1.5, EtOH).

Anal. calcd. for C₁₄H₁₇N₁O₃F₂: C, 58.94; H, 6.01; N, 4.91; F, 13.32.

Found C, 58.61; H, 6.13; N, 4.79; F, 13.01.

IR (Nujol): ν 3279, 2907, 1730, 1670, 1460, 852 cm⁻¹.

$^1\text{H-NMR}$ (400 MHz, DMSO): δ 8.89 (1H, d, $J = 7.6$ Hz, -NH-), 7.51-7.58 (1H, m, -ArH 6), 7.26-7.39 (2H, m, -ArH 4 & 5), 4.48-4.54 (1H, m, α -H), 3.68 (3H, s, -OCH₃), 1.51-1.76 (3H, m, -CH₂- & -CH-), 0.92 (3H, d, $J = 6.4$ Hz, -CH₃), 0.90 (3H, d, $J = 6.4$ Hz, -CH₃).

$^{13}\text{C-NMR}$ (100 MHz, DMSO): δ 172.9 (-COOCH₃), 163.4 (d, -ArCO-), 150.1 (dd, -ArC 3), 147.5 (dd, -ArC 2), 126.4 (d, -ArC 1), 125.2 (d, -ArC 4), 125.1 (d, -ArC 5), 119.6 (d, -ArC 6), 52.2 (-OCH₃), 51.3 (α -C), 39.6 (-CH₂-, -VE DEPT), 24.7 (-CH-), 23.1 (-CH₃), 21.3 (-CH₃).

$^{19}\text{F-NMR}$ (376 MHz, DMSO): δ -63.1 - -63.2 (m), -64.9 - -65.0 (m).

***N*-2,4-difluorobenzoyl-L-leucine methyl ester 109**

2,4-Difluorobenzoyl chloride (1.99 g, 11.3 mmol) was used. Recrystallisation from ethyl acetate furnished **109** as a viscous yellow oil (2.28 g, 71%).

$[\alpha]_{\text{D}}^{25} = -14^\circ$ (c, 1.5, EtOH).

Anal. calcd. for C₁₄H₁₇N₁O₃F₂: C, 58.94; H, 6.01; N, 4.91; F, 13.32.

Found C, 58.55; H, 6.33; N, 4.86; F, 13.14.

IR (Nujol): ν 3284, 2918, 1750, 1648, 1361, 856 cm⁻¹.

$^1\text{H-NMR}$ (400 MHz, DMSO): δ 8.70 (1H, d, $J = 7.6$ Hz, -NH-), 7.65-7.71 (1H, m, -ArH 6), 7.26-7.32 (1H, m, -ArH 5), 7.13-7.18 (1H, m, -ArH 3), 4.48-4.54 (1H, m, α -H), 3.68 (3H, s, -OCH₃),

1.56-1.77 (3H, m, $-CH_2-$ & $-CH-$), 0.91 (3H, d, $J = 6.4$ Hz, $-CH_3$), 0.89 (3H, d, $J = 6.4$ Hz, $-CH_3$).
 ^{13}C -NMR (100 MHz, DMSO): δ 173.0 ($-COOCH_3$), 163.8 (dd, $-ArC$ 4), 163.6 (d, $-ArCO-$), 160.1 (dd, $-ArC$ 2), 132.1 (dd, $-ArC$ 6), 120.6 (dd, $-ArC$ 1), 111.9 (dd, $-ArC$ 3), 104.7 (t, $-ArC$ 5), 52.1 ($-OCH_3$), 51.2 ($\alpha-C$), 39.6 ($-CH_2-$, $-VE$ DEPT), 24.7 ($-CH-$), 23.0 ($-CH_3$), 21.3 ($-CH_3$).
 ^{19}F -NMR (376 MHz, DMSO): δ -31.0 (qt, $J = 9$ Hz), -33.8 (q, $J = 9.4$ Hz).

***N*-2,5-difluorobenzoyl-L-leucine methyl ester 110**

2,5-Difluorobenzoyl chloride (1.99 g, 11.3 mmol) was used. Recrystallisation from ethyl acetate furnished **110** as a colourless viscous oil (1.89 g, 59%).

$[\alpha]_D^{25} = -14^\circ$ (c, 1.5, EtOH).

Anal. calcd. for $C_{14}H_{17}N_1O_3F_2$: C, 58.94; H, 6.01; N, 4.91; F, 13.32.

Found C, 59.02; H, 5.99; N, 4.65; F, 13.50.

IR (Nujol): ν 3268, 2957, 1750, 1638, 1342, 798 cm^{-1} .

1H -NMR (400 MHz, DMSO): δ 8.80 (1H, d, $J = 7.6$ Hz, $-NH-$), 7.32-7.43 (3H, m, $-ArH$ 3, 4 & 6), 4.45-4.51 (1H, m, $\alpha-H$), 3.67 (3H, s, $-OCH_3$), 1.53-1.75 (3H, m, $-CH_2-$ & $-CH-$), 0.91 (3H, d, $J = 6.4$ Hz, $-CH_3$), 0.89 (3H, d, $J = 6.4$ Hz, $-CH_3$).

^{13}C -NMR (100 MHz, DMSO): δ 172.8 ($-COOCH_3$), 163.2 ($-ArCO-$), 158.0 (dd, $-ArC$ 5), 155.6 (dd, $-ArC$ 2), 125.3 (dd, $-ArC$ 1), 119.3 (dd, $-ArC$ 4), 118.3 (dd, $-ArC$ 3), 116.4 (dd, $-ArC$ 6), 52.2 ($-OCH_3$), 51.2 ($\alpha-C$), 39.6 ($-CH_2-$, $-VE$ DEPT), 24.6 ($-CH-$), 23.0 ($-CH_3$), 21.4 ($-CH_3$).

^{19}F -NMR (376 MHz, DMSO): δ -43.0 - -43.1 (m), -44.1 - -44.2 (m).

***N*-2,6-difluorobenzoyl-L-leucine methyl ester 111**

2,6-Difluorobenzoyl chloride (1.99 g, 11.3 mmol) was used. Recrystallisation from ethyl acetate furnished **111** as an orange crystalline solid (2.02 g, 63%).

m.p. = 70-72 $^\circ C$. $[\alpha]_D^{25} = -18^\circ$ (c, 1.5, EtOH).

Anal. calcd. for $C_{14}H_{17}N_1O_3F_2$: C, 58.94; H, 6.01; N, 4.91; F, 13.32.

Found C, 58.16; H, 6.03; N, 4.74; F, 13.42.

IR (KBr): ν 3268, 2920, 1756, 1654, 1442, 816 cm^{-1} .

1H -NMR (400 MHz, DMSO): δ 9.15 (1H, d, $J = 8.4$ Hz, $-NH-$), 7.49-7.56 (1H, m, $-ArH$ 4), 7.13-7.19 (2H, m, $-ArH$ 3 & 5), 4.48-4.54 (1H, m, $\alpha-H$), 3.68 (3H, s, $-OCH_3$), 1.58-1.75 (3H, m, $-CH_2-$ & $-CH-$), 0.91 (6H, t, $J = 6.6$ Hz, $-CH_3$).

^{13}C -NMR (100 MHz, DMSO): δ 172.7 (-COOCH₃), 160.4 (d, -ArC 2) 160.2 (-ArCO-), 157.9 (d, -ArC 6), 132.0 (t, -ArC 4), 115.2 (t, -ArC 1), 112.2 (d, -ArC 3), 112.0 (d, -ArC 5), 52.2 (-OCH₃), 50.9 (α -C), 39.7 (-CH₂-, -VE DEPT), 24.5 (-CH-), 23.0 (-CH₃), 21.2 (-CH₃).

^{19}F -NMR (376 MHz, DMSO): δ -38.5 (t, J = 6.8 Hz).

***N*-3,4-difluorobenzoyl-L-leucine methyl ester 112**

3,4-Difluorobenzoyl chloride (1.12 g, 6.3 mmol) and L-leucine methyl ester (1.14 g, 6.3 mmol) were used. Recrystallisation from ethyl acetate furnished **112** as a brown powder (0.92 g, 51%).

m.p. = 75-76 °C. $[\alpha]_{\text{D}}^{25}$ = -16° (c, 3.0, EtOH).

Anal. calcd. for C₁₄H₁₇N₁O₃F₂: C, 58.94; H, 6.01; N, 4.91; F, 13.32.

Found C, 58.63; H, 6.16; N, 5.11; F, 13.18.

IR (KBr): ν 3287, 2961, 1747, 1638, 1551, 779 cm⁻¹.

^1H -NMR (400 MHz, DMSO): δ 8.81 (1H, d, J = 7.6 Hz, -NH-), 7.91-7.96 (1H, m, -ArH 6), 7.80-7.83 (1H, m, -ArH 2), 7.39-7.46 (1H, m, -ArH 5), 4.51-4.56 (1H, m, α -H), 3.65 (3H, s, -OCH₃), 1.68-1.82 (3H, m, -CH₂- & -CH-), 0.91 (3H, d, J = 6.4 Hz, -CH₃), 0.87 (3H, d, J = 6.4 Hz, -CH₃).

^{13}C -NMR (100 MHz, DMSO): δ 173.2 (-COOCH₃), 164.7 (-ArCO-), 152.0 (dd, -ArC 4), 149.4 (dd, -ArC 3), 131.2 (t, -ArC 1), 125.2 (dd, -ArC 2), 117.4 (d, -ArC 5), 117.1 (d, -ArC 6), 51.9 (-OCH₃), 51.4 (α -C), 39.5 (-CH₂-, -VE DEPT), 24.6 (-CH-), 22.8 (-CH₃), 21.1 (-CH₃).

^{19}F -NMR (376 MHz, DMSO): δ -59.0 - -59.1 (m), -62.8 - -62.9 (m).

***N*-3,5-difluorobenzoyl-L-leucine methyl ester 113**

3,5-Difluorobenzoyl chloride (1.99 g, 11.3 mmol) and L-leucine methyl ester (2.05 g, 11.3 mmol) were used. Recrystallisation from ethyl acetate furnished **113** as a brown powder (2.35 g, 73%).

m.p. = 69-71 °C. $[\alpha]_{\text{D}}^{25}$ = -15° (c, 1.5, EtOH).

Anal. calcd. for C₁₄H₁₇N₁O₃F₂: C, 58.94; H, 6.01; N, 4.91; F, 13.32.

Found C, 58.75; H, 5.90; N, 5.04; F, 12.98.

IR (KBr): ν 3268, 2913, 1727, 1642, 1468, 721 cm⁻¹.

^1H -NMR (400 MHz, DMSO): δ 8.93 (1H, d, J = 7.6 Hz, -NH-), 7.38-7.52 (3H, m, -ArH 2, 4 & 6), 4.46-4.52 (1H, m, α -H), 3.68 (3H, s, -OCH₃), 1.52-1.73 (3H, m, -CH₂- & -CH-), 0.90 (3H, d, J = 6.4 Hz, -CH₃), 0.86 (3H, d, J = 6.4 Hz, -CH₃).

^{13}C -NMR (100 MHz, DMSO): δ 173.0 (-COOCH₃), 164.3 (t, -ArCO-), 163.8 (d, -ArC 3), 161.3 (d, -ArC 5), 137.3 (t, -ArC 1), 111.2 (d, -ArC 2), 111.0 (d, -ArC 6), 107.3 (t, -ArC 4), 52.2 (-OCH₃), 51.4 (α -C), 39.4 (-CH₂-, -VE DEPT), 24.7 (-CH-), 23.0 (-CH₃), 21.3 (-CH₃).

^{19}F -NMR (376 MHz, DMSO): δ -33.7 (t, J = 8.3 Hz).

***N*-pentafluorobenzoyl-L-leucine methyl ester 114**

Pentafluorobenzoyl chloride (2.19 g, 11.3 mmol) was used. Recrystallisation from ethyl acetate furnished **114** as white needles (1.55 g, 45%) that were of sufficient quality for an X-ray diffraction study.

m.p. = 64-66 °C. $[\alpha]_{\text{D}}^{25} = -18^\circ$ (c, 1.5, EtOH).

Anal. calcd. for C₁₄H₁₄N₁O₃F₅: C, 49.56; H, 4.16; N, 4.13; F, 28.00.

Found C, 49.50; H, 4.09; N, 3.83; F, 27.54.

IR (KBr): ν 3233, 3067, 1752, 1655, 1519, 996 cm⁻¹.

^1H -NMR (400 MHz, DMSO): δ 9.39 (1H, d, J = 7.6 Hz, -NH-), 4.47-4.53 (1H, m, α -H), 3.69 (3H, s, -OCH₃), 1.54-1.73 (3H, m, -CH₂- & -CH-), 0.92 (3H, d, J = 6.4 Hz, -CH₃), 0.90 (3H, d, J = 6.4 Hz, -CH₃).

^{13}C -NMR (100 MHz, DMSO): δ 172.3 (-COOCH₃), 157.1 (-ArCO-), 144.7-144.8 (m, -ArC 2), 140.3-142.8 (m, -ArC 4), 142.1-142.3 (m, -ArC 6), 138.3-138.6 (m, -ArC 3), 136.0-136.1 (m, -ArC 5), 112.3 (t, -ArC 1), 52.3 (-OCH₃), 51.2 (α -C), 39.6 (-CH₂-, -VE DEPT), 24.5 (-CH-), 22.9 (-CH₃), 21.1 (-CH₃).

^{19}F -NMR (376 MHz, DMSO): δ -66.7 (dd, 2F, $J^4 = 6.4$ Hz, $J^3 = 22.9$ Hz), -77.8 (t, 1F, $J = 21.8$ Hz), -86.3 - -86.4 (m, 2F).

***N*-pentafluorobenzoyl-L-tryptophan methyl ester 115**

A solution of pentafluorobenzoyl chloride (1.45 g, 6.3 mmol) in dichloromethane (10 mls) was added dropwise to a solution of L-tryptophan methyl ester (1.60 g, 6.3 mmol) and triethylamine (1.27 g) in dichloromethane (10 mls). The solution was stirred for 8 hrs then washed with 5% NaHCO₃, 5% HCl and water. The organic extract was then dried over MgSO₄ and the solvent was removed *in vacuo* furnished and recrystallisation from ethyl acetate/hexane furnished **115** as a brown powder (1.12 g, 43%).

m.p. = 139-140 °C. $[\alpha]_{\text{D}}^{25} = -9.1^\circ$ (c, 1.8, EtOH).

Mass Spectrum: $[\text{M}+\text{Na}]^+$ found 435.0.

$C_{19}H_{13}N_2O_3F_5Na_1$ requires 435.3.

IR (KBr): ν 3392, 1754, 1678, 1518, 1004 cm^{-1} .

1H -NMR (400 MHz, DMSO): 10.91 (1H, bs, -NH-), 9.49 (1H, d, $J = 7.6$ Hz, -NH-), 7.51 (1H, d, $J = 7.6$ Hz, -PhH 1), 7.36 (1H, d, $J = 8.0$ Hz, -PhH 4), 7.18 (1H, d, $J = 2.4$ Hz, -C=C-H), 7.08 (1H, t, $J = 8.0$ Hz, -PhH 2), 7.00 (1H, t, $J = 8.0$ Hz, -PhH 3), 4.71-4.75 (1H, m, α -H), 3.66 (3H, s, -OCH₃), 3.13-3.29 (2H, m, -CH₂-).

^{13}C -NMR (100 MHz, DMSO): δ 171.7 (-COOCH₃), 157.2 (-ArCO-), 144.7-144.8 (m, -ArC 2), 140.3-142.8 (m, -ArC 4), 142.1-142.3 (m, -ArC 6), 138.3-138.5 (m, -ArC 3), 136.4 (-C=C-H), 135.8-136.0 (m, -ArC 5), 127.2 (-PhC 5), 124.1 (-C=C-H), 121.4 (-PhC 2), 118.8 (-PhC 3), 118.2 (-PhC 4), 112.3 (t, -ArC 1), 111.8 (-PhC1), 109.1 (-PhC 6), 54.0 (α -C), 52.5 (-OCH₃), 27.1 (-CH₂-, -VE DEPT).

^{19}F -NMR (376 MHz, DMSO): δ -66.5 (dd, 2F, $J^4 = 6.4$ Hz, $J^3 = 22.9$ Hz), -78.2 (t, 1F, $J = 22.5$ Hz), -86.5 - -86.6 (m, 2F).

2.7 References

- 1 a) DeRuiter, J., Swearingen, B.E., Wandrekar, V., Mayfield, C.A., *J. Med. Chem.* **1989**,
32, 1033. b) Leone-Bay, A., McInnes, C., Wang, N., DeMorin, F., Achan, D., Lercara,
2 C., Sarubbi, D., Haas, S., Press, J., Barantsevich, E., O'Broin, B., Milstein, S., Paton, D.,
J. Med. Chem. **1995**, *38*, 4257. c) Burdick, D.J., Paris, K., Weese, K., Stanley, M.,
Beresini, M., Clark, K., McDowell, R.S., Marsters Jr., J.C., Gadek, T.R., *Bioorg. Med.*
Chem. Lett. **2003**, *13*, 1015.
- 3 Benvenuti, S., Severi, F., Costantino, L., Vampa, G., Melegari, M., *Farmacolo* **1998**, *53*,
439.
- 4 Lee, H., Angus, R.H., Storer, A.C., Carey, P.R., *J. Mol. Struct.* **1989**, *214*, 1.
- 5 O'Brien, S.E., Browne, H.L., Bradshaw, T.D., Westwell, A.D., Stevens, M.F.G.,
Laughton, C.A., *Org. Biomol. Chem.* **2003**, *3*, 493.
- 6 Thomas, G., "*Medicinal Chemistry*", Wiley and Sons **2000**.
- 7 Park, B.K., Kitteringham, N.R., O'Neill, P.M., *Annu. Rev. Pharmacol. Toxicol.* **2001**, *41*,
443.
- 8 a) Reddy, T.J., Chan, L., Turcotte, N., Proulx, M., Periera, O.Z., Das, S.K., Siddiqui, A.,
Wang, W., Poisson, C., Yannopoulos, C.G., Bilimoria, D., L'Heureux, L., Alaoui,
H.M.A., Nguyen-Ba, N., *Bioorg. Med. Chem. Lett.* **2003**, *13*, 3341. b) Beguin, C.,
LeTiran, A., Stables, J.P., Voyksner, R.D., Kohn, H., *Bioorg. Med. Chem.* **2004**, *12*,
3079. c) Le, V.L., Mak, C.C., Lin, Y.C., Elder, J.H., Wong, C.H., *Bioorg. Med. Chem.*
2001, *9*, 1185.
- 9 Banks, R.E., Smart, B.E., "*Organofluorine Chemistry*" Kluwer Academic Publishing
1994.
- 10 Moillet, J.S., *J. Fluorine Chem.* **2001**, *109*, 13.
- 11 Smith, M.B., March, J., "*March's Advanced Organic Chemistry*", Wiley and Sons
2001.
- 12 Yoneda, N., Fukuhara, T., *Tetrahedron* **1996**, *52*, 23.
- 13 Olah, G.A., Nojima, M., Kerekes, I., *Synthesis* **1973**, 779.
- 14 Tsuji, M., Kuwano, E., Saito, T., Eto, M., *Biosci. Biotech. Biochem.* **1992**, *56*, 778.
- Pretsch, E., Clerc, T., Seibl, J., Simon, W., "*Spectral data for structure determination of*

-
- organic compounds*”, Springer-Verlag **1989**.
- 15 Dewick, P.M., “*Medicinal Natural Products*”, Wiley and Sons **2003**.
- 16 X. Ge, Y.M. Fu, Y.Q. Li, G.G. Meadows, *Arch. Biochem. Biophys.* **2002**, *403*, 50.
- 17 Fujita, T., Nose, T., Matsushima, A., Okada, K., Asai, D., Yamauchi, Y., Shirasu, N.,
Honda, T., Shigehiro, D., Shimohigashi, Y., *Tetrahedron Lett.* **2000**, *41*, 923.
- 18 Gaskell, S.J., *J. Mass. Spectrom.* **1997**, *32*, 677.
- 19 Williams, D.H., Fleming, I., “*Spectroscopic Methods in Organic Chemistry*”, McGraw-
Hill publishers, **1995**, 5th edition.
- 20 Coates, J.H., Coghlan, D.R., Easton, C.J., Hoskins, B.F., Lincoln, S.F., Tiekink, E.R.T.,
Z. Kristallographie **1989**, *188*, 131.
- 21 Gonzalez Manzano, R., Versanvoort, C., Wright, K., Twentyman, P.R., *Eur. J. Cancer*
1996, *32*, 2136.
- 22 Larsen, A.K., Escargueil A.E., Skladanowski, A., *Pharmacology and Therapeutics* **2000**,
85, 217.
- 23 Bradley, G., Ling, V., *Cancer Metastasis Rev.* **1994**, *13*, 223.
- 24 Cole, S.P.C., Bhardwaj, G., Gerlach, J.H., Mackie, J.E., Grant, C.E., Almquist, K.C.,
Stewart, A.J., Kurz, E.U., Duncan, A.M., Deeley, R.G., *Science* **1992**, *258*, 1650.
- 25 Jensen, P. B., Wessel, I., Falck, I. J. Mirski, S., Cole S. P. C., Sehested, M., *Lung*
Cancer, **1997**, *18*, 143.
- 26 Teodori, E., Dei, S., Scapecchi, S., Gualteiri, F., *Farmaco* **2002**, *57*, 385.
- 27 Tavares, F.X., Boncek, V., Deaton, D.N., Hassell, A.M., Long, S.T., Miller, A.B., Payne,
A.A., Miller, L.R., Shewchuk, L.M., Wells-Knecht, K., Willard Jr., D.H., Wright, L.L.,
Zhou, H.Q. *J. Med. Chem.* **2004**, *47*, 588.
- 28 http://www.fda.gov/ohrms/dockets/ac/99/slides/3521S1_03_PharmaciaUpjohn.ppt
- 29 <http://www.cancerquest.org/index.cfm?page=1196>
- 30 <http://www.ncbi.nlm.nih.gov/books/bv.fcgi?rid=cmed.section.11653>
- 31 http://www.plwc.org/plwc/MainConstructor/1,1744,_12-001148-00_14-00News%20-00_17-001029-00_18-0026675-00_19-0026676-00_20-001-00_21-008,00.asp
- 32 Jensen, B.V., Skovsgaard, T., Nielsen, S.L., *Lancet* **1996**, *347*, 297.
- 33 Davey, R.A., Longhurst, T.J., Davey, M.W., Belov, L., Harvie, R.M., Hancox, D.,

Wheeler, H., *Leukemia Research* **1995**, *19*, 275.

34 Wang, S., Folkes, A., Chuckowree, I., Cockcroft, X., Sohal, S., Miller, W., Milton, J., Wren, S., Vicker, N., Depledge, P., Scott, J., Smith, L., Jones, H., Mistry, P., Faint, R., Thompson, D., Cocks, S., *J. Med. Chem.* **2004**, *47*, 1329.

35 Conway, S.C., Perni, R.B., *Synthetic Communication* **1998**, *28*, 1539.

Chapter 3

Fluorobenzoyl dipeptidyl derivatives as inhibitors of the *Fasciola hepatica* cathepsin L endoproteases

3.1 Introduction

The group of cysteine proteases known as the cathepsins have been shown to play a crucial function in diseases such as osteoporosis, rheumatoid arthritis, cancer metastasis and infectious diseases.¹ Cathepsins are important targets for the development of inhibitors as therapeutic agents. Fasciolosis is caused by infection with *Fasciola hepatica* and *Fasciola gigantica* parasites. It is not only an important human disease but also affects cattle and sheep worldwide causing economic losses of approx 2 billion dollars.² It is caused by the ingestion of vegetation or water contaminated with the encysted infectious liver fluke larvae known as metacercariae.³ It has become clear that the predominant protease activity in this parasite was associated with cells of the gut epithelium.⁴ Like many other parasitic helminths, *Fasciola hepatica* liver flukes release many proteolytic enzymes that belong to the group of cysteine proteases. It has been suggested that these proteases may be involved in protecting the parasite against immune attack.⁵ Most of the current approaches to cathepsin inhibition involve molecules of a peptidic nature. The hydrolysable amide is replaced by an electrophilic functionality and the catalytic thiol of the enzyme reacts with the inhibitor to form a covalent complex. Until recently the most potent cysteine protease inhibitors were irreversible inhibitors with the electrophilic functionality alkylating the enzyme. Inhibitors containing electrophilic moieties such as aldehyde, halomethyl ketone and epoxide have been shown to be potent cysteine protease inhibitors.⁶ Previous work in these laboratories has identified *N*-benzoyl dipeptidyl derivatives as potent inhibitors of *Fasciola hepatica* protease. For this study all of the compounds prepared are based on a fluorobenzoyl dipeptidyl scaffold. The fluorobenzoyl moiety has been shown to be an effective *N*-terminal substitution in various potent inhibitors.⁷ There are generally two consequences of introducing fluorine into a drug molecule. Firstly there are the physicochemical properties, *i.e.* increased lipophilicity, increased acidity, decreased basicity and a change in hydrogen bonding properties. The inductive electron withdrawing effect of fluorine

is expected due to its electronegative nature but electron donation by resonance effects attributed to the three lone pair electrons is a distinctive property of fluorine. Secondly, there is the influence of fluorine substitution on the biological stability of a drug molecule through altering susceptibility to metabolism. Fluorine has been used as a means to developing safer and more reactive pharmaceuticals due to the strength of the carbon-fluorine bond that is very difficult to metabolise, so harmful and unproductive side reactions are unlikely to occur.

3.2 Synthesis of dipeptidyl derivatives.

The synthesis of dipeptides containing the amino acids L-leucine, glycine, β -alanine and γ -aminobutyric acid with *N*- and *C*-terminal modifications was carried out. The amino acids were coupled using an activating agent 1,3-dicyclohexylcarbodiimide (DCC) **119**. The mode of action of DCC involves the formation of an *O*-acylisourea intermediate **120** that is a potent acylating agent (Figure 3.1).

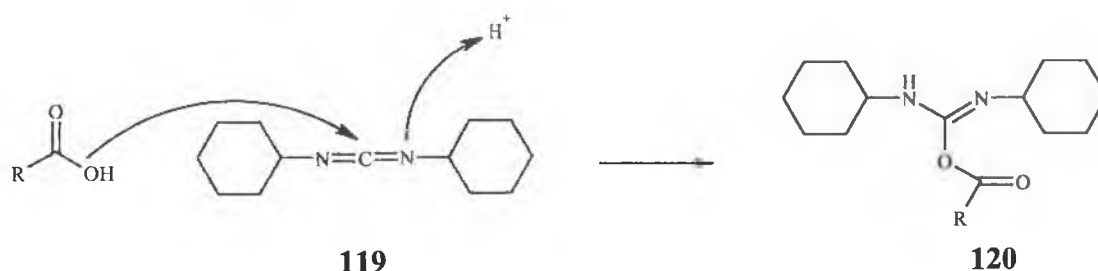


Figure 3.1 Mode of action of peptide coupling with 1,3-dicyclohexylcarbodiimide.

Unfortunately there are some disadvantages in using DCC as a coupling agent. Activation by **119** is shown to cause racemisation of the carboxy terminal residue. Reactive intermediates produced during coupling contain a basic center, which causes an intramolecular proton abstraction from the chiral carbon atom (Figure 3.2).

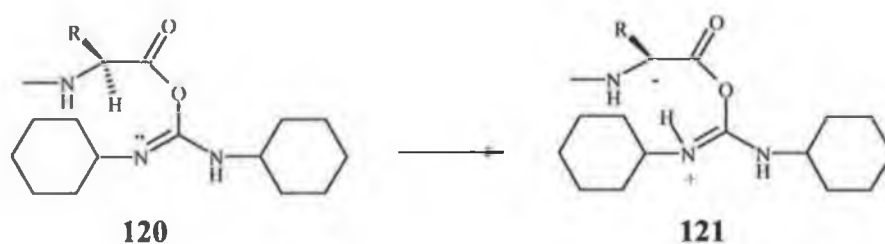


Figure 3.2 The mode of racemisation of the carbonyl terminal residue upon activation with 1,3-dicyclohexylcarbodiimide.

Chiral integrity can be preserved by the use of 1-hydroxybenzotriazole (HOBt) **122**. HOBt acts as an auxiliary nucleophile and reduces the lifetime of the *O*-acylisourea intermediate thus decreasing the occurrence of racemisation. An acylating agent of lower potency is formed which is still reactive to aminolysis, but is less susceptible to racemisation or other side reactions. 1-hydroxybenzotriazole also offers an acidic hydrogen that can be more easily removed by bases than the proton at the chiral center.

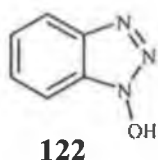


Figure 3.3 Structure of 1-hydroxybenzotriazole (HOBt).

Low yields are often another feature of peptide coupling using 1,3-dicyclohexylcarbodiimide **119**. These low yields can be accounted for due to the formation of a *N*-acylurea derivative **123** via an intramolecular rearrangement of the *O*-acyl derivative **120** formed by activation with 1,3-dicyclohexylcarbodiimide **119** (Figure 3.4). The attack of the activated carbonyl group by the nearby nucleophilic -NH- results in an *O* to *N* shift yielding a *N*-acylurea side product **123**.

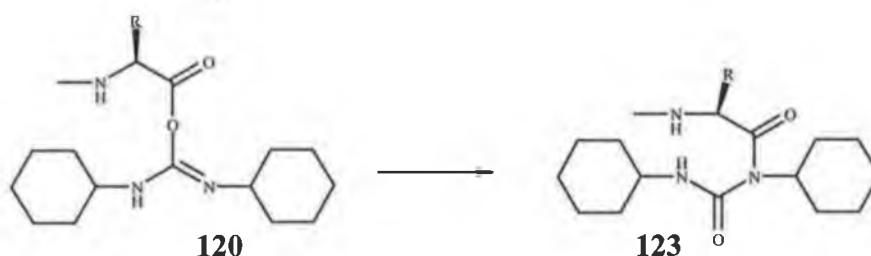


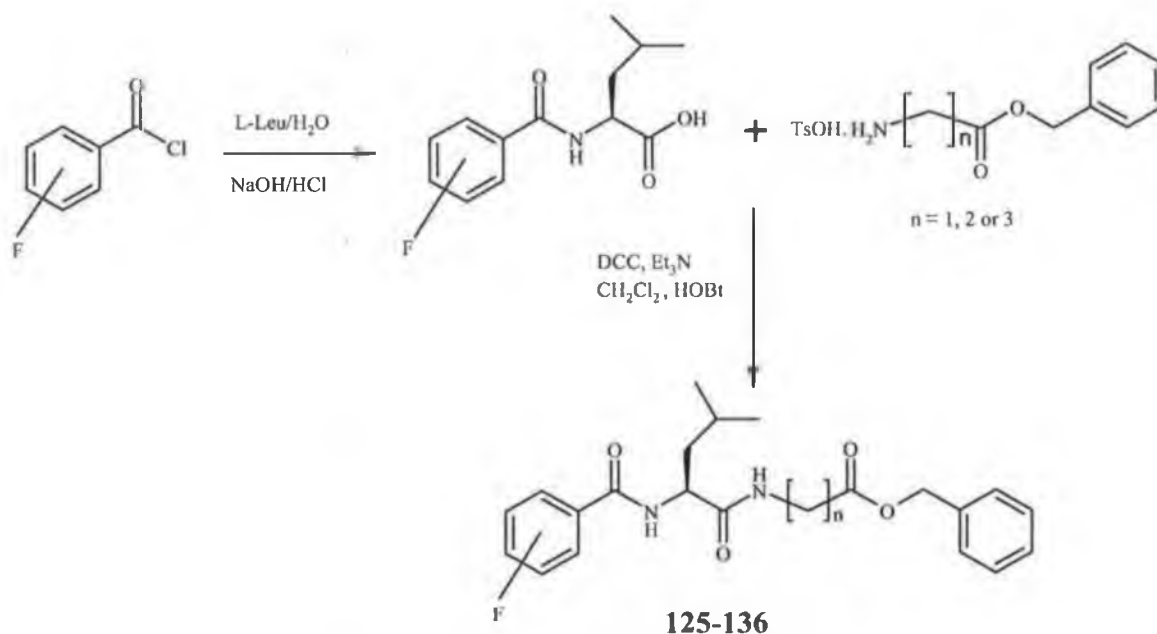
Figure 3.4 Formation of an *N*-acyl derivative **123** via intramolecular rearrangement of the *O*-acylisourea derivative.

The disadvantages of coupling peptides with 1,3-dicyclohexylcarbodiimide include low yields and poor reaction rates. The employment of HOBt and similar derivatives has greatly enhanced the ability of DCC to couple amino acids effectively. More recently, the design of peptide coupling reagents has concentrated on the ability of the reagent to limit the onset of racemisation while at the same time offer a highly competent coupling agent whose side products

can be easily removed. This method of design has resulted in coupling reagents incorporating the coupling ability of DCC and the racemisation suppression activity of HOBt being developed and utilised as effective combination type reagents.⁸

3.2.1 Synthesis and characterization of *N*-fluorobenzoyl dipeptidyl benzyl esters

Dipeptidyl derivatives have been shown to be effective inhibitors of the liver fluke *Fasciola hepatica* cysteine cathepsin L over the known commercial inhibitor *Z*-Phe-Ala-CHN₂ **124** at varying concentrations.⁹ The synthesis of a series of benzoyl dipeptidyl benzyl esters incorporating a fluorine atom into four different positions on the phenyl ring was undertaken to assess the effect of the fluorobenzoyl substituent. It has been shown that benzyl esters are potent protease inhibitors mainly due to their potential prodrug ability.¹⁰ A series of derivatives were synthesized as illustrated in Scheme 3.1.



Scheme 3.1 Synthesis of *N*-fluorobenzoyl dipeptidyl benzyl ester derivatives.

The benzyl ester tosylate salts were synthesized by refluxing the amino acid, *p*-toluenesulphonic acid, benzyl alcohol and toluene in a Dean and Stark apparatus.¹¹ The obtained yields ranged between 75 and 95 %. The fluorobenzoyl amino acids were synthesized in high yields (>75%) but often contained the by-product benzoic acid and therefore were purified by recrystallisation from ethanol and water. The fluorobenzoyl leucine derivatives displayed a tendency to absorb water and several recrystallisations were often needed. It was found that the

hydrolysis of *N*-fluorobenzoyl-L-leucine methyl ester derivatives using sodium hydroxide caused racemisation at the chiral center. In general the pentafluorobenzoyl dipeptidyl derivatives gave the lowest yields. This is probably due to two factors. Firstly, *N*-pentafluorobenzoyl-L-leucine was obtained as a viscous oil. Several attempts to recrystallise failed to furnish any crystalline solid. From the ^{19}F NMR of this compound the purity of this starting material was estimated at approx 95%. Secondly, *N*-pentafluorobenzoyl-L-leucine was found to be only partially soluble in dichloromethane, the solvent of choice for peptide coupling. The utilization of chloroform or tetrahydrofuran failed to improve the solubility of this compound. When the reaction was carried out at elevated temperatures increased solubility occurred but inactivation of the coupling reagents was prevalent.

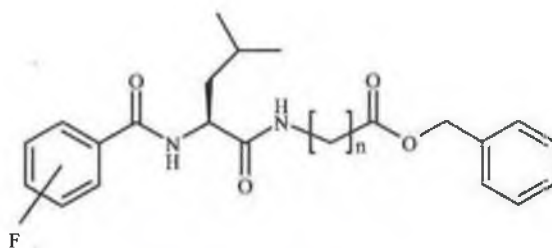


Table 3.1. *N*-fluorobenzoyl dipeptidyl ester derivatives

Compound	F	n	% Yield
<i>N</i> -2-fluorobenzoyl-L-Leu-Gly-OBn 125	2-F	1	37
<i>N</i> -3-fluorobenzoyl-L-Leu-Gly-OBn 126	3-F	1	45
<i>N</i> -4-fluorobenzoyl-L-Leu-Gly-OBn 127	4-F	1	66
<i>N</i> -pentafluorobenzoyl-L-Leu-Gly-OBn 128	2,3,4,5,6-F	1	42
<i>N</i> -2-fluorobenzoyl-L-Leu- β -Ala-OBn 129	2-F	2	58
<i>N</i> -3-fluorobenzoyl-L-Leu- β -Ala-OBn 130	3-F	2	50
<i>N</i> -4-fluorobenzoyl-L-Leu- β -Ala-OBn 131	4-F	2	46
<i>N</i> -pentafluorobenzoyl-L-Leu- β -Ala-OBn 132	2,3,4,5,6-F	2	47
<i>N</i> -2-fluorobenzoyl-L-Leu- γ -ABA -OBn 133	2-F	3	63
<i>N</i> -3-fluorobenzoyl-L-Leu- γ -ABA-OBn 134	3-F	3	50
<i>N</i> -4-fluorobenzoyl-L-Leu- γ -ABA -OBn 135	4-F	3	63
<i>N</i> -pentafluorobenzoyl-L-Leu- γ -ABA -OBn 136	2,3,4,5,6-F	3	46

3.2.2 ^1H NMR Study of the *N*-fluorobenzoyl dipeptidyl benzyl esters

The ^1H NMR spectra of the *N*-fluorobenzoyl dipeptidyl benzyl ester derivatives show the characteristic aromatic protons between δ 7 and 8. Due to the effect of ^1H - ^{19}F coupling the aromatic peaks of the fluorobenzoyl group appear as multiplets. The amide protons appear

between δ 8 and 9 with the aryl amide appearing at a lower field. One of the most interesting results shows that the amide proton of the 2-fluorobenzoyl dipeptides appears as double doublets. It has been proposed that a coplanar arrangement of the phenyl and amide residue is beneficial for inhibition and this is enhanced by an interaction between the 2-fluorine and the amide hydrogen bond.¹² A fluorine atom in any other position on the phenyl ring prevents coplanarity and additional ^{19}F - ^1H coupling is not seen. This conformational control feature of a single 2-fluorine substituent has been incorporated into many anti-cancer drugs.¹³ The methylene group of the benzyl moiety appears as a singlet at δ 5.1 due the electron deshielding effect of the attached oxygen atom. The methyl groups of the leucyl t butyl side chain appear as two individual doublets at δ 0.85 although they seem to appear in the same chemical environment. The methylene group of glycine appears as a double doublet due to its diastereotopic nature. The methylene groups of β -Ala appear as a triplet at δ 2.5 and a multiplet at δ 3.4. The methylene units of the γ -aminobutyric acid derivatives appear as a quartet at δ 3.13, a triplet at δ 2.38 and a multiplet centered at δ 1.63. The ^1H NMR spectrum of compound **129** is shown in Figure 3.5.

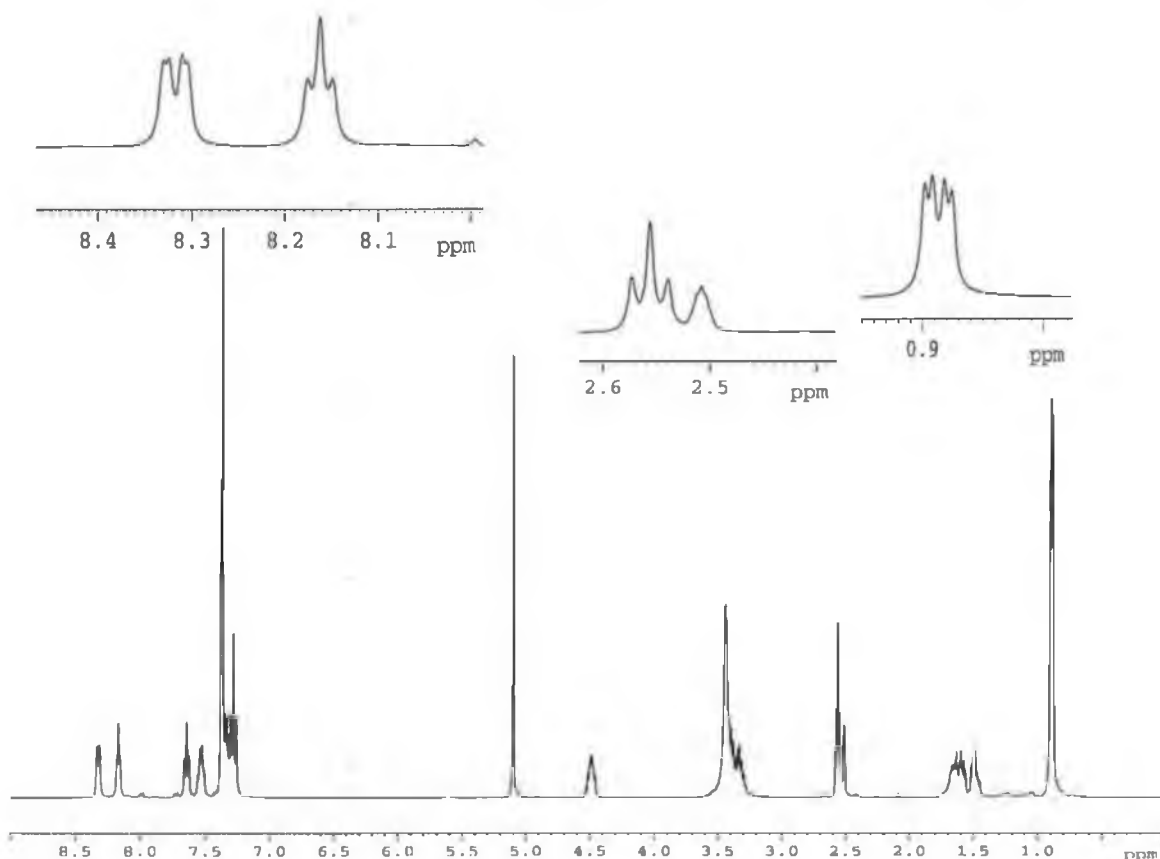


Figure 3.5 ^1H NMR spectrum of *N*-2-fluorobenzoyl-L-leucine- β -alanine benzyl ester **129**.

Table 3.2 Selected ^1H NMR data (δ) for the *N*-fluorobenzoyl dipeptidyl benzyl esters

Compound No.	NH	NH	α -H	-CH ₂ -
125	8.49	8.35	4.52-4.66	3.99, 3.88
128	9.13	8.70	4.60-4.64	4.03, 3.84
130	8.58	8.17	4.46-4.52	3.29-3.43, 2.54
134	8.55	8.06	4.44-4.50	3.10, 2.37, 1.50-1.73
136	9.16	8.23	4.48-4.51	3.09-3.16, 2.40, 1.47-1.75

The ^{13}C NMR spectra show distinctive doublets representing the carbon atoms attached to the fluorine atoms at approximately δ 160. The carbon atoms on the fluorobenzoyl ring system appear as doublets due to the effect of ^{13}C - ^{19}F coupling. The methyl groups of the leucine side chain appear at δ 21 and δ 23. The Infrared spectra show distinct peaks at 1642 and 1727 cm^{-1} due to amide and ester carbonyls respectively. Peaks at 1468 cm^{-1} can be attributed to N-H bending and C-N stretching of the C-N-H group. A peak at 3268 cm^{-1} is due to N-H stretching.

3.2.3 Synthesis and characterisation of *N*-pentafluorobenzoyl dipeptidyl methyl esters

N-pentafluorobenzoyl-L-alanine derivatives have been shown to be bioactive compounds. Dipeptidyl derivatives containing the *N*-pentafluorobenzoyl-L-alanine scaffold and the amino acid methyl esters of glycine **137**, β -alanine **138**, γ -aminobutyric acid **139**, L-alanine **140**, L-leucine **141**, L-phenylalanine **142**, L-valine **143**, L-tryptophan **144**, L-aspartic acid **145** and L-methionine **146** were prepared (Scheme 3.2). It is hoped that by varying the size and hydrophobicity of the side chain of the amino acid in the P1 position an optimized dipeptidyl compound will be achieved. These compounds will be tested for their biological activity as protease inhibitors of the liver fluke *Fasciola hepatica* cysteine cathepsin L endoproteases.

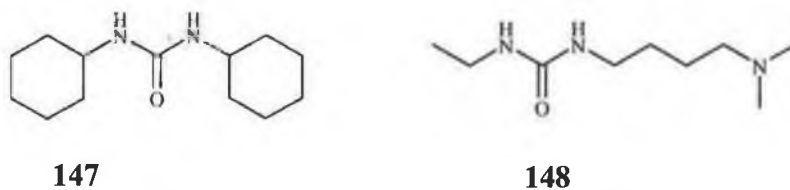


Figure 3.6 Urea side products formed by DCC **147** and EDC **148**

The dipeptidyl derivatives were synthesized using the coupling reagent 1-ethyl-3-(3-dimethylaminopropyl)carbodiimide (EDC) **149**. The mode of action of EDC is analogous to DCC **119** with the main advantage of EDC over DCC being the fact that the urea side product **148** formed during the reaction is water-soluble and hence purification is simplified. EDC has

been proposed to exist as a tautomeric mixture.¹⁴ It has been shown that both tautomers are potentially involved in the addition reactions of nucleophiles to EDC.¹⁵

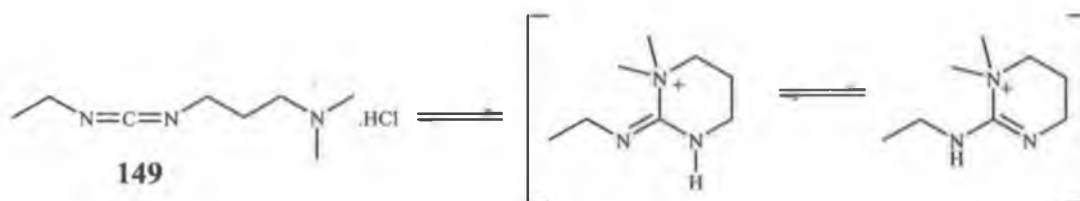
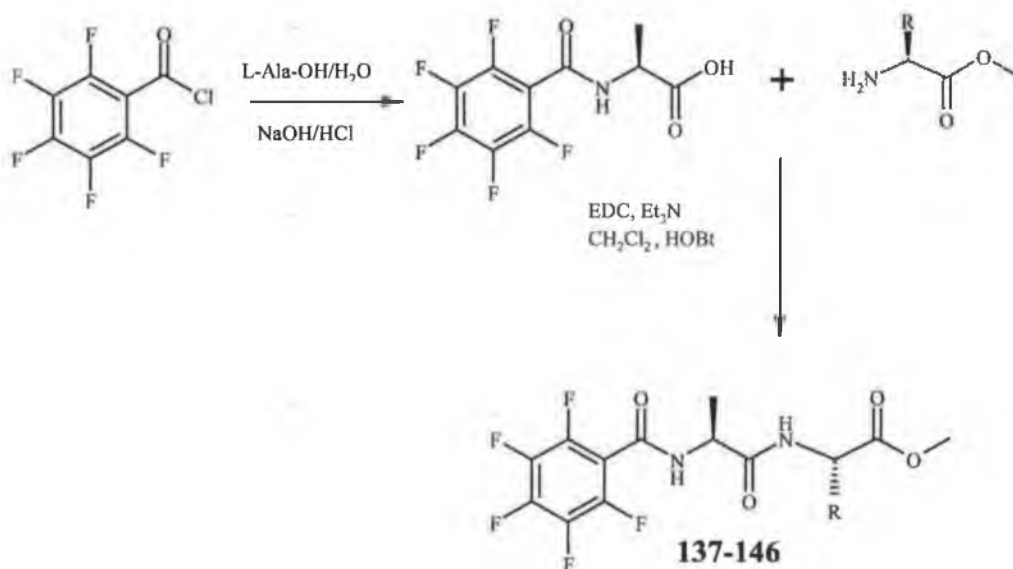


Figure 3.7 Tautomerisation of EDC

N-pentafluorobenzoyl-L-alanine was synthesized in an analogous manner to *N*-pentafluorobenzoyl-L-leucine. The pentafluorobenzoic acid impurity was removed by recrystallisation from ethanol and water. The amino acid methyl esters were prepared as hydrochloride salts using thionyl chloride and methanol.¹⁶ Yields for this reaction were as high as 80%. The dipeptidyl derivatives were purified using an acid water wash cycle.



Scheme 3.2 Synthesis of the *N*-pentafluorobenzoyl dipeptidyl derivatives.

Compound **145** gave the highest yield of 61%. The ester moiety of the L-aspartic acid side chain is the most polar derivative prepared. This compound gave a crystalline solid although due to its fine nature an x-ray crystal structure was not possible. The L-phenylalanine derivative **142** gave the lowest yield of 34%. The benzyl side chain of L-phenylalanine is one of the largest groups present on a naturally occurring amino acid. L-tryptophan has a similarly large aromatic

side chain and its derivative **144** only gave a yield of 37%. This indicates that a bulky aromatic side chain has a distinct steric effect on the yield of these dipeptidyl derivatives.

The ^1H NMR spectra of the *N*-pentafluorobenzoyl dipeptidyl derivatives have the characteristic α -hydrogens located between δ 4 and δ 5. The amide proton signal appears downfield at $\delta \sim 9.4$ due to the deshielding effect of a pentafluorobenzoyl moiety. The methyl group of alanine is found as a doublet at δ 1.2. The ^{19}F NMR shows three peaks, a double doublet representing the fluorine atoms in the 2- and 6- positions, a multiplet representing the fluorine atoms in the 3- and 5- positions and one triplet that represents the 4-fluoro substituent. The Infrared spectra show distinct peaks at 1653 and 1752 cm^{-1} due to amide and ester carbonyls respectively. Peaks at 1560 cm^{-1} can be attributed to N-H bending and C-N stretching of the C-N-H group. At 3292 cm^{-1} a peak due to N-H stretching is observed.

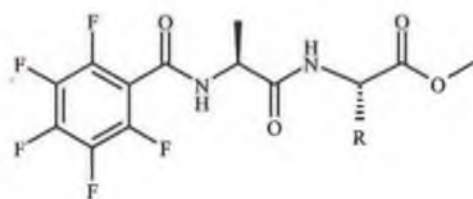


Table 3.3 *N*-pentafluorobenzoyl dipeptidyl ester derivatives

Compound	R	% Yield
<i>N</i> -pentafluorobenzoyl-L-Ala-Gly-OMe 137	-CH ₂	42
<i>N</i> -pentafluorobenzoyl-L-Ala- β -Ala-OMe 138	-(CH ₂) ₂	54
<i>N</i> -pentafluorobenzoyl-L-Ala- γ -ABA-OMe 139	-(CH ₂) ₃	49
<i>N</i> -pentafluorobenzoyl-L-Ala-L-Ala-OMe 140	-CH ₃	58
<i>N</i> -pentafluorobenzoyl-L-Ala-L-Leu-OMe 141	-CH ₂ CH(CH ₃) ₂	55
<i>N</i> -pentafluorobenzoyl-L-Ala-L-Phe-OMe 142	-CH ₂ Ph	34
<i>N</i> -pentafluorobenzoyl-L-Ala-L-Val-OMe 143	-CH(CH ₃) ₂	51
<i>N</i> -pentafluorobenzoyl-L-Ala-L-Try-OMe 144	-CH ₂ -Indole	37
<i>N</i> -pentafluorobenzoyl-L-Ala-L-Asp-OMe 145	-CH ₂ COOCH ₃	61
<i>N</i> -pentafluorobenzoyl-L-Ala-L-Met-OMe 146	-(CH ₂) ₂ SCH ₃	52

3.2.4 ^{13}C NMR study of the *N*-pentafluorobenzoyl-L-alanine dipeptidyl methyl esters

The ^{13}C NMR spectrum of *N*-pentafluorobenzoyl-L-Ala-L-Asp-(OMe)₂ **145** is shown in Figure 3.8. The two ester carbonyls of L-aspartic acid dimethyl ester appear at $\delta \sim 171$. The peptide carbonyl appears further downfield at $\delta \sim 172$ with the carbonyl of the benzoyl group shown at $\delta \sim 156$. The carbon atoms of the pentafluorobenzoyl moiety show a very distinct pattern. Four multiplets are shown centered at $\delta \sim 145$, ~ 142 , ~ 138 and ~ 136 . These multiplets represent the *ortho* and *meta* carbons. Two further multiplets are located at $\delta \sim 140$ and $\delta \sim 143$. These multiplets represent the *para* carbon. Finally the *ipso* carbon is located as a triplet at $\delta \sim 111$. The methyl esters appear as individual carbons at $\delta \sim 52$ due to the deshielding effect of the attached oxygen atom.

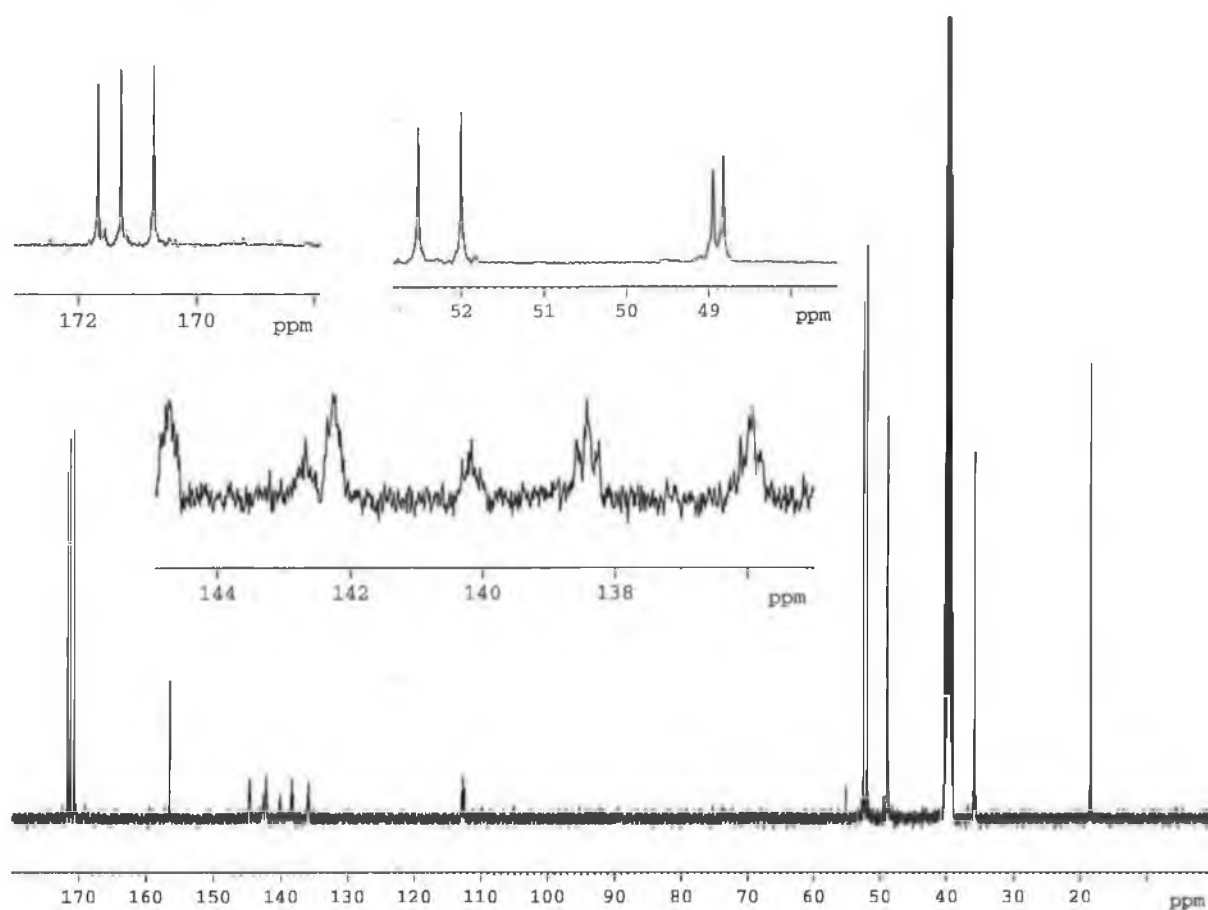


Figure 3.8 ^{13}C NMR spectrum of *N*-pentafluorobenzoyl-L-Ala-L-Asp dimethyl ester **145**.

The methylene group of L-aspartic acid appears at $\delta \sim 38$. This was confirmed by the DEPT 135 spectrum. The α -carbons of alanine and aspartic acid are located at $\delta \sim 48.9$ and $\delta \sim 48.8$

respectively with the methyl group of the alanine side chain appearing at $\delta \sim 18$. The α -carbon of the L-valine derivative **143** appears the furthest downfield at approx δ 57.6 due to the proximity of the i propyl side chain.

Table 3.4 Selected ^{13}C NMR data (δ) for the *N*-fluorobenzoyl-L-alanine dipeptidyl methyl esters

Compound No.	C=O _{Ester}	C=O _{Amide}	C=O _{Amide}	α -C	-OMe
137	170.5	156.6	172.2	49.0, 40.8	52.0
140	171.5	156.5	173.2	48.9, 47.9	52.1
143	172.0	156.5	172.4	48.9, 57.6	52.1
144	171.7	156.5	172.4	48.9, 53.5	52.1
146	171.9	156.5	172.4	49.0, 51.2	52.3

3.2.5 Synthesis and characterisation of *N*-fluorobenzoyl dipeptidyl nitrile derivatives

Peptidic molecules bearing the electrophilic nitrile warhead have been reported to be potent inhibitors of cathepsin proteases.¹⁷ One of the first such examples was the dipeptidyl derivative *N*-benzoyl-L-Leu-Gly-CN synthesized by Suzue *et al* in 1968.¹⁸ Previous work in our group has shown this to be a potent inhibitor of the liver fluke *Fasciola hepatica* cathepsin L endoproteases. The majority of recent research with nitrile derivatives has concentrated on developing the *N*-terminal substituent next to the P2 position with the fluorobenzoyl moiety showing increased selectivity.¹⁹ Dipeptidyl nitrile derivatives are believed to function as reversible inhibitors with the nitrile moiety undergoing attack by the activated thiol group of cysteine in the active site of the protease (Figure 3.9).

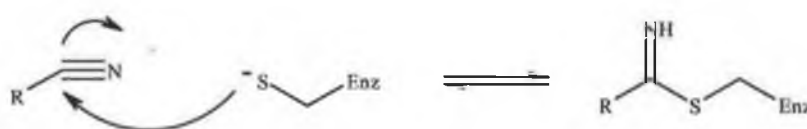
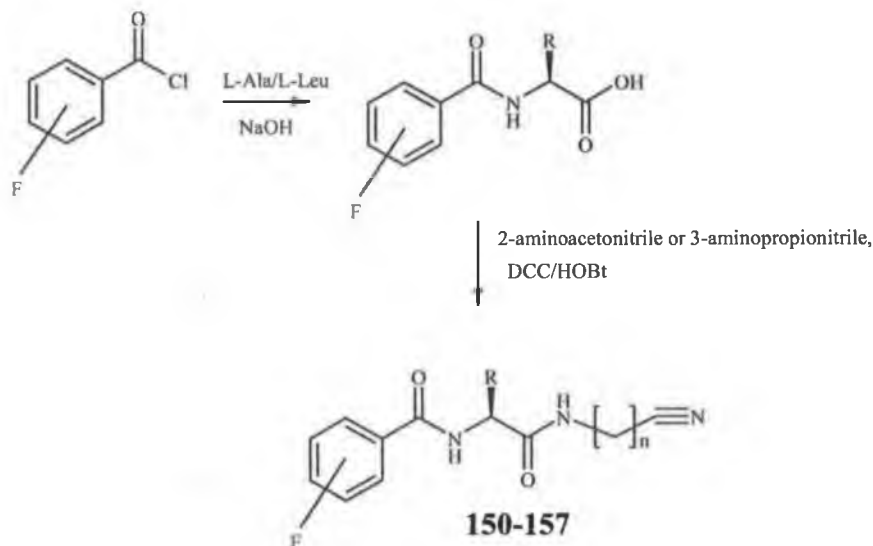


Figure 3.9 Mechanism of nitrile inhibition of cysteine proteases.

^1H NMR studies have shown that inhibition occurs through the formation of a thioimidate intermediate and this process is fully reversible.²⁰ A series of fluorobenzoyl dipeptidyl nitrile derivatives based on the *N*-benzoyl-L-Leu-Gly-CN scaffold have been synthesised. It is hoped that by extending the number of methylene units in the P1 position and the size of the P2 position, superior inhibitory activities will result. The fluorobenzoyl amino acids were prepared as previously described using the *Schotten-Baumann* reaction.



Scheme 3.3 Synthesis of *N*-fluorobenzoyl dipeptidyl nitrile derivatives.

The dipeptidyl derivatives gave yields varying from 42 to 69 % (Table 3.5). The highest yields recorded were for the 2-fluorobenzoyl-L-leucine derivatives with both the glycyl **150** and β -alanyl **154** analogues giving yields of over 68 %. The lowest yield recorded was for compound **153**. This pentafluorobenzoyl derivative was obtained in a yield of just 42 %. The fluorobenzoyl dipeptidyl nitriles were found to be partially insoluble in organic solvents but they were completely insoluble in aqueous media. These solubility problems often hindered successful isolation. A large amount of solvent was often required to dissolve the nitrile derivatives completely. The pentafluoro derivatives were found to be the least soluble in organic solvents such as dichloromethane, chloroform, ethyl acetate or methanol. Overall the L-leucine derivatives gave higher yields than their L-alanine analogues. This is probably due to the fact that the leucine derivatives were slightly more soluble in an organic medium.

The ^1H NMR spectra of these compounds show the distinctive amide protons appearing at $\delta \sim 8.5$. The α -hydrogen of L-leucine or L-alanine shows up as a multiplet due to coupling with the amide and the side chain group at approx δ 4.5. The methylene protons of the glycyl derivatives appear as singlets at $\delta \sim 4.15$. This is in sharp contrast to the previously discussed benzyl ester derivatives **125-136** where the methylene group appears as a double doublet due to its diastereotopic nature where coupling with both the amide proton and the methylene protons occurs. The ^{13}C NMR spectra show a distinctive peak for the nitrile moiety at $\delta \sim 117$. The nitrile moiety shifted the chemical shifts of the attached methylene units upfield. The methylene carbon

atom of the amino acid glycine usually appears at $\delta \sim 40.5$ but the methylene unit of glycine nitrile is seen appearing at approximately $\delta 27.4$. The fluorobenzoyl moiety causes the carbon atoms of the phenyl ring to appear as doublets and triplets due to ^{13}C - ^{19}F coupling. The ^{19}F NMR spectra of these compounds show the monofluoro derivatives appearing as multiplets due to ^{19}F - ^1H coupling. The Infrared spectra of these compounds show a distinctive band at $\sim 2370\text{ cm}^{-1}$ responsible for the nitrile moiety. The amide bond is represented by two peaks. Peaks at $\sim 1505\text{ cm}^{-1}$ can be attributed to N-H bending and C-N stretching of the C-N-H group. A peak at $\sim 3286\text{ cm}^{-1}$ is due to N-H stretching.

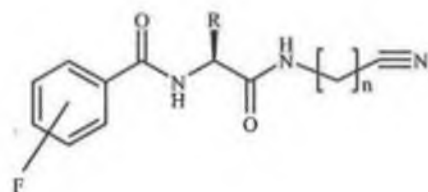


Table 3.5 *N*-pentafluorobenzoyl dipeptidyl nitrile derivatives

Compound	F	R	n	% Yield
150	2-F	$-\text{CH}_2\text{CH}(\text{CH}_3)_2$	1	69
151	4-F	$-\text{CH}_2\text{CH}(\text{CH}_3)_2$	1	64
152	2-F	$-\text{CH}_3$	1	55
153	Penta-F	$-\text{CH}_3$	1	42
154	2-F	$-\text{CH}_2\text{CH}(\text{CH}_3)_2$	2	68
155	4-F	$-\text{CH}_2\text{CH}(\text{CH}_3)_2$	2	53
156	2-F	$-\text{CH}_3$	2	49
157	Penta-F	$-\text{CH}_3$	2	53

3.2.6 HMQC study of 4-fluorobenzoyl-L-leucine-glycine nitrile 151

Table 3.6 and Figure 3.10 show the C-H correlation spectrum of *N*-4-fluorobenzoyl-L-leucine-glycine nitrile 151.

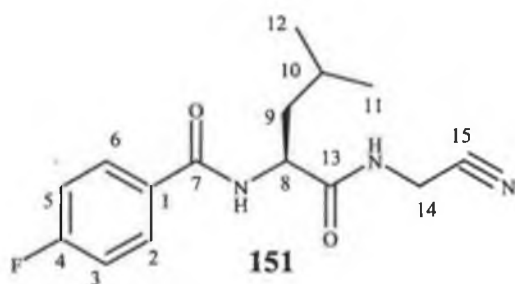


Table 3.6 C-H correlation of *N*-4-fluorobenzoyl-L-leucine-glycine nitrile **151**

Site	¹ H	¹³ C	HMQC
1		130.7	
2	7.99-8.02		130.66
3	7.28-7.32		115.5
4		164.3	
5	7.28-7.32		115.3
6	7.99-8.02		130.62
7		165.7	
8	4.48-4.54		51.9
9	1.52-1.76		40.2
10	1.52-1.76		24.7
11	0.90		23.3
12	0.86		21.5
13		173.3	
14	4.14		27.4
15		117.9	

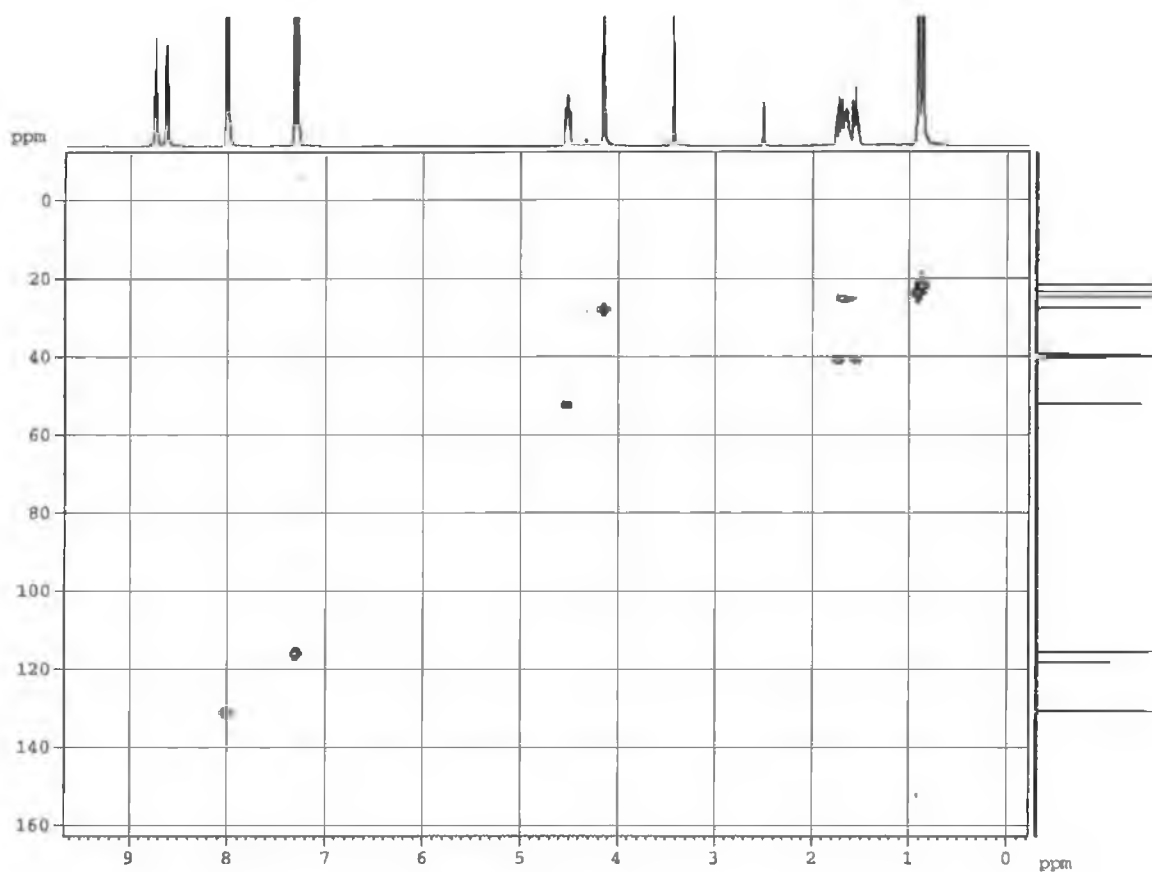


Figure 3.10 HMQC Spectrum of *N*-4-fluorobenzoyl-L-leucine-glycine nitrile **151**.

3.3 Protease inhibitory activity of *N*-fluorobenzoyl dipeptidyl derivatives

3.3.1 Introduction

Cathepsins are a complex group of cysteine proteases that cleave peptide bonds. They have been implicated as essential components of various diseases such as rheumatoid arthritis, cancer and malaria.¹ Their broad-spectrum biological activities render them as key therapeutic targets. Fasciolosis or liver fluke as it is commonly known has been estimated to be present in up to 2 million humans worldwide and its economic losses on cattle and sheep livestock is estimated at \$2 billion annually.² Increasing resistance to the present chemotherapy against fasciolosis in animals requires novel chemotherapeutic approaches. A series of potential cathepsin inhibitors have been developed and their bioactivity was assessed with the cathepsin protease *Fasciola hepatica* that has been implicated in the reproduction of the parasites.²¹

Commercially available peptide substrates with substituents added to either the *N*- or *C*-termini are most commonly used to assay, characterize and perform inhibition studies on proteases. The *C*-terminal substituents usually involve a chromophoric amine such as 4-naphthylamine(-NHNap) or a fluorogenic group such as 7-amino-4-methylcoumarin (-NHMec) **159**. These species are highly absorbent or fluorescent when cleaved from the substrate and can be detected spectrophotometrically or fluorometrically. The fluorogenic substrates are far more sensitive due to the ability of fluorescence to be detected against a low background in contrast to absorption spectrophotometry that requires measurement of transmitted light relative to high incident light levels at the same wavelength.²² Although these substrates are useful in evaluating the inhibitory potency of potential therapeutic agents, *in vivo* testing has shown the physicochemical properties of the enzyme can vary against natural protein substrates.

3.3.2 Fluorescent assay to determine the inhibitory potency of dipeptidyl derivatives against the *Fasciola hepatica* cysteine cathepsin L endoproteases

A standard fluorometric assay has been developed using a fluorogenic substrate to test the activity of these compounds. In this assay activity was determined by measuring the release of the fluorescent species 7-amino-4-methyl-coumarin (-NHMec) **159** from the substrate Z-Phe-Arg-NHMec **158** upon enzymatic hydrolysis by cathepsin L protease isolated from *Fasciola hepatica*. Assays were carried out using a final concentration of 10 μ M substrate in 0.1 M sodium acetate buffer pH 10, containing 0.5 mM dithiotheritol in a final volume of 1 ml. The

mixture of enzyme and inhibitor were incubated together at 37 °C for 15 mins. The substrate was then added and the mixture was further incubated for 30 mins. The reaction was stopped by the addition of 200 µL of a 10% acetic acid solution. The amount of 7-amino-4-methyl-coumarin (-NHMeC) **159** released was measured using a Perkin-Elmer fluorescence spectrophotometer with excitation at 370 nm and emission at 440 nm. The positive control contained only the enzyme extract and the substrate Z-Phe-Arg-NHMeC **158**. There were two negative controls used. One contained the enzyme and inhibitor and the other contained just the inhibitor and the substrate. All assays were performed in triplicate with the mean result being taken.

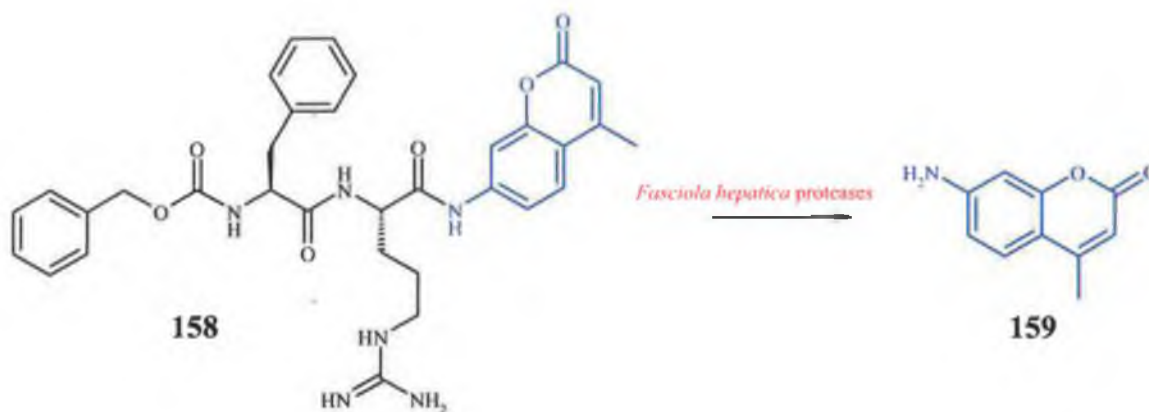


Figure 3.11 Hydrolysis of Z-Phe-Arg-NHMeC **158** by cathepsin L protease with liberation of the fluorescent 7-amino-4-methyl coumarin (-NHMeC) **159**.

3.3.3 Protease inhibition of the *N*-fluorobenzoyl dipeptidyl benzyl ester derivatives

The *N*-benzoyl-L-Leu-Gly scaffold has been shown to be crucial for the inhibition of various cathepsins. Benzyl esters increase the lipophilicity of amino acid derivatives but they are easily hydrolyzed by cellular processes. It is proposed that the benzyl ester moiety will function as a prodrug with the deprotected acid derivative in fact being the potent derivative. It is hoped that by modifying the length of the P1 side chain between one and three methylene groups, employing glycine, β -alanine and γ -aminobutyric acid will furnish potent inhibitors of *Fasciola hepatica* cathepsin L endoproteases. The benefits of introducing fluorine into a molecule have been well documented.

The γ -amino butyric acid derivatives were found to be the most effective inhibitors. The incorporation of three methylene units into the P1 position gave inhibitors with activity up to 2-

fold greater than their β -alanine analogues and as much as 7-fold greater than the glycine derivatives. The most active compound was found to be *N*-2-fluorobenzoyl-L-leucine- γ -aminobutyric acid benzyl ester **133** with an IC_{50} value of 15.32 μ M (Table 3.7). The P3 substitutions demonstrated an influence on the overall activity of these derivatives. In the case of the β -Ala and γ -ABA derivatives mono-substitution of the benzoyl ring gave the best results but it was the pentafluoro group that gave the best results with glycine compounds. Overall the benzyl ester moiety failed to achieve single digit micromolar inhibition due to the fact that the benzyl ester moiety is probably not electrophilic enough.

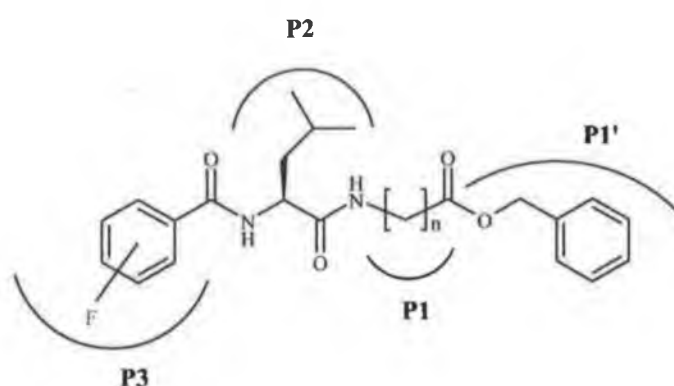


Table 3.7 Inhibitory activity of *N*-fluorobenzoyl dipeptidyl benzyl ester derivatives

Compound	% Protease Inhibition			IC_{50} μ M
	10 μ M	50 μ M	100 μ M	
125	3.46	26.50	33.71	> 100
126	4.29	12.79	20.53	> 100
127	16.12	54.21	74.67	43.35
128	18.55	57.23	80.87	39.52
129	24.68	66.32	86.50	29.38
130	18.24	56.85	79.32	40.08
131	13.33	44.26	59.34	62.34
132	14.87	47.08	70.42	57.68
133	46.52	74.65	92.24	15.32
134	34.88	67.04	87.75	24.78
135	42.34	69.82	90.15	19.25
136	38.58	68.58	89.21	21.38

3.3.4 Protease inhibition of the *N*-pentafluorobenzoyl dipeptidyl methyl ester derivatives

We have shown that *N*-pentafluorobenzoyl-L-alanine derivatives are efficient inhibitors of the MRP-1 cancer resistant mechanism. We were interested to assess the potential biological activity of analogous dipeptidyl derivatives on the inhibition of *Fasciola hepatica* cathepsin L endoproteases. It was hoped that by modifying the size and hydrophobicity of the P1 substituent an optimum dipeptidyl scaffold will be prepared.

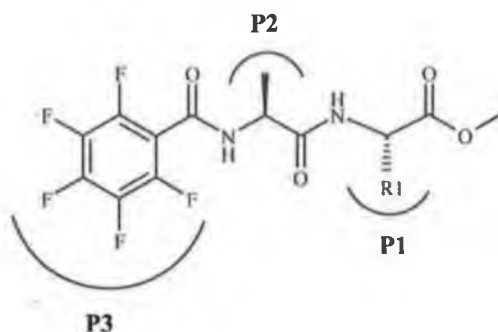


Table 3.8 Inhibitory activity of *N*-pentafluorobenzoyl dipeptidyl methyl ester derivatives

Compound	% Protease Inhibition			
	10 μ M	50 μ M	100 μ M	IC ₅₀ μ M
137	12.10	51.02	65.56	48.58
138	8.47	46.35	60.73	59.82
139	6.40	14.79	20.11	> 100
140	20.62	61.14	74.36	29.34
141	33.25	69.84	83.20	18.69
142	24.95	65.22	79.38	20.21
143	23.87	62.88	77.64	23.65
144	16.70	57.42	70.09	35.47
145	1.22	3.68	7.98	> 100
146	3.45	4.24	8.54	> 100

N-pentafluorobenzoyl-L-Ala-L-Leu-OMe **141** was found to be the most potent inhibitor of the pentafluoro derivatives with an IC₅₀ value of 18.69 μ M (Table 3.8). Previously it has been shown that an ^tbutyl group in the P2 position is often needed for efficient inhibition. In this case the leucyl side chain is in the P1 position but similarities persist. Compound **143** has an ^tpropyl

group in the P1 substitution. The hydrogen bonding interactions, hydrophobicity and polarity of this group are very similar to the 'butyl group and inhibitory potency seems to be similar with compound **142** having an IC_{50} value of 20.21 μ M. The two most polar compounds, the aspartic acid derivative **145** and the methionine derivative **146** recorded IC_{50} values of greater than 100 μ M. This illustrates that the presence of a polar side chain in the P1 position is not suitable for efficient inhibition of the *Fasciola hepatica* cathepsin L endoproteases.

3.3.5 Protease inhibition of the *N*-fluorobenzoyl dipeptidyl nitrile derivatives

N-benzoyl-L-Leu-Gly nitrile is a potent inhibitor of *Fasciola hepatica* cathepsin L endoproteases.⁹ The electrophilic nature of the nitrile moiety is believed to be crucial to the effectiveness of this compound as a potent inhibitor. Fluorinated analogues of similar derivatives have been prepared with modifications to the P1 and P2 positions carried out.

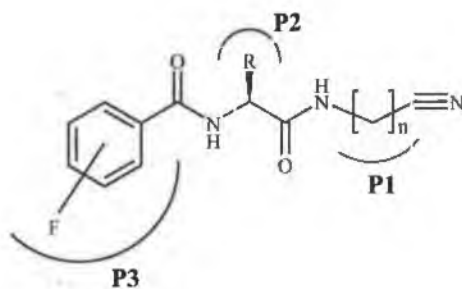


Table 3.9 Inhibitory activity of *N*-fluorobenzoyl dipeptidyl nitrile derivatives

Compound	% Protease Inhibition			IC_{50} μ M
	10 μ M	50 μ M	100 μ M	
150	77.74	93.17	95.61	3.04
151	82.92	93.91	96.05	2.78
152	10.35	33.51	54.23	87.55
153	13.54	41.43	67.11	68.34
154	35.25	68.58	88.02	24.32
155	39.22	69.95	91.12	21.61
156	7.24	25.78	41.54	>100
157	9.31	29.33	42.68	>100

By modifying the length of the side chain in the P2 position and by extending number of methylene units in the P1 position it was hoped to improve the inhibitory activity. The inhibitory activities of the compounds are shown in Table 3.9. Modifications of the P1, P2 and P3 positions were carried out. Three different fluorine positions on the phenyl ring were analysed. The pentafluoro and 4-fluoro derivatives were shown to be more potent derivatives than the 2-fluoro analogues. A reduction of the P2 substituent size by using L-alanine resulted in a decrease in activity of up to 30 fold. To increase the number of methylene units present at the P1 position a β -Alanine derivative was employed in place of glycine. By increasing the number of methylene units to two, the inhibitory activity was shown to decrease by up to 8 fold. This clearly shows that a glycine residue in the P1 position and a leucine residue in the P2 position are essential for effective inhibition.

3.3.6 True inhibitory activity of the most potent protease inhibitors

The activity of *Fasciola hepatica* cysteine cathepsin L endoprotease against the substrate Z-Phe-Arg-NHMec can be blocked by micromolar concentrations of the commercially available diazomethane, Z-Phe-Ala-CHN₂ **124**.²³ An assay comparing the nitrile derivatives, **150** and **151** to Z-Phe-Ala-CHN₂ **124** was undertaken in order to evaluate the true inhibitory potency of the nitrile analogues. The assay was carried out using six different micromolar concentrations of each compound and inhibition was measured as previously described. From this study the inhibitory activity of *N*-2-fluorobenzoyl-L-leu-gly nitrile **150** was shown to be slightly less than the activity of **124**. Compound **150** records an IC₅₀ value of 3.04 μ M compared to 2.96 μ M of compound **124**. However compound **150** records greater inhibition at concentrations of 1.25 and 20 μ M over compound **124**.

Table 3.10 Bioactivity of compounds **150**, **151** and **124** against *Fasciola hepatica* endoprotease

Compound	% Protease Inhibition						
	0.63 μ M	1.25 μ M	2.5 μ M	5 μ M	10 μ M	20 μ M	IC ₅₀ μ M
150	9.38	29.49	35.64	59.67	77.74	88.10	3.04
151	10.41	21.62	48.21	69.89	82.92	90.57	2.78
124	11.92	28.11	45.56	63.75	78.80	87.47	2.96

Alternatively it was found that compound **151** has superior inhibitory potency than the commercial inhibitor **124** at almost all concentrations. *N*-4-fluorobenzoyl-L-leucine-glycine nitrile **151** was found to have an IC₅₀ value of 2.78 μM compared to the 2.96 μM for compound **124**. At a concentration of 5 μM compound **151** is approximately 4% more effective as an inhibitor of *Fasciola hepatica* cathepsin L endoproteases than compound **124**. These results show that *N*-fluorobenzoyl dipeptidyl nitrile derivatives have potential as commercial inhibitors of *Fasciola hepatica* cysteine cathepsin L endoprotease.

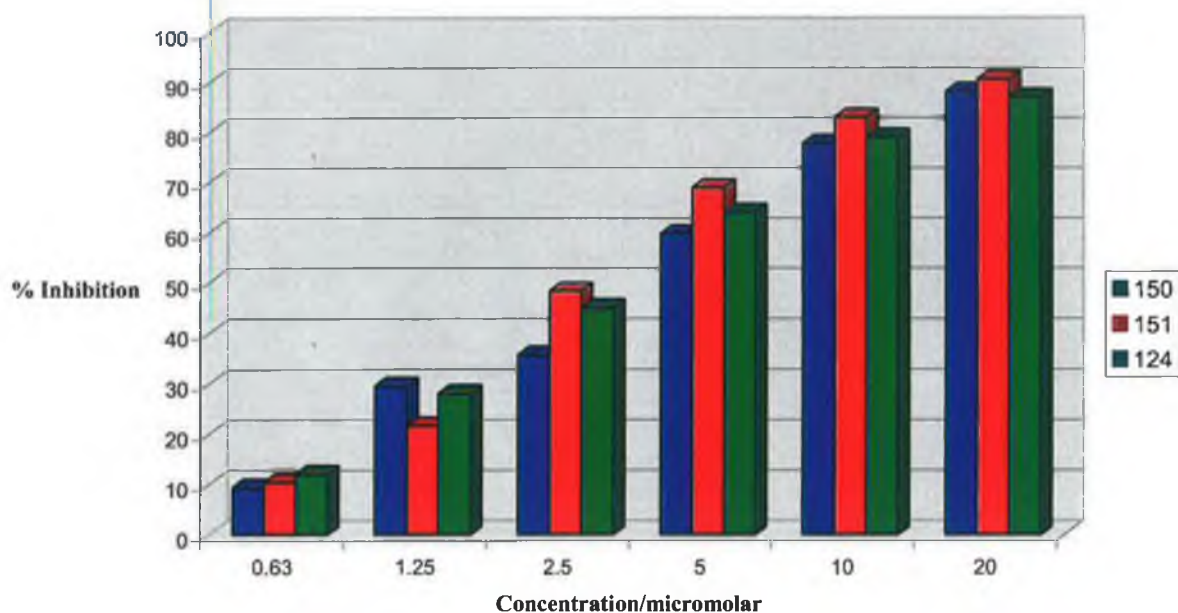


Figure 3.12 A bar graph illustration of the % inhibition of *N*-2-fluorobenzoyl-L-Leu-Gly-CN **150**, *N*-4-fluorobenzoyl-L-Leu-Gly-CN **151** and Z-Phe-Ala-CHN₂ **124** towards *Fasciola hepatica* cysteine cathepsin L endoprotease at varying concentration /μM

3.4 Conclusion

In summary, we have identified potent inhibitors of the *Fasciola hepatica* liver fluke cathepsin L proteases with the two most successful derivatives being the nitrile compounds **150** and **151**. From the protease inhibition results it is very clear that the presence of an electrophilic isostere adjacent to the P1 position is essential for effective inhibition. It has been shown that the introduction of a benzyl or methyl ester moiety decreases the inhibitory activity in comparison

with the nitrile moiety. We have also shown that the importance of the L-Leu-Gly scaffold varies as the C-terminal is modified. The scaffold is the most effective dipeptide when a nitrile moiety is attached. This is not the case with the benzyl ester derivatives with the dipeptide L-Leu- γ -ABA producing the most active derivatives. It has been shown that different fluoro-substitution patterns on the benzoyl ring have a distinct effect on the inhibitory ability of these compounds. The most effective substitution is monofluorination although this is often dependent on the structure of the remaining molecule. From this study it has been shown that the fluorobenzoyl moiety is an effective N-terminal substituent for dipeptidyl inhibitors of the *Fasciola hepatica* cathepsin L endoproteases. The inhibitory potency of the nitrile compounds N-2-fluorobenzoyl-L-leucine-glycine nitrile **150** and N-4-fluorobenzoyl-L-leucine-glycine nitrile **151** relative to the commercial inhibitor Z-Phe-Ala-CHN₂ **124** shows that such fluorobenzoyl dipeptidyl derivatives may have a role to play as commercial inhibitors of *Fasciola hepatica* cathepsin L endoproteases.

3.5 Experimental

General Procedures.

All chemicals were purchased from Sigma/Aldrich and used as received. When necessary solvents were purified prior to use and stored under nitrogen. Dichloromethane was distilled from CaH₂ and triethylamine was distilled and stored over potassium hydroxide pellets. Commercial grade reagents were used without further purification. Riedel-de Haën silica gel was used for thin layer and column flash chromatography. Melting points were determined using a Griffin melting point apparatus and are uncorrected. Specific rotation $[\alpha]_D$ studies were recorded on a Perkin Elmer 241 polarimeter. Infrared spectra (IR) were recorded on a Nicolet 405 FT-IR spectrometer. Elemental analysis was carried out by the Microanalytical Laboratory at University College Dublin. Electrospray mass spectra were recorded on a Bruker Esquire 3000 series LC/MS. NMR spectra were obtained on a Bruker AC 400 NMR spectrometer operating at 400 MHz for ¹H NMR, 376 MHz for ¹⁹F NMR and 100 MHz for ¹³C NMR. The ¹H and ¹³C NMR chemical shifts (ppm) are relative to tetramethylsilane and the ¹⁹F NMR chemical shifts (ppm) are relative to trifluoroacetic acid. All coupling constants (*J*) are in Hertz.

General procedure for the synthesis of N-fluorobenzoyl dipeptides 125-136

***N*-2-fluorobenzoyl-L-leucine-glycine benzyl ester 125**

N-2-fluorobenzoyl-L-leucine (0.8 g, 3.16 mmol) was dissolved in dichloromethane (50 ml) with glycine benzyl ester tosylate (1.12 g, 3.16 mmol), 1-hydroxybenzotriazole (0.43 g, 3.16 mmol) and triethylamine (0.44 ml). The mixture was cooled to 0 °C, and 1,3-dicyclohexylcarbodiimide (0.65 g, 3.16 mmol) was added. After 30 min. the solution was raised to room temperature and the reaction was allowed to proceed for 8 hrs. The precipitated *N,N*-dicyclohexylurea was removed by filtration and the filtrate was washed with 10% potassium hydrogen carbonate, 10% citric acid, water and dried over magnesium sulphate. The solvent was evaporated *in vacuo* and recrystallisation from ethyl acetate/hexane furnished **125** as a white powder (0.45 g, 37%).

m.p. = 101-103 °C. $[\alpha]_D^{25} = -18.2^\circ$ (c, 3.0, EtOH).

Anal. calcd. for C₂₂H₂₅N₂O₄F₁: C, 65.98; H, 6.29; N, 6.99.

Found C, 65.59; H, 6.04; N, 7.12.

Mass Spectrum: $[M+Na]^+$ found 423.2.

C₂₂H₂₅N₂O₄F₁Na₁ requires 423.44.

IR (KBr): ν 3290, 2957, 1720, 1638, 1542, 752 cm^{-1} .

$^1\text{H-NMR}$ (400 MHz, DMSO): δ 8.49 (1H, t, $J = 6.0$ Hz, -NH-), 8.35 (1H, dd, $J^{\text{H-F}} = 2.8$ Hz, $J^{\text{H-H}} = 8.4$ Hz, -NH-), 7.62-7.66 (1H, m, -ArH 6), 7.50-7.55 (1H, m, -ArH 4), 7.24-7.36 (7H, m, -ArH 3, 5 & -PhH), 5.12 (2H, s, -OCH₂-), 4.52-4.66 (1H, m, α -H), 3.99 (1H, dd, $J^3 = 6.4$ Hz, $J^2 = 17.2$ Hz, -CH₂-), 3.88 (1H, dd, $J^3 = 5.6$ Hz, $J^2 = 17.6$ Hz, -CH₂-), 1.50-1.73 (3H, m, -CH₂- & -CH-), 0.89 (3H, d, $J = 3.6$ Hz, -CH₃), 0.88 (3H, d, $J = 3.6$ Hz, -CH₃).

$^{13}\text{C-NMR}$ (100 MHz, DMSO): δ 172.9 (-CONH-), 169.9 (-COOCH₂Ph), 164.0 (-ArCO-), 159.5 (d, -ArC 2), 136.1 (-PhC 1), 132.9 (d, -ArC 4), 130.5 (d, -ArC 6), 128.7 (-PhC 3 & 5), 128.4 (-PhC 4), 128.2 (-PhC 2 & 6), 124.7 (d, -ArC 5), 123.8 (d, -ArC 1), 116.4 (d, -ArC 3), 66.2 (-OCH₂-, -VE DEPT), 51.8 (α -C), 41.1 (-CH₂-, -VE DEPT), 41.0 (-CH₂-, -VE DEPT), 24.6 (-CH-), 23.3 (-CH₃), 21.7 (-CH₃).

$^{19}\text{F-NMR}$ (376 MHz, DMSO): δ -38.7 - -38.8 (m).

***N*-3-fluorobenzoyl-L-leucine-glycine benzyl ester 126**

N-3-fluorobenzoyl-L-leucine (0.8 g, 3.16 mmol) and glycine benzyl ester tosylate (1.12 g, 3.16 mmol) were used. Recrystallisation from ethyl acetate/hexane furnished **126** as a white powder (0.55 g, 45%).

m.p. = 76-78 °C. $[\alpha]_{\text{D}}^{25} = -21.3^\circ$ (c, 3.2, EtOH).

Anal. calcd. for C₂₂H₂₅N₂O₄F₁: C, 65.98; H, 6.29; N, 6.99.

Found C, 65.72; H, 6.41; N, 6.88.

Mass Spectrum: $[\text{M}+\text{Na}]^+$ found 423.1.

C₂₂H₂₅N₂O₄F₁Na₁ requires 423.44.

IR (KBr): ν 3275, 2958, 1744, 1637, 1560, 754 cm^{-1} .

$^1\text{H-NMR}$ (400 MHz, DMSO): δ 8.63 (1H, d, $J = 8.4$ Hz, -NH-), 8.49 (1H, t, $J = 6.0$ Hz, -NH-), 7.73-7.79 (2H, m, -ArH 2 & 6), 7.49-7.53 (1H, m, -ArH 5), 7.31-7.41 (6H, m, -ArH 4 & -PhH), 5.12 (2H, s, -OCH₂-), 4.54-4.58 (1H, m, α -H), 3.95 (1H, dd, $J^3 = 6.0$ Hz, $J^2 = 17.6$ Hz, -CH₂-), 3.87 (1H, dd, $J^3 = 5.6$ Hz, $J^2 = 17.2$ Hz, -CH₂-), 1.54-1.74 (3H, m, -CH₂- & -CH-), 0.89 (3H, d, $J = 6.4$ Hz, -CH₃), 0.85 (3H, d, $J = 6.0$ Hz, -CH₃).

$^{13}\text{C-NMR}$ (100 MHz, DMSO): δ 173.1 (-CONH-), 170.0 (-COOCH₂Ph), 165.3 (d, -ArCO-), 162.2 (d, -ArC 3), 136.7 (d, -ArC 1), 136.2 (-PhC 1), 130.6 (d, -ArC 5), 128.7 (-PhC 3 & 5), 128.4 (-PhC 4), 128.2 (-PhC 2 & 6), 124.1 (d, -ArC 6), 118.5 (d, -ArC 4), 114.7 (d, -ArC 2), 66.2

(-OCH₂-, -VE DEPT), 52.0 (α -C), 41.1 (-CH₂-, -VE DEPT) 40.6 (-CH₂-, -VE DEPT), 24.6 (-CH-), 23.3 (-CH₃), 21.6 (-CH₃).

¹⁹F-NMR (376 MHz, DMSO): δ -37.8 - -37.9 (m).

***N*-4-fluorobenzoyl-L-leucine-glycine benzyl ester 127**

N-4-fluorobenzoyl-L-leucine (0.8 g, 3.16 mmol) and glycine benzyl ester tosylate (1.12 g, 3.16 mmol) were used. Recrystallisation from ethyl acetate/hexane furnished **127** as a brown powder (0.80 g, 66%).

m.p. = 108-110 °C. $[\alpha]_D^{25} = -22.2^\circ$ (c, 3.2, EtOH).

Anal. calcd. for C₂₂H₂₅N₂O₄F₁: C, 65.98; H, 6.29; N, 6.99.

Found C, 65.77; H, 6.31; N, 7.21.

Mass Spectrum: [M+Na]⁺ found 423.2.

C₂₂H₂₅N₂O₄F₁Na₁ requires 423.44.

IR (KBr): ν 3285, 2957, 1742, 1632, 1502, 695 cm⁻¹.

¹H-NMR (400 MHz, DMSO): δ 8.51 (1H, d, $J = 8.4$ Hz, -NH-), 8.43 (1H, t, $J = 6.0$ Hz, -NH-), 7.92-7.98 (2H, m, -ArH 2 & 6), 7.26-7.40 (7H, m, -ArH 3, 5 & -PhH), 5.10 (2H, s, -OCH₂-), 4.50-4.56 (1H, m, α -H), 3.93 (1H, dd, $J^3 = 6.0$ Hz, $J^2 = 17.6$ Hz, -CH₂-), 3.84 (1H, dd, $J^3 = 6.0$ Hz, $J^2 = 17.2$ Hz, -CH₂-), 1.52-1.71 (3H, m, -CH₂- & -CH-), 0.88 (3H, d, $J = 6.4$ Hz, -CH₃), 0.84 (3H, d, $J = 6.4$ Hz, -CH₃).

¹³C-NMR (100 MHz, DMSO): δ 173.2 (-CONH-), 170.0 (-COOCH₂Ph), 165.6 (-ArCO-), 164.2 (d, -ArC 4), 136.1 (-PhC 1), 130.8 (-ArC 1), 130.6 (-ArC 2), 130.5 (-ArC 6), 128.7 (-PhC 3 & 5), 128.3 (-PhC 4), 128.2 (-PhC 2 & 6), 115.4 (-ArC 3), 115.2 (-ArC 5), 66.1 (-OCH₂-, -VE DEPT), 51.9 (α -C), 41.1 (-CH₂-, -VE DEPT) 40.6 (-CH₂-, -VE DEPT), 24.7 (-CH-), 23.3 (-CH₃), 21.6 (-CH₃).

¹⁹F-NMR (376 MHz, DMSO): δ -34.1 - -34.2 (m).

***N*-pentafluorobenzoyl-L-leucine-glycine benzyl ester 128**

N-pentafluorobenzoyl-L-leucine (2.64 g, 8.1 mmol) and glycine benzyl ester tosylate (2.88 g, 8.1 mmol) were used. Recrystallisation from ethyl acetate/hexane furnished **128** as a white powder (1.56 g, 42%).

m.p. = 165-167 °C. $[\alpha]_D^{25} = -20.8^\circ$ (c, 1.5, EtOH).

Anal. calcd. for C₂₂H₂₁N₂O₄F₅: C, 55.93; H, 4.48; N, 5.93.

Found C, 56.15; H, 4.62; N, 6.11.

Mass Spectrum: $[M+Na]^+$ found 495.1.

$C_{22}H_{21}N_2O_4F_5Na_1$ requires 495.39.

IR (KBr): ν 3287, 2966, 1745, 1662, 1546, 996 cm^{-1} .

1H -NMR (400 MHz, DMSO): δ 9.13 (1H, d, $J = 8.4$ Hz, -NH-), 8.70 (1H, t, $J = 6.0$ Hz, -NH-), 7.31-7.38 (5H, m, -PhH), 5.13 (2H, s, -OCH₂-), 4.60-4.64 (1H, m, α -H), 4.03 (1H, dd, $J^3 = 6.0$ Hz, $J^2 = 17.2$ Hz, -CH₂-), 3.84 (1H, dd, $J^3 = 6.0$ Hz, $J^2 = 17.6$ Hz, -CH₂-), 1.49-1.70 (3H, m, -CH₂- & -CH-), 0.90 (3H, d, $J = 6.4$ Hz, -CH₃), 0.89 (3H, d, $J = 6.4$ Hz, -CH₃).

^{13}C -NMR (100 MHz, DMSO): δ 172.0 (-CONH-), 169.9 (-COOCH₂Ph), 156.6 (-ArCO-), 144.7-144.8 (m, -ArC 2), 140.3-142.8 (m, -ArC 4), 142.1-142.3 (-ArC 6), 138.4-138.6 (m, -ArC 3), 136.1 (-PhC 1), 135.9-136.1 (m, -ArC 5), 128.7 (-PhC 3 & 5), 128.4 (-PhC 4), 128.3 (-PhC 2 & 6), 112.7 (t, -ArC 1), 66.2 (-OCH₂-, -VE DEPT), 51.7 (α -C), 41.3 (-CH₂-, -VE DEPT) 40.1 (-CH₂-, -VE DEPT), 24.4 (-CH-), 23.3 (-CH₃), 21.6 (-CH₃).

^{19}F -NMR (376 MHz, DMSO): δ -66.5 dd, 2F, $J^4 = 6.7$ Hz, $J^3 = 22.9$ Hz), -78.1 (t, $J = 16.1$ Hz), -86.4 - -86.5 (m, 2F).

***N*-2-fluorobenzoyl-L-leucine- β -alanine benzyl ester 129**

N-2-fluorobenzoyl-L-leucine (0.8 g, 3.16 mmol) and β -alanine benzyl ester tosylate (1.16 g, 3.16 mmol) were used. Recrystallisation from ethyl acetate/hexane furnished **129** as a brown powder (0.73 g, 58%).

m.p. = 69-71 °C. $[\alpha]_D^{25} = -4.2^\circ$ (c, 1.4, EtOH).

Anal. calcd. for $C_{23}H_{27}N_2O_4F_1$: C, 66.65; H, 6.56; N, 6.75.

Found C, 66.60; H, 6.62; N, 6.77.

Mass Spectrum: $[M+Na]^+$ found 437.2.

$C_{23}H_{27}N_2O_4F_1Na_1$ requires 437.46.

IR (KBr): ν 3268, 2913, 1727, 1642, 1468, 721 cm^{-1} .

1H -NMR (400 MHz, DMSO): δ 8.31 (1H, dd, $J^{H-F} = 2.4$ Hz, $J^{H-H} = 8.0$ Hz, -NH-), 8.16 (1H, t, $J = 5.6$ Hz, -NH-), 7.61-7.65 (1H, m, -ArH 6), 7.50-7.55 (1H, m, -ArH 4), 7.24-7.36 (7H, m, -ArH 3, 5 & -PhH), 5.09 (2H, s, -OCH₂-), 4.46-4.50 (1H, m, α -H), 3.29-3.44 (2H, m, β -CH₂), 2.54 (2H, t, $J = 6.8$ Hz, α -CH₂), 1.46-1.67 (3H, m, -CH₂- & -CH-), 0.89 (3H, d, $J = 2.8$ Hz, -CH₃), 0.87 (3H, d, $J = 2.8$ Hz, -CH₃).

¹³C-NMR (100 MHz, DMSO): δ 172.2 (-CONH-), 171.5 (-COOCH₂Ph), 163.8 (-ArCO-), 159.5 (d, -ArC 2), 136.3 (-PhC 1), 132.8 (d, -ArC 4), 130.5 (d, -ArC 6), 128.7 (-PhC 3 & 5), 128.3 (-PhC 4), 128.2 (-PhC 2 & 6), 124.7 (d, -ArC 5), 123.9 (d, -ArC 1), 116.4 (d, -ArC 3), 65.9 (-OCH₂-, -VE DEPT), 52.0 (α-C), 41.1 (-CH₂-, -VE DEPT), 35.1 (β-CH₂-, -VE DEPT), 34.0 (α-CH₂-, -VE DEPT), 24.6 (-CH-), 23.3 (-CH₃), 21.8 (-CH₃).

¹⁹F-NMR (376 MHz, DMSO): δ -38.7 - -38.8 (m).

N*-3-fluorobenzoyl-*L*-leucine-β-alanine benzyl ester **130*

N-3-fluorobenzoyl-*L*-leucine (0.8 g, 3.16 mmol) and β-alanine benzyl ester tosylate (1.16 g, 3.16 mmol) were used. Recrystallisation from ethyl acetate/hexane furnished **130** as a brown powder (0.63 g, 50%).

m.p. = 63-65 °C. $[\alpha]_D^{25} = -9.1^\circ$ (c, 2.4, EtOH).

Anal. calcd. for C₂₃H₂₇N₂O₄F₁: C, 66.65; H, 6.56; N, 6.75.

Found C, 66.89; H, 6.90; N, 6.55.

Mass Spectrum: [M+Na]⁺ found 437.2.

C₂₃H₂₇N₂O₄F₁Na₁ requires 437.46.

IR (KBr): ν 3324, 2960, 1736, 1655, 1542, 752 cm⁻¹.

¹H-NMR (400 MHz, DMSO): δ 8.58 (1H, d, *J* = 8.0 Hz, -NH-), 8.17 (1H, t, *J* = 5.6 Hz, -NH-), 7.67-7.78 (2H, m, -ArH 2 & 6), 7.48-7.53 (1H, m, -ArH 5), 7.28-7.39 (6H, m, -ArH 4 & -PhH), 5.07 (2H, s, -OCH₂-), 4.46-4.52 (1H, m, α-H), 3.29-3.43 (2H, m, β-CH₂), 2.54 (2H, t, *J* = 6.8 Hz, α-CH₂), 1.47-1.72 (3H, m, -CH₂- & -CH-), 0.88 (3H, d, *J* = 6.4 Hz, -CH₃), 0.85 (3H, d, *J* = 6.4 Hz, -CH₃).

¹³C-NMR (100 MHz, DMSO): δ 172.6 (-CONH-), 171.5 (-COOCH₂Ph), 165.3 (d, -ArCO-), 162.2 (d, -ArC 3), 136.7 (d, -ArC 1), 136.3 (-PhC 1), 130.6 (d, -ArC 5), 128.7 (-PhC 3 & 5), 128.3 (-PhC 4), 128.2 (-PhC 2 & 6), 124.0 (d, -ArC 6), 118.4 (d, -ArC 4), 114.6 (d, -ArC 2), 65.9 (-OCH₂-, -VE DEPT), 52.0 (α-C), 40.7 (-CH₂-, -VE DEPT), 35.1 (β-CH₂-, -VE DEPT), 34.0 (α-CH₂-, -VE DEPT), 24.7 (-CH-), 23.3 (-CH₃), 21.6 (-CH₃).

¹⁹F-NMR (376 MHz, DMSO): δ -37.6 - -37.7 (m).

***N*-4-fluorobenzoyl-L-leucine- β -alanine benzyl ester 131**

N-4-fluorobenzoyl-L-leucine (0.8 g, 3.16 mmol) and β -alanine benzyl ester tosylate (1.16 g, 3.16 mmol) were used. Recrystallisation from ethyl acetate/hexane furnished **131** as a brown powder (0.58 g, 46%).

m.p. = 103-105 °C. $[\alpha]_D^{25} = -12.3^\circ$ (c, 1.6, EtOH).

Anal. calcd. for C₂₃H₂₇N₂O₄F₁: C, 66.65; H, 6.56; N, 6.75.

Found C, 66.29; H, 6.35; N, 6.49.

Mass Spectrum: [M+Na]⁺ found 437.2.

C₂₃H₂₇N₂O₄F₁Na₁ requires 437.46.

IR (KBr): ν 3330, 2959, 1734, 1632, 1502, 857 cm⁻¹.

¹H-NMR (400 MHz, DMSO): δ 8.49 (1H, d, $J = 8.0$ Hz, -NH-), 8.14 (1H, t, $J = 5.6$ Hz, -NH-), 7.96-7.99 (2H, m, -ArH 2 & 6), 7.26-7.36 (7H, m, -ArH 3, 5 & -PhH), 5.07 (2H, s, -OCH₂-), 4.46-4.48 (1H, m, α -H), 3.29-3.39 (2H, m, β -CH₂), 2.54 (2H, t, $J = 6.8$ Hz, α -CH₂), 1.47-1.70 (3H, m, -CH₂- & -CH-), 0.88 (3H, d, $J = 6.4$ Hz, -CH₃), 0.85 (3H, d, $J = 6.4$ Hz, -CH₃).

¹³C-NMR (100 MHz, DMSO): δ 172.6 (-CONH-), 171.5 (-COOCH₂Ph), 165.5 (-ArCO-), 164.3 (d, -ArC 4), 136.4 (-PhC 1), 130.9 (-ArC 1), 130.6 (-ArC 2), 130.5 (-ArC 6), 128.7 (-PhC 3 & 5), 128.3 (-PhC 4), 128.2 (-PhC 2 & 6), 115.5 (-ArC 3), 115.3 (-ArC 5), 65.9 (-OCH₂-, -VE DEPT), 52.1 (α -C), 40.7 (-CH₂-, -VE DEPT), 35.1 (β -CH₂-, -VE DEPT), 34.0 (α -CH₂-, -VE DEPT), 24.7 (-CH-), 23.3 (-CH₃), 21.7 (-CH₃).

¹⁹F-NMR (376 MHz, DMSO): δ -34.1 - -34.2 (m).

***N*-pentafluorobenzoyl-L-leucine- β -alanine benzyl ester 132**

N-pentafluorobenzoyl-L-leucine (2.93 g, 9.0 mmol) and β -alanine benzyl ester tosylate (3.33 g, 9.0 mmol) were used. Recrystallisation from ethyl acetate/hexane furnished **132** as a brown oil (1.99 g, 47%).

$[\alpha]_D^{25} = -6.5^\circ$ (c, 2.1, EtOH).

Anal. calcd. for C₂₃H₂₃N₂O₄F₅: C, 56.79; H, 4.76; N, 5.75.

Found C, 56.61; H, 4.85; N, 6.01.

Mass Spectrum: [M+Na]⁺ found 509.2.

C₂₃H₂₃N₂O₄F₅Na₁ requires 509.42.

IR (KBr): ν 3267, 3083, 1745, 1638, 1560, 734 cm⁻¹.

¹H-NMR (400 MHz, DMSO): δ 9.16 (1H, d, *J* = 8.4 Hz, -NH-), 8.35 (1H, t, *J* = 5.6 Hz, -NH-), 7.31-7.38 (5H, m, -PhH), 5.10 (2H, s, -OCH₂-), 4.51-4.55 (1H, m, α-H), 3.30-3.44 (2H, m, β-CH₂), 2.56 (2H, t, *J* = 6.4 Hz, α-CH₂), 1.45-1.64 (3H, m, -CH₂- & -CH-), 0.90 (3H, d, *J* = 6.4 Hz, -CH₃), 0.89 (3H, d, *J* = 6.4 Hz, -CH₃).

¹³C-NMR (100 MHz, DMSO): δ 171.4 (-COOCH₂Ph & -CONH-), 156.6 (-ArCO-), 144.5-144.7 (m, -ArC 2), 140.0-142.2 (m, -ArC 4), 142.1-142.3 (-ArC 6), 138.2-138.4 (m, -ArC 3), 136.4 (-PhC 1), 135.8-136.0 (m, -ArC 5), 128.7 (-PhC 3 & 5), 128.3 (-PhC 4), 128.1 (-PhC 2 & 6), 112.7 (t, -ArC 1), 65.9 (-OCH₂-, -VE DEPT), 51.9 (α-C), 41.3 (-CH₂-, -VE DEPT), 35.1 (β-CH₂-, -VE DEPT), 33.9 (α-CH₂-, -VE DEPT), 24.4 (-CH-), 23.1 (-CH₃), 21.7 (-CH₃).

¹⁹F-NMR (376 MHz, DMSO): δ -66.6 (dd, 2F, *J*⁴ = 6.8 Hz, *J*³ = 23.6 Hz), -78.4 (t, *J* = 21.6 Hz), -86.6 - -86.7 (m, 2F).

***N*-2-fluorobenzoyl-L-leucine-γ-aminobutyric acid benzyl ester 133**

N-2-fluorobenzoyl-L-leucine (0.8 g, 3.16 mmol) and γ-aminobutyric acid benzyl ester tosylate (1.21 g, 3.16 mmol) were used. Recrystallisation from ethyl acetate/hexane furnished **133** as a brown oil (0.79 g, 63%).

$[\alpha]_{\text{D}}^{25} = -19^{\circ}$ (c, 0.18, EtOH).

Anal. calcd. for C₂₄H₂₉N₂O₄F₁: C, 67.27; H, 6.82; N, 6.53.

Found C, 67.60; H, 6.58; N, 6.32.

Mass Spectrum: [M+Na]⁺ found 451.2.

C₂₄H₂₉N₂O₄F₁Na₁ requires 451.49.

IR (KBr): ν 3301, 2985, 1737, 1662, 1435, 728 cm⁻¹.

¹H-NMR (400 MHz, DMSO): δ 8.30 (1H, dd, *J*^{H-F} = 2.4 Hz, *J*^{H-H} = 8.0 Hz, -NH-), 8.05 (1H, t, *J* = 5.6 Hz, -NH-), 7.61-7.65 (1H, m, -ArH 6), 7.49-7.55 (1H, m, -ArH 4), 7.24-7.38 (7H, m, -ArH 3, 5 & -PhH), 5.08 (2H, s, -OCH₂-), 4.45-4.50 (1H, m, α-H), 3.13 (2H, q, *J* = 6.8 Hz, γ-CH₂), 2.38 (2H, t, *J* = 7.6 Hz, α-CH₂), 1.48-1.73 (5H, m, β-CH₂-, -CH₂- & -CH-), 0.89 (6H, t, *J* = 6.4 Hz, -CH₃).

¹³C-NMR (100 MHz, DMSO): δ 172.9 (-CONH-), 172.1 (-COOCH₂Ph), 163.8 (-ArCO-), 159.5 (d, -ArC 2), 136.5 (-PhC 1), 132.8 (d, -ArC 4), 130.5 (d, -ArC 6), 128.7 (-PhC 3 & 5), 128.3 (-PhC 4), 128.2 (-PhC 2 & 6), 124.7 (-ArC 5), 123.9 (d, -ArC 1), 116.3 (d, -ArC 3), 65.7 (-OCH₂-,

-VE DEPT), 52.2 (α -C), 41.1 (-CH₂-, -VE DEPT), 38.1 (γ -CH₂-, -VE DEPT), 31.1 (α -CH₂-, -VE DEPT), 24.75 (-CH-), 24.72 (β -CH₂-, -VE DEPT), 23.2 (-CH₃), 21.9 (-CH₃).

¹⁹F-NMR (400 MHz, DMSO): δ -38.7 - -38.8 (m).

***N*-3-fluorobenzoyl-L-leucine- γ -aminobutyric acid benzyl ester 134**

N-3-fluorobenzoyl-L-leucine (0.8 g, 3.16 mmol) and γ -aminobutyric acid benzyl ester tosylate (1.21 g, 3.16 mmol) were used. Recrystallisation from ethyl acetate/hexane furnished **134** as a white powder (0.63 g, 50%).

m.p. = 69-71 °C. $[\alpha]_D^{25} = -2.5^\circ$ (c, 1.2, EtOH).

Anal. calcd. for C₂₄H₂₉N₂O₄F₁: C, 67.27; H, 6.82; N, 6.53.

Found C, 67.65; H, 7.01; N, 6.38.

Mass Spectrum: [M+Na]⁺ found 451.2.

C₂₄H₂₉N₂O₄F₁Na₁ requires 451.49.

IR (KBr): ν 3330, 2954, 1725, 1634, 1534, 754 cm⁻¹.

¹H-NMR (400 MHz, DMSO): δ 8.55 (1H, d, $J = 8.0$ Hz, -NH-), 8.06 (1H, t, $J = 5.6$ Hz, -NH-), 7.70-7.77 (2H, m, -ArH 2 & 6), 7.47-7.54 (1H, m, -ArH 5), 7.29-7.39 (6H, m, -ArH 4 & -PhH), 5.07 (2H, s, -OCH₂-), 4.44-4.50 (1H, m, α -H), 3.10 (2H, q, $J = 6.4$ Hz, γ -CH₂), 2.37 (2H, t, $J = 7.2$ Hz, α -CH₂), 1.50-1.73 (5H, m, β -CH₂-, -CH₂- & -CH-), 0.89 (3H, d, $J = 6.0$ Hz, -CH₃), 0.85 (3H, d, $J = 6.0$ Hz, -CH₃).

¹³C-NMR (100 MHz, DMSO): δ 172.9 (-CONH-), 172.4 (-COOCH₂Ph), 165.3 (d, -ArCO-), 162.2 (d, -ArC 3), 136.7 (t, -ArC 1), 136.5 (-PhC 1), 130.6 (d, -ArC 5), 128.7 (-PhC 3 & 5), 128.3 (-PhC 4), 128.2 (-PhC 2 & 6), 124.0 (d, -ArC 6), 118.4 (d, -ArC 4), 114.6 (d, -ArC 2), 65.7 (-OCH₂-, -VE DEPT), 52.4 (α -C), 40.7 (-CH₂-, -VE DEPT), 38.1 (γ -CH₂-, -VE DEPT), 31.1 (α -CH₂-, -VE DEPT), 24.79 (-CH-), 24.77 (β -CH₂-, -VE DEPT), 23.3 (-CH₃), 21.7 (-CH₃).

¹⁹F-NMR (376 MHz) (DMSO): δ -37.7 - -37.8 (m).

***N*-4-fluorobenzoyl-L-leucine- γ -aminobutyric acid benzyl ester 135**

N-4-fluorobenzoyl-L-leucine (0.8 g, 3.16 mmol) and γ -aminobutyric acid benzyl ester tosylate (1.21 g, 3.16 mmol) were used. Recrystallisation from ethyl acetate/hexane furnished **135** as a brown powder (0.73 g, 63%).

m.p. = 83-85 °C. $[\alpha]_D^{25} = -2.9^\circ$ (c, 1.2, EtOH).

Anal. calcd. for C₂₄H₂₉N₂O₄F₁: C, 67.27; H, 6.82; N, 6.53.

Found C, 67.55; H, 7.13; N, 6.69.

Mass Spectrum: $[M+Na]^+$ found 451.2.

$C_{24}H_{29}N_2O_4F_1Na_1$ requires 451.49.

IR (KBr): ν 3330, 2954, 1725, 1634, 1534, 754 cm^{-1} .

1H -NMR (400 MHz, DMSO): δ 8.49 (1H, d, $J = 8.0$ Hz, -NH-), 8.06 (1H, t, $J = 5.6$ Hz, -NH-), 7.96-8.02 (2H, m, -ArH 2 & 6), 7.25-7.39 (7H, m, -ArH 3, 5 & -PhH), 5.08 (2H, s, -OCH₂-), 4.44-4.50 (1H, m, α -H), 3.11 (2H, q, $J = 6.4$ Hz, γ -CH₂), 2.37 (2H, t, $J = 7.2$ Hz, α -CH₂), 1.50-1.73 (5H, m, β -CH₂, -CH₂- & -CH-), 0.89 (3H, d, $J = 6.4$ Hz, -CH₃), 0.86 (3H, d, $J = 6.4$ Hz, -CH₃).

^{13}C -NMR (100 MHz, DMSO): δ 172.9 (-CONH-), 172.5 (-COOCH₂Ph), 165.6 (-ArCO-), 164.4 (d, -ArC 4), 136.5 (-PhC 1), 130.9 (-ArC 1), 130.6 (-ArC 2), 130.5 (-ArC 6), 128.7 (-PhC 3 & 5), 128.3 (-PhC 4), 128.2 (-PhC 2 & 6), 115.4 (-ArC 3), 115.2 (-ArC 5), 65.7 (-OCH₂-, -VE DEPT), 52.3 (α -C), 40.8 (-CH₂-, -VE DEPT), 38.1 (γ -CH₂-, -VE DEPT), 31.1 (α -CH₂-, -VE DEPT), 24.8 (-CH-), 24.7 (β -CH₂-, -VE DEPT), 23.3 (-CH₃), 21.7 (-CH₃). ^{19}F -NMR (376 MHz, DMSO): δ -34.1 - -34.2 (m).

***N*-pentafluorobenzoyl-L-leucine- γ -aminobutyric acid benzyl ester 136**

N-pentafluorobenzoyl-L-leucine (2.69 g, 8.2 mmol) and γ -aminobutyric acid benzyl ester tosylate (3.15 g, 8.2 mmol) were used. Recrystallisation from ethyl acetate/hexane furnished **136** as a white powder (1.82 g, 46%).

m.p. = 54-56 °C. $[\alpha]_D^{25} = -4.2^\circ$ (c, 1.2, EtOH).

Anal. calcd. for $C_{24}H_{25}N_2O_4F_5$: C, 57.59; H, 5.04; N, 5.59.

Found C, 57.32; H, 4.77; N, 5.91.

Mass Spectrum: $[M+Na]^+$ found 523.1.

$C_{24}H_{25}N_2O_4F_5Na_1$ requires 523.45.

IR (KBr): ν 3329, 2962, 1736, 1655, 1508, 991 cm^{-1} .

1H -NMR (400 MHz, DMSO): δ 9.16 (1H, d, $J = 8.4$ Hz, -NH-), 8.23 (1H, t, $J = 5.6$ Hz, -NH-), 7.31-7.37 (5H, m, -PhH), 5.10 (2H, s, -OCH₂-), 4.48-4.51 (1H, m, α -H), 3.09-3.16 (2H, m, γ -CH₂), 2.40 (2H, t, $J = 7.2$ Hz, α -CH₂), 1.47-1.75 (5H, m, β -CH₂, -CH₂- & -CH-), 0.90 (6H, t, $J = 6.0$ Hz, -CH₃).

^{13}C -NMR (100 MHz, DMSO): δ 172.8 (-CONH-), 171.3 (-COOCH₂Ph), 156.6 (-ArCO-), 144.5-144.7 (m, -ArC 2), 140.0-142.6 (m, -ArC 4), 142.1-142.3 (-ArC 6), 138.2-138.5 (m, -ArC 3), 136.5 (-PhC 1), 135.8-136.0 (m, -ArC 5), 128.7 (-PhC 3 & 5), 128.3 (-PhC 4), 128.1 (-PhC 2 & 6), 112.7 (t, -ArC 1), 65.7 (-OCH₂-, -VE DEPT), 52.1 (α -C), 41.3 (-CH₂-, -VE DEPT), 38.1 (γ -CH₂-, -VE DEPT), 31.0 (α -CH₂-, -VE DEPT), 24.7 (β -CH₂-, -VE DEPT), 24.5 (-CH-), 23.1 (-CH₃), 21.7 (-CH₃).

^{19}F -NMR (376 MHz, DMSO): δ -66.6 (dd, 2F, $J^4 = 6.8$ Hz, $J^3 = 23.3$ Hz), -78.4 (t, $J = 22.1$ Hz), -86.6 - -86.7 (m, 2F).

General procedure for the synthesis of N-pentafluorobenzoyl-L-alanine dipeptides 137-146

N-pentafluorobenzoyl-L-alanine-glycine methyl ester 137

N-pentafluorobenzoyl-L-alanine (1.13 g, 4 mmol), glycine methyl ester (0.5 g, 4 mmol), triethylamine (0.56 ml) and 1-hydroxybenzotriazole hydrate (0.54 g, 4 mmol) were dissolved in dichloromethane (50 ml). The mixture was cooled to 0 °C, and 1-[3-dimethylaminopropyl]-3-ethyl carbodiimide hydrochloride (EDC) (0.84 g, 4.4 mmol) was added. After 30 min. the solution was raised to room temperature and the reaction was allowed to proceed for 8 hrs. The filtrate was washed with 10% citric acid, water and dried over magnesium sulphate. The solvent was evaporated *in vacuo* and recrystallisation from ethyl acetate/hexane furnished **137** as a light yellow powder (0.60 g, 42%).

m.p. = 144-146 °C. $[\alpha]_{\text{D}}^{25} = -15.1^\circ$ (c, 1.6, EtOH).

Anal. calcd. for C₁₃H₁₁N₂O₄F₅: C, 44.07; H, 3.13; N, 7.91.

Found C, 44.02; H, 2.92; N, 7.80.

IR (KBr): ν 3292, 3105, 1752, 1653, 1560, 995 cm⁻¹.

^1H -NMR (400 MHz, DMSO): δ 9.19 (1H, d, $J = 8.0$ Hz, -NH-), 8.53 (1H, t, $J = 5.6$ Hz, -NH-), 4.56-4.61 (1H, m, α -H), 3.96 (1H, dd, $J^3 = 6.0$ Hz, $J^2 = 17.6$ Hz, -CH₂-), 3.86 (1H, dd, $J^3 = 6.0$ Hz, $J^2 = 17.6$ Hz, -CH₂-), 3.65 (3H, s, -OCH₃), 1.32 (3H, d, $J = 7.2$ Hz, -CH₃).

^{13}C -NMR (100 MHz, DMSO): δ 172.2 (-CONH-), 170.5 (-COOCH₃), 156.6 (-ArCO-), 144.7-144.8 (m, -ArC 2), 140.3-142.8 (m, -ArC 4), 142.1-142.3 (-ArC 6), 138.3-138.5 (m, -ArC 3), 135.8-136.0 (m, -ArC 5), 112.7 (t, -ArC 1), 52.0 (-OCH₃), 49.0 (α -C), 40.8 (-CH₂-, -VE DEPT), 18.6 (-CH₃).

^{19}F -NMR (376 MHz, DMSO): δ -66.6 (dd, 2F, $J^4 = 6.8$ Hz, $J^3 = 23.7$ Hz), -78.4 (t, $J = 21.8$ Hz), -86.7 - -86.8 (m, 2F).

***N*-pentafluorobenzoyl-L-alanine- β -Alanine methyl ester 138**

β -Alanine methyl ester (0.56 g, 4 mmol) was used. Recrystallisation from ethyl acetate/hexane furnished **138** as a white powder (0.80 g, 54%).

m.p. = 154-155 °C. $[\alpha]_{\text{D}}^{25} = -8.2^\circ$ (c, 1.5, EtOH).

Anal. calcd. for $\text{C}_{14}\text{H}_{13}\text{N}_2\text{O}_4\text{F}_5$: C, 45.66; H, 3.56; N, 7.61.

Found C, 45.59; H, 3.29; N, 7.52.

IR (KBr): ν 3289, 3110, 1738, 1646, 1523, 992 cm^{-1} .

^1H -NMR (400 MHz, DMSO): δ 9.13 (1H, d, $J = 7.6$ Hz, -NH-), 8.17 (1H, t, $J = 5.6$ Hz, -NH-), 4.43-4.48 (1H, m, α -H), 3.60 (3H, s, -OCH₃), 3.24-3.38 (2H, m, β -CH₂), 2.48 (2H, t, $J = 6.4$ Hz, α -CH₂), 1.26 (3H, d, $J = 6.8$ Hz, -CH₃).

^{13}C -NMR (100 MHz, DMSO): δ 172.0 (-CONH-), 171.6 (-COOCH₃), 156.5 (-ArCO-), 144.7-144.8 (m, -ArC 2), 140.3-142.8 (m, -ArC 4), 142.1-142.3 (-ArC 6), 138.3-138.5 (m, -ArC 3), 135.8-136.0 (m, -ArC 5), 112.7 (t, -ArC 1), 51.6 (-OCH₃), 49.2 (α -C), 35.1 (β -CH₂, -VE DEPT), 33.8 (α -CH₂, -VE DEPT), 18.6 (-CH₃).

^{19}F -NMR (376 MHz, DMSO): δ -66.7 (dd, 2F, $J^4 = 6.8$ Hz, $J^3 = 23.3$ Hz), -78.5 (t, $J = 21.8$ Hz), -86.7 - -86.8 (m, 2F).

***N*-pentafluorobenzoyl-L-alanine- γ -aminobutyric acid methyl ester 139**

γ -Aminobutyric acid methyl ester (0.61 g, 4 mmol) was used. Recrystallisation from ethyl acetate/hexane yielded the title product as a light yellow powder (0.75 g, 49%).

m.p. = 138-139 °C. $[\alpha]_{\text{D}}^{25} = -2.9^\circ$ (c, 1.7, EtOH).

Anal. calcd. for $\text{C}_{15}\text{H}_{15}\text{N}_2\text{O}_4\text{F}_5$: C, 47.12; H, 3.96; N, 7.33.

Found C, 47.00; H, 3.70; N, 7.26.

IR (KBr): ν 3331, 2960, 1736, 1648, 1560, 992 cm^{-1} .

^1H -NMR (400 MHz, DMSO): δ 9.13 (1H, d, $J = 7.6$ Hz, -NH-), 8.10 (1H, t, $J = 5.6$ Hz, -NH-), 4.43-4.48 (1H, m, α -H), 3.60 (3H, s, -OCH₃), 3.08-3.14 (2H, m, γ -CH₂), 2.33 (2H, t, $J = 7.6$ Hz, α -CH₂), 1.64-1.71 (2H, m, β -CH₂), 1.28 (3H, d, $J = 7.2$ Hz, -CH₃).

^{13}C -NMR (100 MHz, DMSO): δ 173.4 (-CONH-), 171.4 (-COOCH₃), 156.5 (-ArCO-), 144.7-144.8 (m, -ArC 2), 140.3-142.8 (m, -ArC 4), 142.1-142.3 (-ArC 6), 138.3-138.5 (m, -ArC 3),

135.8-136.0 (m, -ArC 5), 112.7 (t, -ArC 1), 51.6 (-OCH₃), 49.3 (α -C), 38.1 (γ -CH₂, -VE DEPT), 30.8 (α -CH₂, -VE DEPT), 24.7 (β -CH₂, -VE DEPT), 18.6 (-CH₃).

¹⁹F-NMR (376 MHz, DMSO): δ -66.6 (dd, 2F, $J^4 = 6.8$ Hz, $J^3 = 22.9$ Hz), -78.5 (t, $J = 21.8$ Hz), -86.7 - -86.8 (m, 2F).

***N*-pentafluorobenzoyl-L-alanine-L-alanine methyl ester 140**

L-Alanine methyl ester (0.56 g, 4 mmol) was used. Recrystallisation from ethyl acetate/hexane furnished **140** as a white powder (0.85 g, 58 %).

m.p. = 188-190 °C. $[\alpha]_D^{25} = -34.1^\circ$ (c, 3.0, EtOH).

Anal. calcd. for C₁₄H₁₃N₂O₄F₅: C, 45.66; H, 3.56; N, 7.61.

Found C, 45.55; H, 3.27; N, 7.54.

IR (KBr): ν 3299, 2961, 1740, 1643, 1560, 994 cm⁻¹.

¹H-NMR (400 MHz, DMSO): δ 9.17 (1H, d, $J = 7.6$ Hz, -NH-), 8.10 (1H, d, $J = 7.2$ Hz, -NH-), 4.52-4.59 (1H, m, α -H), 4.28-4.35 (1H, m, α -H), 3.64 (3H, s, -OCH₃), 1.33 (3H, d, $J = 3.2$ Hz, -CH₃), 1.31 (3H, d, $J = 2.8$ Hz, -CH₃).

¹³C-NMR (100 MHz, DMSO): δ 173.2 (-CONH-), 171.5 (-COOCH₃), 156.5 (-ArCO-), 144.6-144.8 (m, -ArC 2), 140.3-142.8 (m, -ArC 4), 142.1-142.3 (-ArC 6), 138.3-138.5 (m, -ArC 3), 135.8-136.0 (m, -ArC 5), 112.7 (t, -ArC 1), 52.1 (-OCH₃), 48.9 (α -C), 47.9 (α -C), 18.4 (-CH₃), 17.0 (-CH₃).

¹⁹F-NMR (376 MHz, DMSO): -66.7 (dd, 2F, $J^4 = 6.8$ Hz, $J^3 = 22.9$ Hz), -78.4 (t, $J = 21.8$ Hz), -86.7 - -86.8 (m, 2F).

***N*-pentafluorobenzoyl-L-alanine-L-leucine methyl ester 141**

L-Leucine methyl ester (0.73 g, 4 mmol) was used. Recrystallisation from ethyl acetate/hexane furnished **141** as a white powder (0.9 g, 55%).

m.p. = 140-142 °C. $[\alpha]_D^{25} = -28.6^\circ$ (c, 3.8, EtOH).

Anal. calcd. for C₁₇H₁₉N₂O₄F₅: C, 49.76; H, 4.67; N, 6.83.

Found C, 49.72; H, 4.38; N, 6.80.

IR (KBr): ν 3260, 2963, 1752, 1648, 1555, 995 cm⁻¹.

¹H-NMR (400 MHz, DMSO): δ 9.15 (1H, d, $J = 7.6$ Hz, -NH-), 8.43 (1H, d, $J = 7.6$ Hz, -NH-), 4.53-4.60 (1H, m, α -H), 4.31-4.35 (1H, m, α -H), 3.63 (3H, s, -OCH₃), 1.48-1.70 (3H, m, -CH₂- &

-CH-), 1.30 (3H, d, $J = 6.8$ Hz, -CH₃), 0.91 (3H, d, $J = 6.4$ Hz, -CH₃), 0.86 (3H, d, $J = 6.4$ Hz, -CH₃).

¹³C-NMR (100 MHz, DMSO): 173.1 (-CONH-), 171.7 (-COOCH₃), 156.5 (-ArCO-), 144.7-144.8 (m, -ArC 2), 140.3-142.8 (m, -ArC 4), 142.2-142.3 (-ArC 6), 138.3-138.5 (m, -ArC 3), 135.8-136.0 (m, -ArC 5), 112.7 (t, -ArC 1), 52.1 (-OCH₃), 50.6 (α-C), 48.9 (α-C), 40.0 (-CH₂-, -VE DEPT), 24.5 (-CH-), 22.9 (-CH₃), 21.5 (-CH₃), 18.4 (-CH₃).

¹⁹F-NMR (376 MHz, DMSO): δ -66.7 (dd, 2F, $J^4 = 6.8$ Hz, $J^3 = 22.9$ Hz), -78.4 (t, $J = 21.4$ Hz), -86.7 - -86.8 (m, 2F).

***N*-pentafluorobenzoyl-L-alanine-L-phenylalanine methyl ester 142**

L-Phenylalanine methyl ester (0.86 g, 4 mmol) was used. Recrystallisation from ethyl acetate/hexane furnished **142** as a white powder (0.6 g, 34%).

m.p. = 184-186 °C. $[\alpha]_D^{25} = -9.1^\circ$ (c, 2.6, EtOH).

Anal. calcd. for C₂₀H₁₇N₂O₄F₅: C, 54.09; H, 3.86; N, 6.30.

Found C, 54.10; H, 3.61; N, 6.15.

IR (KBr): ν 3302, 2954, 1740, 1643, 1508, 995 cm⁻¹.

¹H-NMR (400 MHz, DMSO): 9.13 (1H, d, $J = 7.6$ Hz, -NH-), 8.54 (1H, d, $J = 7.6$ Hz, -NH-), 7.20-7.30 (5H, m, -PhH), 4.49-4.58 (2H, m, α-H), 3.59 (3H, s, -OCH₃), 2.95-3.07 (2H, m, -CH₂-), 1.28 (3H, d, $J = 6.8$ Hz, -CH₃).

¹³C-NMR (100 MHz, DMSO): 172.0 (-CONH-), 171.7 (-COOCH₃), 156.5 (-ArCO-), 144.5-144.7 (m, -ArC 2), 140.3-142.8 (m, -ArC 4), 142.1-142.3 (-ArC 6), 138.3-138.5 (m, -ArC 3), 137.2 (-PhC 1), 135.8-136.0 (m, -ArC 5), 129.3 (-PhC 3 & 5), 128.6 (-PhC 2 & 6), 126.9 (-PhC 4), 112.7 (t, -ArC 1), 54.0 (α-C), 52.1 (-OCH₃), 48.9 (α-C), 36.8 (-CH₂-, -VE DEPT), 18.6 (-CH₃).

¹⁹F-NMR (376 MHz, DMSO): -66.6 (dd, 2F, $J^4 = 6.8$ Hz, $J^3 = 23.3$ Hz), -78.3 (t, $J = 21.8$ Hz), -86.6 - -86.7 (m, 2F).

***N*-pentafluorobenzoyl-L-alanine-L-valine methyl ester 143**

L-Valine methyl ester (0.67 g, 4 mmol) was used. Recrystallisation from ethyl acetate/hexane furnished **143** as a white powder (0.8 g, 51%).

m.p. = 152-154 °C. $[\alpha]_D^{25} = -25.2^\circ$ (c, 2.7, EtOH).

Anal. calcd. for C₁₆H₁₇N₂O₄F₅: C, 48.49; H, 4.32; N, 7.07.

Found C, 48.39; H, 4.04; N, 6.93.

IR (KBr): ν 3256, 2976, 1751, 1648, 1508, 994 cm^{-1} .

$^1\text{H-NMR}$ (400 MHz, DMSO): δ 9.17 (1H, d, $J = 7.2$ Hz, -NH-), 8.29 (1H, d, $J = 8.0$ Hz, -NH-), 4.62-4.67 (1H, m, α -H), 4.20-4.24 (1H, m, α -H), 3.63 (3H, s, -OCH₃), 2.04-2.09 (1H, m, -CH-), 1.29 (3H, d, $J = 7.2$ Hz, -CH₃), 0.90 (6H, t, $J = 6.8$ Hz, -CH₃).

$^{13}\text{C-NMR}$ (100 MHz, DMSO): δ 172.1 (-CONH-), 172.0 (-COOCH₃), 156.5 (-ArCO-), 144.7-144.8 (m, -ArC 2), 140.3-142.8 (m, -ArC 4), 142.1-142.3 (-ArC 6), 138.3-138.5 (m, -ArC 3), 135.8-136.0 (m, -ArC 5), 112.6 (t, -ArC 1), 57.6 (α -C), 52.1 (-OCH₃), 48.9 (α -C), 30.2 (-CH-), 19.1 (-CH₃), 18.35 (-CH₃), 18.31 (-CH₃).

$^{19}\text{F-NMR}$ (376 MHz, DMSO): δ -66.7 (dd, 2F, $J^4 = 6.8$ Hz, $J^3 = 22.6$ Hz), -78.4 (t, $J = 21.8$ Hz), -86.6 - -86.7 (m, 2F).

***N*-pentafluorobenzoyl-L-alanine-L-tryptophan methyl ester 144**

L-Tryptophan methyl ester (1.02 g, 4 mmol) was used. Recrystallisation from ethyl acetate/hexane furnished **144** as a brown powder (0.71 g, 37%).

m.p. = 174-175 °C. $[\alpha]_{\text{D}}^{25} = +10.1^\circ$ (c, 1.8, EtOH).

Anal. calcd. for C₂₂H₁₈N₃O₄F₅: C, 54.66; H, 3.75; N, 8.69.

Found C, 54.34; H, 3.62; N, 8.51.

IR (KBr): ν 3315, 2973, 1736, 1648, 1508, 995 cm^{-1} .

$^1\text{H-NMR}$ (400 MHz, DMSO): 10.91 (1H, bs, -NH-), 9.16 (1H, d, $J = 7.6$ Hz, -NH-), 8.53 (1H, d, $J = 7.2$ Hz, -NH-), 7.51 (1H, d, $J = 8.0$ Hz, -PhH 1), 7.35 (1H, d, $J = 8.0$ Hz, -PhH 4), 7.20 (1H, d, $J = 2.0$ Hz, -C=C-H), 7.08 (1H, t, $J = 7.2$ Hz, -PhH 2), 7.00 (1H, t, $J = 7.2$ Hz, -PhH 3), 4.55-4.63 (2H, m, α -H), 3.58 (3H, s, -OCH₃), 3.12-3.23 (2H, m, -CH₂-), 1.31 (3H, d, $J = 6.8$ Hz, -CH₃).

$^{13}\text{C-NMR}$ (100 MHz, DMSO): δ 172.4 (-CONH-), 171.7 (-COOCH₃), 156.5 (-ArCO-), 144.7-144.8 (m, -ArC 2), 140.3-142.6 (m, -ArC 4), 142.1-142.3 (-ArC 6), 138.3-138.5 (m, -ArC 3), 136.4 (-C=C-H), 135.8-136.0 (m, -ArC 5), 127.4 (-PhC 5), 124.0 (-C=C-H), 121.3 (-PhC 2), 118.7 (-PhC 3), 118.3 (-PhC 4), 112.6 (t, -ArC 1), 111.7 (-PhC 1), 109.4 (-PhC 6), 53.5 (α -C), 52.1 (-OCH₃), 48.9 (α -C), 27.1 (-CH₂-, -VE DEPT), 18.3 (-CH₃).

$^{19}\text{F-NMR}$ (376 MHz, DMSO): δ -66.5 (dd, 2F, $J^4 = 6.8$ Hz, $J^3 = 23.3$ Hz), -78.2 (t, $J = 22.5$ Hz), -86.5 - -86.6 (m, 2F).

***N*-pentafluorobenzoyl-L-alanine-L-aspartic acid dimethyl ester 145**

L-Aspartic acid dimethyl ester (0.79 g, 4 mmol) was used. Recrystallisation from ethyl acetate/hexane furnished **145** as yellow crystals (1.04 g, 61%).

m.p. = 124-125 °C. $[\alpha]_D^{25} = -12.5^\circ$ (c, 1.2, EtOH).

Anal. calcd. for C₁₆H₁₅N₂O₆F₅: C, 45.08; H, 3.55; N, 6.57.

Found C, 44.99; H, 3.49; N, 6.72.

IR (KBr): ν 3299, 2958, 1744, 1654, 1508, 994 cm⁻¹.

¹H-NMR (400 MHz, DMSO): δ 9.18 (1H, d, $J = 7.6$ Hz, -NH-), 8.57 (1H, d, $J = 8.0$ Hz, -NH-), 4.64-4.71 (1H, m, α -H), 4.53-4.59 (1H, m, α -H), 3.63 (6H, s, -OCH₃), 2.74-2.87 (2H, m, -CH₂-), 1.30 (3H, d, $J = 7.2$ Hz, -CH₃).

¹³C-NMR (100 MHz, DMSO): 171.6 (-CONH-), 171.2 (-COOCH₃), 170.7 (-COOCH₃), 156.5 (-ArCO-), 144.7-144.8 (m, -ArC 2), 140.3-142.8 (m, -ArC 4), 142.1-142.3 (-ArC 6), 138.3-138.5 (m, -ArC 3), 135.8-136.0 (m, -ArC 5), 112.7 (t, -ArC 1), 52.4 (-OCH₃), 51.9 (-OCH₃), 48.9 (α -C), 48.8 (α -C), 35.7 (-CH₂-, -VE DEPT), 18.4 (-CH₃).

¹⁹F-NMR (376 MHz, DMSO): δ -66.7 (dd, 2F, $J^4 = 6.8$ Hz, $J^3 = 22.9$ Hz), -78.4 (t, $J = 21.8$ Hz), -86.8 - -86.9 (m, 2F).

***N*-pentafluorobenzoyl-L-alanine-L-methionine methyl ester 146**

L-Methionine methyl ester (0.8 g, 4 mmol) was used. Recrystallisation from ethyl acetate/hexane furnished **146** as a light yellow powder (0.90 g, 52%).

m.p. = 116-118 °C. $[\alpha]_D^{25} = -17^\circ$ (c, 2.5, EtOH).

Anal. calcd. for C₁₆H₁₇N₂O₄S₁F₅: C, 44.86; H, 4.00; N, 6.54.

Found C, 44.73; H, 3.78; N, 6.26.

IR (KBr): ν 3299, 2973, 1743, 1648, 1522, 994 cm⁻¹.

¹H-NMR (400 MHz, DMSO): 9.18 (1H, d, $J = 7.2$ Hz, -NH-), 8.57 (1H, d, $J = 7.2$ Hz, -NH-), 4.43-4.56 (2H, m, α -H), 3.64 (3H, s, -OCH₃), 2.52 (2H, t, $J = 7.0$ Hz, -CH₂S-), 1.88-2.04 (5H, m, -CH₂- & -SCH₃), 1.30 (3H, d, $J = 6.8$ Hz, -CH₃).

¹³C-NMR (100 MHz, DMSO): δ 172.4 (-CONH-), 171.9 (-COOCH₃), 156.5 (-ArCO-), 144.7-144.8 (m, -ArC 2), 140.3-142.8 (m, -ArC 4), 142.1-142.3 (-ArC 6), 138.3-138.5 (m, -ArC 3), 135.8-136.0 (m, -ArC 5), 112.6 (t, -ArC 1), 52.3 (-OCH₃), 51.2 (α -C), 49.0 (α -C), 30.8 (-CH₂-, -VE DEPT), 29.7 (-CH₂S-, -VE DEPT), 18.4 (-CH₃), 14.8 (-SCH₃).

^{19}F -NMR (376 MHz, DMSO): -66.6 (dd, 2F, $J^4 = 6.8$ Hz, $J^3 = 22.9$ Hz), -78.2 (t, $J = 21.8$ Hz), -86.6 - -86.7 (m, 2F).

General procedure for the synthesis of *N*-fluorobenzoyl dipeptidyl nitriles 150-157

***N*-2-fluorobenzoyl-L-leucine-glycine nitrile 150**

N-2-fluorobenzoyl-L-leucine (1.01 g, 4 mmol) was dissolved in dichloromethane (50 ml) with glycine nitrile hydrochloride (0.37 g, 4 mmol), 1-hydroxybenzotriazole (0.54 g, 4 mmol) and triethylamine (0.56 ml). The mixture was cooled to 0 °C, and 1,3-dicyclohexylcarbodiimide (0.83 g, 4 mmol) was added. After 30 min. the solution was raised to room temperature and the reaction was allowed to proceed for 8 hrs. The precipitated *N,N*-dicyclohexylurea was removed by filtration and the filtrate was washed with 10% potassium hydrogen carbonate, 10% citric acid, water and dried over magnesium sulphate. The solvent was evaporated *in vacuo* and recrystallisation from ethyl acetate/hexane furnished **150** as a white powder (0.81 g, 69%).

m.p. = 91-92 °C. $[\alpha]_{\text{D}}^{25} = -4.5^\circ$ (c, 2.1, EtOH).

Anal. calcd. for $\text{C}_{15}\text{H}_{18}\text{N}_3\text{O}_2\text{F}_1$: C, 61.84; H, 6.23; N, 14.42.

Found C, 61.98; H, 6.18; N, 14.17.

IR (KBr): ν 3277, 2961, 2372, 1637, 1534, 751 cm^{-1} .

^1H -NMR (400 MHz, DMSO): δ 8.78 (1H, t, $J = 5.6$ Hz, -NH-), 8.35 (1H, d, $J = 7.6$ Hz, -NH-), 7.60-7.65 (1H, m, -ArH 6), 7.51-7.56 (1H, m, -ArH 4), 7.26-7.34 (2H, m, -ArH 3 & 5), 4.48-4.53 (1H, m, α -H), 4.17 (2H, d, $J = 5.6$ Hz, -CH₂-), 1.47-1.72 (3H, m, -CH₂- & -CH-), 0.90 (6H, t, $J = 3.6$ Hz, -CH₃).

^{13}C -NMR (100 MHz, DMSO): δ 172.9 (-CONH-), 164.2 (-ArCO-), 159.5 (d, -ArC 2), 132.8 (d, -ArC 4), 130.5 (d, -ArC 6), 124.6 (d, -ArC 5), 124.0 (d, -ArC 1), 117.9 (-CN), 116.4 (d, -ArC 3), 51.7 (α -C), 40.5 (-CH₂-, -VE DEPT), 27.4 (-CH₂-, -VE DEPT), 24.6 (-CH-), 23.3 (-CH₃), 21.6 (-CH₃).

^{19}F -NMR (376 MHz, DMSO): δ -38.5 - -38.7 (m).

***N*-4-fluorobenzoyl-L-leucine-glycine nitrile 151**

N-4-fluorobenzoyl-L-leucine (1.01 g, 4 mmol) and glycine nitrile hydrochloride (0.37 g, 4 mmol) were used. Recrystallisation from ethyl acetate/hexane furnished **151** as a white powder (0.75 g, 64%).

m.p. = 138-139 °C. $[\alpha]_{\text{D}}^{25} = -8.6^\circ$ (c, 2.2, EtOH).

Anal. calcd. for C₁₅H₁₈N₃O₂F₁: C, 61.84; H, 6.23; N, 14.42.

Found C, 61.72; H, 6.27; N, 14.29.

IR (KBr): ν 3286, 3070, 2346, 1674, 1634, 1505, 854 cm⁻¹.

¹H-NMR (400 MHz, DMSO): δ 8.76 (1H, t, J = 5.6 Hz, -NH-), 8.43 (1H, d, J = 8.0 Hz, -NH-), 7.99-8.02 (2H, m, -ArH 2 & 6), 7.28-7.32 (2H, m, -ArH 3 & 5), 4.48-4.54 (1H, m, α -H), 4.14 (2H, d, J = 5.6 Hz, -CH₂-), 1.52-1.76 (3H, m, -CH₂- & -CH-), 0.90 (3H, d, J = 6.4 Hz, -CH₃), 0.86 (3H, d, J = 6.0 Hz, -CH₃).

¹³C-NMR (100 MHz, DMSO): δ 173.3 (-CONH-), 165.7 (-ArCO-), 164.3 (d, -ArC 4), 130.7 (-ArC 1), 130.66 (-ArC 2), 130.62 (-ArC 6), 117.9 (-CN), 115.5 (-ArC 3), 115.2 (-ArC 5), 51.9 (α -C), 40.2 (-CH₂-, -VE DEPT) 27.4 (-CH₂-, -VE DEPT), 24.7 (-CH-), 23.3 (-CH₃), 21.5 (-CH₃).

¹⁹F-NMR (376 MHz, DMSO): δ -33.8 - -34.0 (m).

***N*-2-fluorobenzoyl-L-alanine-glycine nitrile 152**

N-2-fluorobenzoyl-L-alanine (0.84 g, 4 mmol) and glycine nitrile hydrochloride (0.37 g, 4 mmol) were used. Recrystallisation from ethyl acetate/hexane furnished **152** as a white powder (0.55 g, 55%).

m.p. = 109-111 °C. $[\alpha]_D^{25} = -12.2^\circ$ (c, 1.6, EtOH).

Anal. calcd. for C₁₂H₁₂N₃O₂F₁: C, 57.83; H, 4.85; N, 16.86.

Found C, 57.91; H, 4.77; N, 16.56.

IR (KBr): ν 3336, 2944, 2364, 1677, 1638, 1534, 758 cm⁻¹.

¹H-NMR (400 MHz, DMSO): δ 8.71 (1H, t, J = 5.6 Hz, -NH-), 8.51 (1H, d, J = 6.4 Hz, -NH-), 7.67-7.71 (1H, m, -ArH 6), 7.52-7.57 (1H, m, -ArH 4), 7.27-7.31 (2H, m, -ArH 3 & 5), 4.45-4.52 (1H, m, α -H), 4.18 (2H, d, J = 5.6 Hz, -CH₂-), 1.33 (3H, d, J = 7.2 Hz, -CH₃).

¹³C-NMR (100 MHz, DMSO): δ 173.0 (-CONH-), 163.8 (-ArCO-), 159.7 (d, -ArC 2), 133.0 (d, -ArC 4), 130.7 (d, -ArC 6), 124.7 (d, -ArC 5), 123.7 (d, -ArC 1), 117.9 (-CN), 116.4 (d, -ArC 3), 49.0 (α -C), 27.5 (-CH₂-, -VE DEPT), 18.0 (-CH₃).

¹⁹F-NMR (376 MHz, DMSO): δ -38.4 - -38.6 (m).

***N*-pentafluorobenzoyl-L-alanine-glycine nitrile 153**

N-pentafluorobenzoyl-L-alanine (1.13 g, 4 mmol) and glycine nitrile hydrochloride (0.37 g, 3.16 mmol) were used. Recrystallisation from ethyl acetate/hexane furnished **153** as a white powder (0.54 g, 42%).

m.p. = 150-151 °C. $[\alpha]_D^{25} = -16.8^\circ$ (c, 2.4, EtOH).

Anal. calcd. for $C_{12}H_8N_3O_2F_5$: C, 44.87; H, 2.51; N, 13.08.

Found C, 45.04; H, 2.44; N, 12.93.

IR (KBr): ν 3293, 3061, 2258, 1662, 1523, 999 cm^{-1} .

1H -NMR (400 MHz, DMSO): δ 9.30 (1H, d, $J = 7.2$ Hz, -NH-), 8.86 (1H, t, $J = 5.6$ Hz, -NH-), 4.47-4.54 (1H, m, α -H), 4.20 (2H, d, $J = 5.6$ Hz, -CH₂-), 1.30 (3H, d, $J = 7.2$ Hz, -CH₃).

^{13}C -NMR (100 MHz, DMSO): δ 172.2 (-CONH-), 156.6 (-ArCO-), 144.7-144.8 (m, -ArC 2), 140.2-142.7 (m, -ArC 4), 142.1-142.3 (-ArC 6), 138.2-138.5 (m, -ArC 3), 135.8-136.0 (m, -ArC 5), 117.8 (-CN), 112.5 (t, -ArC 1), 48.9 (α -C), 27.4 (-CH₂-, -VE DEPT), 18.1 (-CH₃).

^{19}F -NMR (376 MHz, DMSO): δ -66.3 (dd, 2F, $J^4 = 6.8$ Hz, $J^3 = 22.9$ Hz), -77.9 (t, $J = 15.4$ Hz), -86.4 - -86.6 (m, 2F).

***N*-2-fluorobenzoyl-L-leucine- β -alanine nitrile 154**

N-2-fluorobenzoyl-L-leucine (1.01 g, 4 mmol) and β -alanine nitrile (0.28 g, 4 mmol) were used. Recrystallisation from ethyl acetate/hexane furnished **154** as a white powder (0.83 g, 68%).

m.p. = 84-85 °C. $[\alpha]_D^{25} = -8.3^\circ$ (c, 1.2, EtOH).

Anal. calcd. for $C_{16}H_{20}N_3O_2F_1$: C, 62.94; H, 6.60; N, 13.76.

Found C, 63.31; H, 6.98; N, 13.40.

IR (KBr): ν 3293, 2960, 2247, 1655, 1542, 755 cm^{-1} .

1H -NMR (400 MHz, DMSO): δ 8.41 (1H, t, $J = 5.6$ Hz, -NH-), 8.37 (1H, d, $J = 7.6$ Hz, -NH-), 7.63-7.67 (1H, m, -ArH 6), 7.50-7.55 (1H, m, -ArH 4), 7.25-7.30 (2H, m, -ArH 3 & 5), 4.48-4.54 (1H, m, α -H), 3.27-3.42 (2H, m, β -CH₂), 2.66 (2H, t, $J = 6.0$ Hz, α -CH₂), 1.51-1.71 (3H, m, -CH₂- & -CH-), 0.92 (3H, d, $J = 6.0$ Hz, -CH₃), 0.90 (3H, d, $J = 6.0$ Hz, -CH₃).

^{13}C -NMR (100 MHz, DMSO): δ 172.6 (-CONH-), 163.9 (-ArCO-), 159.5 (d, -ArC 2), 132.8 (d, -ArC 4), 130.6 (d, -ArC 6), 124.6 (d, -ArC 5), 124.0 (d, -ArC 1), 119.4 (-CN), 116.4 (d, -ArC 3), 52.0 (α -C), 41.1 (-CH₂-, -VE DEPT), 35.2 (β -CH₂-, -VE DEPT), 24.6 (-CH-), 23.3 (-CH₃), 21.8 (-CH₃), 17.8 (α -CH₂-, -VE DEPT).

^{19}F -NMR (376 MHz, DMSO): δ -38.6 - -38.7 (m).

***N*-4-fluorobenzoyl-L-leucine- β -alanine nitrile 155**

N-4-fluorobenzoyl-L-leucine (1.01 g, 4 mmol) and β -alanine nitrile (0.28 g, 4 mmol) were used. Recrystallisation from ethyl acetate/hexane furnished **155** as a white powder (0.64 g, 53%).

m.p. = 119-120 °C. $[\alpha]_D^{25} = -17.5^\circ$ (c, 1.5, EtOH).

Anal. calcd. for $C_{16}H_{20}N_3O_2F_1$: C, 62.94; H, 6.60; N, 13.76.

Found C, 63.14; H, 6.86; N, 13.62.

IR (KBr): ν 3326, 2957, 2249, 1649, 1604, 1502, 847 cm^{-1} .

1H -NMR (400 MHz, DMSO): δ 8.53 (1H, d, $J = 8.4$ Hz, -NH-), 8.36 (1H, t, $J = 8.0$ Hz, -NH-), 7.97-8.01 (2H, m, -ArH 2 & 6), 7.27-7.32 (2H, m, -ArH 3 & 5), 4.45-4.50 (1H, m, α -H), 3.25-3.36 (2H, m, β -CH₂), 2.64 (2H, t, $J = 6.0$ Hz, α -CH₂), 1.52-1.74 (3H, m, -CH₂- & -CH-), 0.90 (3H, d, $J = 6.0$ Hz, -CH₃), 0.87 (3H, d, $J = 6.0$ Hz, -CH₃).

^{13}C -NMR (100 MHz, DMSO): δ 173.1 (-CONH-), 165.6 (-ArCO-), 164.3 (d, -ArC 4), 130.8 (d, -ArC 1), 130.6 (-ArC 2), 130.5 (-ArC 6), 119.5 (-CN), 115.5 (-ArC 3), 115.3 (-ArC 5), 52.1 (α -C), 40.7 (-CH₂-, -VE DEPT) 35.1 (β -CH₂-, -VE DEPT), 24.7 (-CH-), 23.3 (-CH₃), 21.6 (-CH₃), 17.8 (α -CH₂-, -VE DEPT).

^{19}F -NMR (376 MHz, DMSO): δ -34.0 - -34.1 (m).

***N*-2-fluorobenzoyl-L-alanine- β -alanine nitrile 156**

N-2-fluorobenzoyl-L-alanine (0.84 g, 4 mmol) and β -alanine nitrile (0.28 g, 4 mmol) were used. Recrystallisation from ethyl acetate/hexane furnished **156** as a white powder (0.51 g, 49%).

m.p. = 127-128 °C. $[\alpha]_D^{25} = -11.3^\circ$ (c, 1.8, EtOH).

Anal. calcd. for $C_{13}H_{14}N_3O_2F_1$: C, 59.31; H, 5.36; N, 15.96.

Found C, 59.72; H, 5.67; N, 15.69.

IR (KBr): ν 3376, 3278, 2250, 1677, 1648, 1542, 901 cm^{-1} .

1H -NMR (400 MHz, DMSO): δ 8.36-8.39 (2H, m, -NH-), 7.68-7.72 (1H, m, -ArH 6), 7.51-7.56 (1H, m, -ArH 4), 7.27-7.31 (2H, m, -ArH 3 & 5), 4.44-4.48 (1H, m, α -H), 3.27-3.41 (2H, m, β -CH₂), 2.66 (2H, t, $J = 6.4$ Hz, α -CH₂), 1.33 (3H, d, $J = 7.2$ Hz, -CH₃).

^{13}C -NMR (100 MHz, DMSO): δ 172.7 (-CONH-), 163.4 (-ArCO-), 159.7 (d, -ArC 2), 133.0 (d, -ArC 4), 130.7 (d, -ArC 6), 124.7 (d, -ArC 5), 123.6 (d, -ArC 1), 119.4 (-CN), 116.4 (d, -ArC 3), 49.1 (α -C), 35.1 (β -CH₂-, -VE DEPT), 18.6 (-CH₃), 17.8 (α -CH₂-, -VE DEPT).

^{19}F -NMR (376 MHz, DMSO): δ -38.5 - -38.6 (m).

***N*-pentafluorobenzoyl-L-alanine- β -alanine nitrile 157**

N-pentafluorobenzoyl-L-alanine (1.13 g, 4 mmol) and β -alanine nitrile (0.28 g, 4 mmol) were used. Recrystallisation from ethyl acetate/hexane furnished **157** as a white powder (0.71 g, 53%). m.p. = 150-152 °C. $[\alpha]_D^{25} = -13.6^\circ$ (c, 2.3, EtOH).

Anal. calcd. for C₁₃H₁₀N₃O₂F₅: C, 46.57; H, 3.01; N, 12.54.

Found C, 46.92; H, 3.23; N, 12.33.

IR (KBr): ν 3365, 3274, 2252, 1672, 1626, 1522, 992 cm⁻¹.

¹H-NMR (400 MHz, DMSO): δ 9.19 (1H, d, $J = 7.6$ Hz, -NH-), 8.48 (1H, t, $J = 5.6$ Hz, -NH-), 4.45-4.53 (1H, m, α -H), 3.26-3.45 (2H, m, β -CH₂), 2.62-2.70 (2H, m, α -CH₂), 1.31 (3H, d, $J = 7.2$ Hz, -CH₃).

¹³C-NMR (100 MHz, DMSO): δ 171.9 (-CONH-), 156.5 (-ArCO-), 144.6-144.8 (m, -ArC 2), 140.1-142.6 (m, -ArC 4), 142.1-142.3 (m, -ArC 6), 138.3-138.5 (m, -ArC 3), 135.8-136.0 (m, -ArC 5), 119.4 (-CN), 112.7 (t, -ArC 1), 49.2 (α -C), 35.1 (β -CH₂, -VE DEPT), 18.7 (-CH₃), 17.8 (α -CH₂, -VE DEPT).

¹⁹F-NMR (376 MHz, DMSO): δ -66.4 (dd, 2F, $J^4 = 6.8$ Hz, $J^3 = 23.3$ Hz), -78.2 (t, $J = 15.8$ Hz), -86.6 - -86.7 (m, 2F).

3.6 Bibliography

- 1 Otto, H.H., Schirmeister, T., *Chem. Rev.* **1997**, *97*, 133.
- 2 Harmsen, M.M., Cornelissen, J.B.W.J., Buijs, H.E.C.M., Boersma, W.J.A.,
Jeurissen, S.H.M., van Milligen, F.J., *Intl. J. Parasitol.* **2004**, *34*, 675.
- 3 Dalton, J.P., O'Neill S., Stack, C., Collins, P., Walshe, A., Sekiya, M., Doyle, S.,
Mulcahy, G., Hoyle, D., Khaznadji, E., Moiré, N., Brennan, G., Mousley, A.,
Kreshchenko, N., Maule, A. G., Donnelly, S.M., *Intl. J. Parasitol.* **2003**, *33*, 1173.
- 4 Howell, R.M., *Nature* **1966**, *209*, 713.
- 5 Dalton, J.P., Heffernan, M., *Mol. Biochem. Parasitol.* **1989**, *35*, 161.
- 6 Leung, D., Abbenante, G., Fairlie, D.P., *J. Med. Chem.* **2000**, *43*, 305.
- 7 Lim, I.T., Meroueh, S.O., Lee, M., Heeg, M.J., Mobashery, S., *J. Am. Chem. Soc.*
2004, *126*, 10271.
- 8 Han, S.Y., Kim, Y.A., *Tetrahedron* **2004**, *60*, 2447.
- 9 Sheehy, M.J., "The design and synthesis of novel peptide derivatives as malarial
protease inhibitors and electrochemical anion sensing receptors", Dublin City
University, PhD Thesis, **1999**.
- 10 Gour-Salin, B.J., Lachance, P., Bonneau, P.R., Storer, A.C., Kirschke, H., Broemme,
P.R., *Bioorg. Chem.* **1994**, *22*, 227.
- 11 Lash, T.D., Belletini, J.R., Bastian, J.A., Couch, K.B., *Synthesis* **1994**, *2*, 170.
- 12 Thornton, T.J., Jackman, A.L., Marsham, P.R., O'Connor, B.M., Bishop, J.A.M.,
Calvert, A.H., *J. Med. Chem.* **1992**, *35*, 2321.
- 13 Jackman, A.L., Marsham, P.R., Thornton, T.J., Jones, T.R., Bishop, J.A.M.,
O'Connor, B.M., Hughes, L.R., Calvert, A.H., *J. Med Chem.* **1990**, *33*, 3067.
- 14 Sheehan, J.C., Cruickshank, P.A., Boshart, G.L., *J. Org. Chem.* **1961**, *26*, 2525.
- 15 Williams, A., Ibrahim, I.T., *J. Am. Chem. Soc.* **1981**, *103*, 7090.
- 16 Brenner, H., *Helv. Chim. Acta* **1953**, *36*, 1109.
- 17 Robichaud, J., Oballa, R., Prasit, P., Falguyret, J.P., Percival, M.D., Wesolowski, G.,
Rodan, S.B., Kimmel, D., Johnsen, C., Bryant, C., Venkatraman, S., Setti, E.,
Mendonca, R., Palmer, J.T., *J. Med. Chem.* **2003**, *46*, 3709.
- 18 Suzue, S., Irikura, T., *Chem. Pharm. Bull.* **1968**, *16*, 1417.

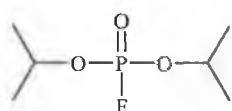
-
- 19 Greenspan, P.D., Clark, K.L., Cowen, S.D., McQuire, L.W., Tomassi, R.A., Farley, D. L., Quadros, E., Coppa, D.E., Du, Z., Fang, Z., Zhou, H., Doughty, J.R., Toscano, K.T., Wigg, A.M., Zhou, S., *Bioorg. Med. Chem. Lett.* **2003**, *13*, 4121.
- 20 Greenspan, P.D., Clark, K.L., Tomassi, R.A., Cowen, S.D., McQuire, L.W., Farley, D. L., van Duzer, J.H., Goldberg, R.L., Zhou, H., Du, Z., Fitt, J.J., Coppa, D.E., Fang, Z., Macchia, W., Zhu, L., Capparelli, M.P., Goldstein, R., Wigg, A.M., Doughty, J.R., Bohacek, R.S., Knap, A.K., *J. Med. Chem.* **2001**, *44*, 4524.
- 21 Zurita, M., Bieber, D., Mansour, T.E., *Mol. Biochem. Parasitol.* **1989**, *37*, 11.
- 22 Valeur, B. "*Molecular Fluorescence*", Wiley-VCH, **2002**.
- 23 Fried, B., Graczyk, T.K., "*Advances in Trematode Biology*", CRC Press LLC, New York, **1997**.

Chapter 4

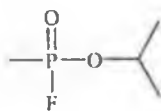
Dipeptidyl phosphonate diphenyl esters as inhibitors of the serine protease bovine pancreas α -chymotrypsin

4.1 Introduction

Serine proteases have been implicated in a number of pathological conditions, including rheumatoid arthritis, tumour metastasis and neurodegenerative diseases.¹ The involvement of serine proteases in proteolysis associated with these diseases has led to the design of synthetic inhibitors as therapeutic agents. Traditional inhibition has been based on the design of inhibitors with electrophilic warheads that alkylate the serine hydroxyl of the active site. This theory has resulted in successful inhibition although some inhibitors have shown some adverse effects.² α -Chymotrypsin (α -CT) is the most well studied serine protease whose structure and catalytic mechanism have been well established.³ The active site of α -CT contains a large hydrophobic pocket in the S1 subsite that prefers to accommodate a P1 residue having a bulky hydrophobic side chain such as phenylalanine or tryptophan. α -CT has served as a prototypical enzyme for a large family of enzymes and has been very useful as a model target enzyme for the development of design strategies that can be applied for other serine proteases of pharmacological interest. Consequentially a vast number of α -CT inhibitors have been reported.⁴



44



158

Serine protease inhibitors containing phosphorus have been known as potent inhibitors for over eighty years. The organophosphorus compound diisopropylfluorophosphate (DFP) **44** is historically one of the most widely used serine protease inhibitors.⁵ Compound **44** is an extremely toxic compound that phosphorylates the active site serine hydroxy group due to the electrophilicity of the phosphorus induced by the adjacent fluorine atom. The phosphorylated enzymes are good transition-state analogues due to the presence of a tetrahedral phosphorus centre, similar to that formed between peptides and enzymes. DFP reacts less rapidly with trypsin-like serine proteases than the α -chymotrypsin-like enzymes. The toxicity of DFP and its instability in aqueous media limits

its practical use as a protease inhibitor.⁶ Compound **44** is considered to be a general serine inhibitor with poor selectivity towards individual enzymes. It cannot discriminate between various serine proteases as it lacks a peptidyl moiety and hence it does not possess structural similarity to natural peptide substrates. Various analogues of DFP have been developed including the nerve gas sarin **158**. Peptidyl analogues of **44** did improve specificity but unwanted alkylation was still prevalent.⁷

The study of phosphorus analogues of the natural α -amino acids began in the late forties and due to recent discoveries of biologically active compounds interest in this area has increased dramatically.⁸ Diphenyl esters of α -aminoalkylphosphonic acids have been shown to be particularly potent and selective inhibitors of various serine proteases.⁹ These derivatives are generally non-toxic and stable in plasma. They have advantageously been shown to be unreactive with nitrogen nucleophiles.¹⁰ Peptidyl α -aminoalkylphosphonate diphenyl esters have been shown to inhibit various α -chymotrypsin like enzymes.⁷ The inhibition of serine proteases involves nucleophilic substitution on the phosphorus atom by the oxygen atom of the catalytic Ser₁₉₅ residue in the active site of the protease. The substitution proceeds through a penta-coordinate phosphorus transition state to give a stable irreversible tetrahedral monophenoxyphosphonyl derivative. X-ray structural studies have shown that the second phenoxy group is hydrolysed during an ageing process.¹¹

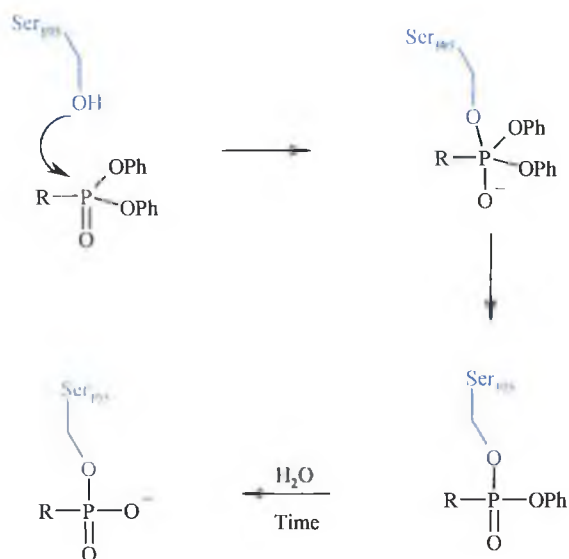


Figure 4.1 Mechanism of inhibition for peptidyl α -aminoalkylphosphonate diphenyl esters

The prodrug potential of phosphonate esters has been the subject of much discussion.¹² Numerous potent phosphonate ester derivatives have been developed that show a hydrolysed phosphate analogue is responsible for the biological activity of the compound.

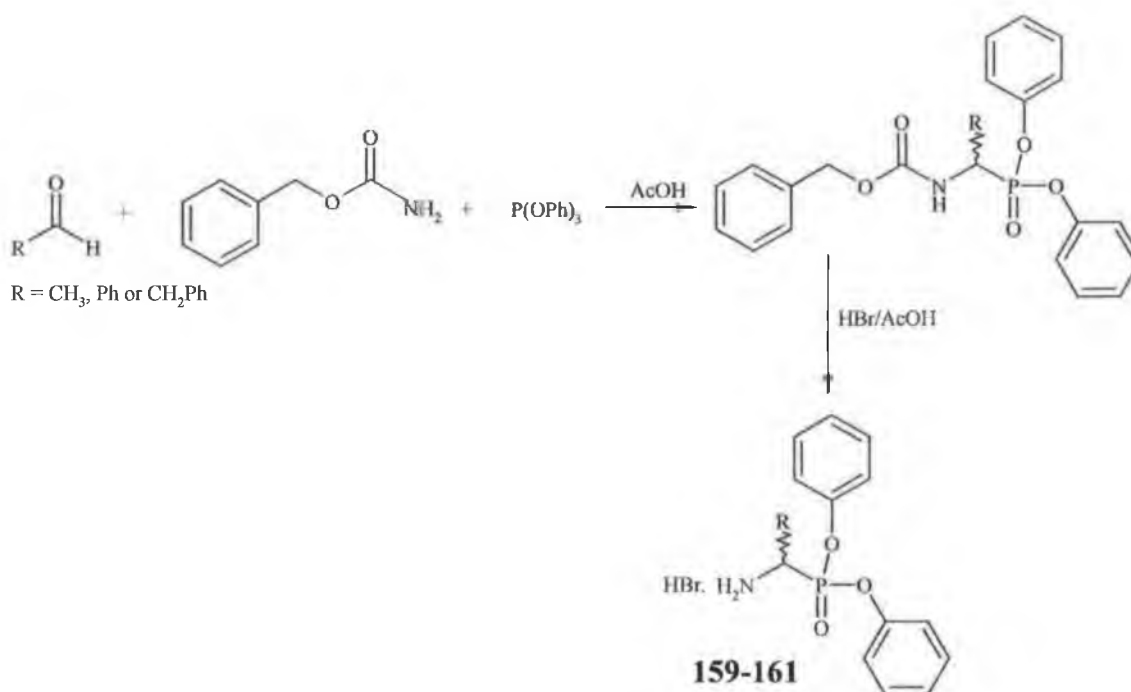
Phosphonic acids usually have a low pK_a value between 1 and 2.¹² When they are subjected to the physiological pH range of 7-7.4 phosphates are deprotonated and therefore negatively charged. These negatively charged species repel other nucleophilic or negatively charged compounds due to Coulombic interactions. This results in phosphates being extremely stable against non-enzymatic hydrolysis with half-lives in the range of hundreds of years.¹³ Phosphates are generally unable to penetrate cellular membranes unless active transport is involved. Therefore phosphates serve as functional units that prevent spreading of the chemical signal from one cell to another.

Chemists have created masking groups such as phenyl esters to allow the delivery of phosphates to the interior of the cell and to increase bioavailability.¹⁴ The resulting non-charged species are usually able to diffuse across the membrane. Once inside the cells, the masking groups are removed by chemical or enzymatic hydrolysis regenerating the charged phosphate species making the molecule impermeable to cell membranes and biologically active. Masking groups for the negative charged species of phosphate that are cleaved by intracellular enzymes but stable outside cells are of particular interest to medicinal chemists. The principal of prodrug action requires sufficient stability of the masked compound to ensure the cells or tissue being investigated are being reached. The design of enzyme activating protecting groups should ensure that these groups are unaffected by enzymes in plasma, blood or other body fluids. Once the phosphonate bearing compounds enter cells, the masking groups should be rapidly broken down by endogenous intracellular enzymes predominantly esterases or more rarely by phosphodiesterases or reductases.

Most bioactivatable masking groups release more or less toxic compounds upon degradation but most cells are equipped to maintain a stable pH. It is the liberation of formaldehyde that usually raises concern due to its potentially carcinogenic properties.¹⁵ Diaryl phosphonates can be viewed as mildly activated esters of phosphonic acids. They should undergo more facile hydrolysis than the corresponding dialkyl phosphonates. The overall rate of hydrolysis is crucial for them to perform as efficient phosphonic acid prodrugs. A diphenyl phosphonate has been hydrolysed rapidly with sodium hydroxide and slowly in strongly acidic medium. The resulting species was not the expected dianion species but in fact the monophenyl phosphonate.¹⁶ The synthesis of dipeptidyl diphenyl phosphonate esters not only offers a possible route to serine protease inhibition but also the incorporation of a masked phosphate group that increases the bioavailability and cellular specificity of the potential therapeutic agent.

4.2 Synthesis and structural characterisation of diphenyl- α -amino phosphonates

α -Aminoalkyl phosphonate esters can be broadly defined as analogues of α -amino acids in which the COOH group is replaced with PO(OR)₂ and have received considerable interest due to the occurrence of analogous derivatives in nature. The discovery of 2-aminoethanephosphonic acid (AEP) in sheep rumen protozoa in 1959 was a seminal discovery.¹⁷ This was the first example of a naturally occurring aminophosphonate and is both the simplest and most common of the natural aminophosphonates. Early studies on naturally occurring aminophosphonates were hindered due to the absence of sensitive methods for the detection of the C-P bond. This has been overcome with the use of ³¹P NMR studies. The synthesis of dipeptidyl α -aminophosphonates has generated potent inhibitors of aminopeptidases and serine proteases.¹⁸



Scheme 4.1 Synthesis of diphenyl- α -amino phosphonates

The diphenyl- α -aminoalkyl phosphonates **159-161** were prepared in a method analogous to Oleksyszyn.¹⁹ Triphenyl phosphite, benzyl carbamate and an aldehyde were reacted together in the presence of acetic acid via a *Michaelis-Arbuzov* reaction to give a racemic *N*-protected diphenyl ester. Yields of this reaction varied between 40 and 60 %. The protected amino group was then deprotected using hydrogen bromide in acetic acid solution. Removal of the benzyloxycarbonyl group was practically quantitative. Although the overall yields of the diphenyl- α -aminoalkyl phosphonates were modest, their synthesis is easily achieved in two steps giving pure compounds. The majority of reported methods involve the

synthesis of a phosphonic acid derivative. The α -aminophosphonic acids are generally prepared by hydrolysis of the diethyl phosphonate ester analogues.²⁰ Diethyl- α -amino phosphonate esters have recently been synthesised from reactions involving solvent-free conditions.²¹ Improved yields have been reported using acidic alumina with microwave irradiation.²² The separation of enantiomers was not deemed essential. Firstly, the α -aminophosphonates are to be coupled to achiral amino acid derivatives yielding racemates. Characterization of these dipeptidyl derivatives will not be hindered by their racemic nature. Secondly the most important aspect of this research is to assess the biological activity of these compounds. It was decided that if a particular compound resulted in potent inhibition in the nanomolar range the racemates would be then separated. It was considered highly unlikely that one enantiomer would have an antagonistic effect on the inhibitory potency of the other enantiomer. The reason the phosphorus analogues of phenylglycine and phenylalanine were synthesised was due to the affinity of α -chymotrypsin for a bulky aromatic side chain in the P1 position. The alanine analogue was not only prepared to further demonstrate this fact but also to reveal that the electrophilic phosphonate ester moiety does have a role to play in the inhibition of serine proteases.

Table 4.1 Diphenyl- α -amino phosphonates

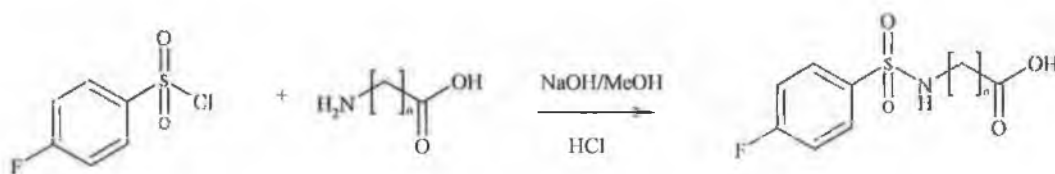
Compound	R	% Yield	³¹ P NMR δ ppm
(<i>D, L</i>)-Phenylglycine ^P -(OPh) ₂ 159	-C ₆ H ₅	59	11.53, d
(<i>D, L</i>)-Phenylalanine ^P -(OPh) ₂ 160	-CH ₂ C ₆ H ₅	43	14.51, m
(<i>D, L</i>)-Alanine ^P -(OPh) ₂ 161	-CH ₃	41	15.72, m

The α -aminophosphonates show a distinctive pattern in the ³¹P NMR spectra (Table 4.1). The phenylalanine and alanine derivatives appear as multiplets due to coupling of the phosphorus nucleus with the nearby protons. The phenylglycine analogue with only one proton in proximity of the phosphorus atom appears as a doublet with a ¹H-³¹P coupling constant of ~ 21 Hz. The chemical shift of these peaks is dependent on the side chain substituent with the methyl group giving the most downfield shift. The ¹³C NMR spectra of these derivatives show the α -carbon atoms appearing as a doublet with coupling constants ranging from 156 to 158 Hz. The effect of ³¹P-¹³C coupling is also seen on the methyl group of the alanine derivative and the methylene group of the phenylalanine analogue. The IR spectra of these derivatives show a strong P=O band at 1275 cm⁻¹ and amino N-H stretching at 3100 cm⁻¹.

4.3 Dipeptidyl phosphonate diphenyl esters

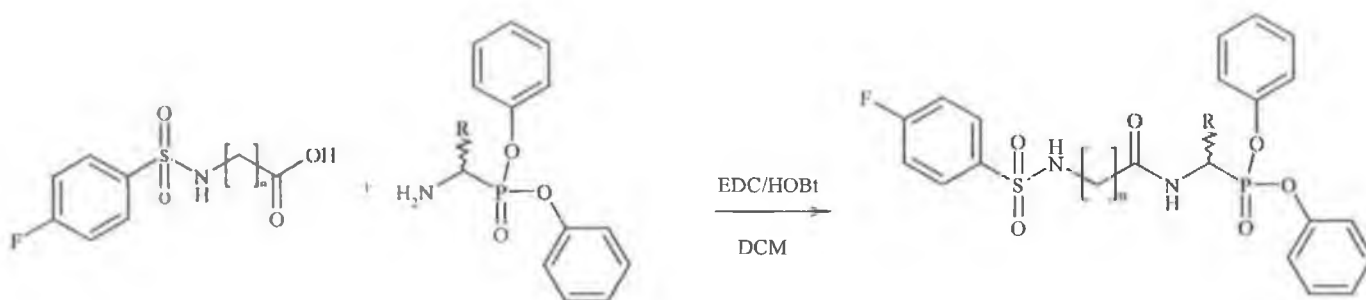
4.3.1 Synthesis and structural characterisation of *N*-4-fluorobenzenesulphonyl dipeptidyl phosphonate diphenyl esters

The series of pharmaceuticals known as the sulphonamides have been one of the greatest success stories in medicinal chemistry. The 4-fluorobenzenesulphonyl moiety has been previously described as an efficient *N*-terminal substitution for potent protease inhibition.²³ Its success can be explained by two reasons. Firstly the fluorobenzenesulphonyl group has an electrophilic centre at the sulphur atom. This centre is strongly electrophilic due to the electron withdrawing nature of the two attached oxygen atoms. This centre has the ability to act as a target for the active site serine residue of serine proteases such as α -chymotrypsin and trypsin. Secondly, it has also been shown that the SO₂ moiety of such inhibitors is involved in several strong hydrogen bonds with amino acid residues in the active site that can strongly stabilize the enzyme-inhibitor adduct.²⁴ The geometry of the sulphonyl group gives a unique configuration unattainable by the planar amide bond.



Scheme 4.2 Synthesis of *N*-4-fluorobenzenesulphonyl amino acids

The first step of the synthesis involves the preparation of *N*-4-fluorobenzenesulphonyl derivatives incorporating the amino acids glycine, β -alanine and γ -aminobutyric acid. This step is carried out in the presence of NaOH and is analogous to the *Schotten Baumann* reaction.²⁵ The presence of a fluorine atom allowed the progress of the reaction to be monitored by ¹⁹F NMR. The starting material 4-fluorobenzenesulphonyl chloride gave a multiplet centred at δ -37.4 whereas the amino acid derivatives gave a multiplet centred at δ -31.7. Yields of up to 80% were recorded for the synthesis of the *N*-4-fluorobenzenesulphonyl amino acid derivatives that were in accordance with the literature.²⁶ The synthesis of these compounds is confirmed by the presence of a triplet at $\sim \delta$ 8.1 in the ¹H NMR spectrum due to the sulphonyl amide proton. The aromatic protons of the benzenesulphonyl moiety appear as multiplets between δ 7 and 8 due to ¹⁹F-¹H internuclear coupling. The Infrared spectra show a distinct peak at 1675 cm⁻¹ due to the amide carbonyl. A strong band at 1155 cm⁻¹ is responsible for the sulphonamide moiety in the Infrared spectra.



Scheme 4.3 Synthesis of *N*-4-fluorobenzenesulphonyl dipeptidyl phosphonate esters

The dipeptidyl phosphonate diphenyl ester derivatives were prepared using standard EDC/HOBt protocol. The dipeptides were purified by an acid water wash cycle followed by recrystallisation from diethyl ether. The yields ranged from 29 to 61 % (Table 4.2). The highest yield recorded was for the alanine derivatives. This is probably due to steric factors as the methyl group of the alanine derivative is considerably smaller than the phenyl or benzyl groups of phenylglycine and phenylalanine respectively.

The *N*-4-fluorobenzenesulphonyl dipeptidyl phosphonate esters (Table 4.2) are characterised by a multiplet at $\delta \sim -31.7$ in the ^{19}F NMR spectra. This appears as a multiplet as the fluorine atom has the ability to interact with each of the four protons present on the aromatic ring. The ^{13}C NMR spectra of these compounds show a distinctive peak at $\delta \sim 167$ that represents the amide carbonyl formed by the coupling reaction. Electrospray ionisation mass spectrometry (ESIMS) carried out on these compounds gave two distinct peaks. The sodium adduct peak was present at molecular ion + 23 mass units while the potassium adduct appeared at m/z molecular ion + 39 mass units.

Table 4.2. *N*-4-fluorobenzenesulphonyl dipeptidyl phosphonate ester derivatives

Compound	n	R	% Yield	^{31}P NMR δ ppm
162	1	-C ₆ H ₅	29	14.83, d
163	2	-C ₆ H ₅	35	15.12, d
164	3	-C ₆ H ₅	29	15.35, d
165	1	-CH ₂ C ₆ H ₅	45	17.65, t
166	2	-CH ₂ C ₆ H ₅	36	17.81, t
167	3	-CH ₂ C ₆ H ₅	33	18.24, t
168	1	-CH ₃	59	19.30, m
169	2	-CH ₃	61	19.57, m
170	3	-CH ₃	50	19.79, m

4.3.2 ^1H NMR Study of *N*-4-fluorobenzenesulphonyl dipeptidyl phosphonate esters

The ^1H NMR spectrum of *N*-4-fluorobenzenesulphonyl-Gly-(*D*, *L*)-Ala^P-(OPh)₂ **168** is shown in Figure 4.2. The effect of ^{19}F - ^1H and ^{31}P - ^1H coupling is seen throughout the spectra of the *N*-4-fluorobenzenesulphonyl dipeptidyl phosphonate esters. The amide protons appear at $\delta \sim 8.6$ and $\delta \sim 8.1$ as a doublet and triplet respectively. The aromatic region of the spectrum shows the peaks responsible for the phenyl ester protons and the hydrogen atoms present on the 4-fluorophenyl rings. The coupling pattern of these protons is complicated due to coupling with nearby phosphorus and fluorine atoms. The α -H is present at $\delta \sim 4.6$ as a multiplet due to coupling with the amide proton, the side chain and also the phosphorus atom of the phosphonate moiety. The methylene group of glycine appears as two double doublets at $\delta \sim 3.5$ and $\delta \sim 3.6$ with coupling constants of ~ 5.6 and ~ 16.4 Hz.

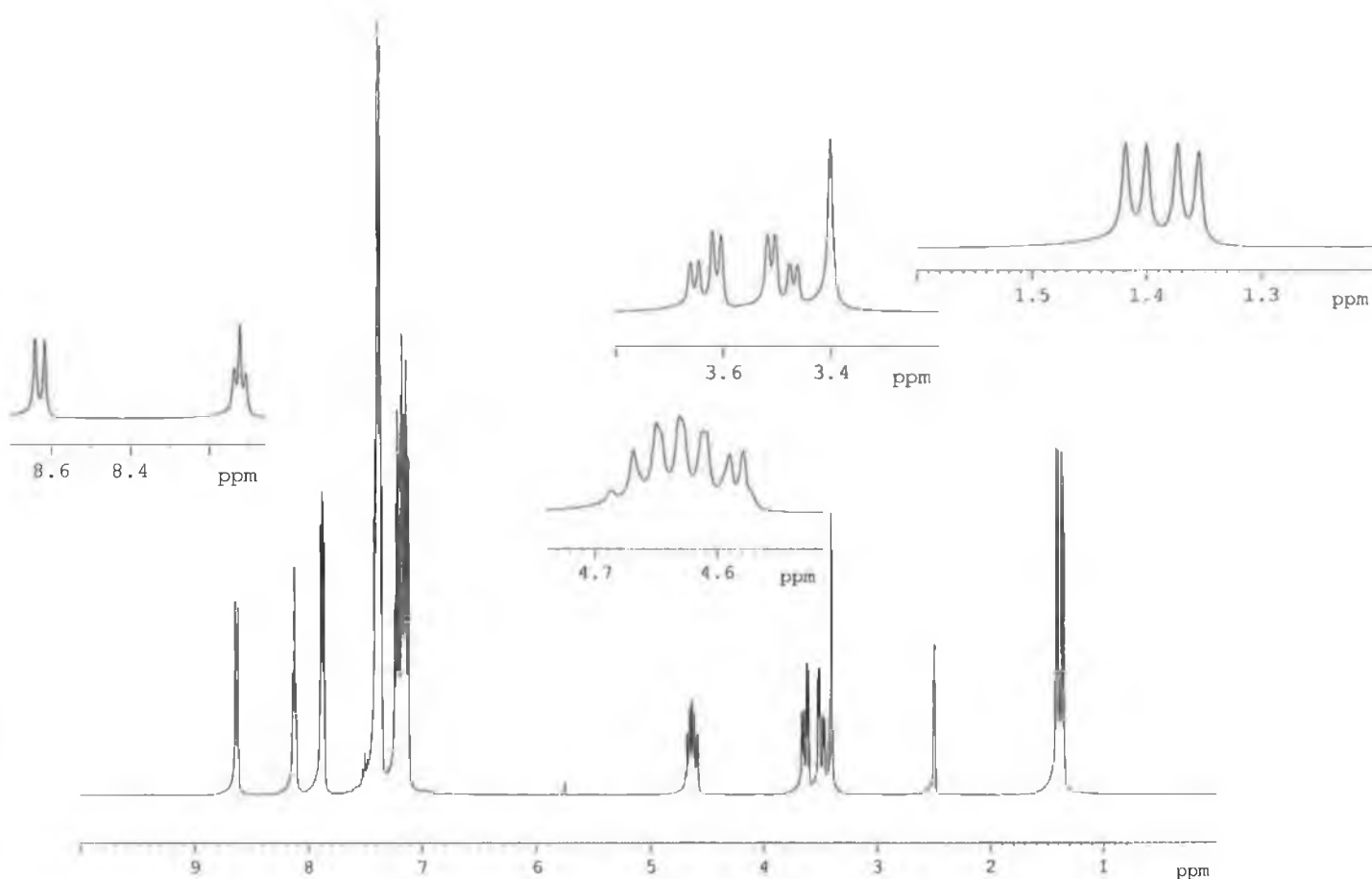


Figure 4.2 ^1H NMR of *N*-4-fluorobenzenesulphonyl-Gly-(*D*, *L*)-Ala^P-(OPh)₂ **168**.

This coupling is due to the diastereotopic nature of these protons and corresponds to coupling between the two methylene protons and further coupling between the methylene protons and the amide proton. The methyl side chain of the phosphorus analogue of alanine appears at $\delta \sim 1.4$ as a double doublet also. This methyl group couples with the α -H to give a coupling constant of 7.2 Hz. The methyl protons also couple with the phosphorus atom three bonds

away. This ^{31}P - ^1H coupling gives a coupling constant of 18.0 Hz. There is a water peak found at ~ 3.5 ppm due to H_2O in the DMSO. Suppression of the water peak also suppressed the methylene protons of glycine. It should be noted that the chemical shift of the α -H is dependent on the side chain substituent. In the case of the phenylglycine derivatives the α -H appears downfield as a double doublet $\delta \sim 5.90$ due to the electron withdrawing effect of the phenyl moiety attached. It appears as a double doublet as the α -H couples with the amide proton and also the phosphorus atom.

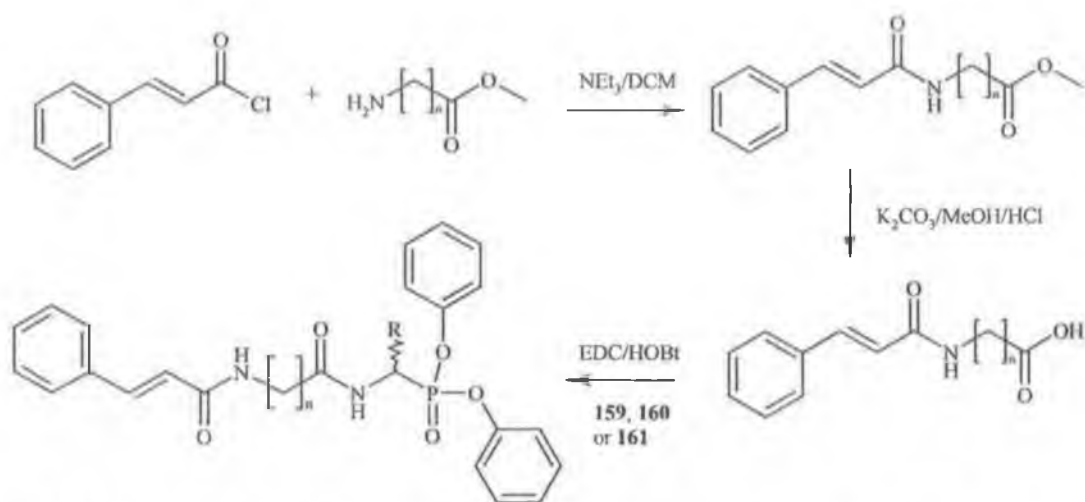
Table 4.3 Selected ^1H NMR data (δ) for the *N*-4-fluorobenzenesulphonyl dipeptidyl phosphonate esters

Compound No.	NH	NH	α -H	-CH ₂ -
162	9.35	8.14	5.81	3.75, 3.63
164	9.33	6.91-7.83	5.92	2.71-2.76, 2.27, 1.60-1.66
166	8.73	7.15-7.85	4.71-4.81	2.69, 2.16-2.22
168	8.66	8.16	4.62-4.71	3.68, 3.54
170	8.69	7.13-7.91	4.71-4.78	2.93-3.00, 2.32-2.43

4.3.3 Synthesis and structural characterisation of *N*-cinnamoyl dipeptidyl phosphonate diphenyl esters

N-terminal cinnamoyl dipeptidyl derivatives have been reported as potent inhibitors of the protease papain.²⁷ The design of such Michael acceptors is based on the fact that the active site nucleophile may attack the strongly electrophilic β -carbon of the unsaturated unit, leading to irreversible covalent bonding to the active site of the enzyme. The concept of extending greater distances from the NH_2 terminal amide with conformational restraint has resulted in enhanced potency due to additional favourable interactions that are unavailable to shorter NH_2 -termini.²⁸

The synthesis of *N*-cinnamoyl amino acid derivatives was carried out in two steps. Cinnamoyl chloride was reacted with glycine, β -alanine and γ -amino butyric acid methyl esters in the presence of triethylamine to yield *N*-cinnamoyl amino acid esters in yields between 57 and 75 %. The esters were then hydrolysed using potassium carbonate to give the free acid moiety. Alternatively, the synthesis of *N*-cinnamoyl amino acid derivatives was carried out by the one step *Schotten-Baumann* reaction with the free amino acid. However the yields obtained were less than 30 %. This low yield was due to the fact that the cinnamoyl chloride was also attacked by the amino acid to form cinnamoyl anhydride derivatives.



Scheme 4.4 Synthesis of *N*-cinnamoyl dipeptidyl phosphonate diphenyl esters

The synthesis of the dipeptidyl derivatives was achieved using the standard EDC/HOBt protocol. Yields ranged from 15 to 55 %. Although these yields were very modest the purity of the compounds was very high as shown by NMR studies. The highest yield was for *N*-cinnamoyl- β -Ala-(*D*, *L*)-Ala^P-(OPh)₂ **178** which gave a value of 55%. The lowest yield recorded was for the phenylglycine derivative compound **172**. The low yield of this compound was also observed in the synthesis of the 4-fluorobenzenesulphonyl derivatives.

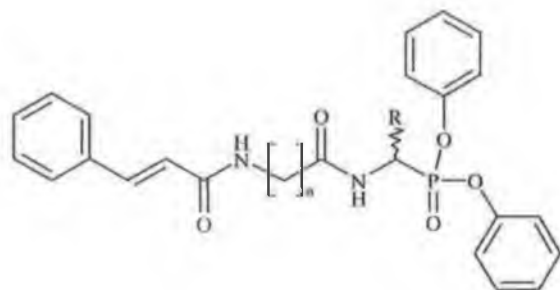


Table 4.4 *N*-cinnamoyl dipeptidyl phosphonate ester derivatives

Compound	n	R	% Yield	³¹ P NMR δ ppm
171	1	-C ₆ H ₅	32	15.15, d
172	2	-C ₆ H ₅	15	15.30, d
173	3	-C ₆ H ₅	37	15.39, d
174	1	-CH ₂ C ₆ H ₅	37	17.99, t
175	2	-CH ₂ C ₆ H ₅	45	18.19, t
176	3	-CH ₂ C ₆ H ₅	36	18.26, t
177	1	-CH ₃	53	19.61, m
178	2	-CH ₃	55	19.75, m
179	3	-CH ₃	49	19.85, m

The ^1H NMR spectra of these compounds show the unsaturated unit appearing as two doublets at $\delta \sim 6.7$ and $\delta \sim 7.9$ with coupling constants of ~ 15.6 Hz. In some cases, the protons of the cinnamoyl double bond are obscured by the aromatic protons of the phenyl esters. The protons of the amide bonds formed between the cinnamoyl group and the amino acid appears downfield at ~ 8.5 due to two factors. Firstly there is the deshielding effect of the cinnamoyl system that shifts the chemical shift to a lower field and secondly there is the effect of using deuterated dimethyl sulphoxide as solvent. The additional hydrogen bonding properties of DMSO- d_6 makes the amide proton resonate at a lower field. The ^{31}P NMR spectra of the cinnamoyl derivatives show an interesting pattern. The chemical shift of the phosphorus atom is influenced by the amino acid bonded to the α -aminophosphonate. The more methylene units that are present in the attached amino acid the more downfield the phosphorus signal appears. This shows the sensitivity of ^{31}P NMR spectroscopy as an analytical tool as the attached amino acid derivatives are at least three bonds away and often further. The *N*-cinnamoyl dipeptidyl phosphonate esters **174**, **175** and **176** appear as triplets in the ^{31}P NMR. This result is due to coupling of the phosphorus atom with two protons and is unique to the phenylalanine containing derivatives. Although the amide bond protons are also only two bond lengths from the phosphorus atom, there is no evidence of ^{31}P - ^1H coupling between the amide protons and phosphorus atom occurring in **174**, **175** or **176**. The Infrared spectra of these compounds show the characteristic amide carbonyl stretching at ~ 1675 and ~ 1590 cm^{-1} . N-H stretching of the amides is seen as a broad band at ~ 3265 cm^{-1} . The phosphonate P=O band is located as a broad peak at ~ 1270 cm^{-1} .

4.3.4 ^{13}C NMR study of *N*-cinnamoyl dipeptidyl phosphonate esters

The ^{13}C NMR spectrum of compound **175** is shown in Figure 4.3. The two amide carbon atoms appear at $\delta \sim 170$ and $\delta \sim 165$. The *ipso* carbons of the phenyl esters show a distinctive pattern. The two phenyl rings come into resonance at slightly different frequencies and each appear as a doublet due to the effect of ^{13}C - ^{31}P coupling in the NMR. The downfield location of these carbon peaks is due to the electron deshielding effect of the attached oxygen atom. The remaining aromatic carbons appear between $\delta \sim 137$ and $\delta \sim 120.7$ as a series of singlets and doublets due to the effects of ^{13}C - ^{31}P internuclear coupling. There is a substantial difference between the chemical shifts of the unsaturated unit carbons. The α -carbon is present at $\delta \sim 138.9$ and the β -carbon of the unsaturated is seen at $\delta \sim 122$. The α -carbon is further downfield due to the attached deshielding carbonyl moiety.

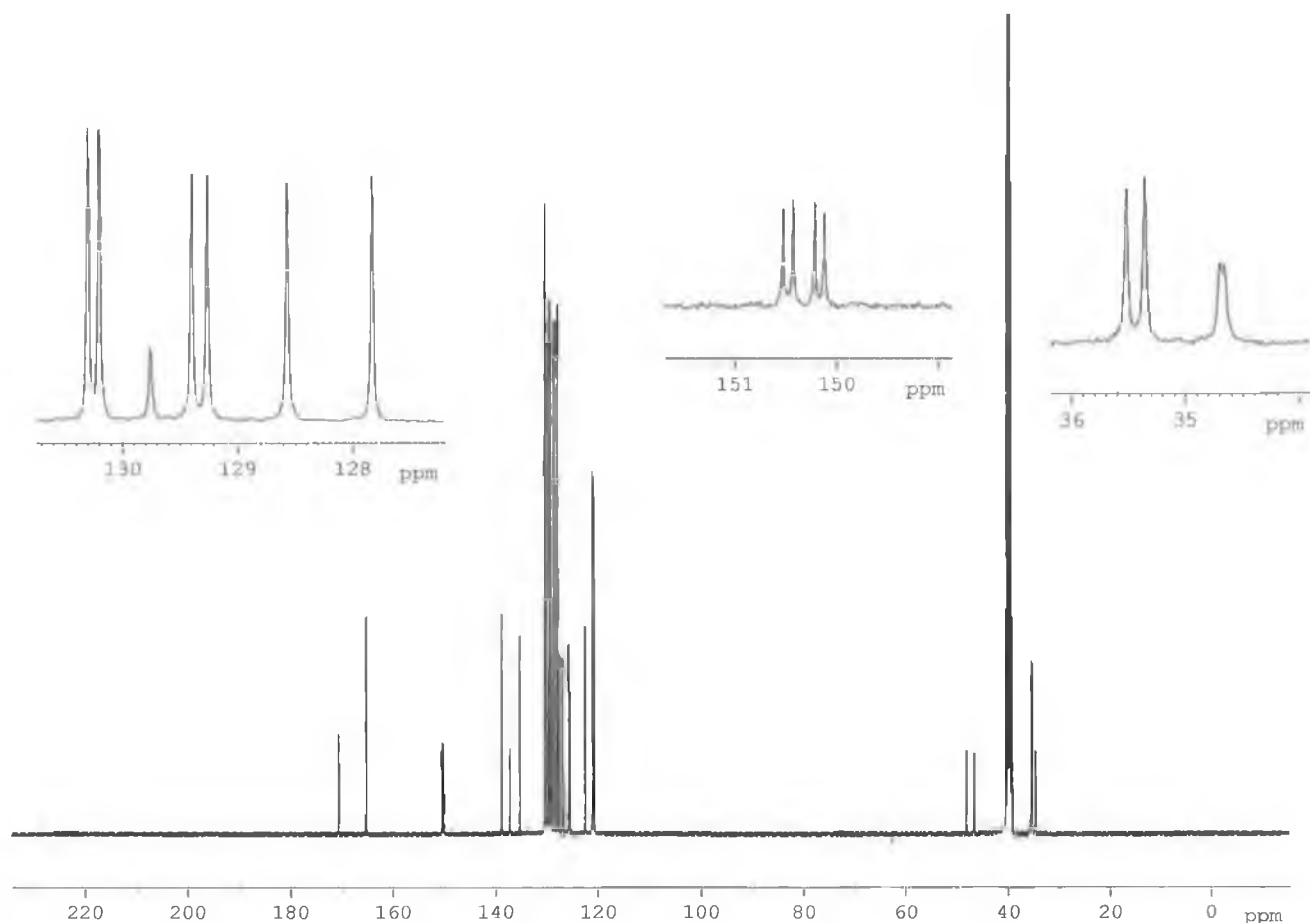


Figure 4.3 ^{13}C NMR of *N*-cinnamoyl- β -Ala-(*D, L*)-Phe^P-(OPh)₂ **175**.

The α -carbon of the phenylalanine derivative **175** appears as a doublet at $\delta \sim 47$ with a ^{31}P - ^{13}C coupling constant of ~ 156.5 Hz. The methylene groups of β -Ala appear as two singlets at $\delta 35.5$ and $\delta 35.3$ and this was confirmed from analysis of the DEPT135 spectra. Finally the side chain methylene group of phenylalanine is found as a doublet at $\delta \sim 34.7$ as it is only three bonds from the phosphorus atom. On the other hand, in the case of the phenylglycine and alanine analogues the α -carbons appear at $\delta \sim 50.4$ and $\delta \sim 41.6$ respectively with similar coupling constants. The methylene groups of γ -aminobutyric acid appear at $\delta \sim 42.5$, $\delta \sim 32.4$ and $\delta \sim 25.6$ with the methylene group attached to the amino group appearing the furthest downfield. The presence of a racemic mixture was undetectable by ^{13}C NMR.

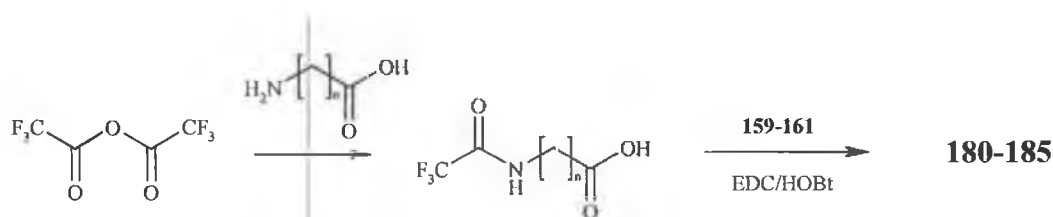
Table 4.5 Selected ^{13}C NMR data (δ) for the *N*-cinnamoyl dipeptidyl phosphonate esters

Compound No.	C=O	C=O _{Aryl}	-OPhC _{ipso}	C=C	α -C
171	169.4	165.7	150.3, 150.1	139.5, 122.1	50.4
173	172.2	165.3	150.4, 150.1	138.9, 122.5	50.3
175	170.7	165.3	150.4, 150.1	138.9, 122.5	47.2
177	169.0	165.6	150.4, 150.1	139.4, 122.2	41.6
179	172.0	165.4	150.4, 150.2	139.0, 122.5	41.2

4.3.5 Synthesis and structural characterisation of *N*-trifluoroacetyl dipeptidyl phosphonate diphenyl esters

The trifluoroacetyl moiety has been shown to be an effective *N*-terminal substituent in potent protease inhibitors.²⁹ The trifluoroacetyl moiety gives a powerful electrophilic substituent that may undergo attack by the serine residue of the α -chymotrypsin active site. The trifluoroacetyl group has been shown to be an effective protecting group for *N*-terminal amino acids and is easily removed by strong acid.²⁹ This indicates that these derivatives may undergo hydrolysis *in vivo* to yield free amino dipeptidyl phosphonate esters.

The *N*-trifluoroacetyl amino acids were synthesised according to the procedure of Giordano *et al.*³⁰ The amino acid was added to trifluoroacetic anhydride at 0 °C and then the reaction was heated at 80 °C for 1 hour. The excess trifluoroacetic acid and trifluoroacetic anhydride were removed to yield *N*-trifluoroacetyl-glycine and β -alanine derivatives as crystalline solids. Previous syntheses of trifluoroacetyl amino acids have used trifluoroacetyl chloride but due to its gaseous nature this was not utilised. The synthesis of *N*-trifluoroacetyl- γ -aminobutyric acid using trifluoroacetic anhydride has not been previously described although success has been achieved with trifluoroacetic methyl ester.³¹ Our attempts to synthesise this compound resulted in a series of oily mixtures. The amino acid derivative was synthesised but in very low yield. This was seen from the ¹⁹F NMR spectra of this reaction. All attempts to remove the acetic acid/anhydride byproducts resulted in a viscous oil. When this oil was coupled with the diphenyl- α -amino phosphonates there was no reaction recorded. This is due to the presence of excess trifluoroacetic acid and trifluoroacetic anhydride present in the reaction. The coupling reagent EDC is not extremely acid stable.



Scheme 4.5 Synthesis of *N*-trifluoroacetyl amino acids

The synthesis of *N*-trifluoroacetyl-dipeptidyl phosphonate esters was achieved using the standard EDC/HOBt protocol. The dipeptidyl derivatives prepared were racemates and this was confirmed by their optical rotation. Yields ranged from 20% for compound **181** to 59% for compound **182**. The glycine derivatives gave the higher yields than the β -alanine analogues used. Uniquely, in comparison to the 4-fluorobenzenesulphonyl- and cinnamoyl analogues, it was the phenylalanine derivatives that gave the highest yields. The reduced size

of the trifluoroacetyl moiety limits the amount of steric hindrance present in the coupling reaction. This also indicates that in fact the *N*-terminal substituents of 4-fluorobenzenesulphonyl and cinnamoyl have a role to play with steric hindrance.

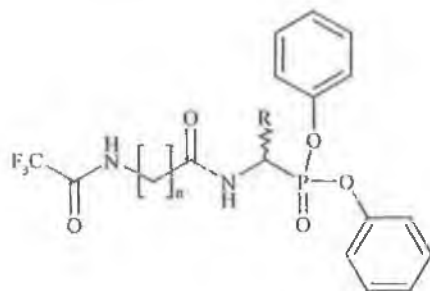


Table 4.6. *N*-trifluoroacetyl dipeptidyl phosphonate ester derivatives

Compound	n	R	% Yield	³¹ P NMR δ ppm
180	1	-C ₆ H ₅	29	15.23, d
181	2	-C ₆ H ₅	20	15.94, d
182	1	-CH ₂ C ₆ H ₅	59	18.01, t
183	2	-CH ₂ C ₆ H ₅	39	18.52, t
184	1	-CH ₃	48	19.71, m
185	2	-CH ₃	40	20.02, m

The *N*-trifluoroacetyl dipeptidyl phosphonates are characterized by the presence of quartets at δ ~157 representing the carbonyl and at δ ~116 representing the trifluoromethyl group in the ¹³C NMR. A singlet at δ ~ 0.9 characterizes the trifluoromethyl moiety in the ¹⁹F NMR spectra. The ¹H, ¹³C and ³¹P NMR spectra correspond favourably to the previously discussed 4-fluorobenzenesulphonyl and cinnamoyl derivatives. The Infrared spectra of these compounds show the characteristic bands of dipeptidyl derivatives. Peaks at ~1255 cm⁻¹ can be attributed to the P=O group. At 3242 cm⁻¹ a peak due to N-H stretching is observed.

4.3.6 HMQC Study of *N*-trifluoroacetyl dipeptidyl phosphonate esters

Heteronuclear multiple quantum correlation (HMQC) is a 2D NMR spectroscopic technique which correlates the carbon and proton spectra. Table 4.7 and Figure 4.4 show the C-H correlation for the structure *N*-trifluoroacetyl-β-Ala-Phe^p-(OPh)₂ **186**.

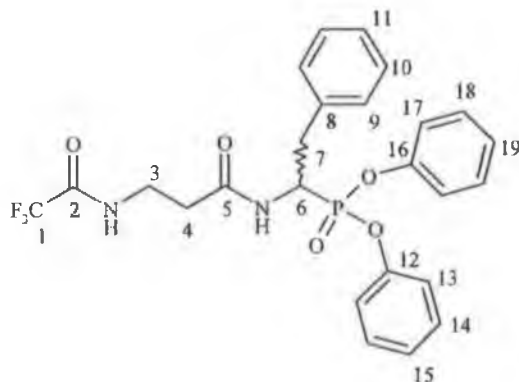


Table 4.7 C-H correlation of *N*-trifluoroacetyl- β -Ala-Phe^P-(OPh)₂ 183

Site	¹ H	¹³ C	HMQC
1		116.6	
2		156.5	
3	3.18-3.22		35.9
4	2.27-2.37		34.1
5		169.8	
6	4.86-4.89		47.3
7	3.29-3.34, 2.95-3.04		34.7
8		137.1	
9	7.18-7.43		128.5
10	7.18-7.43		129.4
11	7.18-7.43		126.9
12		150.4	
13	7.18-7.43		121.0
14	7.18-7.43		130.29
15	7.18-7.43		125.7
16		150.1	
17	7.18-7.43		120.7
18	7.18-7.43		130.21
19	7.18-7.43		125.6

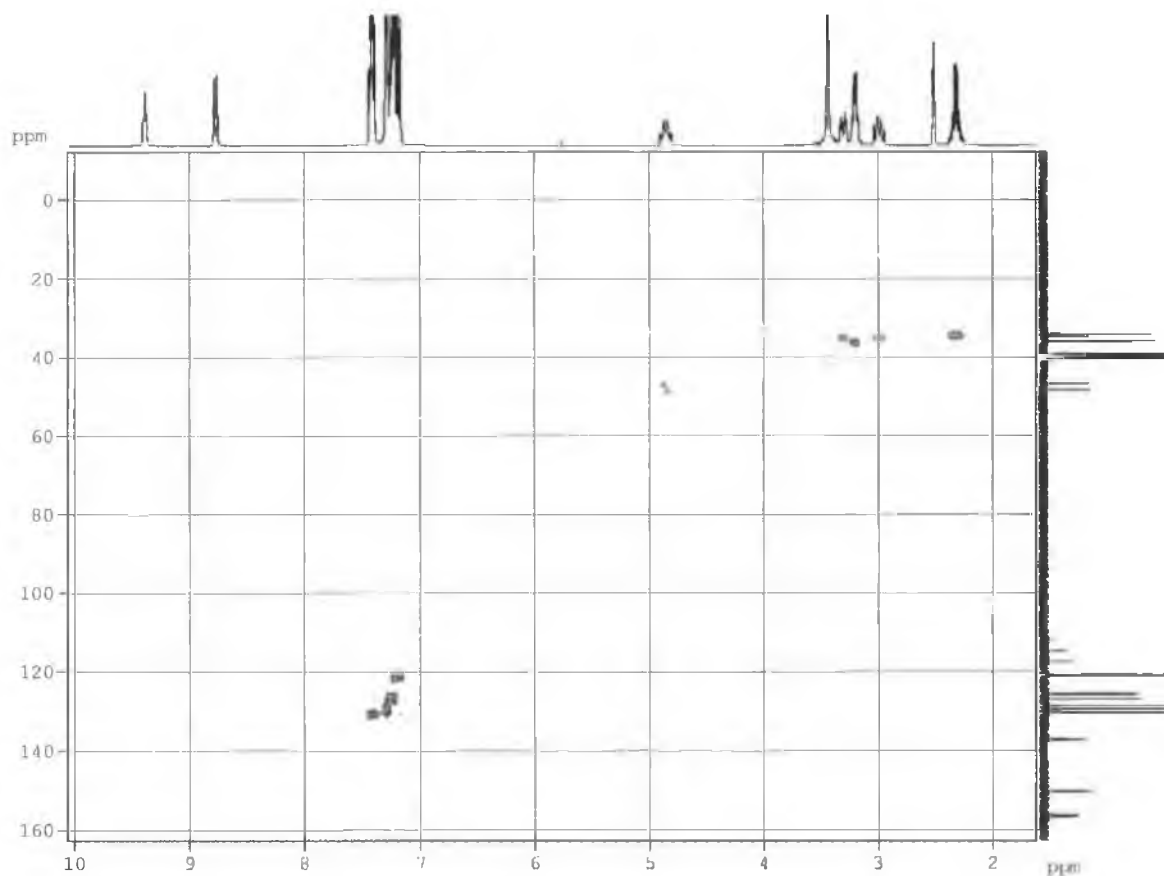


Figure 4.4 HMQC Spectrum of *N*-trifluoroacetyl- β -Ala-Phe^P-(OPh)₂ 183.

4.4 Structural study of the dipeptidyl phosphonate esters

Crystals suitable for single crystal x-ray crystallographic determinations of **164**, **169**, **183** and **184** were grown from methanol, yielding colourless block shaped crystals. All pertinent crystallographic information is summarized in Tables 4.8 and 4.10 and selected bond distances and angles of non-hydrogen atoms are given in Tables 4.9 and 4.11. Figures 4.5 - 4.14 show perspective views of each crystal structure with atomic numbering scheme.

Compound **164** crystallizes in the monoclinic space group $P2_1/n$ with four independent molecules per asymmetric unit. The range of the phenyl C-C bond distances is 1.357(4) to 1.394(3) Å (mean 1.375(3) Å). The sulphonyl S=O distance is 1.436(15) Å. The F-C-C bond angles range from 117.9(19)° to 118.4(19)°. The amide C(O)-N distance C(1)-N(1) 1.340(3) Å and sulphonamide S(O)-N distance S(2)-N(2) 1.608(17) Å exhibit a lot of single bond character. The principle interactions in **164** involve the amide N-H and carbonyl groups of neighbouring residues interacting as N-H...O=C and forming a one-dimensional chain. There is also an intermolecular hydrogen bond formed between the phosphonate P=O and the amide N-H (Figure 4.5).

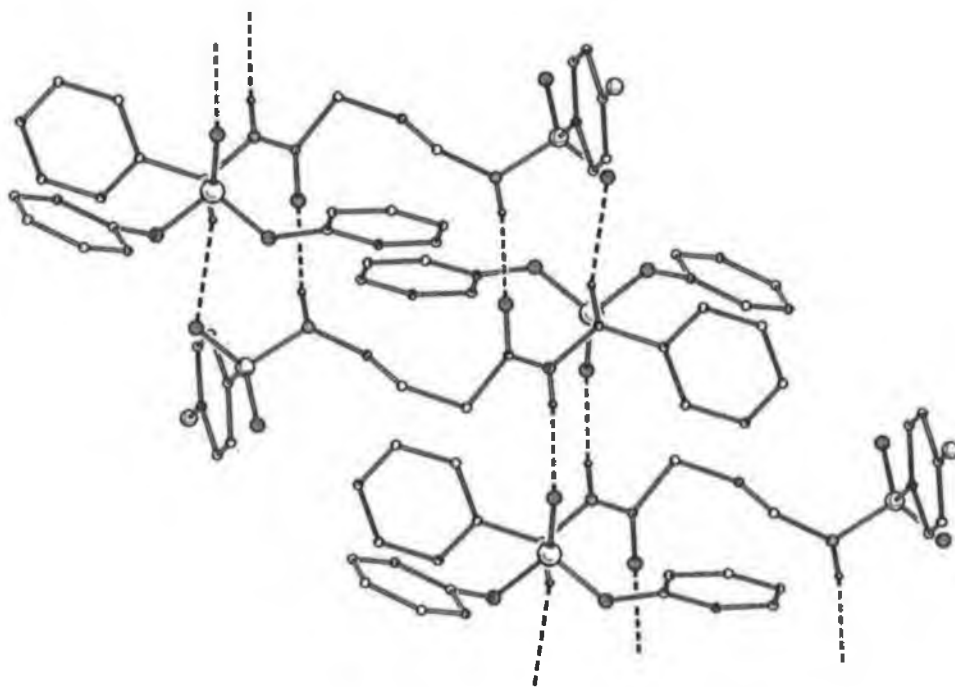


Figure 4.5 PLATON drawing of the X-ray crystal structure of *N*-4-fluorobenzenesulphonyl- γ -aminobutyric acid-(D, L)-phenylglycine^p diphenyl ester **164** depicting the intermolecular interactions.

Table 4.8 Crystal data and structure refinement for *N*-4-fluorobenzenesulphonyl- γ -aminobutyric acid-(D, L)-phenylglycine^p diphenyl ester **164** and *N*-4-fluorobenzenesulphonyl- β -alanine-(D, L)-alanine^p diphenyl ester **169**.

	164	169
Empirical formula	C ₂₉ H ₂₈ N ₂ O ₆ F ₁ S ₁ P ₁	C ₂₃ H ₂₄ N ₂ O ₆ F ₁ S ₁ P ₁
M _r	582.56	506.47
Crystal color	Colorless, block	Colorless, block
Crystal System	Monoclinic	Triclinic
Space group	P2 ₁ /n	P ₁
a/Å	10.0971(2)	9.7421(3)
b/Å	12.0113(2)	15.6322(6)
c/Å	23.2360(6)	16.3509(6)
α /°	-	86.7309(17)
β /°	90.5379(12)	74.052(2)
γ /°	-	87.070(2)
V/Å ³	2817.92(10)	2388.72(15)
Z	4	4
Temperature/K	150	150
D _{calc} /gcm ⁻³	1.373	1.408
F ₍₀₀₀₎	1216	1056
μ /mm ⁻¹	0.224	0.252
Crystal dimensions/mm	0.34 x 0.34 x 0.28	0.24 x 0.22 x 0.16
Index ranges	<i>h</i> , -13-13; <i>k</i> , -14-15; <i>l</i> , -30-30	<i>h</i> , -12-12; <i>k</i> , -20-20; <i>l</i> , -20-21
Max. and min. transmission	0.922 to 0.939	0.942 to 0.961
Refinement method	Full matrix on F ²	Full matrix on F ²
Reflections collected/unique	21343/6448	26371/10888
Data/parameters	4537/370	7181/631
Goodness of fit	1.04	1.02
Final <i>R</i> indices (I>2 σ (I))	0.046 (R ₁), 0.106 (R _w)	0.046 (R ₁), 0.103 (R _w)
Density range in final diff. map/eÅ ³	-0.42, +0.41	-0.47, +0.29

Compound **169** crystallizes in the triclinic space group P₁ with four independent molecules per asymmetric unit. The range of the phenyl C-C bond distances is 1.361(3) to 1.393(3) Å (mean 1.375(3) Å). The sulphonyl S=O distances S(1A)-O(2A) 1.430(14) and S(1A)-O(3A) 1.434(15) Å and S(1B)-O(2B) 1.431(16) and S(1B)-O(3B) 1.434(16) Å compare with the literature values.³² The F-C-C bond angles range from 117.8(2)° to 118.8(2)° in molecule A and 118.0(2)° to 118.2(2)° in molecule B. The amide C(O)-N distances C(1A)-N(1A) 1.343(3) Å and C(1B)-N(1B) 1.342(3) Å and sulphonamide S(O)-N distances S(1A)-N(2A) 1.614(17) Å and S(1B)-N(2B) 1.620(19) Å exhibit a lot of single

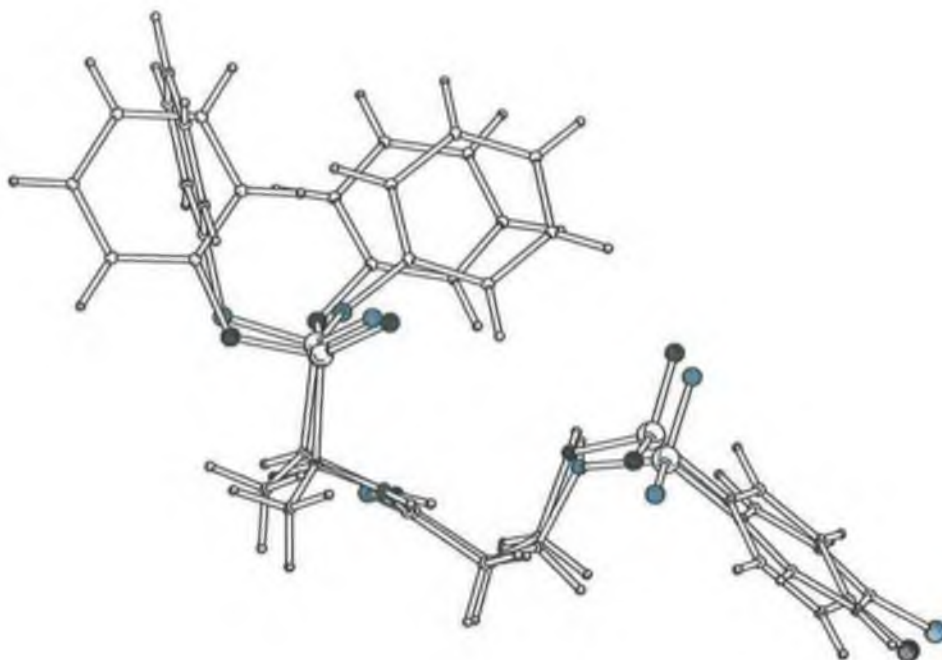


Figure 4.7 PLATON drawing of the X-ray crystal structure of *N*-4-fluorobenzenesulphonyl- γ -aminobutyric acid-(D, L)-phenylglycine^p diphenyl ester **164** depicting the best fit between the two molecules in **164**.

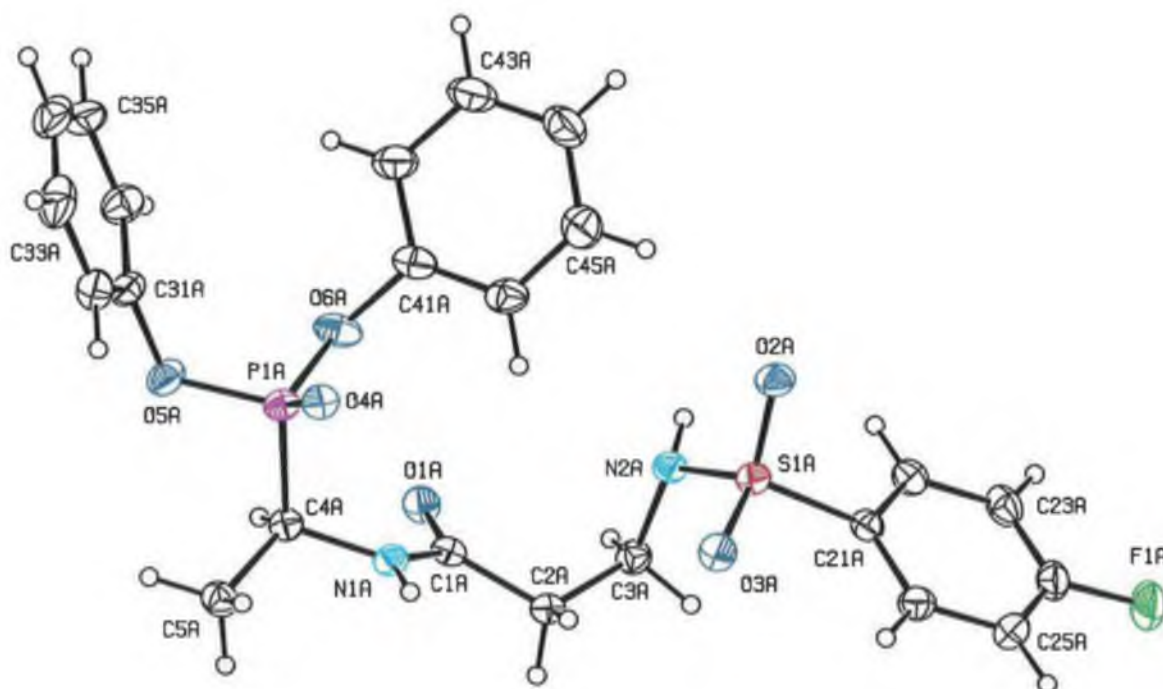


Figure 4.8 ORTEP view of the X-ray crystal structure of *N*-4-fluorobenzenesulphonyl- β -alanine-(D, L)-alanine^p diphenyl ester **169**.

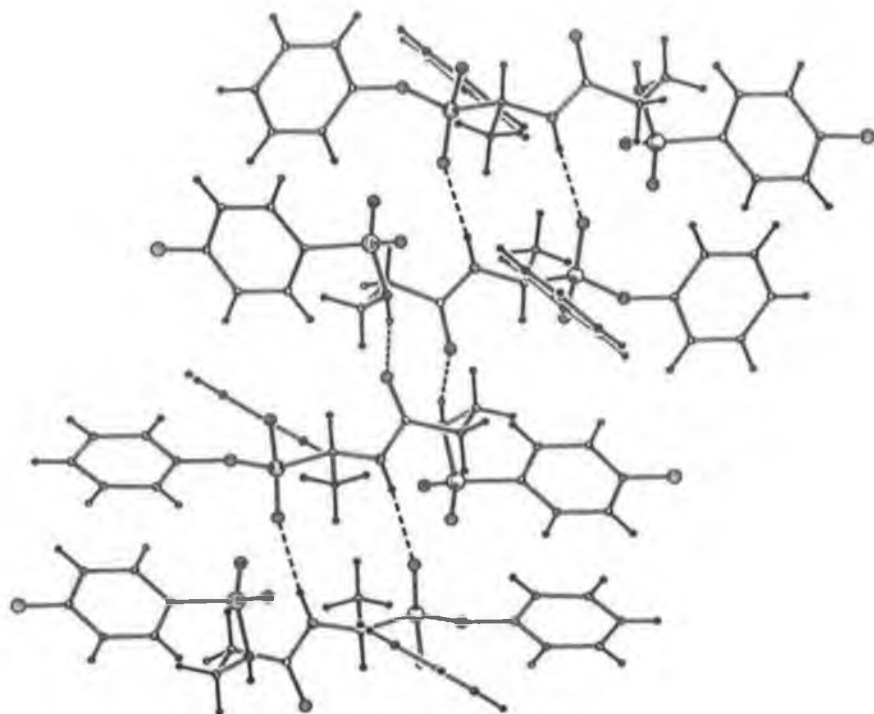


Figure 4.9 PLATON drawing of the X-ray crystal structure of *N*-4-fluorobenzenesulphonyl- β -alanine-(D, L)-alanine^p diphenyl ester **169** depicting the intermolecular interactions.

According to the Cambridge Crystal Structure Database Version 5.25 April 2004 there are only fifteen examples of diphenyl phosphonate esters reported. The average distance of the P=O bond in these derivatives is 1.460 Å which compares favourably with the values of 1.463 Å and 1.465 Å for compounds **164** and **169** respectively. The average angle between the phosphonate double bond and the phenoxy moiety of these fifteen derivatives is reported as 122.66°. Compound **164** and **169** have similar angles of 116.4° and 115.3° respectively. The difference in these angles is probably due to steric effects caused by the peptidyl nature of phosphonate esters **164** and **169**. At present there are only four crystal structures containing the 4-fluorobenzenesulphonamide moiety reported. The average sulphonamide bond distance is 1.633 Å. This is compared to values of 1.608 Å for compound **164** and 1.614 Å for compound **169**. The average sulphonamide (O)-(S)-(N) bond angle has recorded as 106.45°. This corresponds to the value of 106.44° for compound **164** and 106.67° for compound **169**.

There is only one example of a crystal structure of a dipeptidyl diphenyl phosphonate ester previously described.³³ This isoleucyl-proline derivative has an amide bond distance of 1.345 Å and a (O)-(C)-(N) amide bond angle of 122.92°. These values are very close to the values obtained for compounds **164** and **169**.

Compound **183** crystallizes in the monoclinic space group $P2_1/n$ with four independent molecules per asymmetric unit. The range of the phenyl C-C bond distances is 1.369(4) to 1.389(3) Å (mean 1.380(3) Å). The phosphonate P=O distance is 1.461(13) Å. The F-C-C bond angles range from 110.2(2)° to 114.32(19)°. The amide C(O)-N distances C(1)-N(1) 1.341(2) Å and C(4)-N(2) 1.329(3) Å exhibit a lot of single bond character. The principle interactions in **183** involve the amide N-H and carbonyl groups of neighbouring residues interacting as N-H...O=C and forming a one-dimensional chain. There is also an intermolecular hydrogen bond formed between the phosphonate P=O and the amide N-H (Figure 4.10).

Table 4.10 Crystal data and structure refinement for *N*-trifluoroacetyl- β -alanine-(D, L)-phenylalanine^p diphenyl ester **183** and *N*-trifluoroacetyl-glycine-(D, L)-alanine^p diphenyl ester **184**

	183	184
Empirical formula	C ₂₅ H ₂₄ N ₂ O ₅ F ₃ P ₁	C ₁₈ H ₁₈ N ₂ O ₅ F ₃ P ₁
M _r	520.43	430.31
Crystal color	Colorless, block	Colorless, block
Crystal System	Monoclinic	Triclinic
Space group	P2 ₁ /n	P ₁
a/Å	12.2319(5)	10.1264(8)
b/Å	10.3096(4)	11.6424(8)
c/Å	20.2734(5)	17.5757(16)
α /°	-	80.166(5)
β /°	102.685(2)	81.012(4)
γ /°	-	88.841(5)
V/Å ³	2494.20(15)	2016.5(3)
Z	4	4
Temperature/K	150	150
D _{calc} /gcm ⁻³	1.386	1.417
F ₍₀₀₀₎	1080	888
μ /mm ⁻¹	0.171	0.195
Crystal dimensions/mm	0.20 x 0.18 x 0.10	0.26 x 0.26 x 0.10
Index ranges	<i>h</i> , -15-15; <i>k</i> , -13-13; <i>l</i> , -26-26	<i>h</i> , -12-13; <i>k</i> , -15-15; <i>l</i> , -22-22
Max. and min. transmission	0.967 to 0.983	0.951 to 0.981
Refinement method	Full matrix on F ²	Full matrix on F ²
Reflections collected/unique	23370/5717	19628/9096
Data/parameters	3615/333	4846/570
Goodness of fit	1.02	1.03
Final <i>R</i> indices (<i>I</i> >2 σ (<i>I</i>))	0.049 (<i>R</i> ₁), 0.108 (<i>R</i> _w)	0.068 (<i>R</i> ₁), 0.161 (<i>R</i> _w)
Density range in final diff. map/eÅ ³	-0.39, +0.22	-0.47, +0.40

Compound **184** crystallizes in the triclinic space group P_1 with four independent molecules per asymmetric unit and the molecular structure with atomic numbering is depicted in Figure 4.12. The range of the phenyl C-C bond distances is 1.371(5) to 1.388(5) Å (mean 1.380(5) Å). The phosphonate P=O distances P(1A)-O(3A) 1.468(2) Å and P(1B)-O(3B) 1.465(3) Å compare favourably with literature values.³³ The F-C-C bond angles range from 110.6(3)° to 113.40(3)° in molecule A but from 110.2(8)° to 117.20(15)° in molecule B. Refinement has shown that there is disorder associated with molecule B in **184**. The trifluoromethyl group is disordered over two sites which differ in their orientation with respect to the amide moiety and with site occupancy factors subsequently fixed at 50%. The amide C(O)-N distances C(1A)-N(1A) 1.325(4) Å, C(3A)-N(2A) 1.335(5) Å, C(1B)-N(1B) 1.320(5) Å and C(3B)-N(2B) 1.321(5) Å exhibit a lot of single bond character. The principle interactions in **184** involve the amide N-H and carbonyl groups of neighbouring residues interacting as N-H...O=C and forming a one-dimensional chain. There is also an intermolecular hydrogen bond formed between the phosphonate P=O and the amide N-H (Figure 4.13).

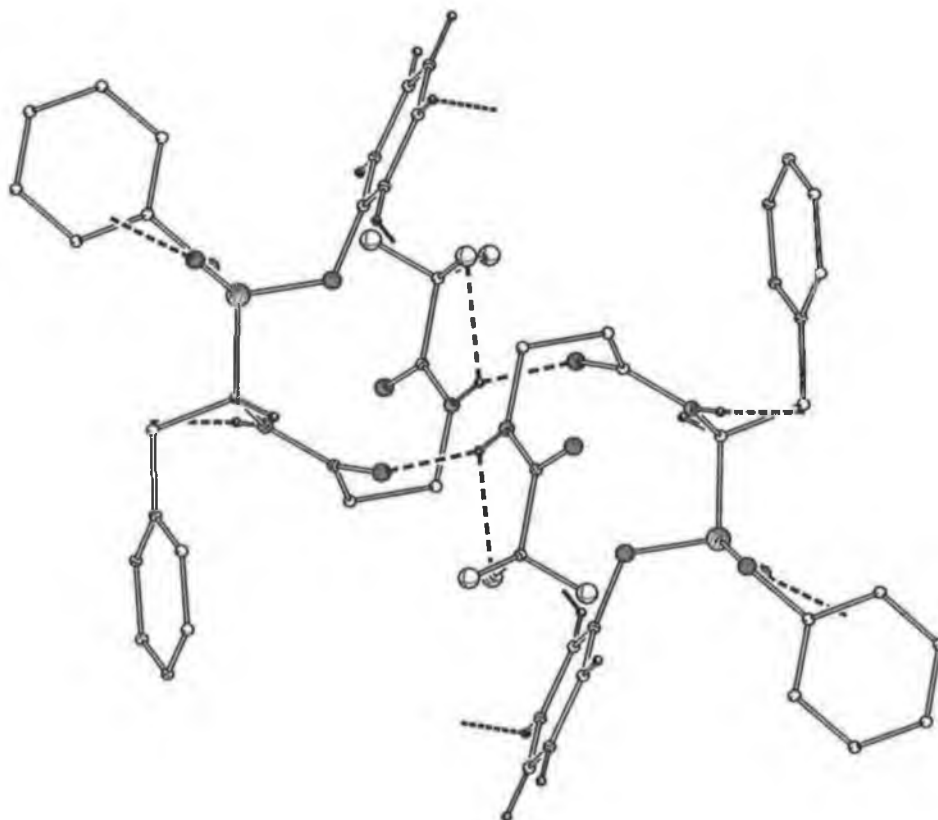


Figure 4.10 PLATON drawing of the X-ray crystal structure of *N*-trifluoroacetyl- β -alanine-(D, L)-phenylalanine^p diphenyl ester **183** depicting the intermolecular interactions.

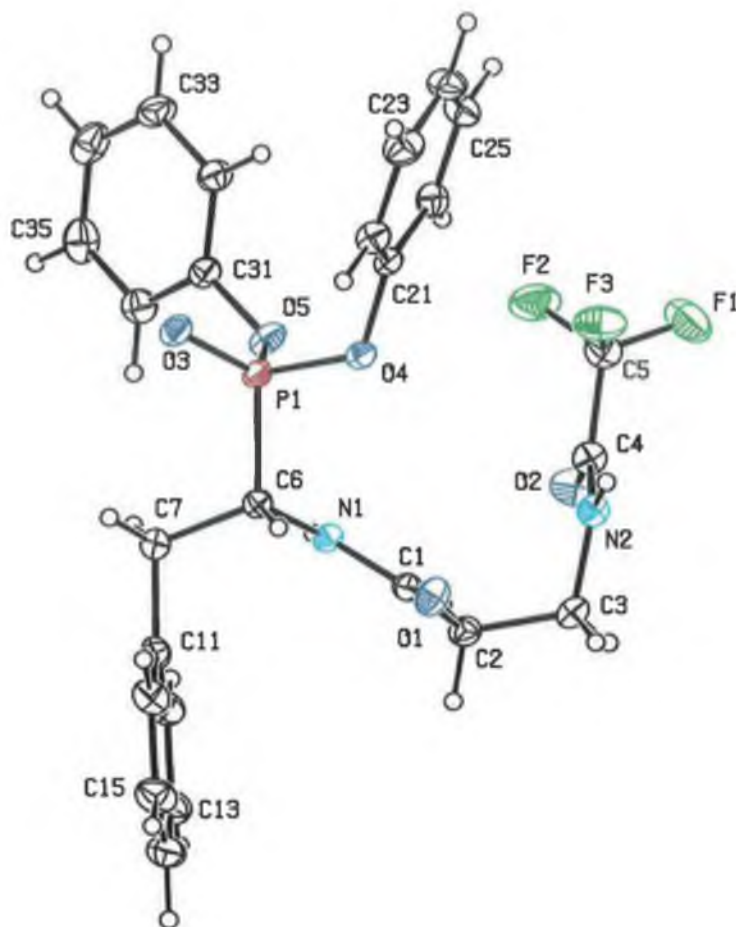


Figure 4.11 ORTEP view of the X-ray crystal structure of *N*-trifluoroacetyl- β -alanine-(D, L)-phenylalanine^P diphenyl ester **183**.

Table 4.11 Selected bond distances (Å) and angles (°) for **183** and **184** with estimated standard deviations.

	183		184	
(a) Bond distances	A	A	B	
P(1)-O(3)	1.461(14)	1.468(2)	1.465(3)	
P(1)-O(4)	1.584(15)	1.577(2)	1.575(3)	
O(1)-C(1)	1.234(2)	1.241(4)	1.230(4)	
N(1)-C(1)	1.341(2)	1.325(4)	1.320(5)	
C(4/3)-N(2)	1.329(3)	1.335(5)	1.321(5)	
C(5/4)-F(1)	1.333(3)	1.321(5)	1.306(8)	
(b) Bond angles				
O(2)-C(4/3)-N(2)	122.60(2)	126.60(3)	126.10(4)	
F(1)-C(5/4)-C(4/3)	111.10(4)	111.90(3)	114.30(5)	
O(1)-C(1)-N(1)	122.28(19)	123.60(3)	123.70(4)	
O(3)-P(1)-O(4)	115.19(9)	114.81(14)	114.75(16)	
P(1)-O(5)-C(31/21)	124.57(13)	120.70(2)	123.20(2)	

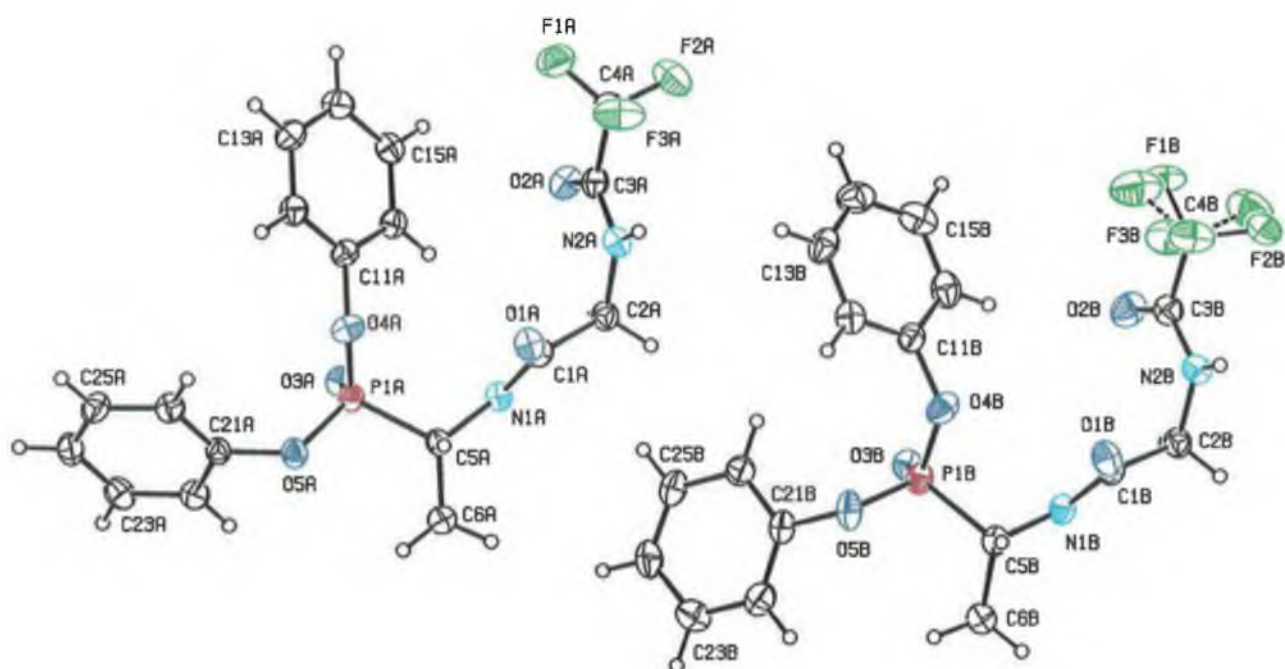


Figure 4.12 ORTEP view of the X-ray crystal structure of *N*-trifluoroacetyl-glycine-(D, L)-alanine^p diphenyl ester **184** showing both molecules present in **184**.

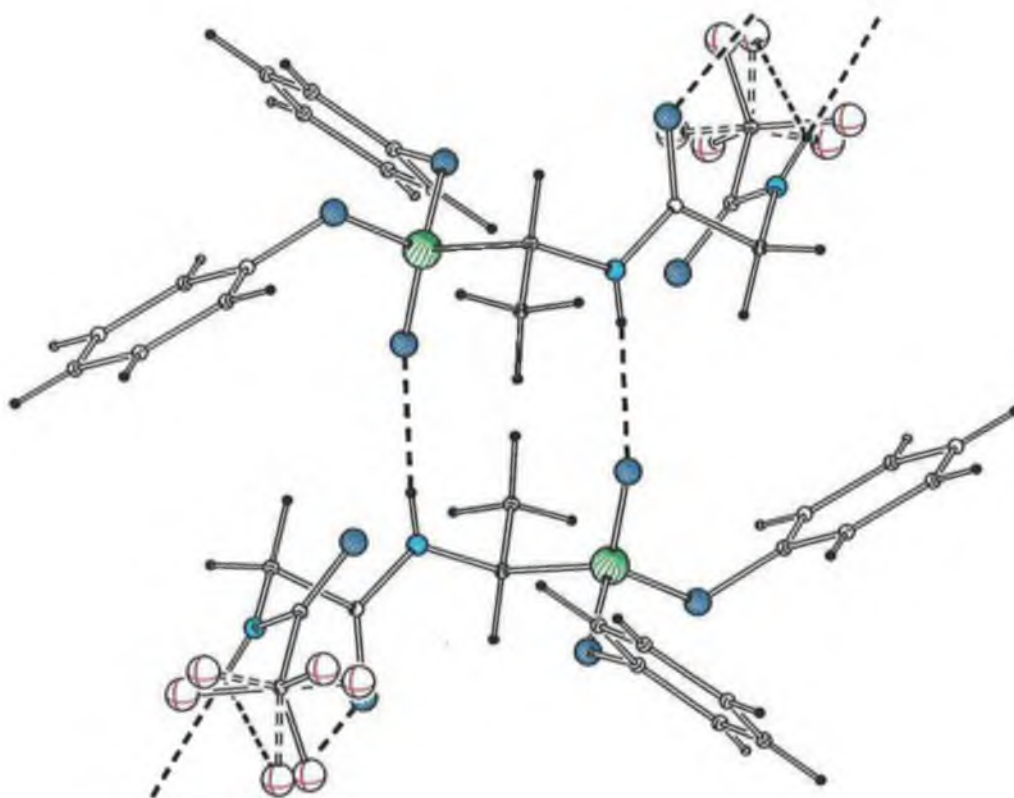


Figure 4.13 PLATON drawing of the X-ray crystal structure of *N*-trifluoroacetyl-glycine-(D, L)-alanine^p diphenyl ester **184** depicting the intermolecular interactions between pairs of B molecules in **184**.

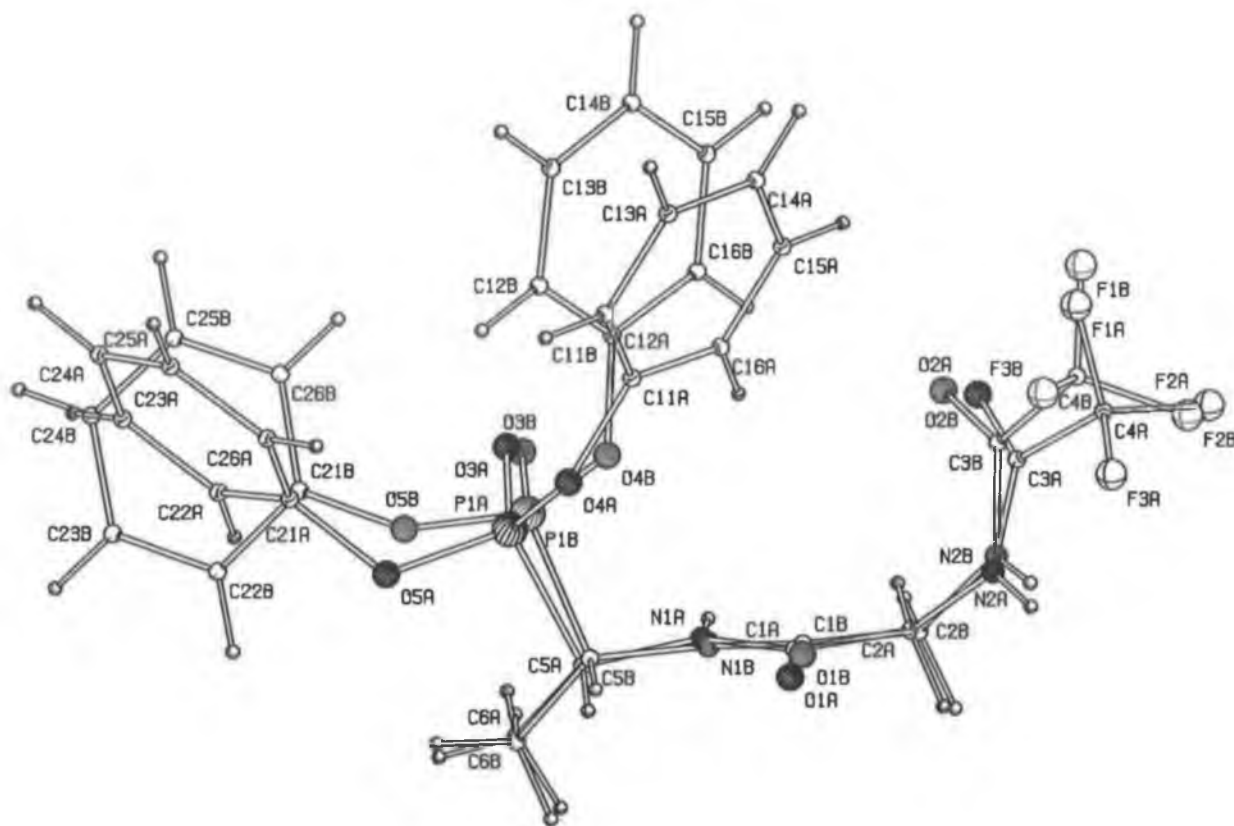


Figure 4.14 Platon drawing of the X-ray crystal structure of *N*-trifluoroacetyl-glycine-(*D, L*)-alanine^p diphenyl ester **184** depicting the best fit between the two molecules in **184**.

The X-ray crystal structure of compounds **183** and **184** relate favourably to the previously described diphenyl phosphonate esters and their dipeptidyl analogues. The Cambridge Crystal Structure Database Version 5.25 April 2004 shows that there are one hundred and thirty one examples of a trifluoroacetamide bond reported. The average bond length of the amide is shown to be 1.329 Å with the bond angle of the amide (O)-(C)-(N) given as 126.12°. Structure **183** has a corresponding bond length of 1.329 Å with a (O)-(C)-(N) bond angle of 122.6°. The average length of the bond between the fluorine atom and the carbon atom in the trifluoromethyl group is 1.315 Å. This value compares with a value of 1.321 Å for structure **184**. Finally the average bond angle between the fluorine atom, the carbon of the trifluoromethyl group and the carbonyl moiety is 111.83°. Compounds **183** and **184** have similar bond angles of 111.10° and 111.90° respectively. The study of the dipeptidyl phosphonate esters show that the structure of these compounds is very similar to previously described structures.

4.5 Protease inhibitory activity of dipeptidyl phosphonate esters

4.5.1 Introduction

Serine proteases have been implicated in a variety of diseases including rheumatoid arthritis, tumour metastasis and neurodegenerative diseases.¹ They are characterised by the presence of the catalytic triad of Asp-His-Ser in the active site. Chymotrypsin-like proteases are the most abundant serine proteases found in nature. They have been shown to be involved in pathological processes such as digestion, apoptosis and immune response.³⁴

Peptidyl phosphonates have been described as potent irreversible inhibitors of serine proteases. They function as transition state analogues whereby the electrophilic phosphorus centre undergoes attack by the active site serine hydroxyl group to give a pentacoordinate intermediate. The loss of a phenoxy and a phenyl group gives a tetrahedral geometry with one of the phosphonate oxygens extended into the oxyanion hole. The inhibitory potency of the synthesised dipeptidyl phosphonates was assessed against α -chymotrypsin due to its use as a model target enzyme for the development of design strategies that can be applied for other serine proteases of pharmacological interest.

4.5.2 Assay to determine the inhibitory potency of dipeptidyl phosphonate esters on bovine pancrease α -chymotrypsin serine protease

A standard ultraviolet assay has been developed using an ultraviolet active substrate to test the activity of these compounds. In this assay activity was determined by measuring the release of the ultraviolet species 4-nitroaniline from the substrate *N*-succinyl-L-Phe-*p*-nitroanilide upon enzymatic hydrolysis by bovine pancrease α -chymotrypsin serine protease purchased from Sigma-Aldrich. The absorbance increase at 405 nm is proportional to chymotrypsin activity. The α -chymotrypsin used was diluted with 1 mM HCl to activate the enzyme. Assays were carried out using a final concentration of 10 μ M substrate in 0.1 M Tris-HCl/20 mM CaCl₂ buffer pH 8.0. The mixture of enzyme and inhibitor were incubated together at 25 °C for 15 mins. The substrate was then added and the mixture was further incubated for 30 mins. The amount of 4-nitroaniline released was measured using an ICN flow multiscan plus MKII titretrek reader with absorbance at 405 nm. The positive control contained only the enzyme extract and the substrate *N*-succinyl-L-Phe-*p*-nitroanilide. This positive control corresponded to 100% inhibition. There were two negative controls used. One contained the enzyme and inhibitor and the other contained just the inhibitor and the substrate. All assays were performed in triplicate with the mean result being taken.

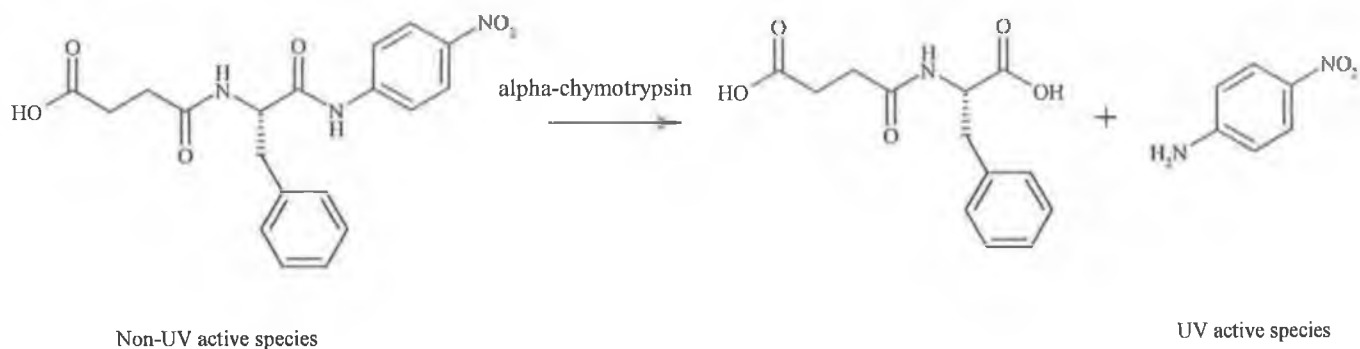


Figure 4.15 Hydrolysis of *N*-succinyl-L-Phe-*p*-nitroanilide by bovine pancreas α -chymotrypsin serine protease with liberation of the ultraviolet species *p*-nitroaniline.

4.5.3 Protease inhibition of the *N*-4-fluorobenzenesulphonyl dipeptidyl phosphonate ester derivatives

Sulphonamide derivatives have been shown to be potent inhibitors of various proteases.³⁵ The geometry and the additional hydrogen bonding properties of the sulphonyl moiety often leads to superior inhibitory potency in contrast to their carbonyl analogues. The presence of a bulky aromatic substituent such as the phenyl ring bonded to the sulphonyl group has been shown to improve activity.³⁶ The introduction of a fluorine atom into a molecule has distinct effects on its physicochemical properties such as lipophilicity and the influence of fluorine substitution on the biological stability of a drug molecule through altering susceptibility to metabolism.³⁷ Scozzafava *et al* have developed a hypothesis that puts forward the possibility that F-H hydrogen bonds between the inhibitor and the active site residues of the protease contribute in stabilizing the enzyme-inhibitor adduct.²⁴

The most potent 4-fluorobenzenesulphonyl inhibitor of bovine pancreas α -chymotrypsin was compound **165**. This compound was shown to have an IC_{50} value of 16.15 μ M. At a concentration of 100 μ M 86.41% inhibition was recorded. The specificity of α -chymotrypsin for an aromatic group in the P1 position is well documented.³ From this study it is very clear that the phenylalanine derivatives are by far the most potent compounds. Surprisingly the phenylglycine derivatives with their aromatic side chain do not show great inhibitory potencies against α -chymotrypsin. The most potent phenylglycine derivative **164** recorded an IC_{50} value of 76.75 μ M. The phenylalanine analogues have inhibitory potencies up to 2-fold greater than the phenylglycine compounds. This shows that the inclusion of a spacer group such as a methylene is crucial for effective inhibition. The alanine derivatives give somewhat expected results. At a concentration of 100 μ M each of the alanyl derivatives fail to achieve greater inhibition than 28%.

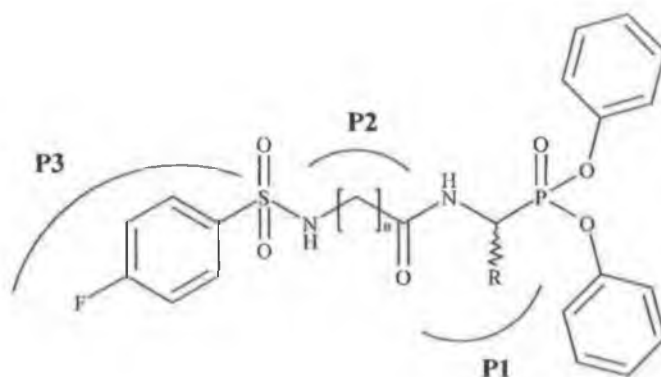


Table 4.12 Inhibitory activity of *N*-4-fluorobenzenesulphonyl dipeptidyl phosphonate ester derivatives

Compound	% Protease Inhibition			
	10 μ M	50 μ M	100 μ M	IC ₅₀ μ M
162	12.90	38.16	41.09	> 100
163	19.31	37.25	47.22	> 100
164	30.60	45.69	51.66	76.75
165	33.23	81.60	86.41	16.15
166	26.84	73.16	83.01	25.76
167	20.82	74.94	83.19	26.73
168	19.08	17.88	27.58	> 100
169	15.62	20.31	24.91	> 100
170	7.56	14.66	14.89	> 100

The small side chain methyl group of alanine has previously not been shown to fit effectively into the S1 subsite of the α -chymotrypsin active site. The effect of increasing the number of methylene units in the P2 position was achieved by using the amino acids glycine, β -alanine and γ -aminobutyric acid. The phenylalanine and alanine derivatives generally give higher inhibition when there is only one methylene unit present in the P1 position. The phenylglycine derivatives gave superior inhibition when γ -aminobutyric acid was used.

4.5.4 Protease inhibition of the *N*-cinnamoyl dipeptidyl phosphonate ester derivatives

N-cinnamoyl peptidyl derivatives are potent inhibitors of angiotension converting enzyme.³⁸ The cinnamoyl moiety is a potential Michael acceptor and may undergo enzyme attack. The phenyl ring in the cinnamoyl group has been shown to bind with the active site of the enzyme with a preferred conformation involving the phenyl ring being twisted out of

plane of the adjacent olefin.²⁸ This conformation has been shown to improve activity substantially. More rigid conformers such as the coumarinoyl moiety have showed decreased activity.²⁸

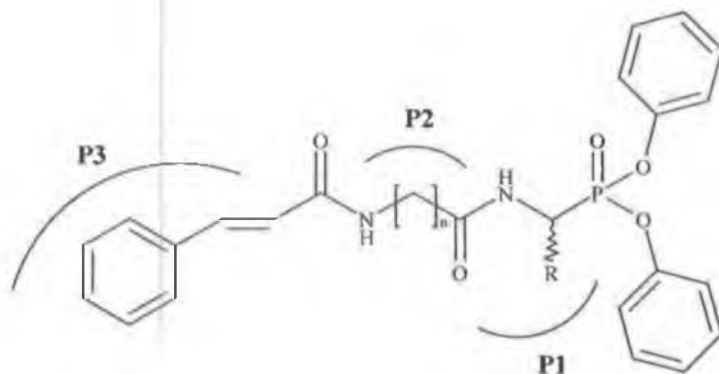


Table 4.13 Inhibitory activity of *N*-cinnamoyl dipeptidyl phosphonate ester derivatives

Compound	% Protease Inhibition			
	10 μ M	50 μ M	100 μ M	IC ₅₀ μ M
171	21.33	49.26	50.71	52.00
172	12.89	21.37	21.89	> 100
173	16.11	16.75	19.57	> 100
174	22.49	81.27	82.36	19.54
175	26.11	58.50	68.99	37.00
176	25.30	49.72	52.75	50.75
177	15.99	23.74	27.76	> 100
178	12.76	14.56	14.99	> 100
179	11.56	15.88	18.27	> 100

The inhibitory potency of the *N*-cinnamoyl dipeptidyl phosphonate esters showed similar results to the 4-fluorobenzenesulphonyl dipeptidyl derivatives. The most active compound was **174** with an IC₅₀ value of 19.54 μ M. The least activity recorded was for compound **178**. At a concentration of 100 μ M a percentage inhibition of just 14.99 was achieved. The phenylalanine derivatives were once again the most potent derivatives. The presence of a benzyl group in the P1 position seems to be the undermining factor in potent inhibition. Once again the phenylglycine derivatives fail to show effective inhibition of α -chymotrypsin. The most potent phenylglycine derivative **171** only records inhibition of 50.71% at the 100 μ M level. The presence of a methyl group in the P1 position reflects very

poor inhibition. The alanine derivatives are probably unable to bind with the S1 subsite of α -chymotrypsin due to the side chain methyl group being extremely short. The presence of a glycine residue in the P2 position has shown the best results. In the case of the phenylglycine derivatives the drug molecules with only one methylene unit are up to three fold more potent than the α -aminobutyric acid analogues.

4.5.5 Protease inhibition of the *N*-trifluoroacetyl dipeptidyl phosphonate ester derivatives

The incorporation of a trifluoroacetyl substituent into a biologically active compound has often improved activity and specificity.³⁹ The trifluoromethyl moiety although very similar sterically to its hydrogen analogue displays distinct properties and is found in various drug compounds such as prozac.⁴⁰ The strongly electron withdrawing trifluoromethyl group causes the amide carbonyl to be increasingly electrophilic and hence the carbon-oxygen bond is more susceptible to enzyme attack. The lipophilic, hydrophilic and hydrogen bonding properties of a molecule are influenced by the introduction of a trifluoroacetyl group.

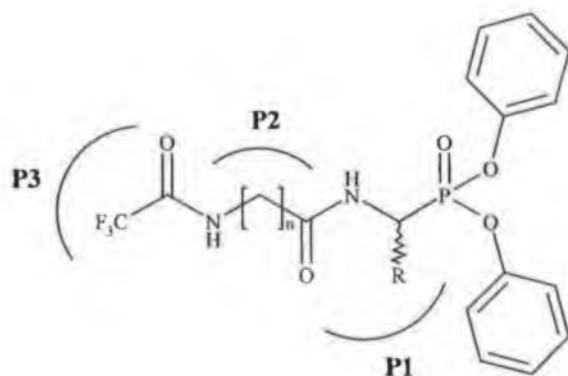


Table 4.14 Inhibitory activity of *N*-trifluoroacetyl dipeptidyl phosphonate ester derivatives

Compound	% Protease Inhibition			
	10 μ M	50 μ M	100 μ M	IC ₅₀ μ M
180	17.80	37.94	55.19	82.38
181	14.53	32.96	44.55	> 100
182	27.06	77.71	89.58	21.15
183	23.61	62.06	79.59	30.67
184	11.56	17.51	16.15	> 100
185	13.24	14.11	18.86	> 100

Due to the unsuccessful synthesis of *N*-trifluoroacetyl- γ -aminobutyric acid we were unable to assess the biological activity of compounds containing three methylene units in the P2 position. This was not deemed imperative, as previous research had indicated that the GABA derivatives synthesised were generally not very potent inhibitors of α -chymotrypsin. The most potent trifluoroacetyl derivative was found to be compound **182**. *N*-trifluoroacetyl-glycine-phenylalanine^P-(OPh)₂ **182** expresses an IC₅₀ value of 21.15 μ M and inhibits 89.58% of α -chymotrypsin at a concentration of 100 μ M. The phenylglycine derivatives **180** and **181** inhibit α -chymotrypsin but up to 2 fold less than their phenylalanine analogues. The alanyl derivatives once again fail to effectively inhibit α -chymotrypsin at micromolar concentrations. At a concentration of 10 μ M compound **184** only inhibits 11.56% of the available enzyme. The glycine derivatives with their one methylene in the P2 position unit gave substantially greater inhibition than their β -alanine analogues.

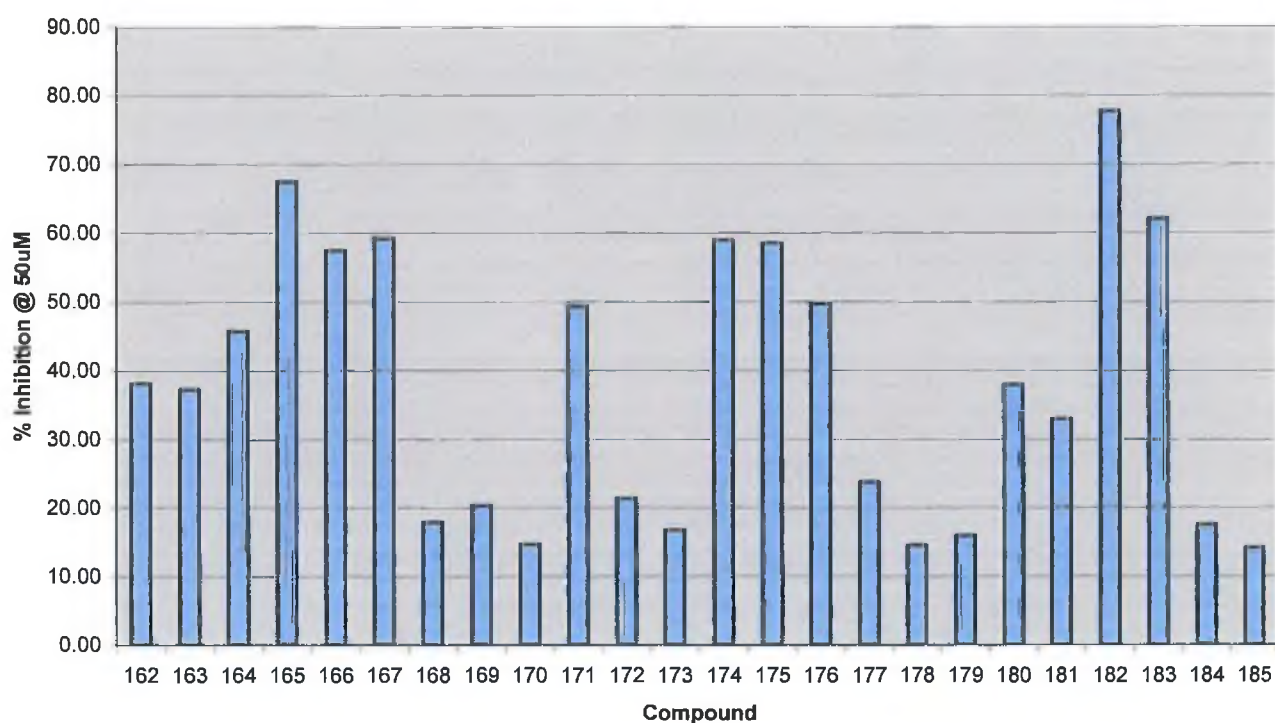


Figure 4.16 Bar graph representing the % inhibition of dipeptidyl phosphonate esters against bovine pancreas α -chymotrypsin at a concentration of 50 μ M.

4.6 Conclusion

We have successfully designed, synthesised and structurally characterized a series of dipeptidyl phosphonate diphenyl esters as potential inhibitors of the serine protease α -chymotrypsin. These derivatives showed varying degrees of biological activity depending on

their amino acid sequence and structure. The most active compound was *N*-4-fluorobenzenesulphonyl-Gly-Phe^P-(OPh)₂ **165** that recorded an IC₅₀ value of 16.15 μM. Three different *N*-terminal substituents were assessed for their effect on the potency of the dipeptidyl derivatives. Concentrating on the most active compounds of each series, it is shown that the 4-fluorobenzenesulphonyl moiety is the most potent *N*-terminal substituent. Compound **165** has an IC₅₀ value of 16.15 μM compared to 19.54 μM for the cinnamoyl derivative **174** and 21.15 μM for the trifluoroacetyl analogue **182**.

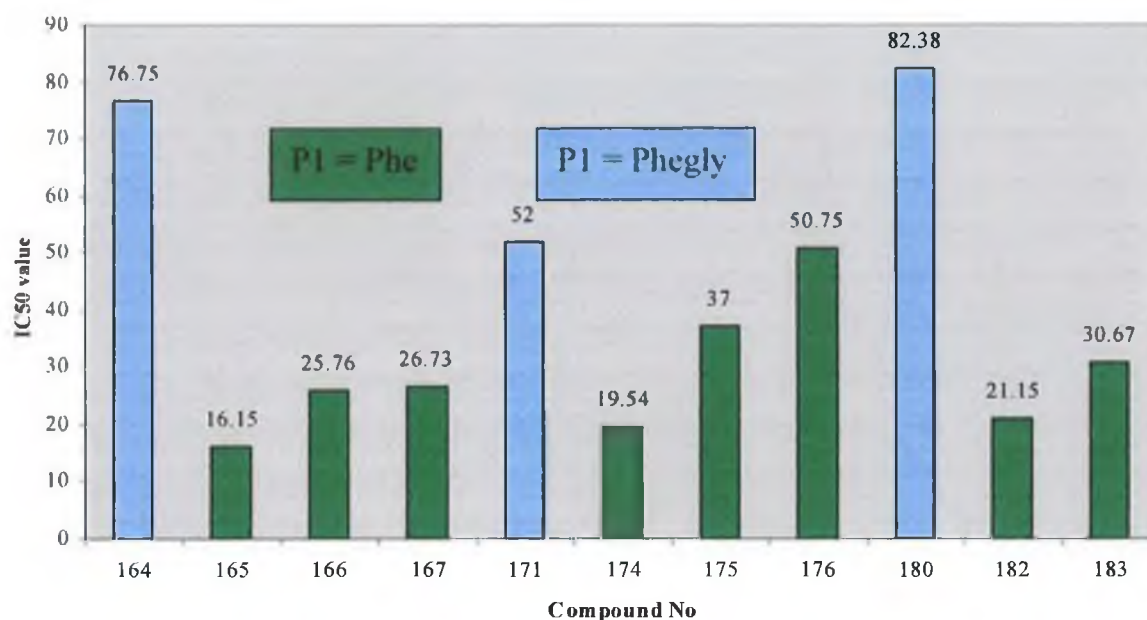


Figure 4.17 Bar chart representing the IC₅₀ values of the most potent dipeptidyl phosphonate esters against bovine pancreas α -chymotrypsin

From this study it is very clear that the most potent dipeptidyl derivatives contain the Gly-Phe^P scaffold. Although the phenylglycine and alanine derivatives do inhibit α -chymotrypsin it is the phenylalanine derivatives that give the most successful results. The specificity of α -chymotrypsin for a phenylalanine unit in the S1 subsite is further demonstrated here. The incorporation of methylene units into the P2 position failed to increase the potency of these derivatives. It was the glycine derivatives with just one methylene unit that showed a higher inhibitory potency.

We have shown that the diphenyl phosphonate ester moiety can be successful as a method for serine protease inhibitor. Although potent inhibition is sequence specific, the inhibition of α -chymotrypsin by unfavourable dipeptidyl arrangements shows that the phosphonate ester moiety has the ability to be a vital ingredient of serine protease inhibitors.

4.7 Experimental

General Procedures.

All chemicals were purchased from Sigma/Aldrich and used as received. When necessary solvents were purified prior to use and stored under nitrogen. Dichloromethane was distilled from CaH₂ and triethylamine was distilled and stored over potassium hydroxide pellets. Commercial grade reagents were used without further purification. Riedel-de Haën silica gel was used for thin layer and column flash chromatography. Melting points were determined using a Griffin melting point apparatus and are uncorrected. Specific rotation [α]_D studies were recorded on a Perkin Elmer 241 polarimeter. Infrared spectra were recorded on a Nicolet 405 FT-IR spectrometer and elemental analysis was carried out by the Microanalytical Laboratory at University College Dublin. Electrospray ionisation mass spectra were recorded on a Bruker Esquire 3000 series LC/MS. NMR spectra were obtained on a Bruker AC 400 NMR spectrometer operating at 400 MHz for ¹H NMR, 376 MHz for ¹⁹F NMR, 161.9 MHz for ³¹P NMR and 100 MHz for ¹³C NMR. The ¹H and ¹³C NMR chemical shifts (ppm) are relative to tetramethylsilane, the ¹⁹F NMR chemical shifts (ppm) are relative to trifluoroacetic acid and the ³¹P NMR chemical shifts are relative to phosphoric acid. All coupling constants (*J*) are in Hertz.

General procedure for the synthesis of dipeptidyl phosphonate esters 162-185

N-4-fluorobenzenesulphonyl-glycine-(D, L)-phenylglycine^P diphenyl ester 162

N-4-fluorobenzenesulphonyl-glycine (1.47 g, 7 mmol), (D, L)-phenylglycine^P diphenyl ester hydrobromide (2.94 g, 7 mmol), triethylamine (0.97 ml) and 1-hydroxybenzotriazole hydrate (0.94 g, 7 mmol) were dissolved in dichloromethane (50 ml). The mixture was cooled to 0 °C, and 1-[3-dimethylaminopropyl]-3-ethyl carbodiimide hydrochloride (EDC) (1.47 g, 7.7 mmol) added. After 30 min. the solution was raised to room temperature and the reaction was allowed to proceed for 8 hrs. The filtrate was washed with 10% citric acid, 10% potassium hydrogen carbonate, water and dried over magnesium sulphate. The solvent was evaporated *in vacuo* and recrystallisation from diethyl ether furnished **162** as a white powder (0.63 g, 29%).

m.p. = 170-172 °C.

Anal. calcd. for C₂₇H₂₄N₂O₆P₁S₁F₁: C, 58.48; H, 4.36; N, 5.05.

Found C, 58.27; H, 4.50; N, 5.04.

Mass Spectrum: [M+Na]⁺ found 577.2.

C₂₇H₂₄N₂O₆P₁S₁F₁Na₁ requires 577.5.

IR (KBr): ν 3261, 3061, 1675, 1590, 1546, 1491, 1155, 940, 691 cm⁻¹.

¹H-NMR (400 MHz, DMSO): δ 9.35 (1H, d, $J = 9.2$ Hz, -NH-), 8.14 (1H, t, $J = 4.4$ Hz, -NH-), 6.90-7.84 (19H, m, -ArH), 5.81 (1H, dd, $J^{\text{H-H}} = 9.6$ Hz, $J^{\text{H-P}} = 21.6$ Hz, α -H), 3.75 (1H, dd, $J^3 = 4.8$ Hz, $J^2 = 16.4$ Hz, -CH₂-), 3.63 (1H, dd, $J^3 = 4.4$ Hz, $J^2 = 16.8$ Hz, -CH₂-).

¹³C-NMR (100 MHz, DMSO): δ 167.9 (d, -CONH-), 164.4 (d, -ArC 4), 150.2 (d, -OPhC 1), 150.0 (d, -OPhC 1), 137.2 (d, -ArC 1), 134.3 (-PhC 1), 130.25 (-OPhC 3), 130.20 (-OPhC 3), 129.8 (-ArC 2), 129.7 (-ArC 6), 128.8 (-PhC 3), 128.7 (-PhC 2), 128.6 (-PhC 4), 125.7 (-OPhC 4), 120.7 (d, -OPhC 2), 120.6 (d, -OPhC 2), 116.9 (-ArC 3), 116.7 (-ArC 5), 49.4 (d, α -C), 45.1 (-CH₂-, -VE DEPT).

¹⁹F-NMR (376 MHz, DMSO): δ -31.6 - -31.7 (m).

³¹P-NMR (161.9 MHz, DMSO): δ 14.83 (d, $J^{\text{P-H}} = 21.5$ Hz).

N*-4-fluorobenzenesulphonyl- β -alanine-(D, L)-phenylglycine^P diphenyl ester **163*

N-4-fluorobenzenesulphonyl- β -alanine (0.90 g, 4 mmol) and (D, L)-phenylglycine^P diphenyl ester hydrobromide (1.68 g, 4 mmol) were used. Recrystallisation from diethyl ether furnished **163** as a white powder (0.77 g, 35%).

m.p. = 138-140 °C.

Anal. calcd. for C₂₈H₂₆N₂O₆P₁S₁F₁: C, 59.15; H, 4.61; N, 4.93.

Found C, 58.85; H, 4.68; N, 4.86.

Mass Spectrum: [M+Na]⁺ found 591.2.

C₂₈H₂₆N₂O₆P₁S₁F₁Na₁ requires 591.5.

IR (KBr): ν 3247, 3058, 1670, 1591, 1542, 1491, 1163, 953, 549 cm⁻¹.

¹H-NMR (400 MHz, DMSO): δ 9.40 (1H, d, $J = 9.2$ Hz, -NH-), 6.93-7.87 (20H, m, -ArH & -NH-), 5.93 (1H, dd, $J^{\text{H-H}} = 10.0$ Hz, $J^{\text{H-P}} = 22.0$ Hz, α -H), 2.92-2.98 (2H, m, β -CH₂), 2.47 (2H, t, $J = 7.2$ Hz, α -CH₂).

¹³C-NMR (100 MHz, DMSO): δ 170.1 (-CONH-), 164.4 (d, -ArC 4), 150.3 (d, -OPhC 1), 150.0 (d, -OPhC 1), 136.8 (d, -ArC 1), 134.6 (-PhC 1), 130.2 (-OPhC 3), 130.1 (-OPhC 3), 129.9 (-ArC 2), 129.8 (-ArC 6), 128.9 (-PhC 3), 128.8 (-PhC 2), 128.5 (-PhC 4), 125.7 (-OPhC 4), 125.6 (-OPhC 4), 120.7 (t, -OPhC 2), 116.8 (-ArC 3), 116.6 (-ArC 5), 50.3 (d, α -C), 39.2 (β -CH₂, -VE DEPT), 35.5 (α -CH₂, -VE DEPT).

¹⁹F-NMR (376 MHz, DMSO): δ -31.5 - -31.6 (m).

³¹P-NMR (161.9 MHz, DMSO): δ 15.12 (d, $J^{\text{P-H}} = 21.9$ Hz).

***N*-4-fluorobenzenesulphonyl- γ -aminobutyric acid-(D, L)-phenylglycine^P diphenyl ester**

164

N-4-fluorobenzenesulphonyl- γ -aminobutyric acid (0.93 g, 4 mmol) and (D, L)-phenylglycine^P diphenyl ester hydrobromide (1.68 g, 4 mmol) were used. Recrystallisation from diethyl ether furnished **164** as a white powder (0.64 g, 29%).

m.p. = 158-160 °C.

Anal. calcd. for C₂₉H₂₈N₂O₆P₁S₁F₁: C, 59.79; H, 4.84; N, 4.81.

Found C, 59.81; H, 4.87; N, 4.71.

Mass Spectrum: [M+Na]⁺ found 605.2.

C₂₉H₂₈N₂O₆P₁S₁F₁Na₁ requires 605.5.

IR (KBr): ν 3266, 3069, 1648, 1591, 1545, 1491, 1165, 958, 763 cm⁻¹.

¹H-NMR (400 MHz, DMSO): δ 9.33 (1H, d, J = 9.2 Hz, -NH-), 6.91-7.83 (20H, m, -ArH & -NH-), 5.92 (1H, dd, $J^{\text{H-H}}$ = 9.6 Hz, $J^{\text{H-P}}$ = 22.0 Hz, α -H), 2.71-2.76 (2H, m, γ -CH₂), 2.27 (2H, t, J = 7.6 Hz, α -CH₂), 1.60-1.66 (2H, m, β -CH₂).

¹³C-NMR (100 MHz, DMSO): δ 171.9 (-CONH-), 164.4 (d, -ArC 4), 150.3 (d, -OPhC 1), 150.0 (d, -OPhC 1), 137.1 (d, -ArC 1), 134.7 (-PhC 1), 130.2 (-OPhC 3), 130.2 (-OPhC 3), 129.8 (-ArC 2), 129.7 (-ArC 6), 128.86 (-PhC 3), 128.8 (-PhC 2), 128.5 (-PhC 4), 125.7 (-OPhC 4), 120.6 (t, -OPhC 2), 116.7 (-ArC 3), 116.5 (-ArC 5), 50.2 (d, α -C), 42.4 (γ -CH₂, -VE DEPT), 32.4 (α -CH₂, -VE DEPT), 25.6 (β -CH₂, -VE DEPT).

¹⁹F-NMR (376 MHz, DMSO): δ -31.7 - -31.8 (m).

³¹P-NMR (161.9 MHz, DMSO): δ 15.35 (d, $J^{\text{P-H}}$ = 21.9 Hz).

***N*-4-fluorobenzenesulphonyl-glycine-(D, L)-phenylalanine^P diphenyl ester 165**

N-4-fluorobenzenesulphonyl-glycine (0.84 g, 4 mmol) and (D, L)-phenylalanine^P diphenyl ester hydrobromide (1.74 g, 4 mmol) were used. Recrystallisation from diethyl ether furnished **165** as a white powder (0.99 g, 45%).

m.p. = 152-154 °C.

Anal. calcd. for C₂₈H₂₆N₂O₆P₁S₁F₁: C, 59.15; H, 4.61; N, 4.93.

Found C, 58.89; H, 4.31; N, 4.54.

Mass Spectrum: [M+Na]⁺ found 591.2.

C₂₈H₂₆N₂O₆P₁S₁F₁Na₁ requires 591.5.

IR (KBr): ν 3262, 3079, 1664, 1592, 1545, 1491, 1151, 939, 771 cm⁻¹.

¹H-NMR (400 MHz, DMSO): δ 8.74 (1H, d, *J* = 9.6 Hz, -NH-), 8.04 (1H, t, *J* = 6.0 Hz, -NH-), 7.32-7.53 (19H, m, -ArH), 4.72-4.82 (1H, m, α-H), 3.36-3.50 (2H, m, -CH₂-), 3.25-3.30 (1H, m, -CH₂Ph), 2.92-3.00 (1H, m, -CH₂Ph).

¹³C-NMR (100 MHz, DMSO): δ 167.7 (d, -CONH-), 164.4 (d, -ArC 4), 150.2 (d, -OPhC 1), 150.0 (d, -OPhC 1), 137.1 (d, -PhC 1), 137.0 (-ArC 1), 130.3 (-OPhC 3), 130.2 (-OPhC 3), 129.9 (-ArC 2), 129.8 (-ArC 6), 129.4 (-PhC 3), 128.6 (d, -PhC 2), 127.0 (-PhC 4), 125.8 (-OPhC 4), 125.7 (-OPhC 4), 121.0 (d, -OPhC 2), 120.8 (d, -OPhC 2), 116.5 (-ArC 3), 116.3 (-ArC 5), 47.7 (d, α-C), 44.9 (-CH₂-, -VE DEPT), 34.7 (d, -CH₂Ph, -VE DEPT).

¹⁹F-NMR (376 MHz, DMSO): δ -31.7 - -31.8 (m).

³¹P-NMR (161.9 MHz, DMSO): δ 17.65 (t, *J*^{P-H} = 7.4 Hz).

***N*-4-fluorobenzenesulphonyl-β-alanine-(D, L)-phenylalanine^P diphenyl ester 166**

N-4-fluorobenzenesulphonyl-β-alanine (0.90 g, 4 mmol) and (D, L)-phenylalanine^P diphenyl ester hydrobromide (1.74 g, 4 mmol) were used. Recrystallisation from diethyl ether furnished **166** as a white powder (0.81 g, 36%).

m.p. = 107-109 °C.

Anal. calcd. for C₂₉H₂₈N₂O₆P₁S₁F₁: C, 59.78; H, 4.85; N, 4.81.

Found C, 60.00; H, 4.87; N, 4.57.

Mass Spectrum: [M+Na]⁺ found 605.2.

C₂₉H₂₈N₂O₆P₁S₁F₁Na₁ requires 605.5.

IR (KBr): ν 3285, 3068, 1670, 1592, 1546, 1490, 1167, 932, 687 cm⁻¹.

¹H-NMR (400 MHz, DMSO): δ 8.73 (1H, d, *J* = 9.6 Hz, -NH-), 7.15-7.85 (20H, m, -ArH & -NH-), 4.71-4.81 (1H, m, α-H), 3.26-3.31 (1H, m, -CH₂Ph), 2.92-3.01 (1H, m, -CH₂Ph), 2.69 (2H, q, *J* = 7.2 Hz, β-CH₂), 2.16-2.22 (2H, m, α-CH₂).

¹³C-NMR (100 MHz, DMSO): δ 169.8 (d, -CONH-), 164.4 (d, -ArC 4), 150.4 (d, -OPhC 1), 150.1 (d, -OPhC 1), 137.1 (d, -PhC 1), 136.7 (d, -ArC 1), 130.3 (-OPhC 3), 130.1 (-OPhC 3), 129.9 (-ArC 2), 129.8 (-ArC 6), 129.4 (-PhC 3), 128.5 (-PhC 2), 126.9 (-PhC 4), 125.7 (-OPhC 4), 125.6 (-OPhC 4), 120.9 (d, -OPhC 2), 120.6 (d, -OPhC 2), 116.8 (-ArC 3), 116.6 (-ArC 5), 47.4 (d, α-C), 39.2 (β-CH₂, -VE DEPT), 35.6 (α-CH₂, -VE DEPT), 34.7 (-CH₂Ph, -VE DEPT).

¹⁹F-NMR (376 MHz, DMSO): δ -31.5 - -31.7 (m)

³¹P-NMR (161.9 MHz, DMSO): δ 17.81 (t, *J*^{P-H} = 7.2 Hz).

***N*-4-fluorobenzenesulphonyl- γ -aminobutyric acid-(D, L)-phenylalanine^P diphenyl ester
167**

N-4-fluorobenzenesulphonyl- γ -aminobutyric acid (0.95 g, 4 mmol) and (D, L)-phenylalanine^P diphenyl ester hydrobromide (1.74 g, 4 mmol) were used. Recrystallisation from diethyl ether furnished **167** as a white powder (0.76 g, 33%).

m.p. = 128-130 °C.

Anal. calcd. for C₃₀H₃₀N₂O₆P₁S₁F₁: C, 60.40; H, 5.07; N, 4.70.

Found C, 60.10; H, 4.95; N, 4.50.

Mass Spectrum: [M+Na]⁺ found 619.3.

C₃₀H₃₀N₂O₆P₁S₁F₁Na₁ requires 619.5.

IR (KBr): ν 3264, 3068, 1664, 1592, 1490, 1153, 946, 768 cm⁻¹.

¹H-NMR (400 MHz, DMSO): δ 8.58 (1H, d, J = 9.2 Hz, -NH-), 7.16-7.82 (20H, m, -ArH & -NH-), 4.81-4.86 (1H, m, α -H), 3.27-3.30 (1H, m, -CH₂Ph), 2.96-3.01 (1H, m, -CH₂Ph), 2.58-2.62 (2H, m, γ -CH₂), 2.02 (2H, t, J = 6.4 Hz, α -CH₂), 1.46-1.50 (2H, m, β -CH₂).

¹³C-NMR (100 MHz, DMSO): δ 171.7 (d, -CONH-), 164.4 (d, -ArC 4), 150.4 (d, -OPhC 1), 150.1 (d, -OPhC 1), 137.3 (d, -PhC 1), 137.1 (d, -ArC 1), 130.28 (-OPhC 3), 130.21 (-OPhC 3), 129.7 (-ArC 2), 129.6 (-ArC 6), 129.3 (-PhC 3), 128.4 (-PhC 2), 126.9 (-PhC 4), 125.7 (-OPhC 4), 125.6 (-OPhC 4), 121.0 (d, -OPhC 2), 120.7 (d, -OPhC 2), 116.7 (-ArC 3), 116.5 (-ArC 5), 47.3 (d, α -C), 42.3 (γ -CH₂, -VE DEPT), 34.6 (-CH₂Ph, -VE DEPT), 32.5 (α -CH₂, -VE DEPT), 25.5 (β -CH₂, -VE DEPT).

¹⁹F-NMR (376 MHz, DMSO): δ -31.7 - -31.9 (m).

³¹P-NMR (161.9 MHz, DMSO): δ 18.24 (t, J^{P-H} = 7.6 Hz).

***N*-4-fluorobenzenesulphonyl-glycine-(D, L)-alanine^P diphenyl ester 168**

N-4-fluorobenzenesulphonylglycine (0.84 g, 4 mmol) and (D, L)-alanine^P diphenyl ester hydrobromide (1.43 g, 4 mmol) were used. Recrystallisation from diethyl ether furnished **168** as a white powder (1.10 g, 59%).

m.p. = 130-132 °C.

Anal. calcd. for C₂₂H₂₂N₂O₆P₁S₁F₁: C, 53.66; H, 4.50; N, 5.69.

Found C, 53.49; H, 4.30; N, 5.65.

Mass Spectrum: [M+Na]⁺ found 515.2.

C₂₂H₂₂N₂O₆P₁S₁F₁Na₁ requires 515.4.

IR (KBr): ν 3221, 3069, 1675, 1591, 1489, 1154, 953, 766 cm⁻¹.

¹H-NMR (400 MHz, DMSO): δ 8.66 (1H, d, $J = 9.2$ Hz, -NH-), 8.16 (1H, t, $J = 6.0$ Hz, -NH-), 7.14-7.93 (14H, m, -ArH), 4.62-4.71 (1H, m, α -H), 3.68 (1H, dd, $J^3 = 6.4$ Hz, $J^2 = 16.8$ Hz, -CH₂-), 3.54 (1H, dd, $J^3 = 5.6$ Hz, $J^2 = 16.4$ Hz, -CH₂-), 1.42 (3H, dd, $J^{\text{H-H}} = 7.2$ Hz, $J^{\text{H-P}} = 18.0$ Hz).

¹³C-NMR (100 MHz, DMSO): δ 167.6 (d, -CONH-), 164.4 (d, -ArC 4), 150.3 (d, -OPhC 1), 150.1 (d, -OPhC 1), 137.2 (d, -ArC 1), 130.24 (-OPhC 3), 130.21 (-OPhC 3), 130.0 (-ArC 2), 129.9 (-ArC 6), 125.7 (-OPhC 4), 125.6 (-OPhC 4), 120.9 (d, -OPhC 2), 120.7 (d, -OPhC 2), 116.6 (-ArC 3), 116.3 (-ArC 5), 45.2 (-CH₂-, -VE DEPT), 41.5 (d, α -C), 15.4 (-CH₃).

¹⁹F-NMR (376 MHz, DMSO): δ -31.5 - -31.7 (m).

³¹P-NMR (161.9 MHz, DMSO): δ 19.16-19.45 (m).

***N*-4-fluorobenzenesulphonyl- β -alanine-(D, L)-alanine^P diphenyl ester 169**

N-4-fluorobenzenesulphonyl- β -alanine (0.90 g, 4 mmol) and (D, L)-alanine^P diphenyl ester hydrobromide (1.43 g, 4 mmol) were used. Recrystallisation from diethyl ether furnished **169** as a white powder (1.18 g, 61%).

m.p. = 123-125 °C.

Anal. calcd. for C₂₃H₂₄N₂O₆P₁S₁F₁: C, 54.54; H, 4.78; N, 5.53.

Found C, 54.48; H, 4.91; N, 5.41.

Mass Spectrum: [M+Na]⁺ found 529.2.

C₂₃H₂₄N₂O₆P₁S₁F₁Na₁ requires 529.4.

IR (KBr): ν 3257, 3066, 1667, 1591, 1491, 1160, 939, 764 cm⁻¹.

¹H-NMR (400 MHz, DMSO): δ 8.69 (1H, d, $J = 9.2$ Hz, -NH-), 7.13-7.91 (15H, m, -ArH & -NH-), 4.71-4.78 (1H, m, α -H), 2.93-3.00 (2H, m, β -CH₂), 2.32-2.43 (2H, m, α -CH₂), 1.45 (3H, dd, $J^{\text{H-H}} = 7.2$ Hz, $J^{\text{H-P}} = 18.0$ Hz).

¹³C-NMR (100 MHz, DMSO): δ 169.7 (d, -CONH-), 164.4 (d, -ArC 4), 150.4 (d, -OPhC 1), 150.1 (d, -OPhC 1), 136.9 (d, -ArC 1), 130.2 (-OPhC 3), 130.1 (-OPhC 3), 129.9 (-ArC 2), 129.8 (-ArC 6), 125.6 (-OPhC 4), 125.5 (-OPhC 4), 120.9 (d, -OPhC 2), 120.8 (d, -OPhC 2), 116.8 (-ArC 3), 116.5 (-ArC 5), 41.4 (d, α -C), 39.2 (β -CH₂-, -VE DEPT), 35.6 (α -CH₂-, -VE DEPT), 15.4 (-CH₃).

¹⁹F-NMR (376 MHz, DMSO): δ -31.5 - -31.7 (m).

³¹P-NMR (161.9 MHz, DMSO): δ 19.37-19.77 (m).

***N*-4-fluorobenzenesulphonyl- γ -aminobutyric acid-(D, L)-alanine^p diphenyl ester 170**

N-4-fluorobenzenesulphonyl- γ -aminobutyric acid (0.95 g, 4 mmol) and (D, L)-alanine^p diphenyl ester hydrobromide (1.43 g, 4 mmol) were used. Recrystallisation from diethyl ether furnished **170** as a white powder (0.99 g, 50%).

m.p. = 129-131 °C.

Anal. calcd. for C₂₄H₂₆N₂O₆P₁S₁F₁: C, 55.38; H, 5.04; N, 5.38.

Found C, 55.25; H, 5.00; N, 5.56.

Mass Spectrum: [M+Na]⁺ found 543.2.

C₂₄H₂₆N₂O₆P₁S₁F₁Na₁ requires 543.5.

IR (KBr): ν 3266, 3060, 1678, 1593, 1490, 1186, 948, 766 cm⁻¹.

¹H-NMR (400 MHz, DMSO): δ 8.55 (1H, d, J = 9.6 Hz, -NH-), 7.12-7.86 (15H, m, -ArH & -NH-), 4.68-4.74 (1H, m, α -H), 2.75 (2H, q, J = 6.8 Hz, γ -CH₂), 2.14-2.20 (2H, m, α -CH₂), 1.63 (2H, qt, J = 7.2 Hz, β -CH₂), 1.42 (3H, dd, $J^{\text{H-H}}$ = 7.2 Hz, $J^{\text{H-P}}$ = 18.4 Hz).

¹³C-NMR (100 MHz, DMSO): δ 171.6 (d, -CONH-), 164.4 (d, -ArC 4), 150.4 (d, -OPhC 1), 150.2 (d, -OPhC 1), 137.1 (d, -ArC 1), 130.2 (-OPhC 3), 130.1 (-OPhC 3), 129.8 (-ArC 2), 129.7 (-ArC 6), 125.6 (-OPhC 4), 125.5 (-OPhC 4), 120.9 (d, -OPhC 2), 120.7 (d, -OPhC 2), 116.7 (-ArC 3), 116.5 (-ArC 5), 42.4 (γ -CH₂, -VE DEPT), 41.4 (d, α -C), 32.5 (α -CH₂, -VE DEPT), 25.5 (β -CH₂, -VE DEPT), 15.5 (-CH₃).

¹⁹F-NMR (376 MHz, DMSO): δ -31.7 - -31.9 (m).

³¹P-NMR (161.9 MHz, DMSO): δ 19.61-19.98 (m).

***N*-cinnamoyl-glycine-(D, L)-phenylglycine^p diphenyl ester 171**

N-cinnamoyl-glycine (0.82 g, 4 mmol) and (D, L)-phenylglycine^p diphenyl ester hydrobromide (1.68 g, 4 mmol) were used. Recrystallisation from diethyl ether furnished **171** as a white powder (0.68 g, 32%).

m.p. = 152-153 °C.

Anal. calcd. for C₃₀H₂₇N₂O₅P₁: C, 68.43; H, 5.17; N, 5.32.

Found C, 68.42; H, 5.18; N, 5.21.

Mass Spectrum: [M+K]⁺ found 565.2.

C₃₀H₂₇N₂O₅P₁K₁ requires 565.6.

IR (KBr): ν 3276, 3075, 1655, 1618, 1490, 1213, 941 cm⁻¹.

¹H-NMR (400 MHz, DMSO): δ 9.53 (1H, d, J = 9.6 Hz, -NH-), 8.50 (1H, t, J = 5.6 Hz, -NH-), 6.98-7.67 (21H, m, -ArH & -C=C-H), 6.82 (1H, d, J = 15.6 Hz, -C=C-H), 5.99 (1H, dd, $J^{\text{H-H}}$ = 10.0 Hz, $J^{\text{H-P}}$ = 22.0 Hz, α -H), 4.09 (2H, d, J = 5.6 Hz, -CH₂-).

^{13}C -NMR (100 MHz, DMSO): δ 169.43 (d, -CONH-), 165.7 (-ArCO-), 150.3 (d, -OPhC 1), 150.1 (d, -OPhC 1), 139.5 (C=C), 135.1 (-ArC 1), 134.6 (-PhC 1), 130.25 (-OPhC 3), 130.22 (-OPhC 3), 129.9 (-ArC 4), 129.3 (-ArC 3), 128.96 (-PhC 3), 128.91 (-PhC 2), 128.6 (-PhC 4), 127.9 (-ArC 2), 125.7 (-OPhC 4), 122.1 (C=C), 120.8 (d, -OPhC 2), 120.7 (d, -OPhC 2), 50.4 (d, α -C), 42.3 (-CH₂-, -VE DEPT).

^{31}P -NMR (161.9 MHz, DMSO): δ 15.15 (d, $J^{\text{P-H}} = 21.9$ Hz).

***N*-cinnamoyl- β -alanine-(D, L)-phenylglycine^P diphenyl ester 172**

N-cinnamoyl- β -alanine (0.88 g, 4 mmol) and (D, L)-phenylglycine^P diphenyl ester hydrobromide (1.68 g, 4 mmol) were used. Recrystallisation from diethyl ether furnished **172** as a white powder (0.33 g, 15%).

m.p. = 163-164 °C.

Anal. calcd. for C₃₁H₂₉N₂O₅P₁: C, 68.88; H, 5.41; N, 5.18.

Found C, 68.59; H, 5.30; N, 5.11.

Mass Spectrum: [M+Na]⁺ found 563.2.

C₃₁H₂₉N₂O₅P₁Na₁ requires 563.5.

IR (KBr): ν 3284, 3068, 1661, 1621, 1489, 1183, 934 cm⁻¹.

^1H -NMR (400 MHz, DMSO): δ 9.43 (1H, d, $J = 9.6$ Hz, -NH-), 8.24 (1H, t, $J = 6.0$ Hz, -NH-), 6.94-7.63 (21H, m, -ArH & -C=C-H), 6.63 (1H, d, $J = 15.6$ Hz, -C=C-H), 5.99 (1H, dd, $J^{\text{H-H}} = 10.0$ Hz, $J^{\text{H-P}} = 22.0$ Hz, α -H), 3.35-3.45 (1H, m, β -CH₂), 2.50-2.57 (1H, m, α -CH₂).

^{13}C -NMR (100 MHz, DMSO): δ 170.87 (d, -CONH-), 165.4 (-ArCO-), 150.3 (d, -OPhC 1), 150.0 (d, -OPhC 1), 139.0 (C=C), 135.2 (-ArC 1), 134.7 (-PhC 1), 130.2 (-OPhC 3), 129.7 (-ArC 4), 129.2 (-ArC 3), 128.9 (-PhC 3), 128.8 (-PhC 2), 128.5 (-PhC 4), 127.8 (-ArC 2), 125.6 (-OPhC 4), 122.4 (C=C), 120.7 (t, -OPhC 2), 50.3 (d, α -C), 35.5 (β -CH₂, -VE DEPT), 35.3 (α -CH₂, -VE DEPT).

^{31}P -NMR (161.9 MHz, DMSO): δ 15.30 (d, $J^{\text{P-H}} = 22.0$ Hz).

***N*-cinnamoyl- γ -aminobutyric acid-(D, L)-phenylglycine^P diphenyl ester 173**

N-cinnamoyl- γ -aminobutyric acid (0.93 g, 4 mmol) and (D, L)-phenylglycine^P diphenyl ester hydrobromide (1.68 g, 4 mmol) were used. Recrystallisation from diethyl ether furnished **173** as a white powder (0.83 g, 37%).

m.p. = 100-101 °C.

Anal. calcd. for C₃₂H₃₁N₂O₅P₁: C, 69.30; H, 5.63; N, 5.05.

Found C, 69.10; H, 5.63; N, 5.04.

Mass Spectrum: $[M+K]^+$ found 593.3.

$C_{32}H_{31}N_2O_5P_1K_1$ requires 593.6.

IR (KBr): ν 3256, 3060, 1654, 1618, 1490, 1182, 940 cm^{-1} .

1H -NMR (400 MHz, DMSO): δ 9.37 (1H, d, $J = 9.6$ Hz, -NH-), 8.20 (1H, t, $J = 5.6$ Hz, -NH-), 6.94-7.64 (21H, m, -ArH & -C=C-H), 6.64 (1H, d, $J = 15.6$ Hz, -C=C-H), 5.98 (1H, dd, $J^{H-H} = 9.6$ Hz, $J^{H-P} = 22.0$ Hz, α -H), 3.20 (2H, q, $J = 6.4$ Hz, γ -CH₂), 2.33 (2H, t, $J = 7.6$ Hz, α -CH₂), 1.70-1.74 (2H, m, β -CH₂).

^{13}C -NMR (100 MHz, DMSO): δ 172.2 (d, -CONH-), 165.3 (-ArCO-), 150.4 (d, -OPhC 1), 150.1 (d, -OPhC 1), 138.9 (C=C), 135.2 (-ArC 1), 134.8 (-PhC 1), 130.2 (-OPhC 3), 129.7 (-ArC 4), 129.2 (-ArC 3), 128.9 (-PhC 3), 128.8 (-PhC 2), 128.5 (-PhC 4), 127.8 (-ArC 2), 125.6 (-OPhC 4), 122.5 (C=C), 120.6 (t, -OPhC 2), 50.3 (d, α -C), 38.7 (γ -CH₂, -VE DEPT), 32.9 (α -CH₂, -VE DEPT), 25.8 (β -CH₂, -VE DEPT).

^{31}P -NMR (161.9 MHz, DMSO): δ 15.39 (d, $J^{P-H} = 22.0$ Hz).

***N*-cinnamoyl-glycine-(D, L)-phenylalanine^P diphenyl ester 174**

N-cinnamoylglycine (0.82 g, 4 mmol) and (D, L)-phenylalanine^P diphenyl ester hydrobromide (1.74 g, 4 mmol) were used. Recrystallisation from diethyl ether furnished **174** as a white powder (1.15 g, 37%).

m.p. = 127-128 °C.

Anal. calcd. for $C_{31}H_{29}N_2O_5P_1$: C, 68.88; H, 5.40; N, 5.18.

Found C, 68.96; H, 5.44; N, 5.12.

Mass Spectrum: $[M+K]^+$ found 579.2.

$C_{31}H_{29}N_2O_5P_1K_1$ requires 579.6.

IR (KBr): ν 3268, 3061, 1656, 1618, 1489, 1189, 940 cm^{-1} .

1H -NMR (400 MHz, DMSO): δ 8.86 (1H, d, $J = 9.2$ Hz, -NH-), 8.35 (1H, bs, -NH-), 7.19-7.59 (21H, m, -ArH & -C=C-H), 6.78 (1H, d, $J = 16.0$ Hz, -C=C-H), 4.86-4.91 (1H, m, α -H), 3.93 (1H, dd, $J^3 = 4.8$ Hz, $J^2 = 16.0$ Hz -CH₂-), 3.75 (1H, dd, $J^3 = 4.8$ Hz, $J^2 = 16.0$ Hz, -CH₂-), 3.30-3.35 (1H, m, -CH₂Ph), 3.00-3.08 (1H, m, -CH₂Ph).

^{13}C -NMR (100 MHz, DMSO): δ 169.2 (d, -CONH-), 165.5 (-ArCO-), 150.3 (d, -OPhC 1), 150.1 (d, -OPhC 1), 139.4 (C=C), 137.2 (d, -PhC 1), 135.1 (-ArC 1), 130.3 (-OPhC 3), 130.2 (-OPhC 3), 129.8 (-ArC 4), 129.4 (-PhC 3), 129.3 (-ArC 3), 128.6 (-PhC 2), 127.9 (-ArC 2), 127.0 (-PhC 4), 125.8 (-OPhC 4), 125.7 (-OPhC 4), 122.1 (C=C), 121.0 (d, -OPhC 2), 120.9 (d, -OPhC 2), 47.7 (d, α -C), 42.1 (-CH₂-, -VE DEPT), 34.7 (d, -CH₂Ph, -VE DEPT).

^{31}P -NMR (161.9 MHz, DMSO): δ 17.99 (t, $J^{P-H} = 7.3$ Hz).

***N*-cinnamoyl- β -alanine-(D, L)-phenylalanine^P diphenyl ester 175**

N-cinnamoyl- β -alanine (0.75 g, 3.45 mmol) and (D, L)-phenylalanine^P diphenyl ester hydrobromide (1.50 g, 3.45 mmol) were used. Recrystallisation from diethyl ether furnished **175** as a white powder (0.85 g, 45%).

m.p. = 116-118 °C.

Anal. calcd. for C₃₂H₃₁N₂O₅P₁: C, 69.30; H, 5.63; N, 5.05.

Found C, 69.08; H, 5.72; N, 5.02.

Mass Spectrum: [M+K]⁺ found 593.3.

C₃₂H₃₁N₂O₅P₁K₁ requires 593.6.

IR (KBr): ν 3268, 3062, 1655, 1618, 1489, 1189, 940 cm⁻¹.

¹H-NMR (400 MHz, DMSO): δ 8.77 (1H, d, J = 9.2 Hz, -NH-), 8.10 (1H, t, J = 5.6 Hz, -NH-), 7.18-7.55 (21H, m, -ArH & -C=C-H), 6.59 (1H, d, J = 16.0 Hz, -C=C-H), 4.87-4.96 (1H, m, α -H), 3.24-3.33 (3H, m, -CH₂Ph & β -CH₂), 2.98-3.06 (1H, m -CH₂Ph), 2.26-2.38 (2H, m, α -CH₂).

¹³C-NMR (100 MHz, DMSO): δ 170.7 (d, -CONH-), 165.3 (-ArCO-), 150.4 (d, -OPhC 1), 150.1 (d, -OPhC 1), 138.9 (C=C), 137.2 (d, -PhC 1), 135.2 (-ArC 1), 130.3 (-OPhC 3), 130.2 (-OPhC 3), 129.7 (-ArC 4), 129.4 (-PhC 3), 129.2 (-ArC 3), 128.5 (-PhC 2), 127.8 (-ArC 2), 126.9 (-PhC 4), 125.7 (-OPhC 4), 125.6 (-OPhC 4), 122.5 (C=C), 121.0 (d, -OPhC 2), 120.7 (d, -OPhC 2), 47.2 (d, α -C), 35.5 (β -CH₂, -VE DEPT), 35.3 (α -CH₂, -VE DEPT), 34.7 (d, -CH₂Ph, -VE DEPT).

³¹P-NMR (161.9 MHz, DMSO): δ 18.19 (t, $J^{\text{P-H}}$ = 6.9 Hz).

***N*-cinnamoyl- γ -aminobutyric acid-(D, L)-phenylalanine^P diphenyl ester 176**

N-cinnamoyl- γ -aminobutyric acid (0.50 g, 2.18 mmol) and (D, L)-phenylalanine^P diphenyl ester hydrobromide (0.95 g, 2.18 mmol) were used. Recrystallisation from diethyl ether furnished **176** as a white powder (0.45 g, 36%).

m.p. = 150-150 °C.

Anal. calcd. for C₃₃H₃₃N₂O₅P₁: C, 69.70; H, 5.85; N, 4.92.

Found C, 69.40; H, 5.88; N, 4.94.

Mass Spectrum: [M+Na]⁺ found 591.3.

C₃₃H₃₃N₂O₅P₁Na₁ requires 591.5.

IR (KBr): ν 3292, 3065, 1651, 1618, 1489, 1187, 942 cm⁻¹.

¹H-NMR (400 MHz, DMSO): δ 8.66 (1H, d, J = 9.6 Hz, -NH-), 8.09 (1H, t, J = 5.6 Hz, -NH-), 7.14-7.57 (21H, m, -ArH & -C=C-H), 6.61 (1H, d, J = 16.0 Hz, -C=C-H), 4.84-4.93 (1H,

m, α -H), 3.29-3.39 (1H, m, -CH₂Ph), 2.95-3.03 (3H, m -CH₂Ph & γ -CH₂), 2.06 (2H, t, J = 7.2 Hz, α -CH₂), 1.48-1.55 (2H, m, β -CH₂).

¹³C-NMR (100 MHz, DMSO): δ 172.1 (d, -CONH-), 165.2 (-ArCO-), 150.4 (d, -OPhC 1), 150.1 (d, -OPhC 1), 138.8 (C=C), 137.2 (d, -PhC 1), 135.2 (-ArC 1), 130.3 (-OPhC 3), 130.2 (-OPhC 3), 129.7 (-ArC 4), 129.4 (-PhC 3), 129.2 (-ArC 3), 128.5 (-PhC 2), 127.8 (-ArC 2), 126.9 (-PhC 4), 125.7 (-OPhC 4), 125.6 (-OPhC 4), 122.5 (C=C), 121.0 (d, -OPhC 2), 120.7 (d, -OPhC 2), 47.3 (d, α -C), 38.5 (γ -CH₂, -VE DEPT), 34.6 (d, -CH₂Ph, -VE DEPT), 33.0 (α -CH₂, -VE DEPT), 25.7 (β -CH₂, -VE DEPT).

³¹P-NMR (161.9 MHz, DMSO): δ 18.26 (t, $J^{\text{P-H}}$ = 7.3 Hz).

***N*-cinnamoyl-glycine-(D, L)-alanine^P diphenyl ester 177**

N-cinnamoylglycine (0.56 g, 2.74 mmol) and (D, L)-alanine^P diphenyl ester hydrobromide (0.98 g, 2.74 mmol) were used. Recrystallisation from diethyl ether furnished **177** as a white powder (0.68 g, 53%).

m.p. = 138-140 °C.

Anal. calcd. for C₂₅H₂₅N₂O₅P₁: C, 64.65; H, 5.43; N, 6.03.

Found C, 64.39; H, 5.30; N, 6.02.

Mass Spectrum: [M+K]⁺ found 503.2.

C₂₅H₂₅N₂O₅P₁K₁ requires 503.5.

IR (KBr): ν 3266, 3071, 1655, 1619, 1489, 1190, 948 cm⁻¹.

¹H-NMR (400 MHz, DMSO): δ 8.76 (1H, d, J = 9.2 Hz, -NH-), 8.44 (1H, t, J = 6.0 Hz, -NH-), 7.16-7.60 (21H, m, -ArH & -C=C-H), 6.80 (1H, d, J = 16.0 Hz, -C=C-H), 4.73-4.81 (1H, m, α -H), 4.02 (1H, dd, J^3 = 6.0 Hz, J^2 = 16.8 Hz, -CH₂-), 3.89 (1H, dd, J^3 = 5.6 Hz, J^2 = 16.8 Hz, -CH₂-), 1.48 (3H, dd, $J^{\text{H-H}}$ = 7.2 Hz, $J^{\text{H-P}}$ = 18.4 Hz, -CH₃).

¹³C-NMR (100 MHz, DMSO): δ 169.0 (d, -CONH-), 165.6 (-ArCO-), 150.4 (d, -OPhC 1), 150.1 (d, -OPhC 1), 139.4 (C=C), 135.1 (-ArC 1), 130.27 (-OPhC 3), 130.22 (-OPhC 3), 129.8 (-ArC 4), 129.3 (-ArC 3), 127.9 (-ArC 2), 125.7 (-OPhC 4), 125.6 (-OPhC 4), 122.2 (C=C), 121.0 (d, -OPhC 2), 120.8 (d, -OPhC 2), 42.3 (-CH₂-, -VE DEPT), 41.6 (d, α -C), 15.5 (-CH₃).

³¹P-NMR (161.9 MHz, DMSO): δ 19.39-19.82 (m).

***N*-cinnamoyl- β -alanine-(D, L)-alanine^P diphenyl ester 178**

N-cinnamoyl- β -alanine (0.43 g, 2.0 mmol) and (D, L)-alanine^P diphenyl ester hydrobromide (0.70 g, 2.0 mmol) were used. Recrystallisation from diethyl ether furnished **178** as a white powder (0.54 g, 55%).

m.p. = 155-156 °C.

Anal. calcd. for C₂₆H₂₇N₂O₅P₁: C, 65.26; H, 5.69; N, 5.85.

Found C, 64.96; H, 5.49; N, 5.93.

Mass Spectrum: [M+Na]⁺ found 501.2.

C₂₆H₂₇N₂O₅P₁Na₁ requires 501.5.

IR (KBr): ν 3249, 3066, 1655, 1618, 1491, 1188, 937 cm⁻¹.

¹H-NMR (400 MHz, DMSO): δ 8.68 (1H, d, J = 9.2 Hz, -NH-), 8.19 (1H, t, J = 5.6 Hz, -NH-), 7.15-7.55 (21H, m, -ArH & -C=C-H), 6.64 (1H, d, J = 15.6 Hz, -C=C-H), 4.74-4.82 (1H, m, α -H), 3.39-3.45 (2H, m, β -CH₂), 2.36-2.49 (2H, m, α -CH₂), 1.47 (3H, dd, $J^{\text{H-H}} = 7.2$ Hz, $J^{\text{H-P}} = 18.4$ Hz, -CH₃).

¹³C-NMR (100 MHz, DMSO): δ 170.5 (d, -CONH-), 165.3 (-ArCO-), 150.4 (d, -OPhC 1), 150.1 (d, -OPhC 1), 138.9 (C=C), 135.2 (-ArC 1), 130.2 (-OPhC 3), 130.1 (-OPhC3), 129.7 (-ArC 4), 129.2 (-ArC 3), 127.8 (-ArC 2), 125.6 (-OPhC 4), 125.5 (-OPhC 4), 122.5 (C=C), 120.9 (d, -OPhC 2), 120.7 (d, -OPhC 2), 41.2 (d, α -C), 35.6 (β -CH₂, -VE DEPT), 35.4 (α -CH₂, -VE DEPT), 15.5 (-CH₃).

³¹P-NMR (161.9 MHz, DMSO): δ 19.55-19.95 (m).

***N*-cinnamoyl- γ -aminobutyric acid-(D, L)-alanine^P diphenyl ester 179**

N-cinnamoyl- γ -aminobutyric acid (0.46 g, 2.0 mmol) and (D, L)-alanine^P diphenyl ester hydrobromide (0.70 g, 2.0 mmol) were used. Recrystallisation from diethyl ether furnished **179** as a white powder (0.48 g, 49%).

m.p. = 150-152 °C.

Anal. calcd. for C₂₇H₂₉N₂O₅P₁: C, 65.85; H, 5.94; N, 5.69.

Found C, 65.58; H, 5.83; N, 5.51.

Mass Spectrum: [M+K]⁺ found 531.2.

C₂₇H₂₉N₂O₅P₁K₁ requires 531.6.

IR (KBr): ν 3256, 3062, 1662, 1628, 1490, 1186, 941 cm⁻¹.

¹H-NMR (400 MHz, DMSO): δ 8.66 (1H, d, J = 9.2 Hz, -NH-), 8.24 (1H, t, J = 5.6 Hz, -NH-), 7.19-7.58 (21H, m, -ArH & -C=C-H), 6.69 (1H, d, J = 16.0 Hz, -C=C-H), 4.77-4.85 (1H,

m, α -H), 3.24-3.32 (2H, m, γ -CH₂), 2.23-2.30 (2H, m, α -CH₂), 1.73-1.80 (2H, m, β -CH₂), 1.47 (3H, dd, $J^{\text{H-H}} = 7.2$ Hz, $J^{\text{H-P}} = 18.4$ Hz, -CH₃).

¹³C-NMR (100 MHz, DMSO): δ 172.0 (d, -CONH-), 165.4 (-ArCO-), 150.4 (d, -OPhC 1), 150.2 (d, -OPhC 1), 139.0 (C=C), 135.2 (-ArC 1), 130.2 (-OPhC 3), 130.1 (-OPhC 3), 129.7 (-ArC 4), 129.2 (-ArC 3), 127.8 (-ArC 2), 125.6 (-OPhC 4), 125.5 (-OPhC 4), 122.5 (C=C), 120.9 (d, -OPhC 2), 120.7 (d, -OPhC 2), 41.2 (d, α -C), 38.7 (γ -CH₂, -VE DEPT), 33.1 (α -CH₂, -VE DEPT), 25.8 (β -CH₂, -VE DEPT), 15.5 (-CH₃).

³¹P-NMR (161.9 MHz, DMSO): δ 19.65-20.05 (m).

***N*-trifluoroacetyl-glycine-(D, L)-phenylglycine^p diphenyl ester 180**

N-trifluoroacetyl-glycine (0.68 g, 4 mmol) and (D, L)-phenylglycine^p diphenyl ester hydrobromide (1.68 g, 4 mmol) were used. Recrystallisation from diethyl ether furnished **180** as a white powder (0.54 g, 29%).

m.p. = 147-149 °C.

Anal. calcd. for C₂₃H₂₀N₂O₅P₁F₃: C, 56.10; H, 4.09; N, 5.69.

Found C, 55.85; H, 4.02; N, 5.48.

Mass Spectrum: [M+K]⁺ found 531.2.

C₂₃H₂₀N₂O₅P₁F₃K₁ requires 531.4.

IR (Nujol): ν 3270, 3079, 1676, 1535, 1458, 1188, 936 cm⁻¹.

¹H-NMR (400 MHz, DMSO): δ 9.75 (1H, t, $J = 6.0$ Hz, -NH-), 9.61 (1H, d, $J = 9.6$ Hz, -NH-), 6.94-7.64 (15H, m, -ArH), 5.93 (1H, dd, $J^{\text{H-H}} = 10.0$ Hz, $J^{\text{H-P}} = 22.0$ Hz, α -H), 3.35-3.41 (2H, m, -CH₂-).

¹³C-NMR (100 MHz, DMSO): δ 167.5 (d, -CONH-), 157.1 (q, F₃CCO-), 150.2 (d, -OPhC 1), 150.0 (d, -OPhC 1), 134.5 (-PhC 1), 130.25 (-OPhC 3), 130.20 (-OPhC 3), 128.9 (-PhC 3), 128.8 (-PhC 2), 128.7 (-PhC 4), 125.8 (-OPhC 4), 125.7 (-OPhC 4), 120.8 (d, -OPhC 2), 120.7 (d, -OPhC 2), 116.3 (q, F₃C-), 50.6 (d, α -C), 42.0 (-CH₂-, -VE DEPT).

¹⁹F-NMR (376 MHz, DMSO): δ 0.86.

³¹P-NMR (161.9 MHz, DMSO): δ 15.23 (d, $J^{\text{P-H}} = 5.5$ Hz).

***N*-trifluoroacetyl- β -alanine-(D, L)-phenylglycine^p diphenyl ester 181**

N-trifluoroacetyl- β -alanine (0.74 g, 4 mmol) and (D, L)-phenylglycine^p diphenyl ester hydrobromide (1.68 g, 4 mmol) were used. Recrystallisation from diethyl ether furnished **181** as a white powder (0.46 g, 20%).

m.p. = 119-120 °C.

Anal. calcd. for $C_{24}H_{22}N_2O_5P_1F_3$: C, 56.92; H, 4.38; N, 5.53.

Found C, 56.66; H, 4.27; N, 5.39.

Mass Spectrum: $[M+Na]^+$ found 529.2.

$C_{24}H_{22}N_2O_5P_1F_3Na_1$ requires 529.4.

IR (Nujol): ν 3371, 3259, 1773, 1660, 1452, 1171, 953 cm^{-1} .

1H -NMR (400 MHz, DMSO): δ 9.48-9.53 (2H, m, -NH-), 6.94-7.62 (15H, m, -ArH), 6.00 (1H, dd, $J^{H-H} = 9.6$ Hz, $J^{H-P} = 17.6$ Hz, α -H), 3.42-3.45 (2H, m, β -CH₂), 2.58-2.62 (2H, m, α -CH₂).

^{13}C -NMR (100 MHz, DMSO): δ 170.3 (d, -CONH-), 156.7 (q, F₃CCO-), 150.3 (d, -OPhC 1), 150.0 (d, -OPhC 1), 134.5 (-PhC 1), 130.1 (-OPhC 3), 128.8 (-PhC 3), 128.7 (-PhC 2), 128.6 (-PhC 4), 125.7 (-OPhC 4), 120.6 (d, -OPhC 2), 116.3 (q, F₃C-), 50.2 (d, α -C), 36.1 (β -CH₂, -VE DEPT), 34.1 (α -CH₂, -VE DEPT).

^{19}F -NMR (376 MHz, DMSO): δ 0.72.

^{31}P -NMR (161.9 MHz, DMSO): δ 15.94 (d, $J^{P-H} = 21.85$ Hz).

***N*-trifluoroacetyl-glycine-(D, L)-phenylalanine^P diphenyl ester 182**

N-trifluoroacetyl-glycine (0.68 g, 4 mmol) and (D, L)-phenylalanine^P diphenyl ester hydrobromide (1.71 g, 4 mmol) were used. Recrystallisation from diethyl ether furnished **182** as a white powder (1.19 g, 59%).

m.p. = 167-168 °C.

Anal. calcd. for $C_{24}H_{22}N_2O_5P_1F_3$: C, 56.92; H, 4.38; N, 5.53.

Found C, 57.14; H, 4.30; N, 5.46.

Mass Spectrum: $[M+Na]^+$ found 529.2.

$C_{24}H_{22}N_2O_5P_1F_3Na_1$ requires 529.4.

IR (Nujol): ν 3225, 3079, 1727, 1650, 1463, 1188, 953 cm^{-1} .

1H -NMR (400 MHz, DMSO): δ 9.71 (1H, t, $J = 6.0$ Hz, -NH-), 9.00 (1H, d, $J = 6.0$ Hz, -NH-), 7.19-7.44 (15H, m, -ArH), 4.84-4.93 (1H, m, α -H), 3.92 (1H, dd, $J^3 = 6.0$ Hz, $J^1 = 16.8$ Hz, -CH₂-), 3.73 (1H, dd, $J^3 = 6.0$ Hz, $J^2 = 16.8$ Hz, -CH₂-) 3.33-3.38 (1H, m, -CH₂Ph), 3.03-3.09 (1H, m, -CH₂Ph).

^{13}C -NMR (100 MHz, DMSO): δ 167.5 (d, -CONH-), 157.0 (q, F₃CCO-), 150.3 (d, -OPhC 1), 150.1 (d, -OPhC 1), 137.1 (d, -PhC 1), 130.29 (-OPhC 3), 130.24 (-OPhC 3), 129.4 (-PhC 3), 128.6 (-PhC 2), 127.0 (-PhC 4), 125.8 (-OPhC 4), 125.7 (-OPhC 4), 121.0 (d, -OPhC 2), 120.9 (d, -OPhC 2), 116.3 (q, F₃C-), 47.8 (d, α -C), 41.8 (-CH₂-, -VE DEPT), 34.8 (-CH₂Ph, -VE DEPT).

^{19}F -NMR (376 MHz, DMSO): δ 0.92.

^{31}P -NMR (161.9 MHz, DMSO): δ 18.01 (t, $J^{\text{P-H}} = 7.28$ Hz).

***N*-trifluoroacetyl- β -alanine-(D, L)-phenylalanine^P diphenyl ester 183**

N-trifluoroacetyl- β -alanine (0.74 g, 4 mmol) and (D, L)-phenylalanine^P diphenyl ester hydrobromide (1.71 g, 4 mmol) were used. Recrystallisation from diethyl ether furnished **183** as a white powder (0.82 g, 39%).

m.p. = 139-140 °C.

Anal. calcd. for $\text{C}_{25}\text{H}_{24}\text{N}_2\text{O}_5\text{P}_1\text{F}_3$: C, 57.69; H, 4.65; N, 5.38.

Found C, 57.40; H, 4.65; N, 5.25.

Mass Spectrum: $[\text{M}+\text{K}]^+$ found 559.2.

$\text{C}_{25}\text{H}_{24}\text{N}_2\text{O}_5\text{P}_1\text{F}_3\text{K}_1$ requires 559.5.

IR (Nujol): ν 3270, 3086, 1704, 1654, 1446, 1183, 947 cm^{-1} .

^1H -NMR (400 MHz, DMSO): δ 9.39 (1H, t, $J = 5.2$ Hz, -NH-), 8.78 (1H, d, $J = 9.6$ Hz, -NH-), 7.18-7.43 (15H, m, -ArH), 4.86-4.89 (1H, m, α -H), 3.29-3.34 (1H, m, -CH₂Ph), 3.18-3.22 (2H, m, β -CH₂), 2.95-3.04 (1H, m, -CH₂Ph), 2.27-2.37 (2H, m, α -CH₂).

^{13}C -NMR (100 MHz, DMSO): δ 169.8 (d, -CONH-), 156.5 (q, F₃CCO-), 150.4 (d, -OPhC 1), 150.1 (d, -OPhC 1), 137.1 (d, -PhC 1), 130.29 (-OPhC 3), 130.21 (-OPhC 3), 129.4 (-PhC 3), 128.5 (-PhC 2), 126.9 (-PhC 4), 125.7 (-OPhC 4), 125.6 (-OPhC 4), 121.0 (d, -OPhC 2), 120.7 (d, -OPhC 2), 116.6 (q, F₃C-), 47.3 (d, α -C), 35.9 (β -CH₂, -VE DEPT), 34.7 (d, -CH₂Ph, -VE DEPT), 34.1 (α -CH₂, -VE DEPT).

^{19}F -NMR (376 MHz, DMSO): δ 0.74.

^{31}P -NMR (161.9 MHz, DMSO): δ 18.52 (t, $J^{\text{P-H}} = 8.24$ Hz).

***N*-trifluoroacetyl-glycine-(D, L)-alanine^P diphenyl ester 184**

N-trifluoroacetyl-glycine (0.68 g, 4 mmol) and (D, L)-alanine^P diphenyl ester hydrobromide (1.43 g, 4 mmol) were used. Recrystallisation from diethyl ether furnished **184** as a white powder (0.77 g, 48%).

m.p. = 117-119 °C.

Anal. calcd. for $\text{C}_{18}\text{H}_{18}\text{N}_2\text{O}_5\text{P}_1\text{F}_3$: C, 50.24; H, 4.22; N, 6.51.

Found C, 49.95; H, 4.13; N, 6.25.

Mass Spectrum: $[\text{M}+\text{Na}]^+$ found 453.2.

$\text{C}_{18}\text{H}_{18}\text{N}_2\text{O}_5\text{P}_1\text{F}_3\text{Na}_1$ requires 453.3.

IR (Nujol): ν 3242, 3068, 1733, 1676, 1373, 1188, 958 cm^{-1} .

$^1\text{H-NMR}$ (400 MHz, DMSO): δ 9.76 (1H, t, $J = 5.2$ Hz, -NH-), 8.88 (1H, d, $J = 9.2$ Hz, -NH-), 7.15-7.40 (10H, m, -ArH), 4.71-4.79 (1H, m, α -H), 3.96 (1H, dd, $J^3 = 5.6$ Hz, $J^2 = 16.4$ Hz, -CH₂-), 3.87 (1H, dd, $J^3 = 5.6$ Hz, $J^2 = 16.4$ Hz, -CH₂-), 1.47 (3H, dd, $J^{\text{H-H}} = 7.2$ Hz, $J^{\text{H-P}} = 18.4$ Hz, -CH₃).

$^{13}\text{C-NMR}$ (100 MHz, DMSO): δ 167.2 (d, -CONH-), 157.4 (q, F₃CCO-), 150.3 (d, -OPhC 1), 150.1 (d, -OPhC 1), 130.26 (-OPhC 3), 130.22 (-OPhC 3), 125.7 (-OPhC 4), 125.6 (-OPhC 4), 120.9 (d, -OPhC 2), 120.8 (d, -OPhC 2), 116.4 (q, F₃C-), 42.0 (-CH₂-, -VE DEPT), 41.7 (d, α -C), 15.5 (-CH₃).

$^{19}\text{F-NMR}$ (376 MHz, DMSO): δ 0.89.

$^{31}\text{P-NMR}$ (161.9 MHz, DMSO): δ 19.42-20.00 (m).

N*-trifluoroacetyl- β -alanine-(D, L)-alanine^P diphenyl ester **185*

N-trifluoroacetyl- β -alanine (0.74 g, 4 mmol) and (D, L)-alanine^P diphenyl ester hydrobromide (1.43 g, 4 mmol) were used. Recrystallisation from diethyl ether furnished **185** as a white powder (0.67 g, 40%).

m.p. = 129-130 °C.

Anal. calcd. for C₁₉H₂₀N₂O₅P₁F₃: C, 51.36; H, 4.54; N, 6.30.

Found C, 51.06; H, 4.50; N, 6.08.

Mass Spectrum: [M+Na]⁺ found 467.2.

C₁₉H₂₀N₂O₅P₁F₃Na₁ requires 467.3.

IR (Nujol): ν 3276, 3074, 1721, 1648, 1458, 1183, 958 cm⁻¹.

$^1\text{H-NMR}$ (400 MHz, DMSO): δ 9.50 (1H, t, $J = 5.2$ Hz, -NH-), 8.73 (1H, d, $J = 9.2$ Hz, -NH-), 7.15-7.40 (10H, m, -ArH), 4.71-4.79 (1H, m, α -H), 3.41 (2H, q, $J = 6.4$ Hz, β -CH₂), 2.40-2.52 (2H, m, α -CH₂), 1.45 (3H, dd, $J^{\text{H-H}} = 7.2$ Hz, $J^{\text{H-P}} = 18.4$ Hz, -CH₃).

$^{13}\text{C-NMR}$ (100 MHz, DMSO): δ 170.0 (d, -CONH-), 156.6 (q, F₃CCO-), 150.3 (d, -OPhC 1), 150.1 (d, -OPhC 1), 130.2 (-OPhC 3), 130.1 (-OPhC 3), 125.7 (-OPhC 4), 125.6 (-OPhC 4), 120.9 (d, -OPhC 2), 120.6 (d, -OPhC 2), 116.4 (q, F₃C-), 41.4 (d, α -C), 36.1 (β -CH₂-, -VE DEPT), 34.2 (α -CH₂-, -VE DEPT), 15.3 (-CH₃).

$^{19}\text{F-NMR}$ (376 MHz, DMSO): δ 0.68.

$^{31}\text{P-NMR}$ (161.9 MHz, DMSO): δ 19.74-20.30 (m).

4.8 References

- 1 Iyer, R.A., Hanna, P.E., *Bioorg. Med. Chem. Lett.* **1995**, *5*, 89.
- 2 Beynon, R.J., Bond, J., "Proteolytic Enzymes", 2nd Edition Oxford University Press, **2001**.
- 3 Harel, M., Su, C.T., Frolow, F., Silman, I., Sussman, J.L., *Biochemistry* **1991**, *30*, 5217.
- 4 Han, M.S., Oh, D.J., Kim, D.H., *Bioorg. Med. Chem. Lett.* **2004**, *14*, 701.
- 5 Ni, L.M., Powers, J.C., *Bioorg. Med. Chem. Lett.* **1998**, *6*, 1767.
- 6 Senten, K., Daniëls, L., Van der Veken, P., De Meester, I., Lambeir, A.M., Scharpé, S., Haemers, A., Augustyns, K., *J. Comb. Chem.* **2003**, *5*, 336.
- 7 Bartlett, P.A., Lamden, L.A., *Bioorg. Chem.* **1986**, *14*, 356.
- 8 Kafarski, P., Mastalerz, P., "Aminophosphonates: Natural Occurrence, Biochemistry and Biological Properties", Beitr. Wirkstoffforschung, **1984**.
- 9 Hamilton, R., Walker, B., Walker, B.J., *Bioorg. Med. Chem. Lett.* **1998**, *8*, 1655.
- 10 Boduszek, B., Oleksyszyn, J., Kam, C.M., Selzler, J., Smith, R.E., Powers, J.C., *J. Med. Chem.* **1994**, *37*, 3969.
- 11 Jackson, D.S., Fraser, S.A., Ni, L.M., Kam, C.M., Winkler, U., Johnson, D.A., Froelich, C.J., Hudig, D., Powers, J.C., *J. Med. Chem.* **1998**, *41*, 2289.
- 12 Schultz, C., *Bioorg. Med. Chem.* **2003**, *11*, 885.
- 13 Meier, C., *Synlett* **1998**, 233.
- 14 Reichenberg, A., Wiesner, J., Weidemeyer, C., Dreiseidler, E., Sanderbrand, S., Altincicek, B., Beck, E., Schlitzer, M., Jomaa, H., *Bioorg. Med. Chem. Lett.* **2001**, *11*, 833.
- 15 <http://www.formaldehyde-europe.org/pages/?id=47#126>
- 16 De Lombaert, S., Erion, M.D., Tan, J., Blanchard, L., El-Chehabi, L., Ghai, R.D., Sakane, Y., Berry, C., Trapani, A.J., *J. Med. Chem.* **1994**, *37*, 498.
- 17 Horiguchi, M., Kandatsu, M., *Nature* **1959**, *184*, 901.
- 18 a) Lejczac, B., Kafarski, P., Zygmunt, J., *Biochemistry* **1989**, *28*, 3549. b) Van der Veken, P., Senten, K., Kertész, I., Haemers, A., Augustyns, K., *Tetrahedron Lett.* **2003**, *44*, 969.
- 19 Oleksyszyn, J., Subotkowska, L., Mastalerz, P., *Synthesis* **1979**, 985.
- 20 Chambers J.R., Isbell, A.F., *J. Org. Chem.* **1964**, *29*, 832
- 21 Azizi, N., Rajabi, F., Saidi, M.R., *Tet. Lett.* **2004**, *45*, 9233.

- 22 Kaboudin, B., Nazari, R., *Tet. Lett.* **2001**, *42*, 8211.
- 23 MacPherson, L.J., Bayburt, E.K., Capparelli, M.P., Carroll, B.J., Goldstein, R.,
Justice, M.R., Zhu, L., Hu, S., Melton, R.A., Fryer, L., Goldberg, R.L., Doughty, J.R.,
Spirito, S., Blancuzzi, V., Wilson, D., O'Byrne, E.M., Ganu, V., Parker, D.T., *J. Med.*
Chem. **1997**, *40*, 2525.
- 24 Scozzafava, A., Supuran, C.T., *J. Med. Chem.* **2000**, *43*, 1858.
- 25 Smith, M.B., March, J., "*March's Advanced Organic Chemistry*", Wiley and Sons
2001.
- 26 Scozzafava, A., Suparan, C.T., *Eur. J. Med. Chem.* **2000**, *35*, 3, 299.
- 27 Liu, S., Hanzlik, R.P., *J. Med. Chem.* **1992**, *35*, 1067.
- 28 Bernatowicz, M.S., Klimas, C.E., Hartl, K.S., Peluso, M., Allegretto, N.J., Seiler,
S.M., *J. Med. Chem.* **1996**, *39*, 4879.
- 29 Gelmi, M.L., Mottadelli, S., Pocar, D., *J. Med. Chem.* **1999**, *42*, 5272.
- 30 Giordano, O.S., Pestchanker, M.J., Guerreiro, E., Saad, J.R., Enriz, R.D., Rodriguez,
A.M., Jauregui, E.A., Guzman, J., Maria, A.O.M., Wendel, G.H., *J. Med. Chem.*
1992, *35*, 2452.
- 31 Clark, J.S., Hodgson, P.B., Goldsmith, M.D., Street, L.J., *J. Chem. Soc. Perkin Trans.*
1 **2001**, *24*, 3312.
- 32 Blanco, B., Cerezo, S., Moreno-Manas, M., Pleixats, R., Spengler, J., *Tet. Lett.* **2001**,
42, 9001.
- 33 Blaton, N.M., Peeters, O.M., De Ranter, C.J., *Acta Cryst.* **1997**, *C53*, 1952.
- 34 Hedstrom, L. *Chem. Rev.* **2002**, *102*, 4501.
- 35 a) Parmee, E.R., He, J., Mastracchio, A., Edmondson, S.D., Colwell, L., Eiermann,
G., Feeney, W.P., Habulihaz, B., He, H., Kilburn, R., Leiting, B., Lyons, K., Marsilio,
F., Patel, R.A., Petrov, A., Di Salvo, J., Wu, J.K., Thornberry, N.A., Weber, A.E.,
Bioorg. Med. Chem. Lett. **2004**, *14*, 43. b) Ma, D., Wu, W., Yang, G., Li, J., Li, J., Ye,
Q. *Bioorg. Med. Chem. Lett.* **2004**, *14*, 47. c) Stranix, B.R., Sauv e, G., Bouzide, A.,
Cot e, A., S evigny, G., Yelle, J., *Bioorg. Med. Chem. Lett.* **2003**, *13*, 4289.
- 36 Harter, W.G., Albrect, H., Brady, K., Caprathe, B., Dunbar, J., Gilmore, J., Hays, S.,
Kostlan, C.R., Lunney, B., Walker, N., *Bioorg. Med. Chem. Lett.* **2004**, *14*, 809.
- 37 Park, B.K., Kitteringham, N.R., O'Neill, P.M., *Annu. Rev. Pharmacol. Toxicol.*
2001, *41*, 443.
- 38 Choo, H.P., Peak, K.H., Park, J., Kim, D.H., Chung, H.S., *Eur. J. Med. Chem.* **2000**,

35, 643.

39 Reed, P.E., Katzenellenbogen, J.A., *J. Med. Chem.* **1991**, *34*, 1162.

40 Banks, R.E., Lowe, K.C., "*Fluorine in Medicine*", UMIST Press, **1994**.

Chapter 5

Fluorinated analogues of resveratrol as potential anticancer agents

5.1 Introduction

Resveratrol **186**, (3, 4', 5-trihydroxy-*trans*-stilbene) is a naturally occurring phytoalexin found in grapes and is formed in response to fungal infections.¹ Resveratrol is present only in small amounts in *Vitis vivifera* (vines) and its quantity is dependent on the stress situation of the plant. The isolation of resveratrol from plant sources is therefore not viable and it was not until synthetic methodologies were developed that the biological activity of resveratrol was completely assessed. It has been shown to exhibit various biological properties including antifungal, antibacterial, anticancer, estrogenic and cardioprotective activities.² Resveratrol came to prominence during the course of research into the so-called 'French paradox'. The 'French paradox' is the realisation that the population of France have a relatively high fat diet accompanied by a steady albeit moderate intake of alcohol in the form of red wine whilst their incidence of coronary heart disease is lower than expected.³ It has been shown that total phenolic compounds extracted from red wine inhibit the oxidation of human low-density lipoproteins (LDL). As the oxidised LDL may be responsible for promoting atherogenesis, resveratrol may play a role in the prevention of cardiovascular diseases.⁴

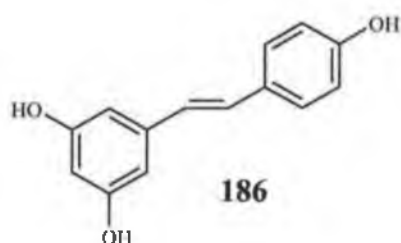


Figure 5.1 Resveratrol

Resveratrol has been suggested as a potential cancer chemopreventative agent based on its striking inhibitory effects on cellular events associated with cancer initiation, promotion and progression.⁵ This triphenolic stilbene has also displayed *in vitro* growth inhibition in a number of human cancer cells.⁶ The mechanistic basis for the wide range of biological activity of resveratrol remains unknown. Numerous studies point to its ability to function as a cellular antioxidant while others have demonstrated the inhibition of signalling kinases as its key function.⁷

5.2 Biosynthetic pathway of resveratrol

Resveratrol is a stilbene derivative formed from a *p*-coumaroyl CoA starter unit, with chain extension using three molecules of malonyl CoA.⁸ Malonyl CoA is derived from the elongation of acetyl CoA units and the *p*-coumaroyl from phenylalanine. Phenylalanine loses the amino group moiety through oxidative deamination catalysed by the enzyme phenylalanine ammonia lyase to yield cinnamic acid which is then converted to 4-coumaric acid by enzymatic hydroxylation.

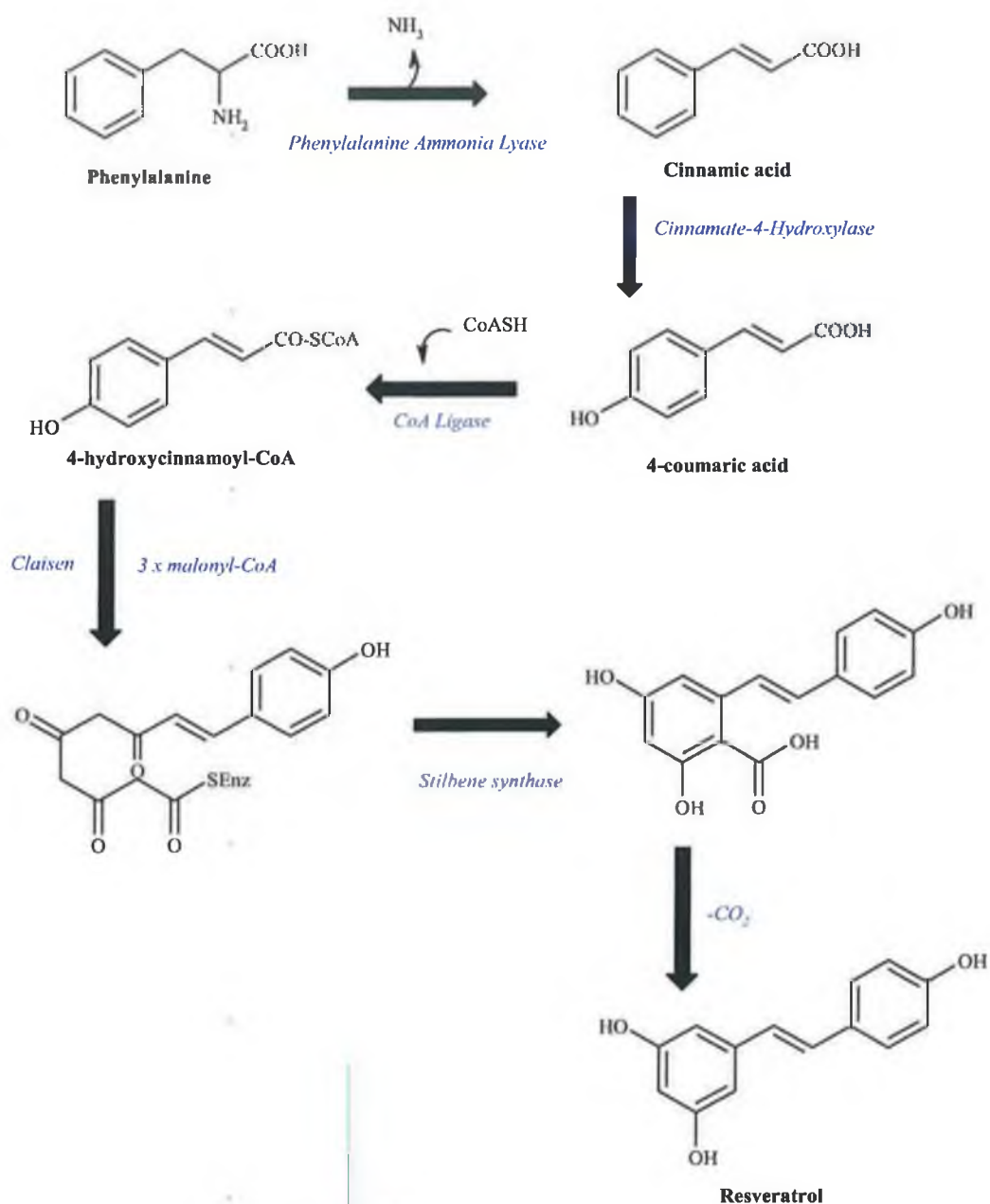


Figure 5.2 The biosynthesis of resveratrol

4-coumaric acid is then transformed to *p*-coumaroyl CoA after treatment with the free co-enzyme of a specific CoA ligase. The condensation of three malonyl CoA units with *p*-

coumaroyl CoA results in a polyketide that undergoes a Claisen condensation to yield a stilbene acid derivative. Four moles of carbon dioxide are released for every mole of resveratrol formed.⁹ The formation of resveratrol is facilitated by a stilbene synthase namely resveratrol synthase that is present in most species of the *Vitaceae*.

5.3 Syntheses of resveratrol

Resveratrol is present only in small amounts in plant sources and its quantity depends on the stress situation of the plant. Isolation from plant sources is not viable, as it has been reported that only 92 µg of resveratrol are present in one gram of dried grape skins.¹⁰ Reliable and efficient synthetic routes to resveratrol are therefore highly desirable. The first synthetic preparation of resveratrol was achieved in 1941 by Späth and Kromp.¹¹ The synthesis of carbon-carbon double bonds can be achieved by various reactions including the Perkin and Suzuki reactions but it was not until the discovery of the Wittig reaction in 1953 that this area of chemistry intensified. The majority of published routes for the synthesis of resveratrol are based on Wittig like reactions.

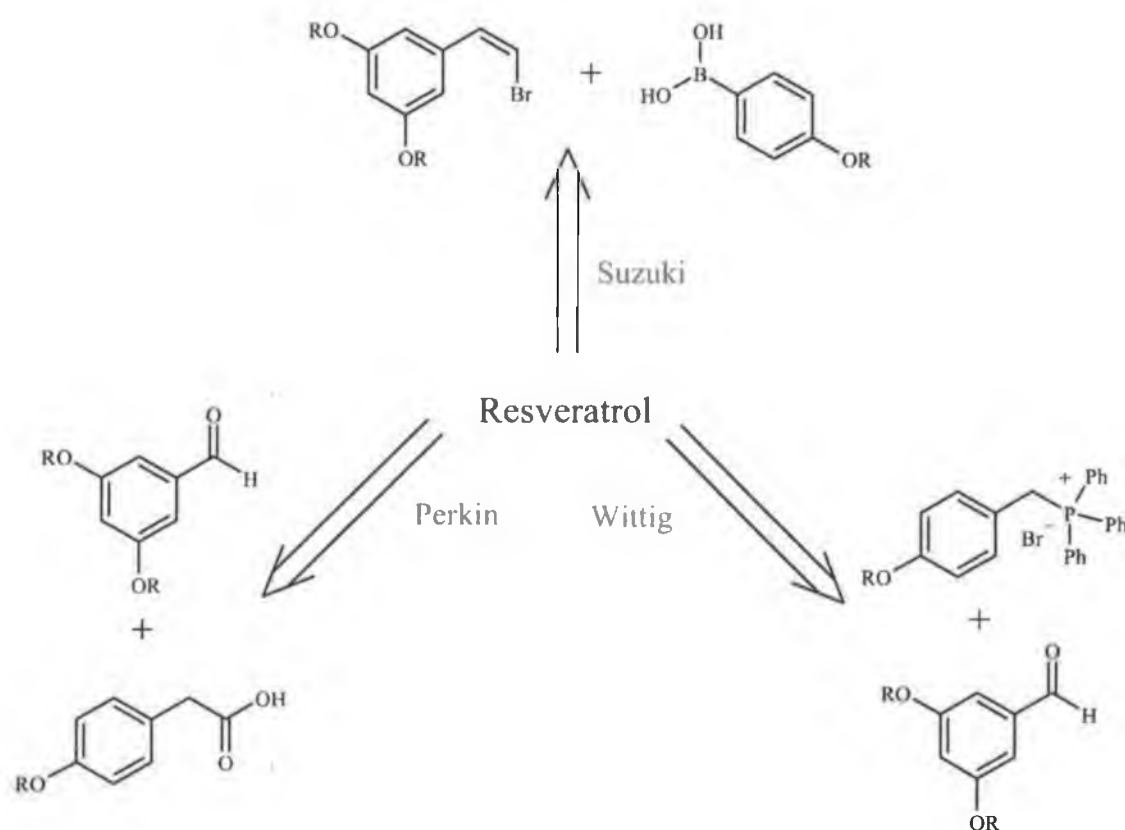


Figure 5.3 Retrosynthetic analysis of resveratrol

The Wittig reaction involves the reaction of an aldehyde or ketone with a phosphorus ylid in the presence of a strong base to furnish an alkene.¹² Phosphorus ylids are prepared by treatment of a phosphonium salt with a base, with the phosphonium salts being prepared from

a phosphine and an alkyl halide. The reaction proceeds with the formation of an oxaphosphetane that in turn due to energetic reasons furnishes a mixture of *E*- and *Z*- alkenes and a triphenylphosphine oxide by-product. The synthesis of resveratrol has been successfully achieved by the Wittig reaction.⁵ The hydroxy groups of the starting materials must be protected for the reaction to proceed successfully. Protection has been achieved with methyl, benzyl and more recently *tert*-butyldimethylsilyl groups.¹³ The main disadvantage of the Wittig reaction is the lack of stereoselectivity in relation to the newly formed double bond. Stereoselectivity has been improved with the use of trialkyl phosphines, a change in solvent or by the addition of salts. The *E*- and *Z*- isomers formed by the Wittig reaction were isolated by column chromatography.⁵

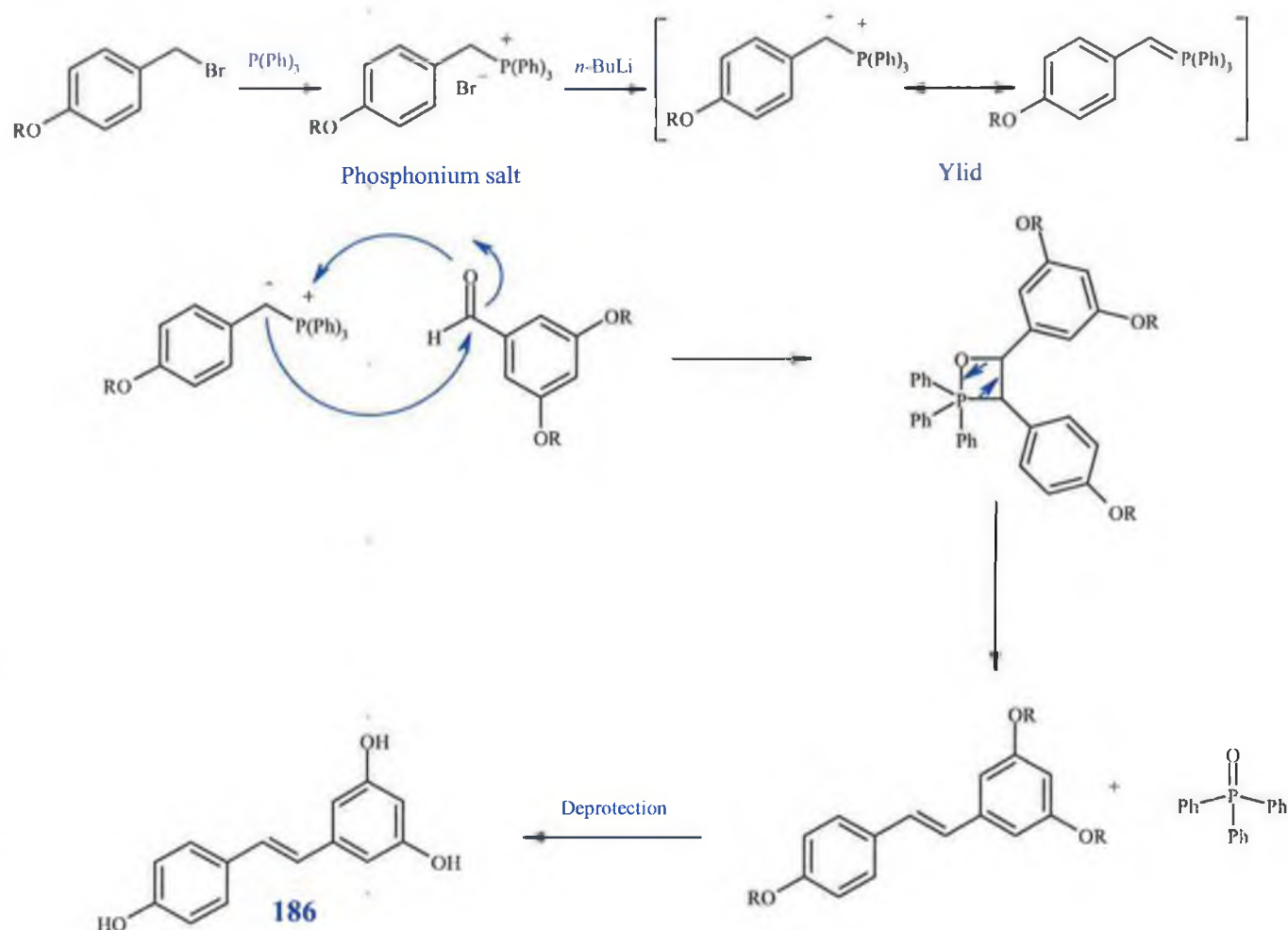


Figure 5.4 Synthesis of resveratrol via the Wittig reaction

The condensation of non-enolizable aromatic aldehydes with anhydrides is called the Perkin reaction.¹⁴ When the anhydride has two α -hydrogen's present, dehydration always occurs giving an aromatic alkenyl carboxylic acid derivative. Usually the salt of the acid is used so that nucleophilic attack on the anhydride regenerates the anhydride. This compound

can then be decarboxylated using a variety of reagents to furnish a mixture of *Z*- and *E*-isomers with the *cis* isomer generally being the most abundant.

Solladié *et al* have developed a synthesis of resveratrol using the Perkin reaction.¹⁵ They reacted 3,5-diisopropoxybenzaldehyde with 4-isopropoxyphenylacetic acid in the presence of acetic anhydride. Isopropyl ethers were used as the protecting groups as they can be easily removed at lower temperatures than their methyl analogues thus avoiding isomerisation of the product. Decarboxylation was carried out using copper chromate yielding the protected resveratrol analogue in a ratio of 79:21 *Z*:- *E*-. Isomerisation was achieved by refluxing the mixture with phenyl disulfide in THF. This step was followed by deprotection of the isopropyl ethers using boron trichloride at -78 °C resulting in a 85% yield of resveratrol.

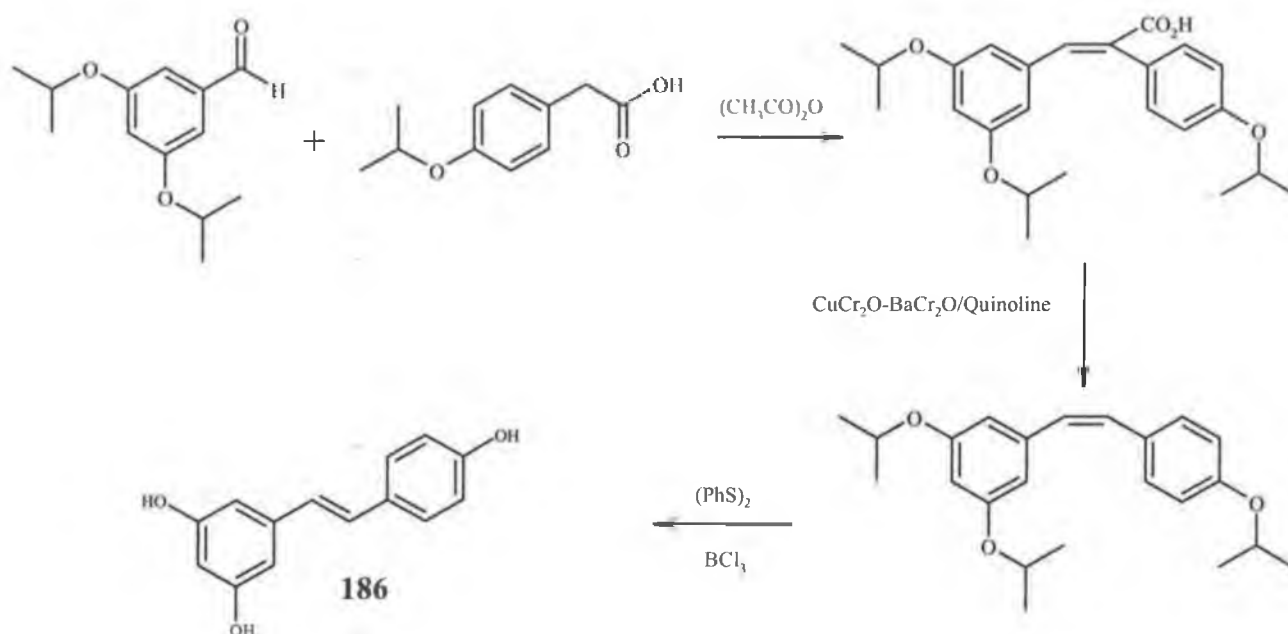


Figure 5.5 Synthesis of resveratrol using the Perkin reaction

The palladium cross coupling of boronic acids with organic halides is known as the Suzuki reaction.¹⁶ It is a highly selective reaction that is generally tolerant of functionality on either coupling partner. This reaction has been used as a successful method for the preparation of fluorinated analogues of resveratrol.¹⁷ The first step of the reaction involved the synthesis of a bromofluoroolefin from the reaction of fluorotribromethane with a substituted aromatic aldehyde in the presence of zinc and a tertiary phosphine. Once again each of the hydroxy groups of resveratrol must be protected. The final step of the reaction involves coupling of the aromatic boronic acid with the bromoolefin. The reaction is

catalysed by a palladium catalyst and is most likely to occur via oxidative addition of Pd(0) to a carbon-boron bond.

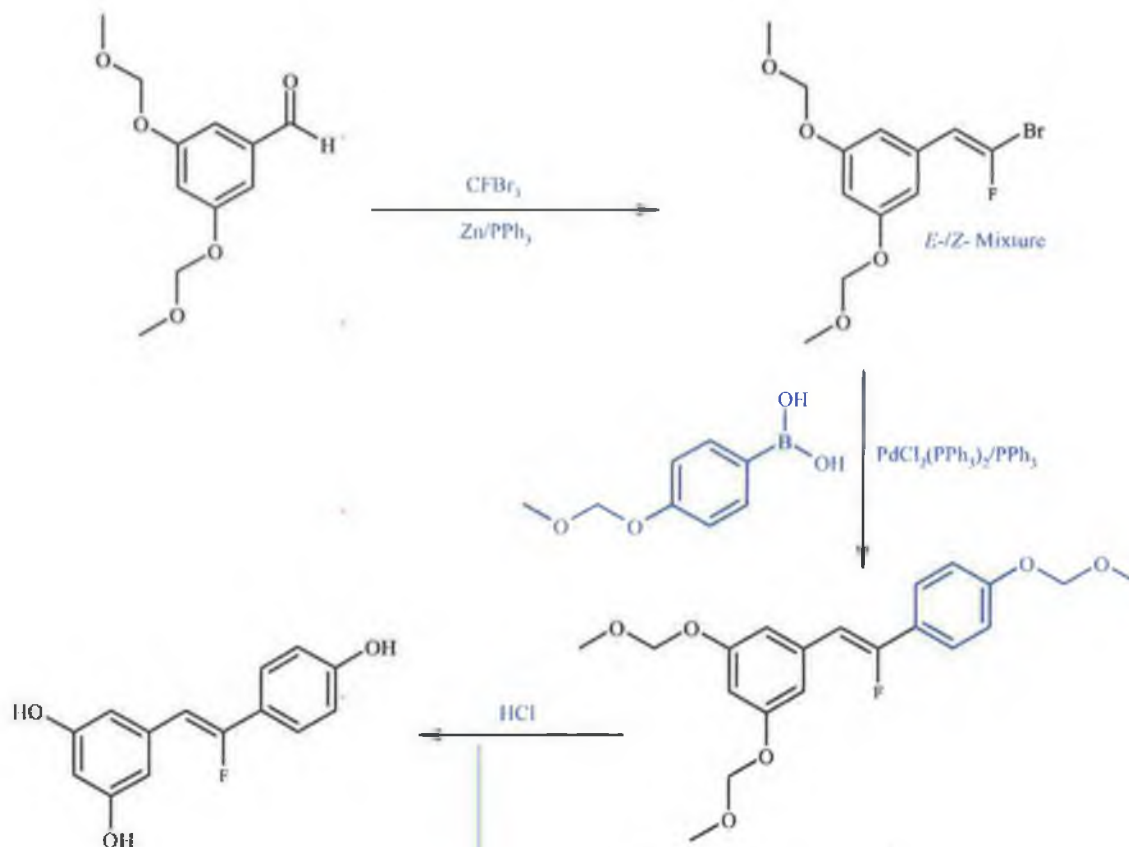


Figure 5.6 Synthesis of fluorinated resveratrol derivatives using the Suzuki reaction.

Resveratrol has been prepared using a variety of synthetic methodologies. The discovery of the Wittig reaction has been seminal in the synthesis of resveratrol and its analogues. To date the majority of synthetic routes available for the synthesis of stilbenes are based loosely on the Wittig reaction with deviations such as the Wadsworth-Emmons and Wittig-Horner prevalent. The success of these routes has been mainly down to the availability of starting materials. The main disadvantage of these routes has been the low yields obtained due in part to the lack of stereoselectivity.

More recently, synthetic routes involving catalysis such as the Heck, Stille and Negishi reactions have come to the fore.¹⁸ These reactions offer a stereospecific synthesis of stilbenes. The main advantage of these coupling reactions is that the yield of a particular isomer is maximised. The other key component with the synthesis of resveratrol analogues is the protection of the hydroxy moieties with easily removable groups. To date there are very few protecting groups that can be removed under mild conditions. This will be a key challenge for the development of stilbene analogues that contain highly reactive substituents.

5.4 Synthesis and structural characterisation of fluorinated analogues of resveratrol

Resveratrol is a natural phytoalexin produced in various plants and has been shown to have a variety of biological properties including antileukemic, antiplatelet aggregation, antifungal, antibacterial, anticancer, estrogenic and cardioprotective activities.² The synthesis of resveratrol has been achieved by various methods including the Wittig, Perkin and Suzuki reactions. Fluorinated resveratrol analogues have been shown to possess potent anti cancer activity.¹⁹ The incorporation of a fluorine atom into a drug molecule has been well documented. Aromatic fluorination increases lipophilicity, acidity and alters the hydrogen bonding properties of a molecule. Fluorine also influences the biological stability of a drug molecule through altering susceptibility to metabolism. Fluorine has been used as a means to developing safer and more reactive pharmaceuticals due to the strength of the carbon-fluorine bond that is very difficult to metabolise, so harmful and unproductive side reactions are unlikely to occur. The replacement of a hydroxyl group by a fluorine atom is a strategy widely used in drug development to alter biological function.²⁰ Fluorine has a Van der Waals radius of 1.47 Å that is positioned between oxygen (1.52 Å) and hydrogen (1.20 Å) allowing it to mimic a hydroxyl group and play a part in hydrogen bonding properties. Fluorine substitution has been widely used to extend the half-life of many synthetic compounds and thereby produce drugs with a longer duration of action.²¹

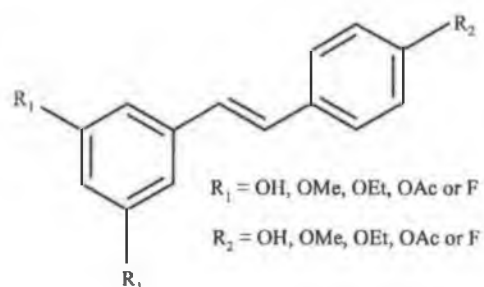


Figure 5.7 Targeted fluorinated analogues of resveratrol

The synthesis of the fluorinated analogues **187-195** was first attempted by the classical Wittig reaction. The triphenyl phosphonium salts were prepared from the reaction of triphenylphosphine and the relevant benzyl bromide in high yield. The benzyl bromides were synthesised from the reaction of the benzyl alcohol and phosphorus tribromide. The Wittig reaction was carried out using *n*-butyl lithium at -78 °C. The Wittig reaction yielded both the *cis* and *trans* isomers in almost equal quantities. Separation of these isomers proved difficult and the overall yield of the *trans* isomer was poor. This problem led to the utilisation of a stereospecific reaction whereby only the required *trans* isomer was prepared. The reaction selected was the Wadsworth-Emmons deviation of the Wittig reaction. The two main

advantages of the Wadsworth-Emmons reaction over the Wittig reaction was that the phosphonate byproduct formed from the Wadsworth-Emmons reaction is water soluble and hence easily removable and secondly the reaction yields only the *E*- configuration. Wadsworth and Emmons believed that the reaction was not in fact stereospecific and that initially both *cis* and *trans* isomers were formed as in the Wittig reaction.²² However under strongly basic conditions at elevated temperatures the isomerisation of *cis*-stilbene to *trans*-stilbene would be expected. The phosphonate esters were prepared from the *Michaelis-Arbuzov* reaction whereby a benzyl bromide was reacted with triethyl phosphite to yield the benzyl phosphonate ester in quantitative yield. These ester derivatives were purified by vacuum distillation. The Wadsworth-Emmons reaction was carried out in 1,2-dimethoxyethane, using sodium hydride as a powerful base. The reaction proceeded as expected but there was a large quantity of unreacted aldehyde observed in the ¹H NMR. The separation of this aldehyde starting material from the product was often unattainable depending on the substitution on the phenyl ring. This failure led to the utilisation of another stereospecific reaction, namely the Heck reaction.

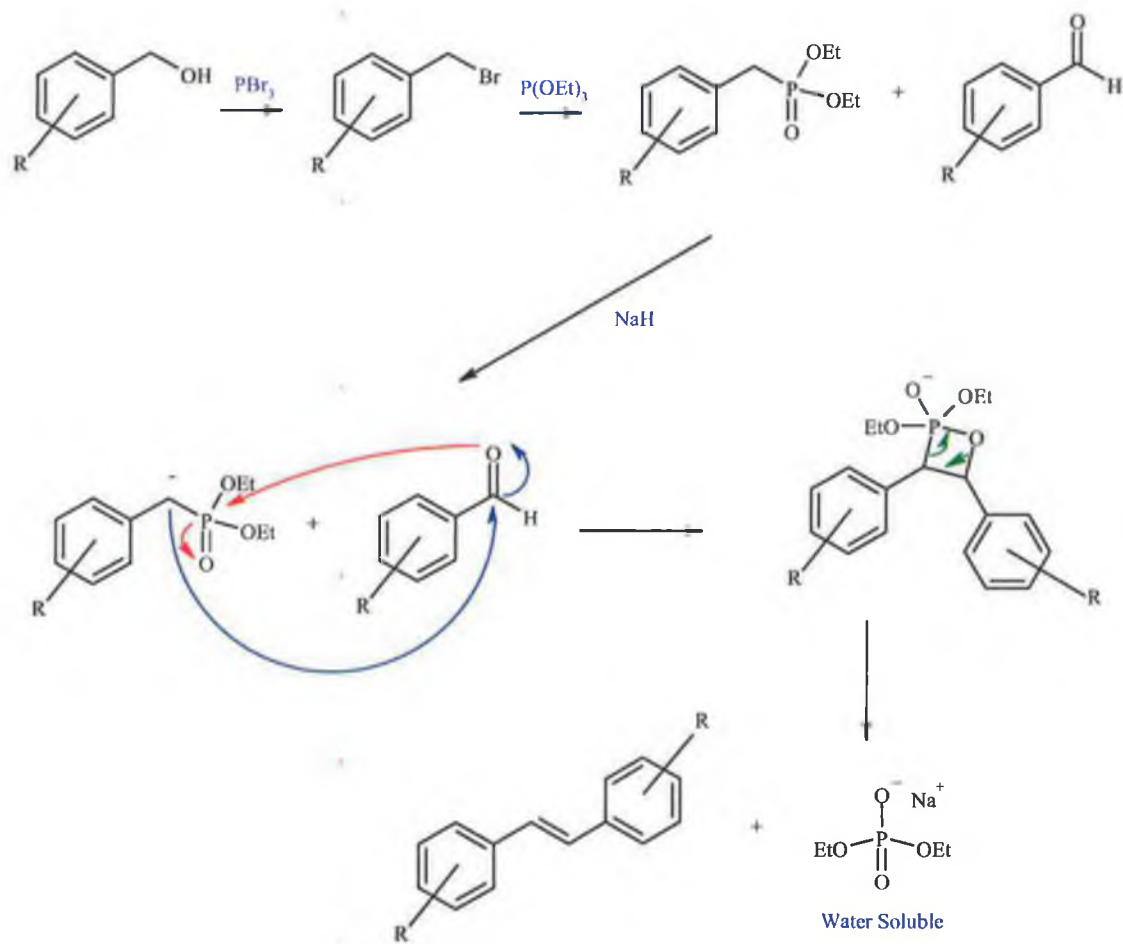


Figure 5.8 The Wadsworth-Emmons reaction

A decarbonylative Heck reaction has been described as an efficient method of synthesising resveratrol.²³ Aryl chlorides react with activated alkenes in presence of a tertiary amine and a catalytic amount of palladium acetate to give arylated alkenes.²⁴ The reaction involves a highly efficient decarbonylation of the aryl chloride. The reaction is not particularly sensitive to substituents in the aryl chloride although strongly electron-donating groups have been shown to be advantageous. With mono-substituted alkenes the trans isomer was formed with almost complete specificity.

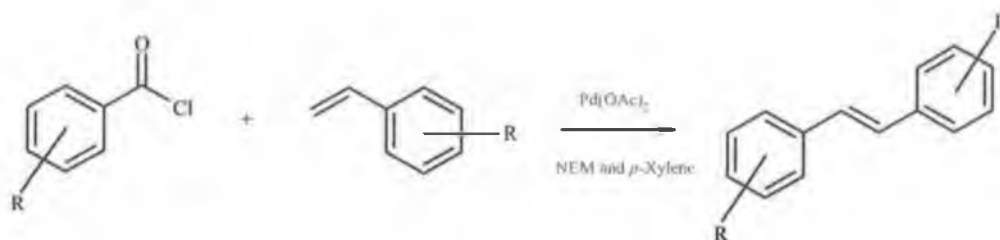


Figure 5.9 The decarbonylative Heck reaction

The best results have been obtained by using tertiary bases with pK_a values in the range 7.5-11. Weak bases were shown to facilitate a slower reaction whereas strong bases would react with the aryl chloride.²⁴ *N*-Ethylmorpholine (NEM) was shown to be the most effective base as it did not react with aryl chlorides nor did it cleave the bond between strongly electron-withdrawing groups and the aryl chloride. The solvent used was *p*-xylene as optimisation of the reaction showed that the best results were achieved at 120-130 °C.

Blaser and Spencer have proposed a mechanism for the decarbonylative Heck reaction.²⁴ Only the reacting groups are shown as little is known about the ligands occupying the vacant coordination sites. The first step is believed to involve oxidative addition of the aryl chloride to a palladium (0) species. The palladium (0) species is believed to be the product of a preliminary reduction of palladium acetate caused by perhaps the alkene or the base. If there are no strongly bound ligands occupying the other coordination sites, aryl migration to the metal should be facilitated. The release of carbon monoxide is expected as there is no ligands present capable of stabilising a palladium (II) carbonyl at high temperature. Alkene coordination is proposed as the next step although it is quite probable that the alkene is present as a ligand throughout the reaction. *Syn* addition of the alkene gives an intermediate that undergoes internal rotation about the central carbon-carbon bond to place H and H-Pd-Cl *syn* to each other. Following this the palladium is cleaved, the double bond is formed with the regeneration of Pd(0). It has been shown that the cumulative effect of multiple electron-withdrawing groups has a detrimental effect on the yield of the reaction.²⁴

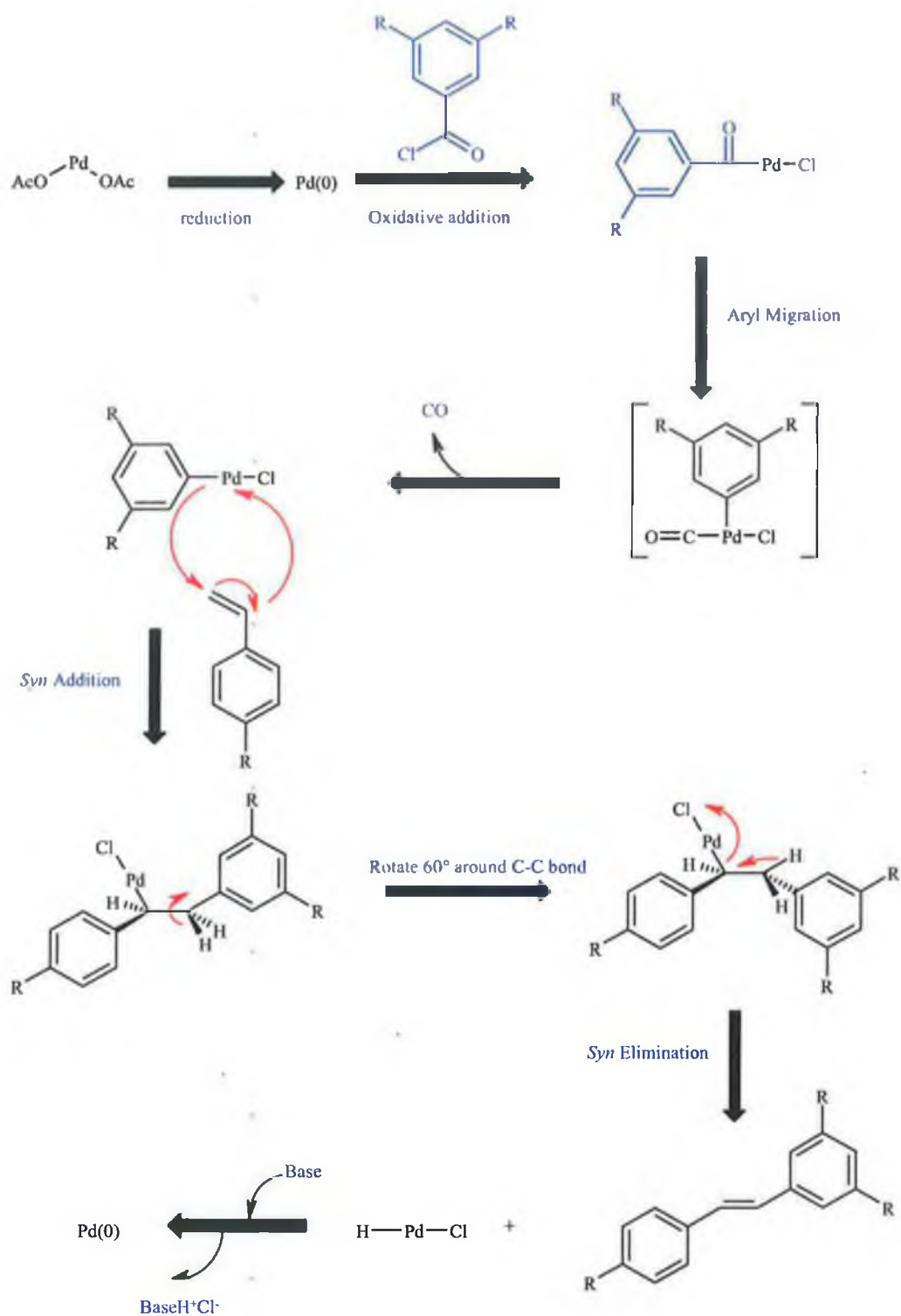


Figure 5.10 Proposed mechanism of the decarbonylative Heck reaction

The decarbonylative Heck reaction gives almost complete specificity for the formation of *E*-isomers with monosubstituted alkenes. There are no sterically bulky ligands present so this steric specificity must be due to electronic factors. The expense of this reaction is somewhat reduced due to the regeneration of a palladium adduct.

The synthesis of the fluorinated analogues **187-195** was successfully achieved using the decarbonylative Heck reaction. 3,5-Diacetoxybenzoyl chloride was prepared from the reaction of 3,5-diacetoxybenzoic acid with phosphorus pentachloride. This benzoic acid was synthesised according to the literature.²⁵ The highest yield recorded for the decarbonylative Heck reaction was 65% for compound **193** with the lowest yield of 19% for compound **190**. The results of this reaction show that the difluoro-substituted phenyl ring always gives a poorer yield in contrast with the yields involving a monofluoro-substituted phenyl ring. For example the difluoro derivative **190** gave a yield of 19%. The analogous monofluoro derivative **191** gave a higher yield of 29%. This fact is due to the cumulative effects of multiple electron-withdrawing groups on the aroyl chloride. Electron-donating groups have been shown to improve the yield of the decarbonylative Heck reaction but electron-withdrawing groups have been shown to have a negative effect on the yield.²⁴ Compound **194** was prepared by firstly synthesising its acetoxy analogue followed by treatment with ammonium acetate to deprotect the acetoxy group.²⁶ Compound **195** was prepared using analogous methodology but in this case ammonium acetate only deprotected one of the available two acetoxy groups.

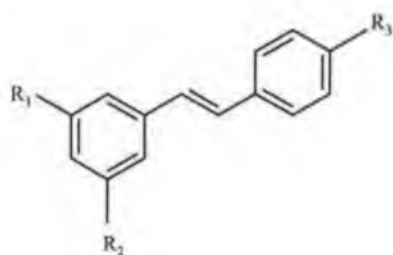


Table 5.1 Fluorinated analogues of resveratrol

Compound	R ₁	R ₂	R ₃	% Yield
187	-F	-F	-F	48
188	-F	-F	-OCH ₃	22
189	-OCH ₃	-OCH ₃	-F	26
190	-F	-F	-OCH ₂ CH ₃	19
191	-OCH ₂ CH ₃	-OCH ₂ CH ₃	-F	29
192	-F	-F	-OCOCH ₃	58
193	-OCOCH ₃	-OCOCH ₃	-F	65
194	-F	-F	-OH	81 ^a
195	-OH	-OCOCH ₃	-F	76 ^a

^a % Yield of deprotection step.

The Infrared spectra of these derivatives show distinctive bands at $\sim 1100\text{ cm}^{-1}$ representing the ether moieties. Compounds **192** and **193** show carbonyl bands at $\sim 1700\text{ cm}^{-1}$. The ^{19}F NMR spectra of these derivatives show the 3,5 difluoro analogues appearing as triplets at $\delta \sim 35$ with coupling constants of approx. 5 Hz. The 4-fluoro derivatives appear as multiplets centred at $\delta \sim 38$ due to the effect of ^{19}F - ^1H coupling.

5.4.1 ^1H NMR study of the fluorinated resveratrol analogues

The ^1H NMR spectrum of compound **191** is shown in Figure 5.12. The stereoselectivity of the decarbonylative Heck reaction was confirmed by ^1H NMR. The unsaturated unit appeared as two doublets at $\delta \sim 7.28$ and $\delta \sim 7.13$ with coupling constants of approx. 16.4 Hz. They appear as doublets due to vicinal coupling with each other. If there was any *Z*-isomer present the double bond protons would also appear as doublets. The main difference between *E*- and *Z*-isomers in ^1H NMR is the size of the coupling constant. *E*-isomers show greater coupling constants due to superior overlap of orbitals. The orbitals of a *Z*-isomer are not parallel so not as much orbital overlap is possible.²⁷ *Z*-isomers generally record coupling constants between 7 and 11 Hz whereas *E*-isomers have coupling constants between 15 and 18 Hz.

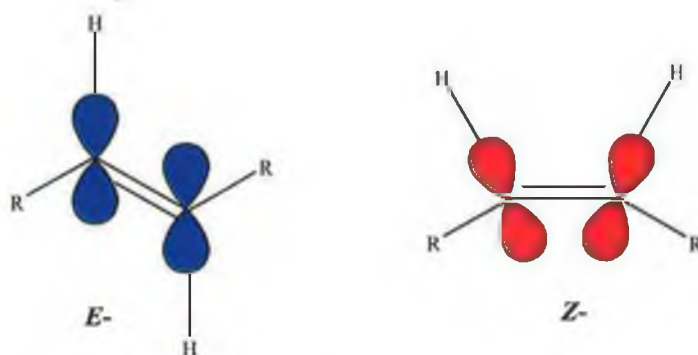


Figure 5.11 Orbital alignment for *E*- and *Z*-isomers

The 3,5-dialkoxy derivatives **189**, **191**, **193** and **195** are good examples of *meta*-coupling in the ^1H NMR. The proton in the *para* position couples with the two protons in the *ortho* positions to give a triplet at $\delta \sim 6.43$ with a coupling constant of ~ 2.4 Hz. This four-bond coupling is facilitated by effective orbital overlap.²⁷ The same coupling is responsible for the doublets that appear for the *ortho* protons in analogous compounds. These appear as doublets at $\delta \sim 6.78$ with a coupling constants of ~ 2.4 Hz. Similar coupling patterns is not seen for the 3,5-difluoro analogues as ^1H - ^{19}F coupling obscures the spectra. The hydrogen atoms attached to fluorinated phenyl rings appear as multiplets due to ^1H - ^{19}F coupling. The only exception is the protons that appear in the *ortho* position next to the fluorine substituent

in compound **191**. The protons in the *meta* positions of this compound appear as multiplets due to ^1H - ^{19}F coupling. The alkoxy substituents appear as expected. The hydroxy, methoxy and acetoxy appear as singlets at $\delta \sim 6.13$, $\delta \sim 3.76$ and $\delta \sim 2.32$ respectively. The ethoxy methylene group appears as a quartet with a coupling constant of 7.2 Hz at δ 4.03 and as a triplet representing the methyl group with a coupling constant of 7.2 Hz at δ 1.33.

Table 5.2 Selected ^1H NMR data (δ) for the fluorinated resveratrol derivatives

Compound No.	ArH 4	ArH 2 & 6	C=C-H	ArH 3 & 5
187	7.15-7.20	7.24-7.32	7.48, 7.24-7.32	7.38-7.41
188	7.01-7.10	7.27-7.30	7.35, 7.01-7.10	6.96
191	6.39	6.74	7.27, 7.10	7.20
192	7.08-7.14	7.32-7.36	7.44, 7.23	7.17
195	6.49	6.78	6.97, 6.85	7.01-7.06

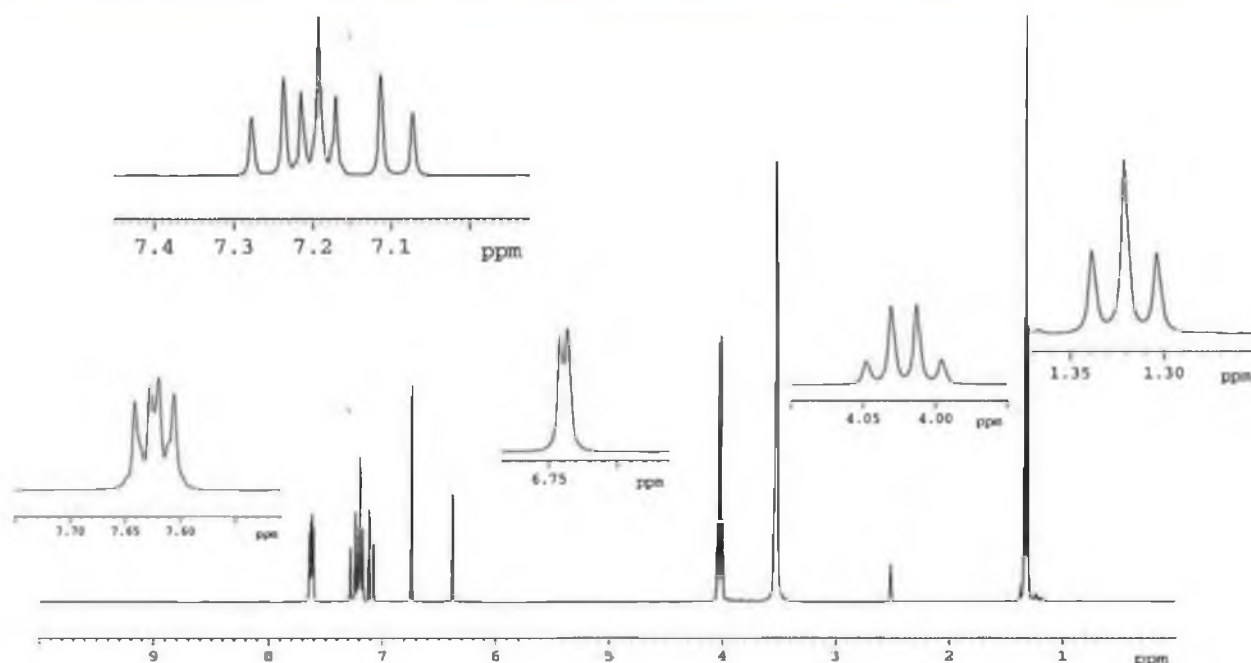


Figure 5.12 ^1H NMR spectrum of (*E*)-1-(4-fluorostyryl)-3,5-diethoxybenzene **191**.

5.4.2 ^{13}C NMR study of the fluorinated resveratrol analogues

The ^{13}C NMR spectrum of compound **191** is shown in Figure 5.13. The effect of ^{19}F - ^{13}C coupling is seen throughout the spectra. The aromatic carbons of the fluorinated ring appear as doublets and triplets due to this coupling. The carbon atom of the phenyl ring to which the fluorine atom is bonded appear as doublets. This appears the furthest downfield at $\delta \sim 163$ due to the electronegative nature of fluorine. There are some notable differences between the mono- and difluoro analogues. The chemical shifts of the double bond carbon atoms in the difluoro derivative compound **188** appear at δ 131.4 and δ 124.2. The chemical

shift of the analogous carbon atoms in the monofluoro derivative compound **189** appear a lot closer together at δ 128.7 and δ 128.0. The trifluoro derivative compound **187** has chemical shifts of $\delta \sim 130$ and $\delta \sim 126$ for the carbon atoms of the unsaturated unit. The carbon atoms of the phenyl rings that are bonded to an oxygen atom appear downfield at $\delta \sim 159$ due to the deshielding effect of the attached oxygen. The acetoxy derivatives **192** and **193** show the analogous carbon atoms appearing further upfield at $\delta \sim 150$. The chemical shift of the *para* carbon in the disubstituted phenyl ring appears at approximately the same resonance frequency for both the difluoro and dialkoxy derivatives. The main difference is the fact that it appears as a triplet in the difluoro- derivatives due to ^{19}F - ^{13}C coupling but as a singlet in the dialkoxy derivatives. The only exceptions are compounds **193** and **195** that have an acetoxy group in the 3- and/or 5- position. The acetoxy moiety has the ability to shift the attached carbon upfield but it also alters the chemical shift of the carbon atom *ortho* to the substituted carbon. The *para* carbon appears downfield at $\delta \sim 114.2$ with the *ortho* carbon also appearing downfield at $\delta \sim 117.2$.

Table 5.3 Selected ^{13}C NMR data (δ) for the fluorinated resveratrol derivatives

Compound No.	C-F	C=C	C-OR	C _{para}
187	164.2, 162.3, 161.8	130.6, 126.4	-	102.9
188	164.2, 161.8	131.4, 124.2	159.8	102.4
191	162.0	128.6, 127.9	160.2	100.9
192	164.2, 161.8	130.8, 126.6	150.7	102.7
195	162.9	129.1, 127.6	157.2, 151.9	108.8

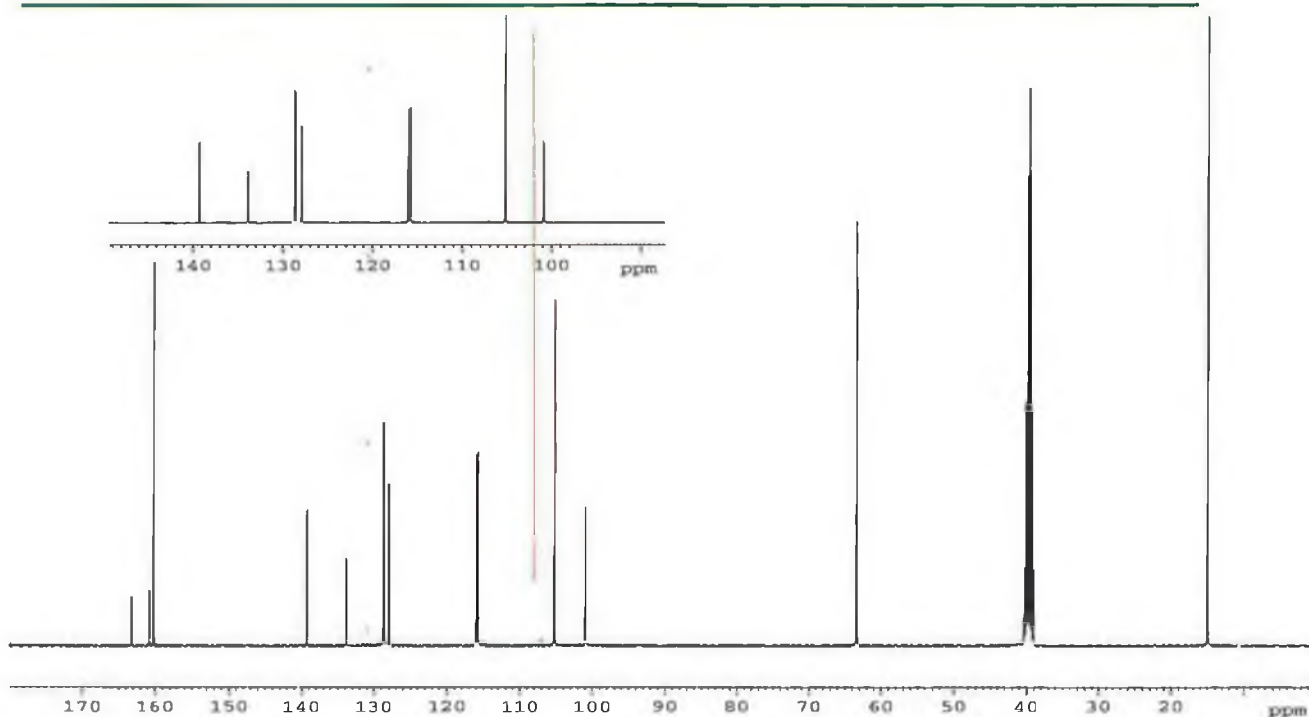


Figure 5.13 ^{13}C NMR spectrum of (*E*)-1-(4-fluorostyryl)-3,5-diethoxybenzene **191**.

5.5 Biological activity of the fluorinated resveratrol analogues

5.5.1 Introduction

Resveratrol exhibits a wide range of biological properties including antifungal, antibacterial, antiviral, estrogenic, platelet aggregation and anticancer activities.² Cancer is a group of diseases characterized by uncontrolled growth and spread of abnormal cells often leading to death.²⁸ Resveratrol has been shown to inhibit the growth of various cancer cell lines. It has been shown to provide cancer chemopreventative effects in different systems based on its potent inhibition of diverse cellular events associated with tumour initiation, promotion and progression.⁵

Chemoprevention can be defined as the prevention or reduction of cancer risk by the ingestion of natural or synthetic compounds with low toxicity that are able to suppress, delay or reverse carcinogenesis.³ The use of tamoxifen in breast cancer is one of the best examples of chemoprevention.³ This stilbene derivative is administered for five years following surgery for breast cancer and it has been found to reduce the risk of tumour recurrence. The cancer chemopreventative activity of resveratrol is due to its ability to activate apoptosis.

Apoptosis is defined as programmed cell death.²⁹ Commonly used chemotherapeutic drugs can induce this form of cell death. Apoptosis may therefore function as a common mechanism of removing unrepairable genetic lesions from cells. Recent studies have shown that cytochrome c release from the mitochondria is a key component in the activation of caspases leading to apoptosis.²⁹ Resveratrol has been shown to have the ability to selectively induce apoptosis in leukemic cells but not in normal haematopoietic cells.³⁰ The p53 gene is one of the most important tumour suppressor genes and mutation or loss of this gene is believed to be responsible for more than half of human cancers.³¹ The p53 protein is critical for apoptosis and lack of p53 expression or function is associated with an increased risk of tumour formation. Resveratrol induces p53 dependent transcriptional activation. Resveratrol induced apoptosis occurs in cells expressing p53 but not in p53 deficient cells. This resveratrol-induced activation of p53 is also partly due to the activities of extracellular signal regulated protein kinases and p38 kinase and their phosphorylation of p53 at serine 15 that plays a critical role in the stabilization, up-regulation and functional activation of p53.³²

The synthesis of fluorinated stilbene analogues has provided potent cell growth inhibitors of leukaemia.¹⁷ The introduction of a fluorine atom often brings about an improvement in bioactivity mainly due to alteration of metabolism and increased lipophilicity. It is hoped that the synthesis of novel fluorinated analogues of resveratrol will produce potent selective drugs with anticancer activity against a range of cancer cell lines.

5.5.2 Anticancer potential of fluorinated resveratrol analogues

Four compounds namely **187**, **188**, **189** and **192** were assessed for their anticancer ability by the National Cancer Institute under the Development Therapeutic Program (DTP). It was hoped that these preliminary results would indicate the potential anticancer activity of the fluorinated resveratrol analogues. The compounds were firstly assessed using a primary anticancer screen. Previous work carried out by the DTP has used an *in vitro* model consisting of 60 human tumour cell lines as the primary anticancer screen. Analysis of this data indicated that approx. 95% of the actives from the 60 cell line screen can be identified using only three lines. For this reason the DTP is now using a three cell line panel consisting of MCF7 (Breast), NCI-H460 (Lung) and SF-268 (CNS) as its primary anticancer assay. This 3-cell line, one dose assay has been in use by the DTP for several years for the evaluation of combinatorial libraries and has proven to be an effective pre-screen. The inclusion of this assay allows for a more detailed evaluation of agents that have exhibited some ability to inhibit the growth of human tumour cells in culture.

In this assay each cell line was inoculated and preincubated on a microtiter plate. Test agents were then added at a single concentration and the culture was incubated for 48 hours. End point determinations were made with alamar blue. Results for each test agent were reported as the percent of growth of the treated cells when compared to the untreated control cells. Compounds that reduce the growth of any one of the cell lines to approx. 32% or less are passed on for evaluation in the full panel of 60 cell lines over a 5-log dosage. Negative numbers indicate cell kill.

Table 5.4 The growth percentage of human tumour cells in culture when treated with various fluorinated analogues of resveratrol compared to the untreated control cells

Compound	Conc. μM	Breast	Lung	CNS
187	100	82	101	111
188	100	84	105	111
189	100	67	60	105
192	100	22	7	1

The results of this assay indicate that fluorinated analogues of resveratrol may have potential as anticancer agents. Compounds **187** and **188** showed mild toxicity against the breast tumour cell lines with approx 20% inhibition recorded but no inhibition of growth was measured against the lung or CNS cell lines. Compound **189** showed improved activity

against both the breast and lung cell lines with 40% inhibition recorded for the lung tumour cell lines. The difluoro derivative compound **192** was the most potent analogue against breast, lung and central nervous system tumour cells. It was shown to limit the growth of breast cancer by 78 %. The lung cancer cells only increased by only 7% when treated with compound **192**. The most interesting result is the fact that this compound managed to limit the growth of CNS tumour cells by 99% over a two-day period. These results indicated that compound **192** was a prime candidate for evaluation in the full panel of 60 cell lines.

Compound **192** was then assessed in the 60 cell line assay that included human tumour cells from leukaemia, lung cancer, colon cancer, central nervous system, melanoma, ovarian cancer, renal cancer, prostate cancer and breast cancer. The IC₅₀ and GI₅₀ values were calculated for each cell line. The IC₅₀ value refers to the concentration required to achieve a 50% survival of the available cells whereas the GI₅₀ value refers to the concentration required to inhibit the growth of the tumour by 50%.

Table 5.5 Pharmacological values of compound **192** against various tumour cell lines

Tumour Cell Line	IC ₅₀ μM	GI ₅₀ μM
Leukaemia HL-60 (TB)	116.74	54.59
Lung EKVX	116.74	78.26
Colon HT29	80.64	73.69
CNS SNB-75	90.92	60.34
Melanoma SK-MEL-28	83.09	70.11
Ovarian SK-OV-3	96.54	83.09
Renal RXF 393	202.35	75.94
Prostate DU-145	127.74	100.48
Breast T-47D	127.74	79.84

From these results it can be seen that compound **192** has broad spectrum anticancer activity. This compound was seen to be most active as an anticancer agent against the colon tumour cell line and gave an IC₅₀ value of 80.64 μM. It was seen to inhibit the growth of cancer most effectively with the leukaemia cell line giving a GI₅₀ value of 54.29 μM. Although the cytotoxicity of compound **192** is not dramatic it is comparable to previously published results.³³ The biological activities of resveratrol analogues have been best utilised by chemoprevention and cancer growth inhibition. Cytotoxicity has not been shown to be an essential component of potent growth inhibition and chemopreventative agents.

5.6 Synthesis and characterisation of 3,5-difluorophenyl resveratrol analogues

Preliminary results indicated that compound **192** exhibited anticancer activity against a variety of tumour cell lines. This led to the development of a series of analogues based on the scaffold of **192**. The unique nature of a 3,5-difluorostilbene exhibiting anticancer properties led to the derivitisation of the 4-position. It was hoped that by altering the lipophilicity, hydrogen bonding properties and steric size of the substituent present at the 4-position that an enhancement of anticancer activity would be achieved. It was decided to incorporate the trichloroacetyl, trifluoroacetyl, trimethylacetyl, methanesulphonyl, 4-fluorobenzenesulphonyl and 2-fluorobenzoyl moieties in an attempt to improve bioactivity.

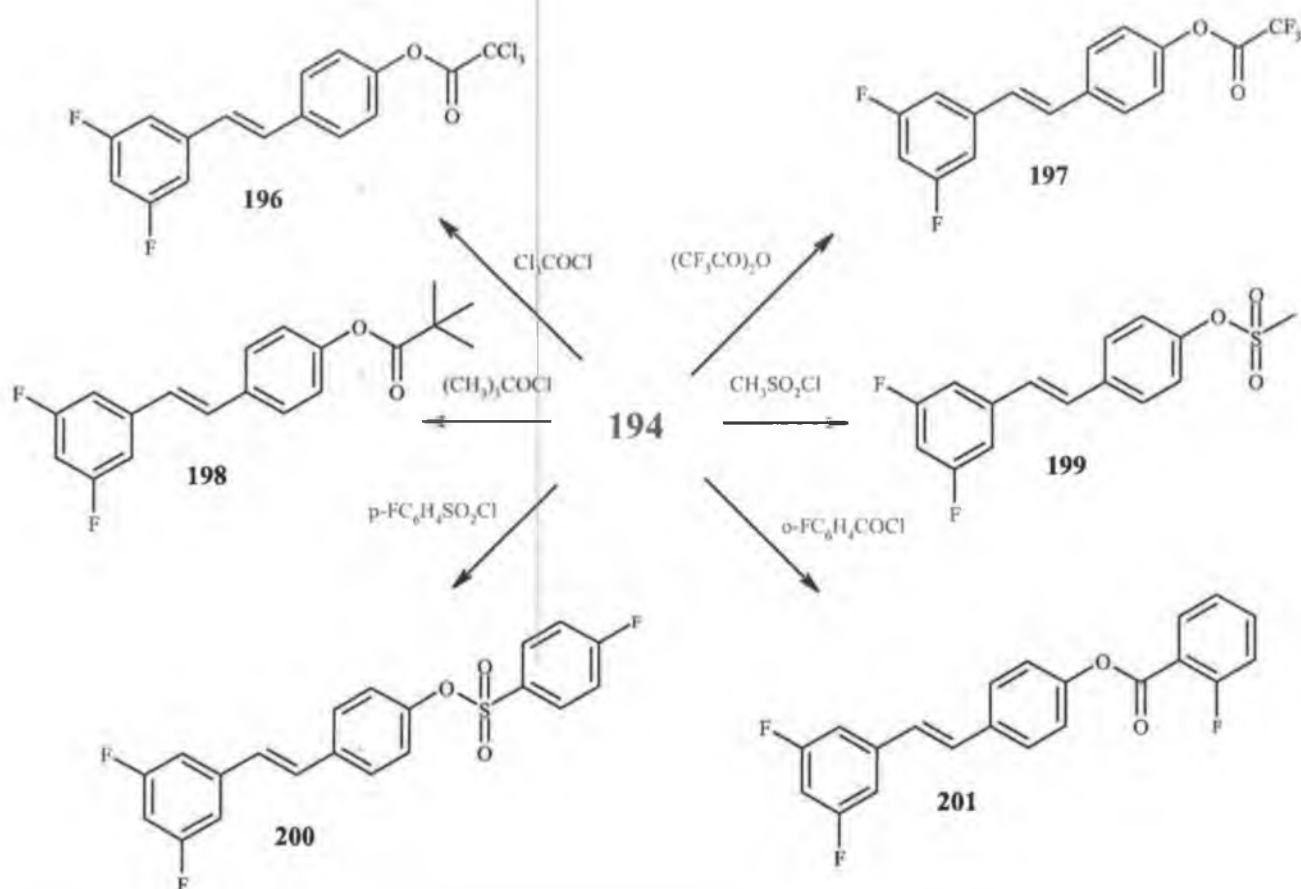


Figure 5.14 Synthesis of 3,5-difluorophenyl resveratrol derivatives

The synthesis of these compounds was achieved by firstly preparing compound **194** from the decarbonylative Heck reaction. This compound was then reacted with a series of chlorides and anhydrides to synthesise the desired derivatives in yields ranging between 50 and 78 %. The highest yield was recorded for compound **198** with a value of 78%. The 4-fluorobenzenesulphonyl derivative **200** gave the lowest yield. Although the trifluoroacetyl moiety is sterically related to the trichloroacetyl and trimethylacetyl groups, the yield of **197** was less than its trichloro- and trimethyl- analogues. This is probably due to the fact that an

anhydride was used to prepare **197** and not a chloride. The use of trifluoroacetyl chloride was not used as it was only available in a gaseous form. The yields of compounds **200** and **201** were the lowest due to steric hindrance as the substituents being introduced were by far the bulkiest groups.

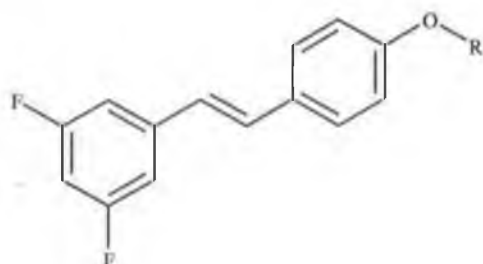


Table 5.6 3,5-difluorinated analogues of resveratrol

Compound	R	¹³ C NMR δ C _{ipso}	m.p. °C	% Yield
196	-COCCl ₃	150.6	92-94	74
197	-COCF ₃	141.4	139-141	61
198	-COC(CH ₃) ₃	151.5	79-81	78
199	-SO ₂ CH ₃	149.2	85-87	71
200	-SO ₂ - <i>p</i> -F-C ₆ H ₄	149.4	71-73	50
201	-CO- <i>o</i> -F-C ₆ H ₄	150.9	118-120	52

The ¹H NMR spectra of these derivatives were very similar to the previously described 3,5-difluoro resveratrol analogues **188**, **190**, **192** and **194**. The substituent present at the 4-position had little effect on the attached phenyl ring. The 2-fluorobenzoyl substituent in compound **201** shifted the protons in the *meta* and *ortho* positions the furthest downfield to δ 7.47 and δ 7.09-7.20 respectively. The *tert*-butyl and methylsulphonyl moieties appear as singlets at δ ~1.27 and δ ~3.08. The ¹³C NMR spectra show analogous pattern to that of the previously discussed 3,5-difluoro resveratrol analogues. The only exception is compound **197** where the effect of the trifluoroacetyl moiety is seen throughout the spectra of the attached phenyl ring. The trifluoromethyl group appears as a triplet at δ 141.4 due to ¹⁹F-¹³C coupling with the carbonyl appearing at δ 156.3. This carbonyl appears at considerably higher field to that of compounds **196** and **201**. The carbonyls of these derivatives generally appear at δ ~162. The carbonyl of the trimethylacetyl moiety is seen the furthest downfield at δ 177.4. The trifluoroacetyl moiety had a distinct effect on the chemical shifts of the carbon atoms in the attached phenyl ring. The *ipso* carbon generally appeared at δ ~150 but in compound **197**

the analogous carbon was shifted upfield to δ 141.4. A similar result was observed for the *ortho* and *para* carbons although this effect was not seen for the *meta* carbons that appeared at a chemical shift common to each derivative. The ^{19}F NMR spectra showed the 3,5-difluorophenyl ring appearing as a triplet at $\delta \sim 34.6$ with a ^{19}F - ^{13}C coupling constant of ~ 7.8 Hz. The fluorine atoms present on the phenyl rings of the benzoyl and benzenesulphonyl moieties appeared as multiplets centred at $\delta \sim 32$ and $\delta \sim 26$ with the benzoyl fluorine appearing at lower field. The fluorine atoms of the trifluoromethyl group appeared as a singlet at $\delta \sim 0.5$ due to their equivalence. The Infrared spectra of these derivatives show C-H stretching of the unsaturated unit appearing at $\sim 3050\text{ cm}^{-1}$. There are two or three bands shown at $\sim 1550\text{ cm}^{-1}$ responsible for the aromatic rings. Compound **199** has two strong bands present at ~ 1200 and 1400 cm^{-1} due to the O-SO₂ moiety. Compounds **196**, **197**, **198** and **201** show absorption peaks due to the carbonyl groups at $\sim 1740\text{ cm}^{-1}$.

5.6.1 HMQC study of (*E*)-4-(3,5-difluorostyryl)phenylmethanesulphonate **199**

Heteronuclear multiple quantum correlation (HMQC) is a 2D NMR spectroscopic technique which correlates the carbon and proton spectra. Table 5.7 and Figures 5.15 to 5.16 show the C-H correlation spectrum of (*E*)-4-(3,5-difluorostyryl)phenylmethanesulphonate **199**.

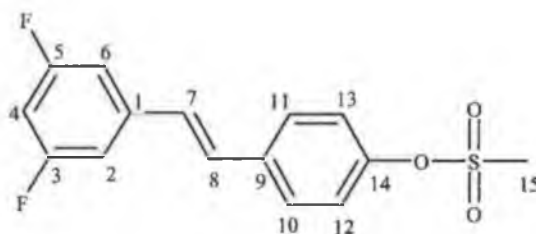


Table 5.7 C-H correlation of (*E*)-4-(3,5-difluorostyryl)phenylmethanesulphonate **199**

Site	^1H	^{13}C	HMQC
1		140.6	
2	6.84-6.92		109.6
3		164.8	
4	6.59-6.62		103.4
5		162.5	
6	6.84-6.92		109.5
7	6.96		128.1
8	6.84-6.92		129.9
9		136.1	
10 & 11	7.43		128.6
12 & 13	7.19		122.8
14		149.2	
15	3.08		37.8

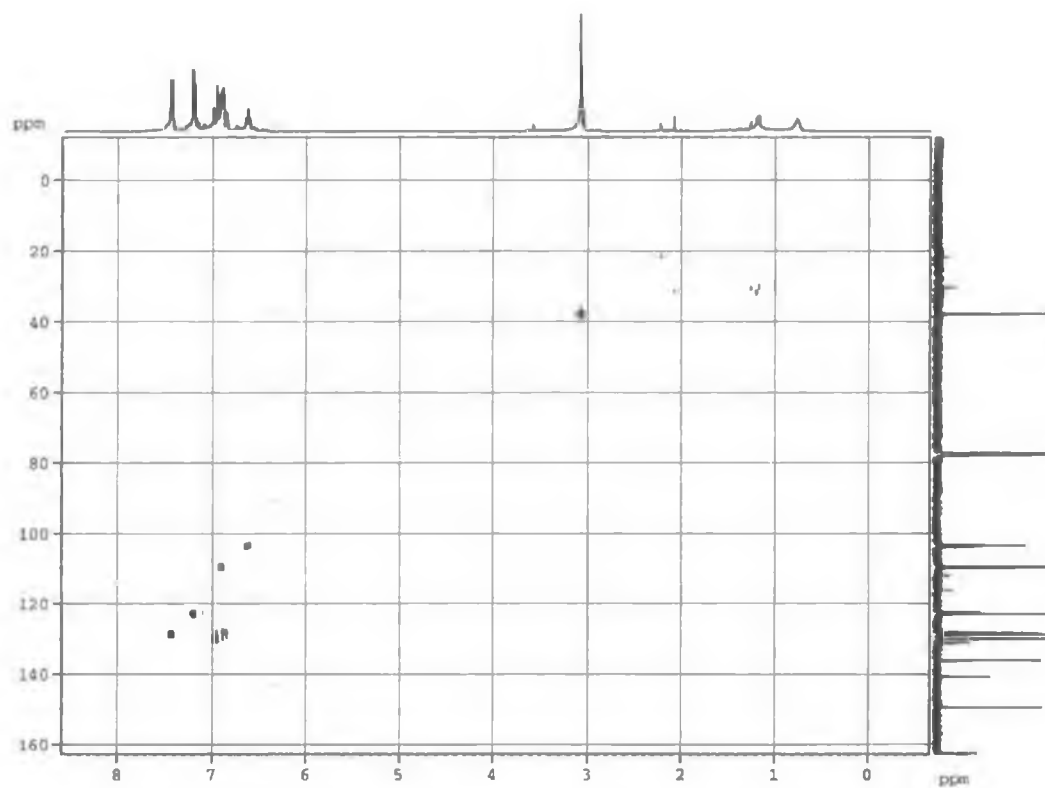


Figure 5.15 HMQC Spectrum of (*E*)-4-(3,5 difluorostyryl)phenylmethanesulphonate **199**

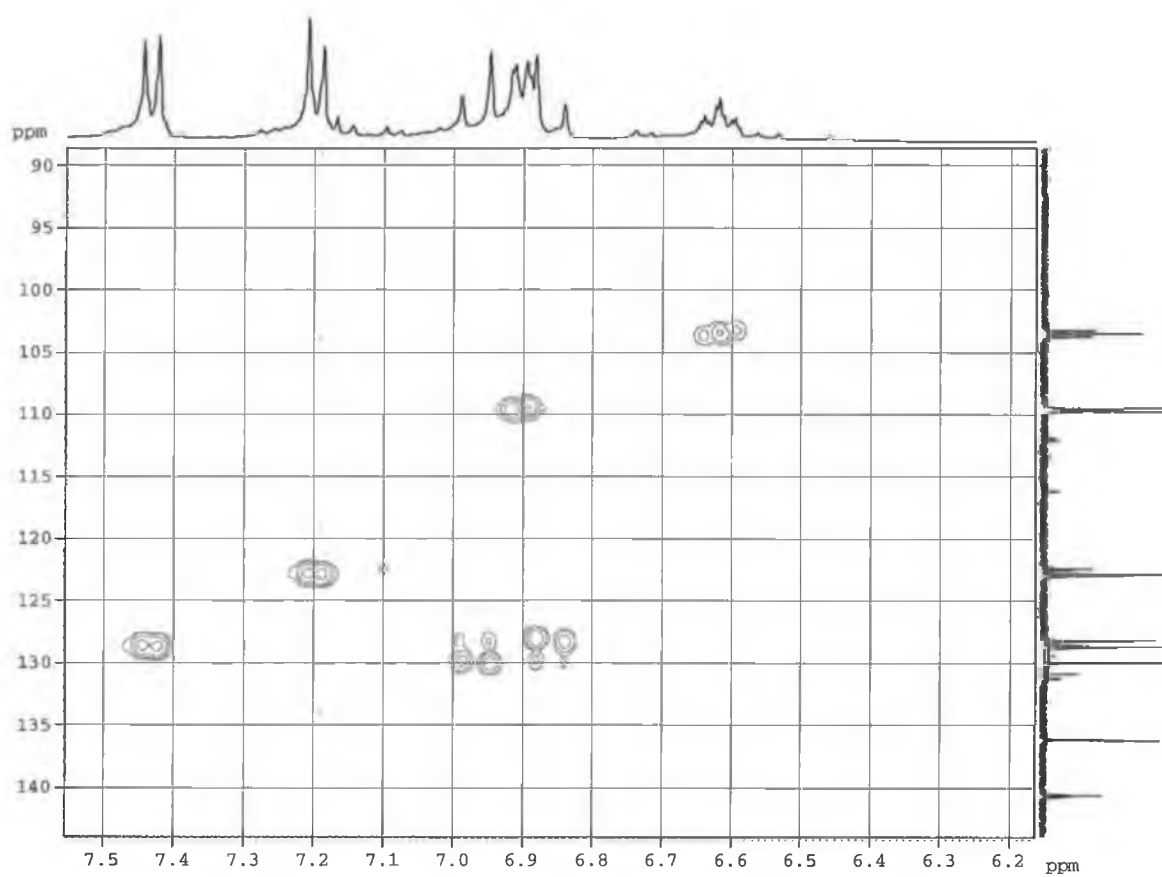


Figure 5.16 Expanded HMQC Spectrum of compound **199**

5.7 Conclusion

The synthesis and characterisation of a series of novel fluorinated analogues of resveratrol has been achieved. Their preparation was carried out using the decarbonylative Heck reaction as devised by Spencer *et al.*²⁴ This reaction was preferentially selected as it formed only the *E*-isomer and the starting materials were readily available. It was shown that the Wittig and Wadsworth-Emmons reactions formed compounds that were difficult to isolate and whose yields were not remarkable. The compounds were characterized by ¹H, ¹³C, ¹⁹F, DEPT and HMQC NMR studies. Structural elucidation was further supplemented by electrospray ionisation mass spectrometry and Infrared spectroscopy.

Preliminary biological results indicated that (*E*)-1-(4-acetoxystyryl)-3,5-difluorobenzene **192** was a potent growth inhibitor of breast, lung and central nervous system cancer lines. At a concentration of 100 μM the growth of central nervous system cancer was inhibited by 99%. Compound **192** was assessed as a prime candidate for evaluation in the full panel of 60 cell lines as used by the National Cancer Institute under the Development Therapeutic Program (DTP). The results of this assay indicated that compound **192** was a broad spectrum anticancer derivative as success was seen against leukaemia, colon, lung, breast, melanoma, prostate, ovarian, central nervous system and renal cancer lines.

These results indicate that fluorinated analogues of resveratrol have the ability to be potent inhibitors of carcinogenesis. Further analogues of compound **192** were prepared based on the 3,5-difluoro-4-oxostilbene scaffold. It is hoped that derivatisation of compound **192** at the 4-oxo position will improve the potency of these derivatives. The anticancer activities of these compounds along with the previously untested compounds are currently under investigation. Further research will be based on the results from these assays.

5.8 Experimental

General Procedures.

All chemicals were purchased from Sigma/Aldrich and used as received. When necessary solvents were purified prior to use and stored under nitrogen. Dichloromethane was distilled from CaH₂ and triethylamine was distilled and stored over potassium hydroxide pellets. Commercial grade reagents were used without further purification. Riedel-de Haën silica gel was used for thin layer and column flash chromatography. Melting points were determined using a Griffin melting point apparatus and are uncorrected. Infrared spectra were recorded on a Nicolet 405 FT-IR spectrometer and elemental analysis was carried out by the Microanalytical Laboratory at University College Dublin. Electrospray ionisation mass spectra were recorded on a Bruker Esquire 3000 series LC/MS. NMR spectra were obtained on a Bruker AC 400 NMR spectrometer operating at 400 MHz for ¹H NMR, 376 MHz for ¹⁹F NMR and 100 MHz for ¹³C NMR. The ¹H and ¹³C NMR chemical shifts (ppm) are relative to tetramethylsilane and the ¹⁹F NMR chemical shifts (ppm) are relative to trifluoroacetic acid. All coupling constants (*J*) are in Hertz.

(*E*)-1-(4'-fluorostyryl)-3,5-difluorobenzene 187

3,5-Difluorobenzoyl chloride (1.45 g, 8.2 mmol) and 4-fluorostyrene (1.0 g, 8.2 mmol) were added to a solution of palladium acetate (0.092 g, 0.41 mmol) and *N*-ethylmorpholine (3.37 g, 8.2 mmol) in xylene (50 mls). The solution was heated at 120 °C for 18 hrs and then filtered. The solvent was removed *in vacuo* to yield a crude brown solid. Recrystallisation from hexane/ethyl acetate 50:1 gave the title product as white crystalline needles (0.93 g, 48%).

m.p. 48-50 °C. Lit.¹⁹ m.p. 47 °C.

Anal. calcd. for C₁₄H₉F₃: C, 71.79; H, 3.87.

Found C, 72.04; H, 3.99.

IR (KBr): ν 2956, 2857, 1597, 1510, 1233, 961, 831 cm⁻¹.

¹H-NMR (400 MHz, DMSO): δ 7.69-7.73 (2H, m, -ArH 2' & 6'), 7.48 (1H, d, *J* = 16.4 Hz, -C=C-H), 7.38-7.41 (2H, m, -ArH 3' & 5'), 7.24-7.32 (3H, m, -ArH 2, 6 & -C=C-H), 7.15-7.20 (1H, m, -ArH 4).

¹³C-NMR (100 MHz, DMSO): δ 164.2 (d, -ArC 3), 162.3 (d, -ArC 4'), 161.8 (d, -ArC 5), 141.4 (t, -ArC 1), 133.2 (d, -ArC 1'), 130.6 (-C=C-H), 129.0 (d, -ArC 2' & 6'), 126.4 (d, -C=C-H), 116.0 (-ArC 3' & 5'), 109.6 (d, -ArC 2), 109.4 (d, -ArC 6), 102.9 (t, -ArC 4).

¹⁹F-NMR (376 MHz, DMSO): δ -34.8 - -34.9 (2F, m), -37.8 - -37.9 (1F, m).

(E)-1-(4'-methoxystyryl)-3,5-difluorobenzene 188

3,5-Difluorobenzoyl chloride (1.32 g, 7.5 mmol) and 4-vinylanisole (1.0 g, 7.5 mmol) were used. Recrystallisation from hexane/ethyl acetate 12:1 furnished **188** as yellow crystalline needles (0.41 g, 22%).

m.p. 107-109 °C. Lit.¹⁹ m.p. 108-110 °C.

Anal. calcd. for C₁₅H₁₂O₁F₂: C, 73.16; H, 4.91.

Found C, 73.49; H, 5.35.

IR (KBr): ν 2963, 2833, 1586, 1511, 1240, 962, 838 cm⁻¹.

¹H-NMR (400 MHz, DMSO): δ 7.54 (2H, d, J = 8.4 Hz, -ArH 2' & 6'), 7.35 (1H, d, J = 16.4 Hz, -C=C-H), 7.27-7.30 (2H, m, -ArH 2 & 6), 7.01-7.10 (2H, m, -ArH 4 & -C=C-H), 6.96 (2H, d, J = 8.8 Hz, -ArH 3' & 5'), 3.76 (3H, s, -OCH₃).

¹³C-NMR (100 MHz, DMSO): δ 164.2 (d, -ArC 3), 161.8 (d, -ArC 5), 159.8 (-ArC 4'), 141.8 (t, -ArC 1), 131.4 (-C=C-H), 129.2 (-ArC 1'), 128.5 (-ArC 2' & 6'), 124.2 (t, -C=C-H), 114.5 (-ArC 3' & 5'), 109.3 (d, -ArC 2), 109.1 (d, -ArC 6), 102.4 (t, -ArC 4), 55.4 (-OCH₃).

¹⁹F-NMR (376 MHz, DMSO): δ -35.0 (2F, t, J^{C-F} = 5.2 Hz).

(E)-1-(4'-fluorostyryl)-3,5-dimethoxybenzene 189

3,5-Dimethoxybenzoyl chloride (1.65 g, 8.2 mmol) and 4-fluorostyrene (1.0 g, 8.2 mmol) were used. Recrystallisation from hexane/ethyl acetate 50:1 furnished **189** as yellow crystalline needles (0.55 g, 26%).

m.p. 48-49 °C. Lit.¹⁹ m.p. 46-48 °C.

Anal. calcd. for C₁₅H₁₂O₁F₂: C, 73.16; H, 4.91.

Found C, 72.93; H, 4.98.

IR (KBr): ν 2933, 2830, 1598, 1506, 1306, 961, 847 cm⁻¹.

¹H-NMR (400 MHz, DMSO): δ 7.62-7.66 (2H, m, -ArH 2' & 6'), 7.28 (1H, d, J = 16.4 Hz, -C=C-H), 7.19-7.23 (2H, m, -ArH 3' & 5'), 7.13 (1H, d, J = 16.4 Hz, -C=C-H), 6.78 (2H, d, J = 2.4 Hz, -ArH 2 & 6), 6.43 (1H, t, J = 2.4 Hz, -ArH 4), 3.78 (6H, s, -OCH₃).

¹³C-NMR (100 MHz, DMSO): δ 162.1 (d, -ArC 4'), 161.0 (-ArC 3 & 5), 139.3 (-ArC 1), 133.8 (-ArC 1'), 128.7 (-C=C-H), 128.6 (d, -ArC 2' & 6'), 128.0 (-C=C-H), 115.9 (d, -ArC 3' & 5'), 104.7 (-ArC 2 & 6), 100.2 (-ArC 4), 55.5 (-OCH₃).

¹⁹F-NMR (376 MHz, DMSO): δ -38.8 - -38.9 (1F, m).

(E)-1-(4'-ethoxystyryl)-3,5-difluorobenzene 190

3,5-Difluorobenzoyl chloride (1.83 g, 6.7 mmol) and 4-ethoxystyrene (1.0 g, 6.7 mmol) were used. Recrystallisation from hexane/ethyl acetate 25:1 furnished **190** as yellow spherical crystals (0.32 g, 19%).

m.p. 82-84 °C.

Anal. calcd. for C₁₆H₁₄O₁F₂: C, 73.83; H, 5.42.

Found C, 73.61; H, 5.85.

IR (KBr): ν 2907, 2357, 1610, 1042, 844, 647 cm⁻¹.

¹H-NMR (400 MHz, DMSO): δ 7.52 (2H, d, J = 8.8 Hz, -ArH 2' & 6'), 7.35 (1H, d, J = 16.4 Hz, -C=C-H), 7.27-7.31 (2H, m, -ArH 2 & 6), 7.03-7.09 (2H, m, -ArH 4 & -C=C-H), 6.94 (2H, d, J = 8.8 Hz, -ArH 3' & 5'), 4.03 (2H, q, J = 6.8 Hz, -OCH₂-), 1.32 (3H, t, J = 6.8 Hz, -OCH₂CH₃).

¹³C-NMR (100 MHz, DMSO): δ 164.2 (d, -ArC 3), 161.8 (d, -ArC 5), 159.1 (-ArC 4'), 141.9 (t, -ArC 1), 131.4 (-C=C-H), 129.0 (-ArC 1'), 128.5 (-ArC 2' & 6'), 124.1 (-C=C-H), 115.0 (-ArC 3' & 5'), 109.2 (d, -ArC 2), 109.1 (d, -ArC 6), 102.4 (t, -ArC 4), 63.4 (-OCH₂-, -VE DEPT), 14.9 (-OCH₂CH₃).

¹⁹F-NMR (376 MHz, DMSO): δ -35.0 (2F, t, J^{C-F} = 5.2 Hz).

(E)-1-(4'-fluorostyryl)-3,5-diethoxybenzene 191

3,5-Diethoxybenzoyl chloride (1.87 g, 8.2 mmol) and 4-fluorostyrene (1.0 g, 8.2 mmol) were used. Recrystallisation from hexane/ethyl acetate 25:1 furnished **191** as yellow crystalline needles (0.68 g, 29%).

m.p. 58-60 °C.

Anal. calcd. for C₁₈H₁₉O₂F₁: C, 75.50; H, 6.68.

Found C, 75.60; H, 6.59.

IR (KBr): ν 2974, 2351, 1591, 1505, 1382, 1184, 968, 832 cm⁻¹.

¹H-NMR (400 MHz, DMSO): δ 7.61-7.65 (2H, m, -ArH 2' & 6'), 7.27 (1H, d, J = 16.0 Hz, -C=C-H), 7.20 (2H, t, J = 8.8 Hz, -ArH 3' & 5'), 7.10 (1H, d, J = 16.4 Hz, -C=C-H), 6.74 (2H, d, J = 2.4 Hz, -ArH 2 & 6), 6.39 (1H, t, J = 2.4 Hz, -ArH 4), 4.03 (4H, q, J = 7.2 Hz, -OCH₂-), 1.33 (6H, t, J = 7.2 Hz, -OCH₂CH₃).

¹³C-NMR (100 MHz, DMSO): δ 162.0 (d, -ArC 4'), 160.2 (-ArC 3 & 5), 139.2 (-ArC 1), 133.9 (d, -ArC 1'), 128.7 (-ArC 2' & 6'), 128.6 (-C=C-H), 127.9 (-C=C-H), 115.9 (d, -ArC 3' & 5'), 105.1 (-ArC 2 & 6), 100.9 (-ArC 4), 63.3 (-OCH₂-, -VE DEPT), 14.9 (-OCH₂CH₃).

¹⁹F-NMR (376 MHz, DMSO): δ -38.8 - -38.9 (1F, m).

(E)-1-(4'-acetoxystyryl)-3,5-difluorobenzene 192

3,5-Difluorobenzoyl chloride (4.38 g, 24.6 mmol) and 4-acetoxystyrene (4.0 g, 24.6 mmol) were used. Recrystallisation from hexane/ethyl acetate 12:1 furnished **192** as yellow planar crystals (3.94 g, 58%).

m.p. 142-144 °C.

Anal. calcd. for C₁₆H₁₂O₂F₂: C, 70.07; H, 4.41.

Found C, 69.72; H, 4.46.

IR (KBr): ν 2926, 2351, 1752, 1616, 1208, 968 cm⁻¹.

¹H-NMR (400 MHz, DMSO): δ 7.63 (2H, d, J = 8.4 Hz, -ArH 2' & 6'), 7.44 (1H, d, J = 16.4 Hz, -C=C-H), 7.32-7.36 (2H, m, -ArH 2 & 6), 7.23 (1H, d, J = 16.4 Hz, -C=C-H), 7.17 (2H, d, J = 8.8 Hz, -ArH 3' & 5'), 7.08-7.14 (1H, m, -ArH 4), 2.29 (3H, s, -CH₃).

¹³C-NMR (100 MHz, DMSO): δ 169.5 (C=O), 164.2 (d, -ArC 3), 161.8 (d, -ArC 5), 150.7 (-ArC 4'), 141.4 (t, -ArC 1), 134.3 (-ArC 1'), 130.8 (-C=C-H), 128.1 (-ArC 2' & 6'), 126.6 (-C=C-H), 122.5 (-ArC 3' & 5'), 109.6 (d, -ArC 2), 109.5 (d, -ArC 6), 102.7 (t, -ArC 4), 21.1 (-CH₃).

¹⁹F-NMR (376 MHz, DMSO): δ -34.8 (2F, t, J^{C-F} = 8.6 Hz).

(E)-1-(4'-fluorostyryl)-3,5-diacetoxybenzene 193

3,5-Diacetoxybenzoyl chloride (1.03 g, 4.0 mmol) and 4-fluorostyrene (0.48 g, 4.0 mmol) were used. Recrystallisation from hexane/ethyl acetate 3:1 furnished **193** as white crystalline needles (0.82 g, 65%).

m.p. 161-162 °C.

Anal. calcd. for C₁₈H₁₅O₄F₁: C, 68.78; H, 4.81.

Found C, 68.91; H, 4.65.

IR (KBr): ν 3119, 2929, 1774, 1655, 1509, 1401, 1197, 912 cm⁻¹.

¹H-NMR (400 MHz, CDCl₃): δ 7.44-7.48 (2H, m, -ArH 2' & 6'), 7.03-7.13 (5H, m, -ArH 2, 6, 3', 5' & -C=C-H), 6.94 (1H, d, J = 16.0 Hz, -C=C-H), 6.84 (1H, t, J = 2.4 Hz, -ArH 4), 2.32 (6H, s, CH₃).

¹³C-NMR (100 MHz, CDCl₃): δ 169.4 (C=O), 162.9 (d, -ArC 4'), 151.6 (-ArC 3 & 5), 139.9 (-ArC 1), 133.2 (d, -ArC 1'), 129.8 (-C=C-H), 128.6 (d, -ArC 2' & 6'), 127.1 (d, -C=C-H), 117.2 (-ArC 2 & 6), 116.1 (d, -ArC 3' & 5'), 114.2 (-ArC 4), 21.5 (-CH₃).

¹⁹F-NMR (376 MHz, CDCl₃): δ -38.0 - -38.1 (1F, m).

(E)-1-(4'-hydroxystyryl)-3,5-difluorobenzene 194

Ammonium acetate (4.5 g, 54.4 mmol) was added to a solution of (E)-1-(4'-acetoxystyryl)-3,5-difluorobenzene (2.0 g, 7.3 mmol) in aqueous methanol (4:1) and the solution was stirred at room temperature for 3 hrs. The title product was extracted with ethyl acetate and dried over MgSO₄. The solvent was removed in vacuo to furnish **194** as an orange solid (1.03 g, 81%).

m.p. 142-144 °C. Lit.³⁴ m.p. 141-142 °C.

Anal. calcd. for C₁₄H₁₀O₁F₂: C, 72.40; H, 4.34.

Found C, 72.27; H, 4.61.

IR (KBr): ν 3364, 2926, 1592, 1246, 1104, 961 cm⁻¹.

¹H-NMR (400 MHz, DMSO): δ 8.04 (1H, s, -OH), 7.43 (2H, d, $J = 8.4$ Hz, -ArH 2' & 6'), 7.24 - 7.31 (3H, m, -ArH 2, 6 & -C=C-H), 6.97-7.01 (2H, m, -ArH 4 & -C=C-H), 6.81 (2H, d, $J = 8.8$ Hz, -ArH 3' & 5').

¹³C-NMR (100 MHz, DMSO): δ 164.2 (d, -ArC 3), 161.8 (d, -ArC 5), 158.3 (-ArC 4'), 142.0 (t, -ArC 1), 131.8 (-C=C-H), 128.7 (-ArC 2' & 6'), 127.6 (-ArC 1'), 123.1 (d, -C=C-H), 116.0 (-ArC 3' & 5'), 109.0 (d, -ArC 2), 108.9 (d, -ArC 6), 102.1 (t, -ArC 4).

¹⁹F-NMR (376 MHz, DMSO): δ -35.0 (2F, t, $J^{C-F} = 8.6$ Hz).

(E)-1-(4'-fluorostyryl)-3-acetoxy-5-hydroxybenzene 195

Ammonium acetate (0.39 g, 5.09 mmol) was added to a solution of (E)-1-(4-fluorostyryl)-3,5-diacetoxybenzene (0.1 g, 0.32 mmol) in aqueous methanol (4:1) and the solution was stirred at room temperature for 3 hrs. The title product was extracted with ethyl acetate and dried over MgSO₄. The solvent was removed *in vacuo* to furnish **195** as a white powder (1.05 g, 76%).

m.p. 118-120 °C.

Anal. calcd. for C₁₆H₁₃O₃F₁: C, 70.58; H, 4.81.

Found C, 70.35; H, 5.00.

IR (KBr): ν 3336, 2364, 1770, 1586, 1509, 1206, 852 cm⁻¹.

¹H-NMR (400 MHz, CDCl₃): δ 7.40-7.43 (2H, m, -ArH 2' & 6'), 7.01-7.06 (2H, m, -ArH 3' & 5'), 6.97 (1H, d, $J = 16.6$ Hz, -C=C-H), 6.85 (1H, d, $J = 16.6$ Hz, -C=C-H), 6.78 (2H, d, $J = 8.8$ Hz, -ArH 2 & 6), 6.49 (1H, t, $J = 2.0$ Hz, -ArH 4), 6.13 (1H, s, -OH), 2.33 (3H, s, CH₃).

¹³C-NMR (100 MHz, CDCl₃): δ 170.6 (C=O), 162.9 (d, -ArC 4'), 157.2 (-ArC 3), 151.9 (-ArC 5), 140.1 (-ArC 1), 133.3 (d, -ArC 1'), 129.1 (-C=C-H), 128.5 (d, -ArC 2' & 6'), 127.6

(-C=C-H), 116.0 (d, -ArC 3' & 5'), 111.9 (-ArC 6), 111.6 (-ArC 2), 108.8 (-ArC 4), 21.6 (-CH₃).

¹⁹F-NMR (376 MHz, CDCl₃): δ -39.3 - -39.4 (1F, m).

(E)-1-(4'-trichloroacetylstyryl)-3,5-difluorobenzene 196

A solution of trichloroacetyl chloride (0.181 g, 1.0 mmol) in dichloromethane (3 mls) was added dropwise to a solution of (E)-1-(4-hydroxystyryl)-3,5-difluorobenzene (0.212 g, 1.0 mmol) and triethylamine (0.14 mls, 1.0 mmol) in dichloromethane (3 mls). The solution was stirred for 8 hrs then washed with 5% HCl and water. The organic extract was then dried over MgSO₄ and the solvent was removed *in vacuo*. Recrystallisation from hexane/ethyl acetate 2:1 furnished **196** as white crystalline needles (279 mg, 74%).

m.p. 92-94 °C.

Anal. calcd. for C₁₆H₉O₂F₂Cl₃: C, 50.89; H, 2.40.

Found C, 51.11; H, 2.63.

IR (KBr): ν 3153, 2928, 1774, 1655, 1400, 1115 cm⁻¹.

¹H-NMR (400 MHz, CDCl₃): δ 7.46 (2H, d, *J* = 7.2 Hz, -ArH 2' & 6'), 7.14 (2H, d, *J* = 7.2 Hz, -ArH 3' & 5'), 6.99 (1H, d, *J* = 16.0 Hz, -C=C-H), 6.86-6.95 (3H, m, -ArH 2, 6 & -C=C-H), 6.60-6.65 (1H, m, -ArH 4).

¹³C-NMR (100 MHz, CDCl₃): δ 164.9 (d, -ArC 3), 162.4 (d, -ArC 5), 160.8 (C=O), 150.6 (-ArC 4'), 140.7 (t, -ArC 1), 135.8 (-ArC 1'), 130.8 (-C=C-H), 128.4 (-ArC 2' & 6'), 128.0 (t, -C=C-H), 121.3 (-ArC 3' & 5'), 109.6 (d, -ArC 2), 109.5 (d, -ArC 6), 103.4 (t, -ArC 4), 89.9 (-CCl₃).

¹⁹F-NMR (376 MHz, CDCl₃): δ -34.6 (2F, t, *J*^{C-F} = 7.8 Hz).

(E)-1-(4'-trifluoroacetylstyryl)-3,5-difluorobenzene 197

Trifluoroacetic anhydride (0.16 g, 0.76 mmol) was used. Recrystallisation from hexane/ethyl acetate 2:1 furnished **197** as white crystalline needles (152 mg, 61%).

m.p. 139-141 °C.

Anal. calcd. for C₁₆H₉O₂F₅: C, 58.54; H, 2.76.

Found C, 58.51; H, 2.75.

IR (KBr): ν 3140, 2928, 1655, 1591, 1400, 1117, 661 cm⁻¹.

¹H-NMR (400 MHz, CDCl₃): δ 7.32 (2H, d, *J* = 8.8 Hz, -ArH 2' & 6'), 6.95 (1H, d, *J* = 16.4 Hz, -C=C-H), 6.88-6.92 (2H, m, -ArH 2 & 6), 6.75-6.79 (3H, m, -ArH 3', 5' & -C=C-H), 6.56-6.61 (1H, m, -ArH 4).

¹³C-NMR (100 MHz, CDCl₃): δ 164.9 (d, -ArC 3), 162.4 (d, -ArC 5), 156.3 (C=O), 141.4 (t, -ArC 4'), 131.1 (t, -ArC 1), 130.7 (-ArC 1'), 129.6 (-C=C-H), 128.7 (-ArC 2' & 6'), 124.8 (t, -C=C-H), 116.1 (-ArC 3' & 5'), 115.7 (-CF₃), 109.2 (d, -ArC 2), 109.0 (d, -ArC 6), 102.7 (t, -ArC 4).

¹⁹F-NMR (376 MHz, CDCl₃): δ -0.5 (3F), -35.1 (2F, t, $J^{C-F} = 7.8$ Hz).

(E)-1-(4'-trimethylacetylstyryl)-3,5-difluorobenzene 198

Trimethylacetyl chloride (0.091 g, 0.76 mmol) was used. Recrystallisation from hexane/ethyl acetate 2:1 furnished **198** as white crystalline needles (188 mg, 78%).

m.p. 79-81 °C.

Anal. calcd. for C₁₉H₁₈O₂F₂: C, 72.13; H, 5.73.

Found C, 72.01; H, 5.83.

IR (KBr): ν 2975, 2365, 1742, 1619, 1120, 670 cm⁻¹.

¹H-NMR (400 MHz, CDCl₃): δ 7.38 (2H, d, $J = 7.6$ Hz, -ArH 2' & 6'), 6.92-6.98 (3H, m, -ArH 3', 5' & -C=C-H), 6.85-6.90 (2H, m, -ArH 2 & 6), 6.81 (1H, d, $J = 16.4$ Hz, -C=C-H), 6.57-6.60 (1H, m, -ArH 4), 1.27 (9H, s, -CH₃).

¹³C-NMR (100 MHz, CDCl₃): δ 177.4 (C=O), 164.9 (d, -ArC 3), 162.4 (d, -ArC 5), 151.5 (-ArC 4'), 141.0 (t, -ArC 1), 134.2 (-ArC 1'), 130.6 (-C=C-H), 128.1 (-ArC 2' & 6'), 126.9 (t, -C=C-H), 122.3 (-ArC 3' & 5'), 109.5 (d, -ArC 2), 109.3 (d, -ArC 6), 103.1 (t, -ArC 4), 39.5 (-C(CH₃)₃), 27.5 (-CH₃).

¹⁹F-NMR (376 MHz, CDCl₃): δ -34.9 (2F, t, $J^{C-F} = 7.8$ Hz).

(E)-4-(3,5-difluorostyryl)phenylmethanesulphonate 199

Methanesulphonyl chloride (0.057 g, 0.50 mmol) was used. Recrystallisation from hexane/ethyl acetate 2:1 furnished **199** as white crystalline needles (110 mg, 71%). m.p. 85-87 °C.

Anal. calcd. for C₁₅H₁₂O₃F₂S₁: C, 58.05; H, 3.89.

Found C, 57.89; H, 4.09.

IR (KBr): ν 3369, 2926, 1619, 1113, 845, 670 cm⁻¹.

¹H-NMR (400 MHz, CDCl₃): δ 7.43 (2H, d, $J = 8.4$ Hz, -ArH 2' & 6'), 7.19 (2H, d, $J = 8.8$ Hz, -ArH 3' & 5'), 6.96 (1H, d, $J = 16.4$ Hz, -C=C-H), 6.84-6.92 (3H, m, -ArH 2, 6 & -C=C-H), 6.59-6.62 (1H, m, -ArH 4), 3.08 (3H, s, -CH₃).

¹³C-NMR (100 MHz, CDCl₃): δ 164.8 (d, -ArC 3), 162.5 (d, -ArC 5), 149.2 (-ArC 4'), 140.6 (t, -ArC 1), 136.1 (-ArC 1'), 129.9 (-C=C-H), 128.6 (-ArC 2' & 6'), 128.1 (t, -C=C-H), 122.8 (-ArC 3' & 5'), 109.6 (d, -ArC 2), 109.5 (d, -ArC 6), 103.4 (t, -ArC 4), 37.8 (-CH₃).

¹⁹F-NMR (376 MHz, CDCl₃): δ -34.6 (2F, t, *J*^{C-F} = 7.8 Hz).

(E)-4-(3,5-difluorostyryl)phenyl-4-fluorobenzenesulphonate 200

4-Fluorobenzenesulphonyl chloride (0.212 g, 1.0 mmol) was used. Recrystallisation from hexane/ethyl acetate 2:1 furnished **200** as white crystalline needles (195 mg, 50%). m.p. 71-73 °C.

Anal. calcd. for C₂₀H₁₃O₃F₃S₁: C, 61.53; H, 3.35.

Found C, 61.45; H, 3.32.

IR (KBr): ν 3118, 2365, 1592, 1400, 1200, 842 cm⁻¹.

¹H-NMR (400 MHz, CDCl₃): δ 7.75-7.79 (2H, m, -Ar(S)H 2 & 6), 7.33 (2H, d, *J* = 8.4 Hz, -ArH 2' & 6'), 7.09-7.14 (2H, m, -Ar(S)H 3 & 5), 6.93 (1H, d, *J* = 16.4 Hz, -C=C-H), 6.86-6.90 (4H, m, -ArH 2, 6, 3' & 5'), 6.83 (1H, d, *J* = 16.4 Hz, -C=C-H), 6.59-6.64 (1H, m, -ArH 4).

¹³C-NMR (100 MHz, CDCl₃): δ 166.4 (d, -Ar(S)C 4), 164.8 (d, -ArC 3), 162.4 (d, -ArC 5), 149.4 (-ArC 4'), 140.6 (t, -ArC 1), 136.0 (-ArC 1'), 131.8 (d, -Ar(S)C 2 & 6), 130.5 (d, -Ar(S)C 1), 129.9 (-C=C-H), 128.3 (-ArC 2' & 6'), 128.1 (t, -C=C-H), 123.1 (-ArC 3' & 5'), 117.0 (d, -Ar(S)C 3 & 5), 109.6 (d, -ArC 2), 109.5 (d, -ArC 6), 103.4 (t, -ArC 4).

¹⁹F-NMR (376 MHz, CDCl₃): δ -26.4 - -26.5 (1F, m), -34.6 (2F, t, *J*^{C-F} = 7.8 Hz).

(E)-4-(3,5-difluorostyryl)phenyl-2-fluorobenzoate 201

2-Fluorobenzoyl chloride (0.158 g, 1.0 mmol) was used. Recrystallisation from hexane/ethyl acetate 2:1 furnished **201** as white crystalline needles (184 mg, 52%). m.p. 118-120 °C.

Anal. calcd. for C₂₁H₁₃O₂F₃: C, 71.18; H, 3.69.

Found C, 71.49; H, 3.41.

IR (KBr): ν 3134, 2345, 1735, 1410, 1292, 847 cm⁻¹.

¹H-NMR (400 MHz, CDCl₃): δ 7.99-8.03 (1H, m, -ArH 6a), 7.48-7.53 (1H, m, -ArH 4a), 7.47 (2H, d, *J* = 8.8 Hz, -ArH 2' & 6'), 7.09-7.20 (4H, m, -ArH 3', 5', 3a & 5a), 7.00 (1H, d, *J* = 16.4 Hz, -C=C-H), 6.84-6.92 (3H, m, -ArH 2, 6 & -C=C-H), 6.58-6.62 (1H, m, -ArH 4).

¹³C-NMR (100 MHz, CDCl₃): δ, 164.9 (d, -ArC 3), 163.0 (d, C=O), 162.7 (d, -ArC 2a), 162.4 (d, -ArC 5), 150.9 (-ArC 4'), 140.9 (t, -ArC 1), 135.7 (d, -ArC 4), 134.7 (-ArC 1'), 132.9 (d, -ArC 6a), 130.6 (-C=C-H), 128.2 (-ArC 2' & 6'), 127.2 (t, -C=C-H), 124.5 (d, -ArC 5a), 122.4

(-ArC 3' & 5'), 118.3 (d, -ArC 1a), 117.6 (d, -ArC 3a), 109.5 (d, -ArC 2), 109.3 (d, -ArC 6), 103.2 (t, -ArC 4).

^{19}F -NMR (376 MHz, CDCl_3): δ -32.7 - -32.8 (1F, m), -34.8 (2F, t, $J^{\text{C-F}} = 7.8$ Hz).

5.9 References

- 1 Nicolosi, G., Spatafora, C., Tringali, C., *J. Mol. Catalysis B* **2002**, *16*, 223.
- 2 Lee, H.J., Seo, J.W., Lee, B.H., Chung, K.H., Chi, D.Y., *Bioorg. Med. Chem. Lett.* **2004**, *14*, 463.
- 3 Ratan, H.L., Steward, W.P., Gescher, A.J., Mellon, J.K., *Urologic Oncology* **2002**, *7*, 223.
- 4 Frémont, L., *Life Sciences* **2000**, *66*, 663.
- 5 Pettit, G.R., Grealish, M.P., Jung, K., Hamel, E., Pettit, R.K., Chapuis, J.C., Schmidt, J.M., *J. Med. Chem.* **2002**, *45*, 2534.
- 6 Botella, L., Najera, C., *Tetrahedron* **2004**, *60*, 5563.
- 7 Savouret, J.F., Quesne, M. *Biomed. Pharmacother.* **2002**, *56*, 84.
- 8 Soleas, G.J., Diamandis, E.P., Goldberg, D.M., *Clin. Biochem.* **1997**, *30*, 91.
- 9 Dewick, P.M., “*Medicinal Natural Products, A Biosynthetic Approach*”, Wiley and Sons, **2003**, 2nd edition.
- 10 Romero-Pérez, A.I., Lameula-Raventós, R.M., Andrés-Laceuva, C., de La Torre-Boronat, M.C., *J. Agric. Food Chem.* **2001**, *49*, 210.
- 11 Späth, E., Kromp, K., *Chem. Ber.* **1941**, *74*, 189.
- 12 Wittig, G., Schollkopf, U., *Chem. Ber.* **1954**, *87*, 1318.
- 13 Roberti, M., Pizzirani, D., Simoni, D., Rondanin, R., Baruchello, R., Bonora, C., Buscemi, F., Grimaudo, S., Tolomeo, M., *J. Med. Chem.* **2003**, *46*, 3546.
- 14 Perkin, W.H., *J. Chem. Soc.* **1868**, *21*, 181.
- 15 Solladié, G., Pasteural-Jacopé, Y., Maignan, J., *Tetrahedron* **2003**, *59*, 3315.
- 16 Miyaura, N., Suzuki, A., *Chem. Rev.* **1995**, *95*, 2457.
- 17 Eddarir, S., Abdelhadi, Z., Rolando, C., *Tetrahedron Lett.* **2001**, *42*, 9127.
- 18 Ferré-Filmon, K., Delaude, L., Demonceau, A., Noels, A.F., *Coord. Chem. Rev.* **2004**, *248*, 2323.
- 19 De Medina, P., Casper, P., Savouret, J.F., Poirot, M., *J. Med. Chem.* **2005**, *48*, 287.
- 20 Welch, J.T., Eswarakrishnan, S., “*Fluorine in Bioorganic Chemistry*”, John Wiley and Sons, **1991**.
- 21 Lawrence, N.J., Hepworth, L.A., Rennison, D., McGown, A.T., Hadfield, J.A., *J. Fluor. Chem.* **2003**, *123*, 101.
- 22 Wadsworth, W.S., Emmons, W.D., *J. Am. Chem. Soc.* **1961**, *83*, 1733.
- 23 Andrus, M.B., Liu, J., Meredith, E.L., Nartey, E., *Tetrahedron Lett.* **2003**, *44*, 4819.

-
- 24 Blaser, H.U., Spencer, A., *J. Organomet. Chem.* **1982**, 233, 267.
- 25 Tobe, M., Isobe, Y., Goto, Y., Obara, F., Tsuchiya, M., Matsui, J., Hirota, K.,
Hayashi, H., *Bioorg. Med. Chem.* **2000**, 8, 2037.
- 26 Ramesh, C., Mahender, G., Ravindranath, N., Das, B, *Tetrahedron* **2003**, 59, 1049.
- 27 Williams, D.H., Fleming, I., “*Spectroscopic Methods in Organic Chemistry*”,
McGraw-Hill publishers, **1995**, 5th edition.
- 28 http://training.seer.cancer.gov/module_cancer_disease/unit2_whatscancer1_definition.html
- 29 Ikeda, K., Negishi, H., Yamori, Y., *Toxicology* **2003**, 189, 55.
- 30 Gao, X., Xu, Y.X., Divine, G., Janakiraman, N., Chapman, R.A., Gautam, S.C., *J.*
Nutr. **2002**, 132, 2076.
- 31 Dong, Z., *Mutat. Res.* **2003**, 523-524, 145.
- 32 She, Q.B., Bode, A.M., Ma, W.Y., Chen, N.Y., Dong, Z. *Cancer Res.* **2001**, 61, 1604.
- 33 Babich, H., Reisbaum, A.G., Zuckerbraun, H.L., *Toxicol. Lett.* **2000**, 114, 143-153.
- 34 Lion, C.J., Matthews, C.S., Stevens, M.F.G., Westwell, A.D., *J. Med. Chem.* **2005**,
48, 1292.

Appendix I

Abbreviations

°C	Degrees Celsius.
Å	Angstrom.
Ac	Acetyl
ACE	Angiotensin converting enzyme.
AIDS	Acquired immunodeficiency syndrome.
Ala	Alanine.
Arg	Arginine.
Asp	Aspartic acid.
ATP	Adenosine triphosphate.
β-Ala	β-alanine.
Boc	<i>Tert</i> -butoxycarbonyl.
CaCl ₂	Calcium chloride.
CDCl ₃	Deuterated chloroform.
CH ₂ Cl ₂	Dichloromethane.
CH ₂ N ₂	Diazomethane.
cm ⁻¹	Per centimetre.
CNS	Central nervous system.
α-CT	α-Chymotrypsin.
COPD	Chronic obstructive pulmonary disease.
Cyp	Cytochrome P450.
Cys	Cysteine.
DCC	Dicyclohexylcarbodiimide.
DCU	<i>N, N'</i> -dicyclohexylurea.
DDQ	2,3-dichloro-5,6-dicyano-1,4-benzoquinone.
DEPT	Distortionless enhancement through polarization transfer.
DFP	Diisopropylfluorophosphate.
DMSO	Dimethyl sulfoxide.
DTP	Development therapeutic program.
EDC	1-ethyl-3-(3-dimethylaminopropyl)carbodiimide.
ESIMS	Electrospray ionisation mass spectroscopy.
Et ₃ N	Triethylamine.

FDA	Food and drug administration.
g	Gram.
γ -ABA	γ -aminobutyric acid.
Glu	Glutamic acid.
Gly	Glycine.
GST	Glutathione <i>S</i> -transferase.
HBr	Hydrogen bromide.
His	Histidine.
HIV	Human immunodeficiency virus.
HMQC	Heteronuclear multiple quantum coherence.
HOBt	1-hydroxybenzotriazole.
HONO	Nitrous acid.
HRV	Human rhinoviruses.
Hz	Hertz.
IC ₅₀	Concentration required to achieve 50% inhibition.
ICE	Interleukin-1 converting enzyme.
Ile	Isoleucine
Iva	Isovaline.
IR	Infrared.
K _i	Rate of inhibition.
Leu	Leucine.
LDL	Low density lipoprotein.
M	Molar.
MDR	Multidrug resistance.
m.p.	Melting point.
MeOH	Methanol.
ml	Millilitre.
mmol	Millimole.
MMP	Matrix metalloproteases.
MRP-1	Multidrug resistance protein 1.
NaBF ₄	Sodium tetrafluoroborate.
NaOH	Sodium hydroxide.
NHMec	7-amino-4-methylcoumarin.
NHNap	4-naphtylamine.

nm	Nanometre.
NMR	Nuclear magnetic resonance.
NO	Nitric oxide.
Pgp	P-glycoprotein.
Phe	Phenylalanine.
Phegly	Phenylglycine.
PMSF	Phenylmethanesulphonyl fluoride.
Py.9HF	Pyridinium polyhydrogen fluoride.
QSAR	Quantitative structure activity relationship.
SAR	Structure activity relationship.
Ser	Serine.
SOCl ₂	Thionyl chloride.
Sta	Statine.
THF	Tetrahydrofuran.
TIMP	Tissue inhibitors of metalloproteases.
TLCK	Tosyl-L-lysine chloromethyl ketone.
TNF- α	Tumor necrosis factor α .
TPCK	Tosylamido-L-phenylethyl chloromethyl ketone.
Tris-HCl	Tris(hydroxymethyl)aminomethane hydrochloride.
TsOH	<i>para</i> -toluenesulphonic acid.
Val	Valine.
Z/CBz	Benzyloxycarbonyl.